REPORT 40

GEOLOGY OF THE JILLAWARRA AREA, BANGEMALL BASIN WESTERN AUSTRALIA

by J.H. Vogt

GEOLOGICAL SURVEY OF WESTERN AUSTRALIA

DEPARTMENT OF MINERALS AND ENERGY

GEOLOGICAL SURVEY OF WESTERN AUSTRALIA

REPORT 40

GEOLOGY OF THE JILLAWARRA AREA, BANGEMALL BASIN, WESTERN AUSTRALIA

by
J. H. Vogt

Perth 1995

MINISTER FOR MINES
The Hon. George Cash, JP, MLC

DIRECTOR GENERAL
K. R. Perry

DIRECTOR, GEOLOGICAL SURVEY OF WESTERN AUSTRALIA
Pietro Guj

REFERENCE

The recommended reference for this publication is:

VOGT, J. H., 1995, Geology of the Jillawarra area, Bangemall Basin, Western Australia: Western Australia Geological Survey, Report 40.

National Library of Australia
Cataloguing-in-publication entry

Vogt, J. H. (Jörn Hubertus), 1955—
Geology of the Jillawarra area, Bangemall Basin, Western Australia.

Bibliography.
ISBN 0 7309 4428 X.

1. Metallogeny — Western Australia — Bangemall Basin.
2. Ore deposits — Western Australia — Bangemall Basin.
3. Rocks, Sedimentary — Western Australia — Bangemall Basin.
4. Geology, Stratigraphic — Proterozoic.
5. Bangemall Basin (W.A.).
I. Geological Survey of Western Australia.
II. Title. (Series: Report (Geological Survey of Western Australia); no. 40).

553/4099412

ISSN 0508–4741

Cover photograph:

View to the west from Manganese Range toward Woodlands Dome and Teano Range.

Contents

Page

Foreword viii

Chapter One Introduction

General 1
Location and access 1
Physiography and climate 1
Previous work 1
Aims of the present study 1

Chapter Two Geology of the Bangemall Basin

Evidence of age 5
Structure and tectonics 5
Tectonic controls 5
Deformation and faulting 5
Conclusion 6
Stratigraphy 6
Facies provinces 6
Stratigraphy of the western facies 8
Development of the western facies 8
Igneous rocks in the Bangemall Basin 8
Mafic rocks 9
Dolerite sills 9
Geochemistry 9
Implications of mafic magmatism 10
Felsic volcanic rocks 10
Rhyolite and felsic lavas 11
Possible felsic volcanic rocks (tuffs) 11
Summary 11

Chapter Three Stratigraphy and sedimentology of the Jillawarra basin

Earlier investigations 13
Basement rocks 13
Coobarra Dome 13
Woodlands Dome 13
The lower Bangemall Group in the Jillawarra basin 15
Gap Well formation (*GW*) 15
Unit *GW1* 16
Unit *GW2* 16
Unit *GW3* 19
Woodlands Arenite Member (*GWW4*) 21
Unit *GW5* 24
Unit *GW6* 30
West Creek formation (*WC*) 36
Unit *WC1* 36
Unit *WC2* 39
Unit *WC3* 43
Unit *WC4* 45
Jillawarra Formation (*Mj*) 46
Unit *Mjd* 47
Unit *Mjs* 47

Chapter Four Structure of the Jillawarra basin

Folding 49
Slump folds 49
Drape folds 49

Tight folds 49
Folds associated with thrusting 50
Variations in fold style 50
Lateral variation 50
Vertical variation 52
Cleavage 52
Faulting 52
Normal faults 53
Reverse faults and thrust faults 53
Summary 54

Chapter Five Igneous rocks of the Jillawarra basin

Mafic intrusions 55
Felsic volcanics of the Coobarra Dome area 55
Rhyolite 55
Lapilli tuff 55
Other volcaniclastic rocks 59
Felsic pipes 59
Summary 59

Chapter Six Development of the Jillawarra basin

Basin limits 61
Earliest deposition 61
Transgression 61
Regression (doming) 61
Transgression (rifting) 61
Further basin development 62
Summary 63

Chapter Seven Abra sub-basin

Stratigraphy of the Abra sub-basin 65
Gap Well formation 65
Stringer zone 66
Black zone 69
Facies of the Black zone 74
Red zone 74
Top of the Red zone 75
Facies of the Red zone 78
The sulfate problem 78
Source rocks for the Abra mineralization 79
Correlation of the Black and Red zones with the Gap Well formation of the Jillawarra basin 82
Summary 82
West Creek formation 83
Unit *WC1* 83
Unit *WC2* 83
Unit *WC3* 83
Structure of the Abra sub-basin 84
Faults 84
Cleavage 84
Development of the Abra sub-basin (a third-order basin) 84
Period representing deposition of middle parts of Unit *GW6* (Stringer zone) 84
Period representing deposition of upper part of Unit GW6 (Black zone) 88
Period representing deposition of uppermost part of Unit *GW6* (top of the Red zone) 88
Period representing deposition of Unit *WC1* (coarse clastites) 88
Period representing deposition of Unit *WC2* (turbidites) 88
Period of folding (present disposition of Abra sub-basin) 88

Chapter Eight Hydrothermal alteration in the Jillawarra basin

Silicification 89
Albitization 89
Chloritization 89

Page

Chapter Nine **Mineralization in the Jillawarra basin (outside the Abra sub-basin)**

Mineralization in the Jillawarra basin 91
Black zone type mineralization 91
Stringer zone type mineralization 95
Metal zonation 96
Quartzite Well Fault mineralization 97
Summary 97

Chapter Ten **Genesis of the Abra mineralization**

Geotectonic setting 99
Source rocks 101
Accumulation of metal-bearing fluids 101
Ascent of hydrothermal fluids 101
Emplacement of the Abra mineralization 103
Summary 103

References 105

Plates

1. Geological map of the Jillawarra area
2. Solid geology of the Jillawarra area

Figures

1. Locality map of the Jillawarra area 2
2. Tectonic setting of the Bangemall Basin 6
3. Structural provinces of the Bangemall Basin in relation to facies provinces and lineaments 7
4. Facies change between western and eastern facies in the Bangemall Basin 8
5. Discrimination diagram of basaltic magma types, using Ti, Zr and Y 10
6. Abundance and distribution of dolerite sills in the Bangemall Basin 10
7. Simplified geological map of the Jillawarra area 14
8. Angular quartz–sericite aggregate 15
9. Diagrammatic stratigraphic correlation through the Jillawarra basin 18
10. Silicified, laminated dolomite of Unit *GW2* 19
11. Part of a disrupted algal layer in micritic carbonate, Unit *GW2* 20
12. Growth of chlorite in the pressure shadow of magnetite grains, siltstone in Unit *GW3* 20
13. Muscovite surrounding euhedral magnetite, siltstone in Unit *GW3* 21
14. Amorphous iron (hydroxide) oxide layer (dark) wrapped around quartz grains, siltstone in Unit *GW3* ... 22
15. Barite vein in coarse-grained Woodlands Arenite (*GWw4*) 22
16. Magnetite grains dispersed in ferroan carbonate, Woodlands Arenite (*GWw4*) 23
17. Zoned subhedral hyalophane in recrystallized quartz, Woodlands Arenite (*GWw4*) 24
18. Quartz phase interstitial to carbonate, containing inclusions of subhedral carbonate, opaques (mainly magnetite) and barite in Woodlands Arenite(*GWw4*) 25
19. Rhythmically interbedded dolomitic siltstone and calcareous wacke, of Unit *GW5* 25
20. Unknown stromatolites in dolomite of the upper part of Unit *GW5* 26
21. Biotite replacing possible authigenic albite, in siltstone of Unit *GW5* 26
22. Authigenic seams of detrital microcline in sandy dolomite, Unit *GW5* 28
23. Barite and chlorite matrix in a coarse-grained quartz sandstone, Unit *GW5* 28
24. Biotite in disequilibrium with chlorite; calcareous wackestone of Unit *GW5* 29
25. Disrupted microbial mats; calcareous siltstone of Unit *GW5* 29
26. Ferruginous pellets in a calcareous wackestone, Unit *GW5* 30
27. Silicification and manganese enrichment at the contact between dolomitic shales (Unit *GW6*) and coarse-grained arenites (Unit *WC1*) 31
28. Red zone-type laminae of hematite (or possible liesegang structures) in dolomitic siltstone of Unit *GW6* 32
29. Soft-sediment deformation in a calcareous mudstone, Unit *GW6* 32
30. Syndiagenetic pyrrhotite layers in micritic dolomite, Unit *GW6* 32
31. Pyrrhotite intergrown with chlorite in dolomite of Unit *GW6* 33

Page

32. Pyrrhotite–quartz–carbonate vein in fine-grained siltstone of Unit *GW6* 33
33. Vein in micaceous fine-grained siltstone of Unit *GW6* 34
34. Quartz with abundant inclusions of carbonate in dolomitic siltstone of Unit *GW6* 34
35. Ferruginous micritic carbonate pellets in a sparitic carbonate in dolomitic siltstone of Unit *GW6* 35
36. Large pellet enriched in biotite–chlorite–pyrite–galena, in quartz–mica rock in Unit *GW6* 35
37. 'Tee-pee' structures in dolomitic cryptalgal laminites, Unit *GW6* 36
38. Authigenic potash feldspar in microsparite, in fine-grained calcareous rock of Unit *GW6* 37
39. Carbonate- and barite-cemented conglomerate, basal conglomerate of Unit *WC1* 38
40. Basal conglomerate in Unit *WC1* 38
41. Moulds of weathered shale clasts in silicified arenite, Unit *WC2* 39
42. Complete Bouma cycle (A to E) in Unit *WC2* 40
43. Ferruginous shale clasts containing pyrite cubes, Unit *WC2* 41
44. Arkose with angular potash feldspar, Unit *WC2* 42
45. Chloritic matrix with chlorite pellet in a coarse-grained wacke, Unit *WC2* 42
46. Ferruginous carbonate grading into chlorite, interstitial to quartz 43
47. Facies distribution in the lower part of West Creek formation (Unit *WC2*) 44
48. Ferruginous and pyritiferous possible ooid in chert horizon of Unit *WC3* 45
49. Coarse-grained arenaceous channel filling within dolomitic siltstone, Unit *WC3* 46
50. Quartzitic appearance of silicified arenite in Unit *WC4* 47
51. Schematic structural cross section through the western part of the Jillawarra basin 51
52. Schematic plan view of tight minor folds 52
53. Locations of felsic volcanogenic rocks in the area of Coobarra Dome 56
54. Lapilli with coarse pumice shards in the core and fine-grained platy shards as rims 58
55. Euhedral quartz grain in siliceous matrix, volcaniclastic rocks 58
56. Plan of the Abra area showing the locations of diamond drillholes, exploration grid, and main structural features 65
57. Block diagram of the Abra area showing the Abra sub-basin 66
58. Cross section of the Abra area 67
59. Drillcore from the Stringer zone showing veins of chalcopyrite, carbonate and quartz in chloritic siltstone 68
60. Brecciation of chloritic siltstone in the Stringer zone 68
61. Partially chloritized potash feldspar, Stringer zone 69
62. Alterned authigenic seams to potash feldspar, Stringer zone 70
63. Drillcore from the Black zone showing magnetite/Fe-carbonate laminae 70
64. Core specimen from the Black zone with crenulated quartz–carbonate–magnetite layering 71
65. Core specimen from the Black zone with magnetite carbonate layering and quartz–pyrite–jaspilite, magnetite layering 71
66. Protrusion of scheelite crystal into hematite/magnetite layer in the Black zone 72
67. Diagenetic growth of barite through hematite/magnetite–pyrite layer in Black zone 72
68. Flamboyant quartz along the margins of angular quartz grains in Black zone 73
69. Relic carbonate layers and carbonate inclusions in quartz in Black zone 73
70. Acicular carbonate crystals along the margins of a micrite nodule in Black zone 74
71. Pyrite layer adjacent to hematite/magnetite layer in Black zone 76
72. Layer of acicular crystals composed of barite and quartz in magnetite–carbonate–quartz laminae of the Black zone 76
73. Drillcore from the Red zone with layers of hematite, jaspilite, quartz, carbonate and magnetite 76
74. Drillcore from laminated Red zone, with layered hematite/magnetite–carbonate vein 77
75. Core specimen from the Red zone showing layers of quartz, barite, pyrite and jaspilite 77
76. Nodule (in Red zone) in micrite at the margin of a thin section 78
77. Sabkha textures in jaspilite–chert of the Red zone 79
78. Mammillated anhydrite structures from the Valence Basin 79
79. Enterolithic structures in sabkha deposits 80
80. Top of Red zone with abundant barite crystals overlain by quartz arenite 81
81. Proterozoic chemical erosion of the top of the Red zone 81
82. A lath-shaped pseudomorph of calcite 82
83. Abra area, deposition of middle of Unit *GW6* 85
84. Abra sub-basin, deposition of upper part of Unit *GW6* 85
85. Abra sub-basin, deposition of uppermost part of Unit *GW6* 86
86. Abra sub-basin, deposition of Unit *WC1* 86
87. Abra sub-basin, deposition of Unit *WC2* 87
88. Abra area, present day 87
89. Stratigraphic position of significant mineralization in the Jillawarra basin 94
90. Black zone-type magnetite–carbonate laminae in core specimen 95
91. Laminated chloritic siltstone with layers of magnetite 95
92. Brecciated dolomicrite 96
93. Chalcopyrite–siderite vein in chloritic siltstone 96
94. Lath-shaped pyrite, in black siliceous shale, Jillawarra Formation 97
95. Atoll pyrite in black siliceous shale, Jillawarra Formation 98

Page

96. Distribution of dolerite in relation to lineaments and structural provinces in the Bangemall Basin 100
97. North–south schematic section showing ascent of hydrothermal fluids derived from red-bed arkose 101
98. Summary of the host rock sequence and the main features of the Abra mineralization 102

Tables

1. Stratigraphy of the western facies, Bangemall Basin 9
2. Stratigraphy of the Jillawarra and Abra basins in relation to the Bangemall Group 16
3. Stratigraphy of the Jillawarra basin 17
4. Chemical analyses of siliceous volcanogenic rocks in the area of Coobarra Dome 57
5. Jillawarra basin and parameters related to potential mineralization 62
6. Features of low-grade mineralization in the Jillawarra basin (excluding Abra) 92
7. Electron microprobe analyses of sphalerite 97

Foreword

This study examines the geological structure and depositional history of the Jillawarra area in the central part of the Bangemall Basin, with particular reference to the Abra sub-basin, where a large, blind, sediment-hosted Pb–Cu–Ba body was discovered in September 1981 by the Geopeko/Amoco Joint Venture. The Abra body is the first base-metal deposit of its kind discovered in Middle Proterozoic sedimentary rocks within the State. It is one of the largest deposits in Australia, but exploration drilling to date has intersected only low-grade mineralization. Nevertheless, the Jillawarra area may still be regarded as one of Australia's most prospective areas for large, blind, sediment-hosted, base-metal orebodies.

This Report covers the results of work carried out by J. H. Vogt for presentation as a doctoral thesis. The naming of some tectonic units, and their relationships, reflect the terminology of 1984. For instance, the Bullen Platform is now known as the Savory Basin.

It should also be noted that the map symbols used in the text and plates of this Report are different from the standard symbols used by the Geological Survey.

Pietro Guj
Director
Geological Survey ofWestern Australia

Chapter One

Introduction

The Jillawarra basin is an easterly trending graben, 60 km long and 9 km wide, in the central part of the Bangemall Basin in Western Australia (Plates 1 and 2). The Bangemall Basin itself is a large intracratonic sedimentary basin, containing Proterozoic rocks assigned to the Bangemall Group (Muhling and Brakel, 1985).

Significant stratabound base-metal mineralization occurs in the Jillawarra basin, within rocks that were formerly assigned to the Irregully and Kiangi Creek formations of the Bangemall Group. A large, low-grade, concealed, lead–copper–barium body, known as Abra, was discovered in September 1981 at the eastern end of the basin by the Geopeko/Amoco Joint Venture (Boddington 1987; Mutton and McInerny, 1987; Vogt and Stumpfl, 1987). Other occurrences of stratabound base metals have been located, between 1975 and 1981, by Geopeko and Amoco elsewhere within the basin.

Location and access

The Jillawarra basin lies in the central part of the Peak Hill Mineral Field, in the northwest of the State (Fig. 1), about 200 km north of the town of Meekatharra. Access is from the sealed Great Northern Highway via the graded Meekatharra–Mount Augustus–Carnarvon road. The Jillawarra area includes the cattle stations of Mulgul and Woodlands, and is named after Jillawarra Bore (latitude 24°41'00"S, longitude 118°23'52"E) on MOUNT EGERTON*. Various station and exploration-company tracks provide reasonable access to most parts of the area.

Physiography and climate

The area is moderately rugged and is dominated by prominent easterly trending strike ridges and scarps. Numerous ephemeral creeks form a dendritic drainage pattern, with a few larger creeks (in broad colluvium-filled valleys) that are part of the drainage systems of the Gascoyne and Ashburton rivers.

The climate is arid to semi-arid with an unreliable and low mean annual rainfall of 200 to 250 mm. The area experiences very hot summers, with an average January maximum between 35 and 40°C. Winters are mild, with an average July maximum of 20°C.

Previous work

The present study examines the regional geology and its controls on mineralization in the Jillawarra basin. Before the study was undertaken, it was thought that mineralization was possibly related to the deposition of Lower Proterozoic sedimentary rocks, believed to be exposed as a basement high, in the central part of the Middle Proterozoic (c.1100 Ma) Bangemall Basin. Muhling and Brakel (1985) suggested that the older mineralized rocks were equivalents of the Glengarry Group or Padbury Group of the Nabberu Basin, and they referred to the basement high as the 'Mulgul Inlier' (here called the Jillawarra basin). However, there were uncertainties about stratigraphic relationships between dolomitic sequences and arenaceous sequences in the proposed 'inlier' and similar lithologies (assigned to the Irregully and Kiangi Creek Formations) of the surrounding Bangemall Group.

Aims of the present study

The study represents a co-research project between the Mining University of Leoben (Austria), the mineral-exploration companies of Geopeko and Amoco Australia, and the Geological Survey of Western Australia. The main aims of the study were

(a) to determine the stratigraphy and structure of the Jillawarra basin, and to produce detailed geological maps of the area;

(b) to examine the stratigraphic relationship between the sedimentary units of the Jillawarra basin and those of the Bangemall Basin;

(c) to identify the stratigraphic and structural setting of mineralization within the Jillawarra basin, with particular emphasis on the Abra sub-basin;

(d) to carry out mineralogical and geochemical investigations of base-metal mineralization in the Jillawarra basin;

* Capitalized names refer to standard map sheets

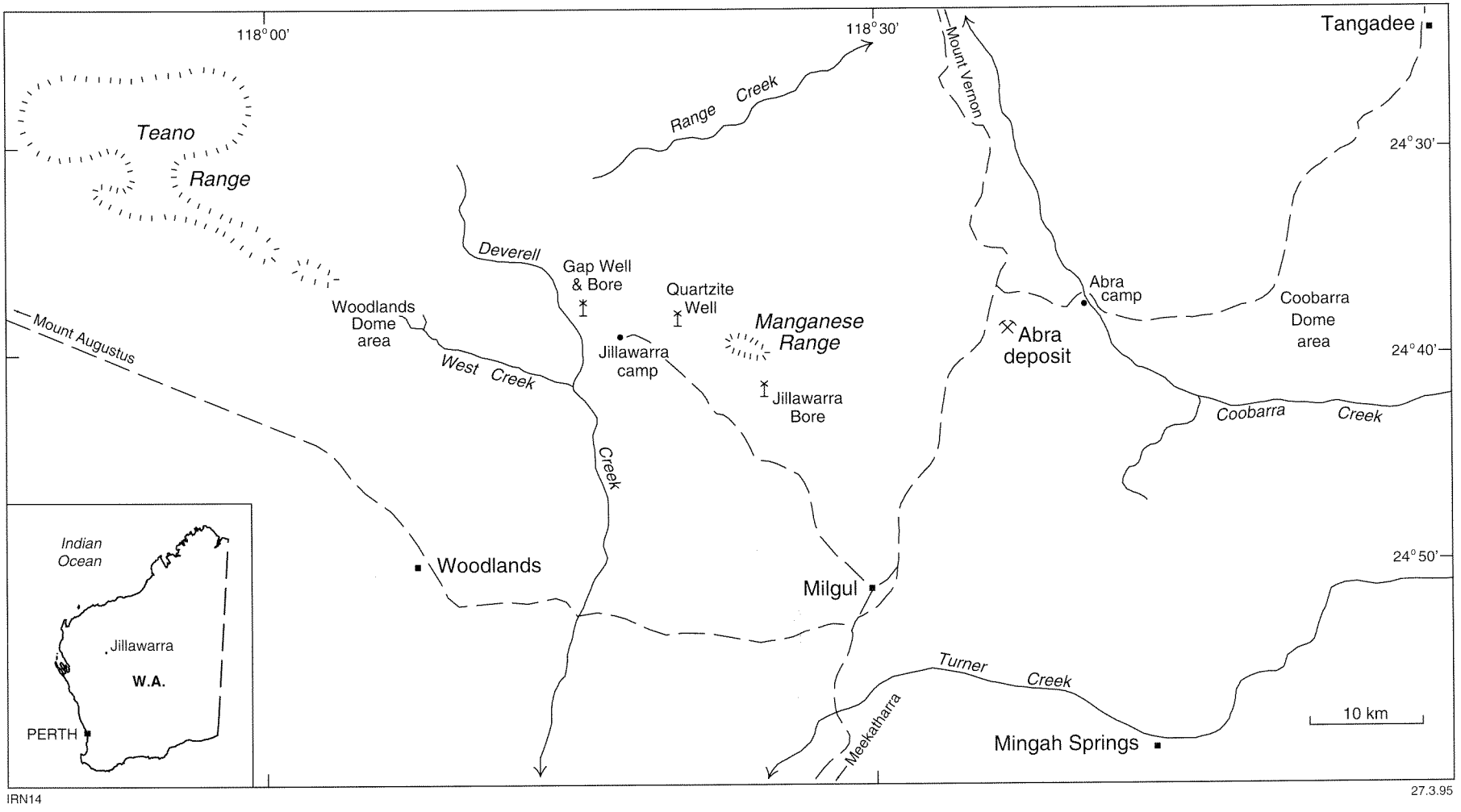

Figure 1. Locality map of the Jillawarra area

(e) to investigate possible ore-forming processes and their relationship to the tectonic evolution of the area;

(f) to develop a genetic model for Abra mineralization that could assist the search for further mineralization of this type in Proterozoic sedimentary rocks.

This report describes those results obtained from the study that pertain to the regional geology of the area, covered by aims (a), (b), and (c). Other results from the study, covered by aims (d), (e), and (f), relate to the economic geology of the area, and these have been presented elsewhere (Vogt, 1984; Vogt and Stumpfl, 1987; Vogt and Kollenberg, 1987).

Chapter Two

Geology of the Bangemall Basin

The Bangemall Basin is a Middle Proterozoic (c. 1100 Ma) intracratonic sedimentary basin, which occupies an area of about 145 000 km² (Muhling and Brakel, 1985). It unconformably overlies older Precambrian sedimentary basins and metamorphic complexes of the Capricorn Orogen in Western Australia (Fig. 2).

Evidence of age

The age of the Bangemall Group is derived from isotopic data obtained from only a few sites. A poor Rb–Sr isochron of about 1080 Ma was obtained by Compston and Arriens (1968) from felsic rocks at Mount Palgrave (in the western part of the Bangemall Basin), believed to be a dyke and a related flow. Compston and Arriens also obtained the same age from black shale in the Curran Formation, which lies about 600 m above the sub-Bangemall unconformity.

Gee et al. (1976) reported a Rb–Sr isochron of 1098 ± 42 Ma from 'rhyolite' within arenites in the Coobarra Formation, 60 m above a basal unconformity, over granitic rocks of the Coobarra Dome at the eastern end of the Jillawarra basin. It should be noted that the rhyolite has an unusually high K_2O content (Muhling and Brakel, 1985), indicating alteration after eruption, so that the ratios date either early devitrification of the volcanic glass or early metamorphism. Although the reliability of the few isotopic ages may be questioned, each one is independent of the others, and when taken together the ages are consistent at around 1.1 Ga.

Apart from isotopic data, Walter (1972) suggested that stromatolites occurring in the Irregully Formation are consistent with an age range of 1350 ± 50 Ma to 950 ± 50 Ma (middle to late Proterozoic).

Structure and tectonics

Tectonic controls

The Bangemall Basin was formed (about 1.1 Ga) as the last phase of activity in the Capricorn Orogen, which separates the Yilgarn and Pilbara cratons. The basin formed initially over two basement components, namely the Gascoyne Complex and the Ashburton Basin, and then extended to the east. The Gascoyne Complex was formerly (2000–1600 Ma) the locus of sedimentation, deformation, igneous plutons and metamorphic activity, during which the Wyloo Group was subjected to medium- to high-grade metamorphism. By contrast, in the Ashburton Basin (formerly a major sedimentary trough), the Wyloo Group was folded but subjected to only low-grade metamorphism. The differences in tectonic style and activity between these two basement components have influenced subsequent sedimentation and deformation events in the cover rocks. These have resulted in contrasting sedimentary and structural styles which characterize the three main structural zones of the Bangemall Basin: the Pingandy Shelf, the Edmund Fold Belt and the Bullen Platform (Fig. 3).

Deformation and faulting

A detailed description and interpretation of the structure of the Bangemall Basin is given by Muhling and Brakel (1985), so only a summary of tectonic style is presented here. The three structural zones not only controlled the regional facies distribution, but they also governed the intensity of deformation and tectonic style. Tectonic activity, which influenced sedimentation in each zone, increased during deformation of the basin.

The Pingandy Shelf overlies a tectonically stable basement, and was not involved in the deformation which affected the Edmund Fold Belt (which overlies the Gascoyne Complex). The sedimentary rocks of the shelf dip gently to the south and west of the Ashburton Basin.

A stable marine shelf, forming the eastern part of the basin, became the Bullen Platform. Here, broad open folds (many of which were domes and basins) formed by the draping of sediments over basement blocks controlled by movement along northeast-trending and northwest-trending faults. The northeasterly trend usually is dominant.

A horst-and-graben terrain developed over an active basement of Gascoyne Complex, and rocks deposited on this terrain were folded into the Edmund Fold Belt. North of the Flint Hill Lineament, southeasterly trending shear zones were dominant in the basement and these interacted with a more widely spaced, subordinate, northeasterly trending set. East of the lineament, northeasterly and easterly trending shear zones controlled deformation. In the Edmund Fold Belt, the horst and graben blocks

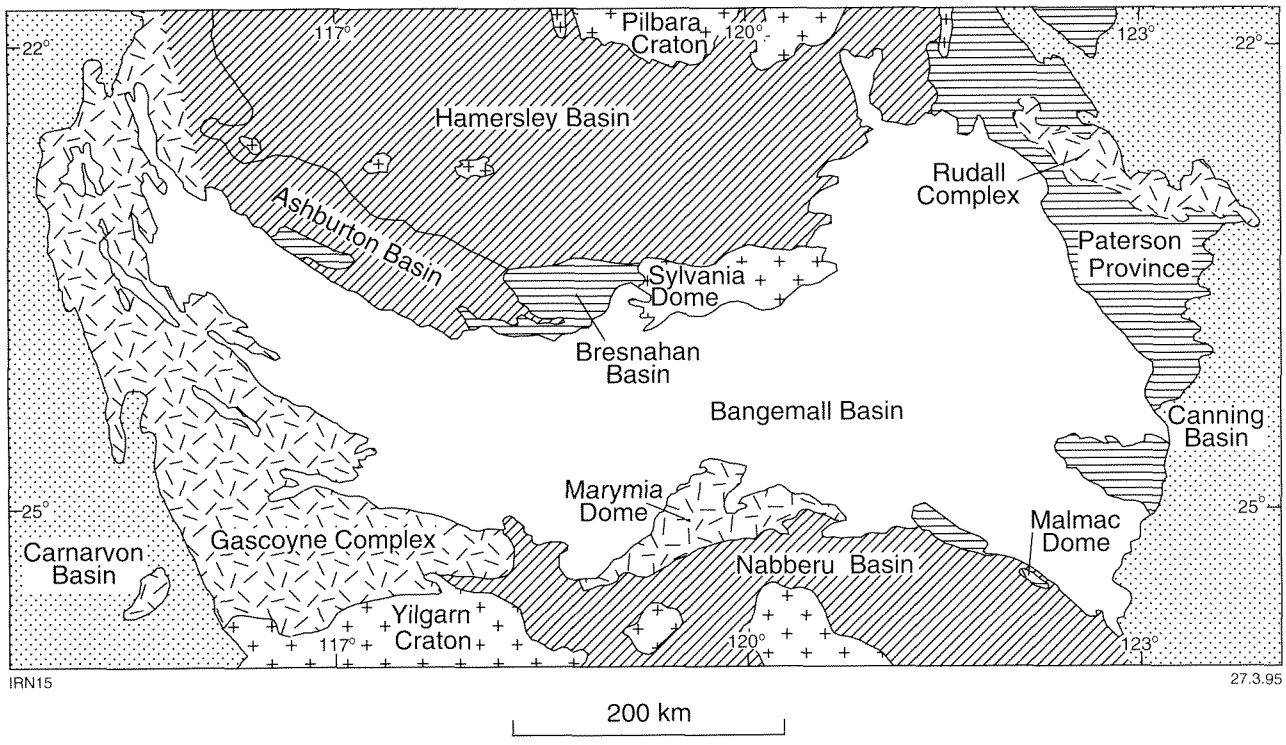

Figure 2. Tectonic setting of the Bangemall Basin, from Muhling and Brakel (1985)

continued to move along normal faults. This caused the overlying sediments to stretch and to form drape folds; block faulting may have occurred in both tensional and compressional tectonic regimes (Chapter Four).

Crustal shortening in the basement was possibly caused by the Gascoyne Complex and Pilbara Craton moving towards each other, to produce north-northeasterly directed forces. This relative movement produced lateral shortening in the cover and caused some fold structures to tighten. It is notable that most regional tight folds occur in a graben setting (e.g. Jillawarra basin).

Strain was concentrated in ductile zones of metasediments in the basement and along faults that formed boundaries between basement blocks. The metasediments behaved incompetently in comparison with the intervening competent blocks of crystalline rocks, and so become folded together with the cover. Although crystalline rocks were not affected by shortening to the same extent, there is a mechanism (discussed in Chapter Four) whereby significant shortening in the cover can also occur over crystalline basement (granite). Total shortening across the western part of the Bangemall Basin is estimated to have been in the order of 10 km.

Conclusion

The tectonic history of the Bangemall Group was controlled by tectonism in the basement rocks. The deformational features observed are compatible with a tectonic regime that was initially tensional and subsequently became compressional.

Stratigraphy

Facies provinces

Three major facies, each with distinctive lithostratigraphic assemblages, have been recognized in the Bangemall Basin: the western, northern, and eastern facies (Brakel and Muhling, 1976). The southeastern part of the basin could constitute a fourth facies. The distribution of the facies corresponds to the structural zones shown in Figure 3.

The change between the western and eastern facies in the easternmost part of the Jillawarra basin (central Bangemall Basin) is shown diagrammatically in Figure 4. In the present study the Kiangi Creek and Coobarra Formations have been combined into the West Creek

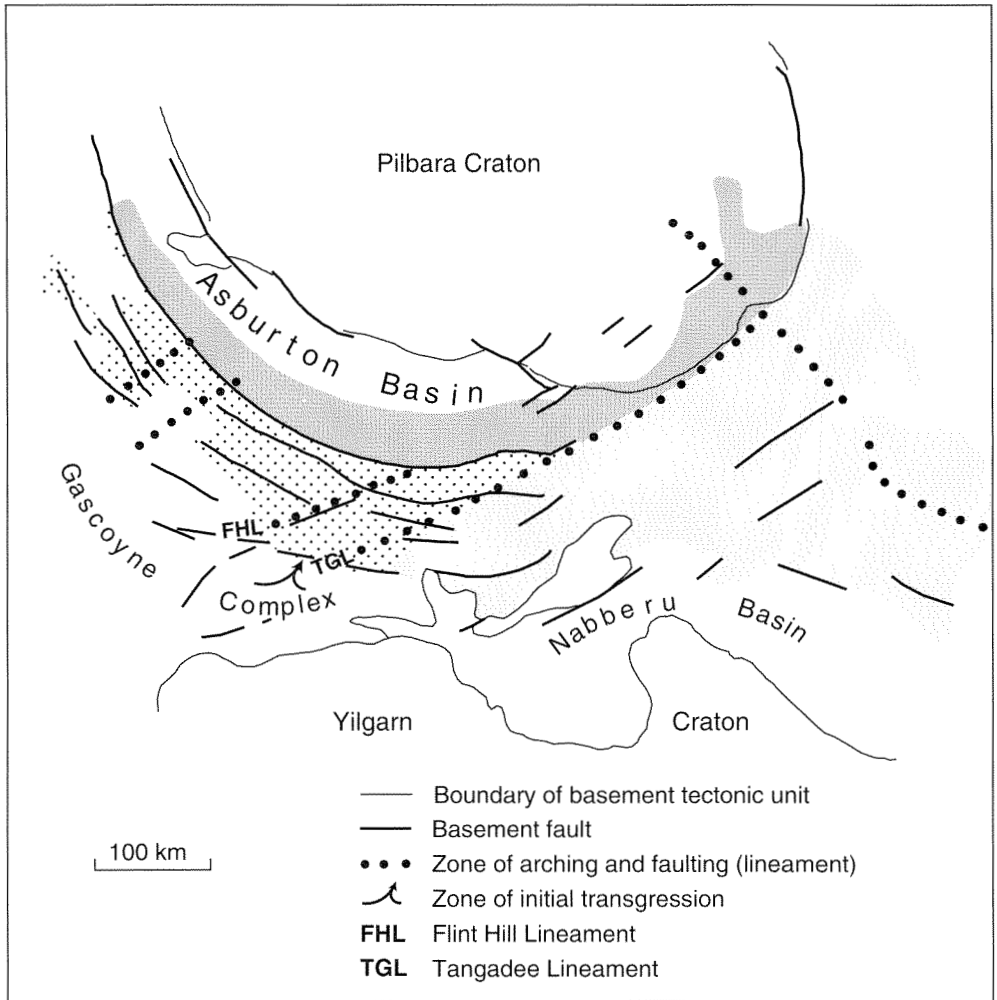

BASEMENT TECTONIC STYLE	FACIES PROVINCE	SEDIMENTARY UNIT STYLE	COVER PROVINCE
Shelf	Northern Facies (Brakel and Muhling, 1976)	Continuous, simple units : carbonate, shale, sandstone	Pingandy shelf
Horst and graben	Western Facies (Brakel and Muhling, 1976)	Discontinuous, complex, interfingering units : shale, sandstone, carbonate, conglomerate	Edmund fold belt
Platform	Eastern Facies (Williams et al., 1976)	Continuous, simple units : sandstone, minor shale Locally complex units only in Kahrban subgroup : shale, sandstone	Bullen platform

IRN16 27.3.95

Figure 3. Structural provinces of the Bangemall Basin in relation to facies provinces and lineaments; modified from Muhling and Brakel (1985)

formation; the Coobarra lithology is regarded as a local facies variety of the latter.

Recent GSWA mapping of BALFOUR DOWNS, in the northeastern part of the Bangemall Basin has revealed some inconsistency in the stratigraphic relation between the eastern and western facies (Williams, I. R., 1982, pers. comm.). It now appears possible that the whole of what Brakel and Muhling (1976) considered as the eastern facies is significantly younger*. The

* *Editor's note*: see Williams, I. R., 1992, Geology of the Savory Basin, Western Australia: Western Australia Geological Survey, Bulletin 141.

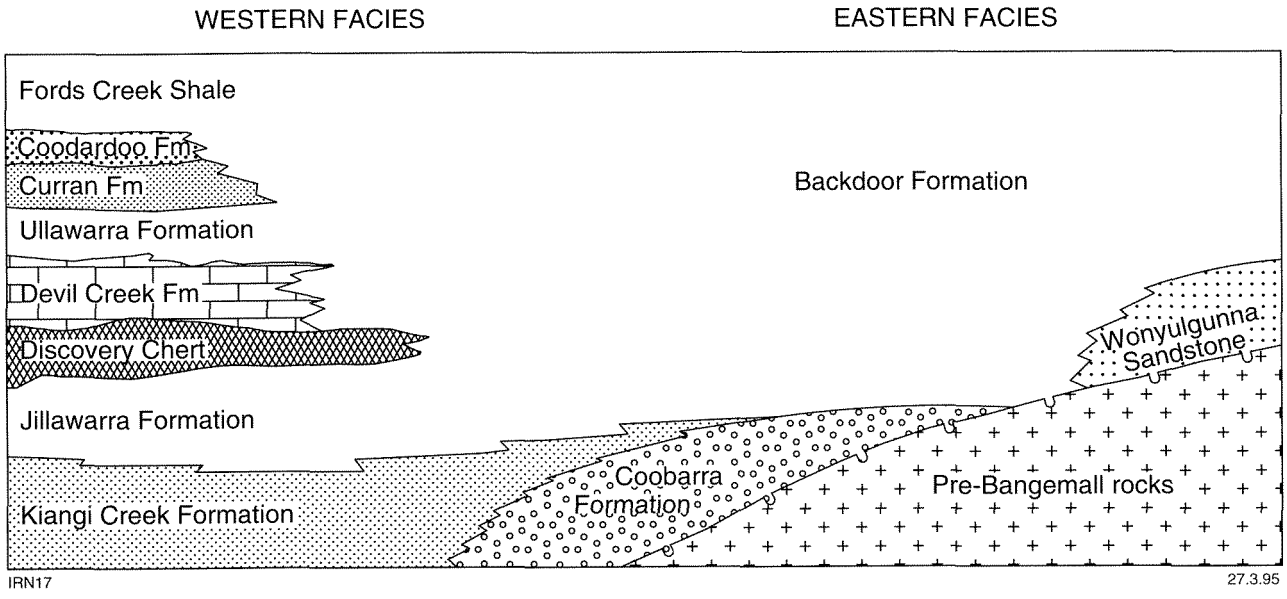

Figure 4. Facies change between western and eastern facies in the Bangemall Basin (Muhling and Brakel, 1976)

existence of a major unconformity between the eastern facies and western facies has thus to be re-examined.

The Jillawarra basin is an easterly trending elongated belt in the central Bangemall Basin, occurring within the western facies province. It is appropriate, therefore, to describe the western facies further. The description that follows is based mainly on Brakel and Muhling (1976), Muhling et al. (1978), Brakel et al. (1982), and Muhling and Brakel (1985).

Stratigraphy of the western facies

The chief lithologies are shale, siltstone, sandstone, dolomite, chert, and conglomerate. The stratigraphic sequence according to Muhling et al. (1978) is shown in Table 1.

All units are marine except the Tringadee Formation, which is a continental fan-delta sequence. The sequence from the Jillawarra Formation upwards shows a simple, laterally persistent stratigraphy. In the lower half of this sequence, lensing and interfingering of units are common. An exception is the Discovery Chert, which is a uniform and continuous unit providing an excellent marker horizon in the western facies of the Bangemall Group. Facies changes in the lower half of the sequence are thought to be the result of an interplay between the lateral migration of contrasting adjacent environments, and varying clastic input (Brakel and Muhling, 1976). A comprehensive description of the stratigraphy of the Bangemall Basin is given by Muhling and Brakel (1985).

Development of the western facies

Sedimentation began in the western part of the basin which overlies the core of the Capricorn Orogen (Gee, 1979) — the Gascoyne Complex. Subsidence of the basement created horsts and grabens along steeply dipping faults.

Alluvial-fan deposits, on the flanks of horst blocks, are overlain by a transgressive marine sequence, which consists of stromatolitic dolomite, sandstone, and pyritic (black) shale. This marine sequence was deposited in lagoon, barrier-bar and shelf (euxinic at times) environments. The basement granitic and metamorphic rocks were the source of the terrigenous clastic sediments.

The transgressive sequence ended with the deposition of the Discovery Chert, which covers an area of 38 000 km² and shows no major facies variations. The presence of gypsum crystal moulds and traces of barite suggest that the chert was deposited in hypersaline water.

A shallow-marine platform sequence overlies the Discovery Chert and represents shoals of carbonate interfingering with terrigenous shale and sandstone. Local debris flows indicate seismic activity. An ensuing phase of widespread subsidence is marked by turbidite sheets which are overlain by marine-shelf shale.

The end of sedimentation in the basin is characterized by a regressional development from the Fords Creek Shale upwards. This is seen as a progradational sequence which could portray the last stage of the infilling of the basin before the end of marine deposition.

Igneous rocks in the Bangemall Basin

The igneous rocks in the Bangemall Basin consist of basic intrusive and felsic volcanogenic rocks. The intrusives represent enormous volumes of basaltic magma, injected chiefly as dolerite sills, but also as dykes.

Table 1. Stratigraphy of the western facies, Bangemall Basin

Age	Group	Map symbol	Formation	Lithology	Thickness (m)	Remarks
MIDDLE PROTEROZOIC	BANGEMALL	*Emq*	Kurabuka Formation	Shale, siltstone, minor dolomite	1 500	
		Emn	Mount Vernon Sandstone	Sandstone	240	
		Ems	Fords Creek Shale	Shale, minor sandstone and siltstone	1 300 – 1 900	
		Emsj	Jeeaila Sandstone Member	Sandstone, with subordinate shale	60 – 80	
		Emc	Coodardoo Formation	Sandstone, minor siltstone and shale	0 – 60	
		Emu	Curran Formation	Shale	250	
		Eml	Ullawarra Formation	Shale, siltstone and minor dolomite	650	Extensively intruded by dolerite
		Emv	Devil Creek Formation	Dolomite and shale	0 – 800 (+)	
		Emd	Discovery Chert	Chert, subordinate shale	50 – 125	Laminated rocks, wavy bedding common
		Emj	Jillawarra Formation	Shale, siltstone, minor chert and dolomite	0 – 1 300	
		Ekm	Kiangi Creek Formation	Sandstone, shale, subordinate dolomite and minor conglomerate conglomerate	0 – 1 800	Stromatolites in one dolomite member
		Emkg	Glen Ross Shale Member	Shale	125 – 525 (+)	
		Emi	Irregully Formation	Dolomite, dolomitic shale, shale and minor sandstone	0 – 2 000	Stromatolites present
		Eme	Tringadee Formation	Sandstone with conglomerate lenses	0 – 1 650	Lenticular basal formation of Bangemall Group

SOURCE: Muhling et al. (1978)

Felsic rocks and basalt occur rarely. The following description is mainly based on Muhling and Brakel (1985).

Mafic rocks

Dolerite sills

Sills may exceed 100 m in thickness, and may be simple tabular bodies or irregular bodies that vary in thickness quite markedly. The most extensive single sheet has a strike length of more than 60 km. Sheets are generally concordant with the bedding of the country rock, but may locally cut across the bedding in zones that range from less than a metre to hundreds of metres in thickness.

Sills are absent from the Tringadee and Coodardoo Formation, and the Mount Augustus Sandstone. In the Irregully Formation they are present only on EDMUND (in the northwestern part of the basin) and they are rare in the Kiangi Creek Formation.

There are apparently two controls on the stratigraphic position of dolerite intrusion:

(a) The nature of the host lithology (e.g. more fissile rocks) may allow magma injection at a specific stratigraphic level.

(b) The absence of dolerite sills in the three lower formations (Tringadee, Irregully, and Kiangi Creek Formations) implies that a tensional crustal tectonic regime had yet to develop before the injection of dolerite could occur.

It is evident that dolerite sills were intruded before rocks of the Bangemall Group were folded, because the sills themselves are folded; also in some fold cores dolerite is altered to chlorite schist.

Geochemistry

There is only a small chemical variation shown by the 13 dolerite samples, collected from the Bangemall Basin by Muhling and Brakel (appendix F; 1985). This is consistent with the uniform appearance of the rocks and the lack of evidence for differentiation. The rocks are tholeiitic, as shown by comparison with chemical compositions and CIPW norms of typical tholeiitic and alkaline basalts elsewhere in the world (Carmichael et al., 1974).

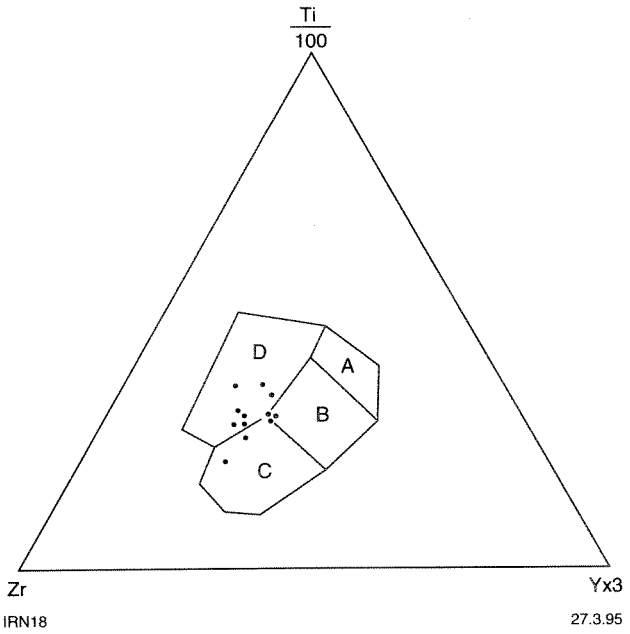

Figure 5. Discrimination diagram of basaltic magma types, using Ti, Zr and Y. Fields for the tectonic setting of basalts are from Pearce and Cann (1973):

D — 'Within plate' basalts, i.e. ocean-island or continental basalts;
B — ocean-floor basalts;
C and D — calc-alkali basalts;
A and B — low potassium tholeiites

A discrimination diagram (Fig. 5), using Ti, Zr and Y, shows that the Bangemall dolerites plot in or near the field of 'within plate' basalts (field D, representing modern oceanic-island and continental occurrences) rather than in the field of 'plate margin' basalts (fields A, B and C, representing volcanic arc and ocean-floor occurrences) (Pearce and Cann, 1973).

Implications of mafic magmatism

It is inferred that passive intrusion took place at shallow depth, where dense, mafic magma flowed gravitationally below less dense sedimentary rocks. The presence of a major tholeiite province, where mantle-derived magma was passively emplaced at shallow depths in a subsiding, infilling basin, implies the existence of a tensional regime in the crust during sedimentation.

The distribution of sills (Fig. 6) shows that the greatest concentrations occur in the western part of the basin and along the southern and northwestern margins of the wider eastern part of the basin. This pattern implies that there was 'an embryonic rift valley which bifurcates into two smaller arms east of a triple junction at the 120° E meridian' (Muhling and Brakel, 1985).

Felsic volcanic rocks

Only two definite occurrences of rhyolite and two probable tuffs were found during regional mapping by the GSWA. Muhling and Brakel (1985) concluded that felsic volcanic

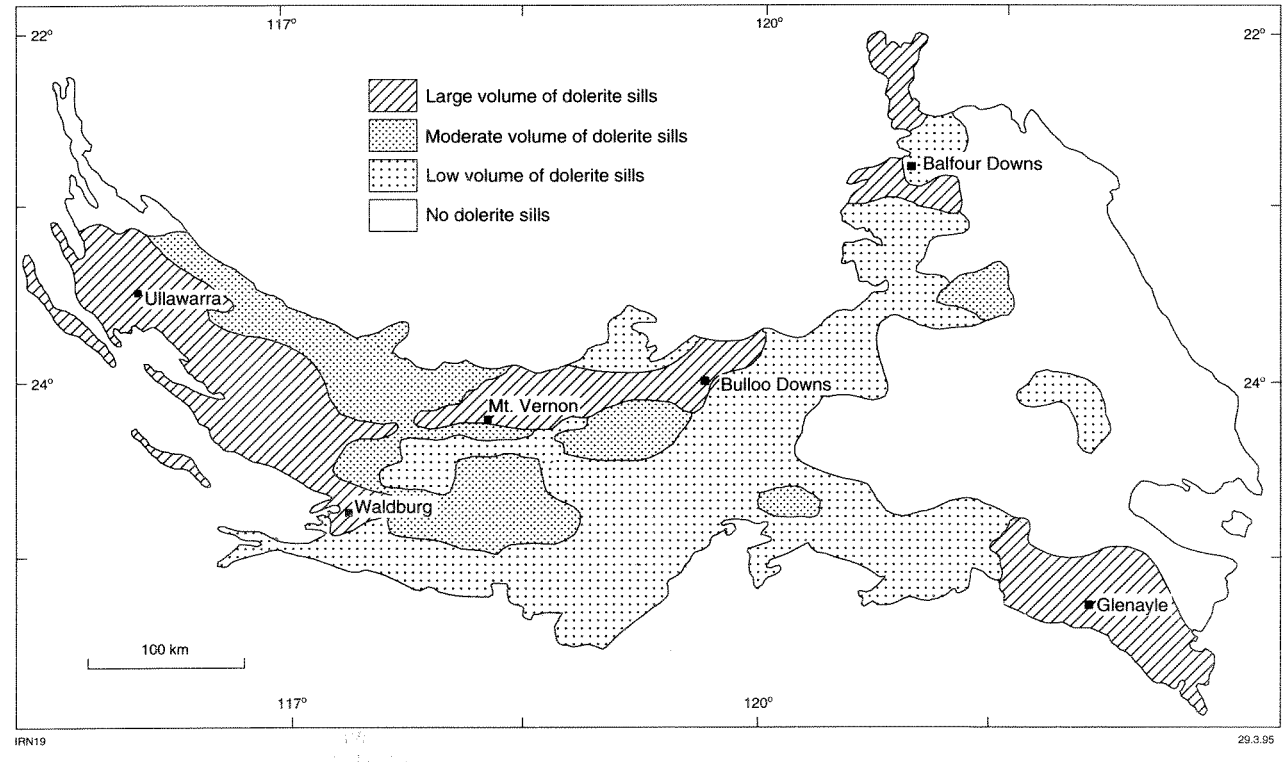

Figure 6. Abundance and distribution of dolerite sills in the Bangemall Basin (Muhling and Brakel, 1985)

activity played a very minor role in the evolution of the Bangemall Basin.

Rhyolite and felsic lavas

The most significant rhyolite occurrence is in the eastern part of the Jillawarra area within the lowermost West Creek formation (formerly called Coobarra Formation). The rhyolite has been studied and dated (1098 ± 42 Ma) by Gee et al. (1976) and is described in Chapter Five.

An occurrence of felsic lava was examined by Compston and Arriens (1968) and a sample yielded an approximate isotopic age of 1080 Ma. The location and petrology of the rock is not documented, but it is believed to form a dyke and related flow in the Jillawarra Formation near Mount Palgrave, in the westernmost part of the Bangemall Basin.

About 11 km southeast of Abra (24° 43' 43"S, 118° 39' 05"E) another felsic rock has been found occurring within ferruginous shale of the Backdoor Formation (eastern facies). The felsic rock is greyish, massive and siliceous, containing angular clasts of altered ferruginous shale; the rock is without any laminations or bedding. The area of outcrop is about 80 x 80 m and rapid pinching out in all directions can be observed. In thin section, the rock consists of a very fine-grained quartz–chlorite groundmass enclosing local angular and/or embayed quartz grains. The shale clasts consist almost entirely of chlorite and other very fine-grained phyllosilicates. The felsic rock has been interpreted as a waterlain tuff by Geopeko petrologists. However, field relationships suggest that it is plug-shaped and cuts across the stratigraphy. It continues along strike for less than 80 m, and contains angular clasts of country rock. The totality of evidence therefore suggests a felsic volcanic vent.

Possible felsic volcanic rocks (tuffs)

Fine-grained highly potassic rocks were found at two localities: one in the Backdoor Formation 12 km northwest of Tangadee (in the eastern facies), and the other in the Ullawarra Formation, about 7 km southeast of Jillawarra Bore.

Summary

The basic igneous rocks of the Bangemall Basin represent large volumes of mantle-derived continental tholeiite. The very few occurrences of felsic rocks probably represent localized crustal melting (Gee et al., 1976).

Chapter Three

Stratigraphy and sedimentology of the Jillawarra basin

Earlier investigations

The Jillawarra basin was mapped by the GSWA during the 1:250 000 regional mapping program of 1973–75. The western half of the basin was mapped first on MOUNT EGERTON (Muhling et al., 1978), where the rocks in the basin were assigned to the Irregully and Kiangi Creek Formations. The eastern half of the basin was mapped later on COLLIER (Brakel et al., 1982), where the rocks were assigned to the Padbury and Glengarry Groups of the western part of the Nabberu Basin.

In their synthesis of regional stratigraphy in the Bangemall Basin, Muhling and Brakel (1985) refer to the Jillawarra basin* as the 'Mulgul Inlier' and imply that the rocks within the inlier are equivalent to units in the western Nabberu Basin.

There are a number of features of the Jillawarra basin which distinguish it from the Bangemall Basin:

(a) An apparent higher metamorphic grade, indicated by some chlorite–biotite–quartz–magnetite schists of the Manganese Range area, and the widespread chloritization of sedimentary rocks within the Jillawarra basin.

(b) The variability of lithologies in chloritic carbonate rocks in the Jillawarra basin compared with the carbonate sequences (dolomitic siltstones and dolomites) of the Irregully Formation in the Bangemall Basin.

(c) The occurrence of tight anticlines and open synclines, both with subsidiary folding on the limbs, while in the Bangemall Basin usually the synclines are tight.

(d) The apparent lack of dolerite sills in the Jillawarra basin; these are so abundant elsewhere in the Bangemall Basin.

Four Pb model ages, obtained from vein galena in drillcore by J. R. Richards after 1981, put further constraints on the age of the Jillawarra basin. For the base-metal mineralization at the Quartzite Well prospect (in the central part of the basin) the TP prospect and the 46–40 prospect in the west of the basin (Plate 2) the calculated Pb model age is in the order of 1.58 to 1.59 Ga. (Richards, 1983). Galena samples from the Abra mineralization show an apparent age of 1.59 to 1.64 Ga. (Richards, J. R., 1986, pers. comm.).

In the following chapters, results are presented which attribute rocks in the Jillawarra basin to the Bangemall Group, so that a stratigraphic and tectonic framework may be established for the genesis of the Abra Cu–Pb–Ba type of mineralization (Fig. 7; Plate 1).

* *Editors note*: Bulletin 128 (Muhling and Brakel, 1985) was published after J. Vogt had completed the manuscript for this report in which he had already proposed the term 'Jillawarra basin' for this central part of the Bangemall Basin.

Basement rocks

Basement rocks occur at the eastern and western ends of the Jillawarra basin, in areas known as the Coobarra Dome (east) and the Woodlands Dome (west). In both areas the rocks are deeply weathered, and while basement occurrences are quite widespread in the Coobarra Dome, the outcrop area of basement rocks is very limited in the Woodlands Dome (Plate 1; Fig. 7).

Coobarra Dome

Granitoid basement rocks, unconformably overlain by Coobarra Formation of the Bangemall Group, occupy a large area of the Coobarra Dome. The predominant granitoid at outcrop is a biotite–muscovite adamellite, which has been deeply weathered. At outcrops the granitoid is a loosely aggregated, gritty material, and no thin sections could be prepared from specimens that were collected during the study. Weathering has ensured that the only main minerals recognized are muscovite and quartz, in a typical granitic texture; foliation is poorly developed. Locally, some quartz–tourmaline veins and pegmatitic phases are present and sporadic veins of colourless fluorite have been noted (Brakel et al., 1982).

Woodlands Dome

The area of outcrop is very small, on the southern slopes of Woodlands Hill. Deeply weathered foliated gneiss (or schist) is intruded by a few pegmatite veins (up to 0.5 m thick) in a narrow creek exposure. The foliated gneiss (or

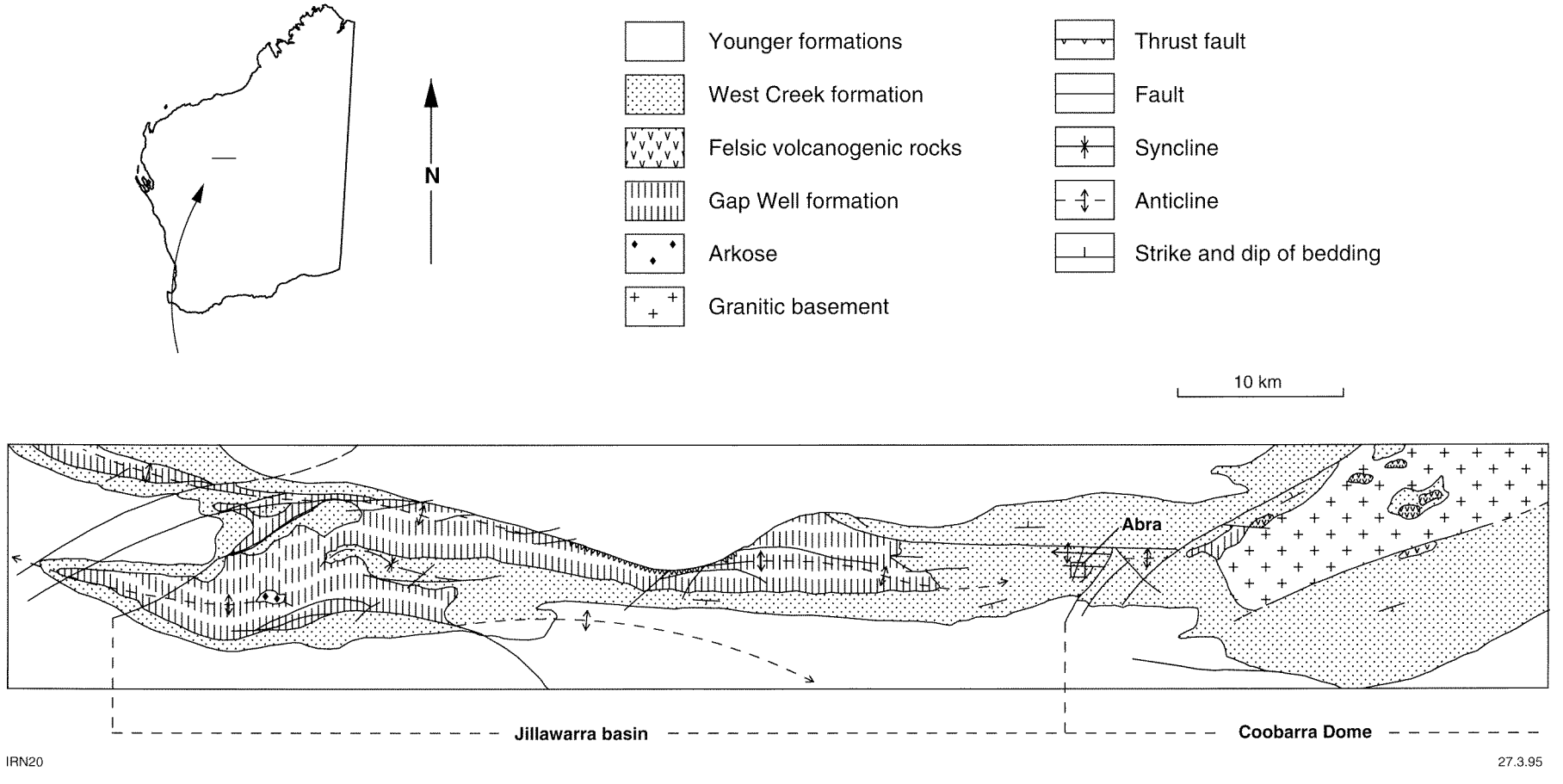

Figure 7. **Simplified geological map of the Jillawarra area, which includes the Jillawarra basin and the basement area of Coobarra Dome. The Abra prospect is located at the eastern margin of the Jillawarra basin. Abra occurs in a special facies, in the upper part of the Gap Well formation, which is not exposed in the area of the Abra prospect. Note the small outcrop of arkose on basement in the western part of the basin**

schist) is overlain by deeply weathered arkose, which shows irregular banding. This is expressed by the arrangement of quartz and muscovite, and the banding may be interpreted either as incipient schistosity or as relic bedding. No feldspars are preserved but the texture resembles sericitized feldspars which have largely been silicified (Fig. 8). In the Coobarra Dome area, rock chips from a percussion drillhole at Coobarra Hill, some 5 km west of the weathered granite outcrops, show textures very similar to the arkose described at Woodlands Dome. The preservation of subangular microcline in this case supports the interpretation of rocks in both areas as arkose. From the evidence that potash feldspar does not appear significantly altered and that muscovite is the only newly formed mineral, a low metamorphic grade is inferred.

It is inferred that the depositional setting at the eastern end of the Jillawarra basin (i.e. a granitic basement high adjacent to a subsiding depository, in the area of the Jillawarra basin) closely resembles the depositional setting of the coarse clastic Tringadee Formation (up to 1650 m thick) of the basal Bangemall Group, elsewhere (Brakel and Muhling, 1976). It is proposed that in the eastern part of the Jillawarra basin a thick, subaerial talus-slope breccia and fluvial arkose unit underlies the Abra deposit. This unit would presumably have been derived from the Coobarra Dome to the east and may have reached 2000 m in thickness.

The lower Bangemall Group in the Jillawarra basin

In view of the distinctive nature of the rocks examined at outcrop and in drillholes in the Jillawarra basin, and their apparent peculiarity, two new stratigraphic names are informally proposed for rocks in the lower Bangemall Group. The lowermost formation exposed in the basin (except the arkose; Fig. 7) is termed the Gap Well formation, and the formation overlying this is termed the West Creek formation. The latter is overlain, in turn, by the Jillawarra Formation and the Discovery Chert. Table 2 shows the stratigraphy of units in the Jillawarra basin and their proposed correlation with sequences in the Bangemall Group.

Mapping of the Gap Well formation, which contains mineralization at Abra and other prospects in the basin, showed that the formation could be subdivided into six units (Table 3). The total thickness of the formation may exceed 1000 m. The overlying West Creek formation, which lacks significant mineralization, consists of four units and its thickness is in the order of 1200 m. In the Jillawarra Formation, within the Jillawarra basin, a lower dolomitic and/or arenaceous unit can be distinguished from a shaly upper unit.

It should be noted that the proposed subdivisions have been established on the basis of the field appearance of lithologies. In fresh drillcore the respective lithological boundaries are sometimes difficult to recognize. In this chapter the stratigraphic units of the Jillawarra basin are described in terms of their distribution in the field (and in drillcores) and their petrographic characteristics. For each unit the possible depositional environment is also discussed.

The classification of the clastic rocks was made with reference to Pettijohn (1975), while that of the carbonate rocks was made with reference to Dunham (1962).

Gap Well formation (*GW*)

This formation may exceed 1000 m in thickness and comprises six subdivisions, sequentially referred to as *GW1* to *GW6*. The lower divisions *GW1* to *GW4* are

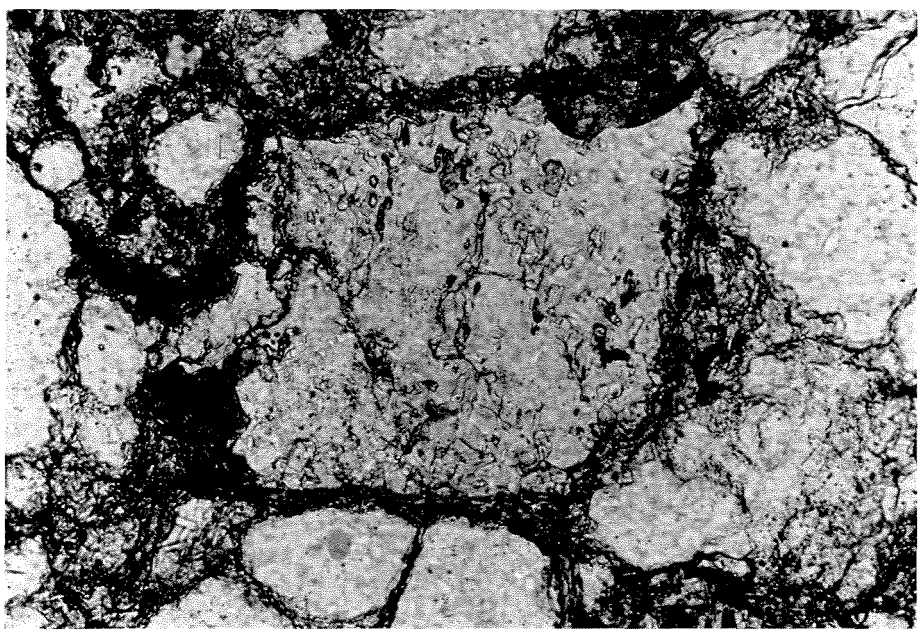

Figure 8. Angular quartz–sericite aggregate resembling sericitized feldspar; in medium- to coarse-grained quartz sandstone. Arkose from the area of Woodlands Dome. Base of picture is 0.9 mm (plane-polarized light)

Table 2. Stratigraphy of the Jillawarra basin and Abra sub-basin in relation to the Bangemall Group

Bangemall Basin (western facies)	*Jillawarra basin*	*Abra sub-basin*
BANGEMALL GROUP		
Upper Cumulative maximum thickness ~5400 m	Overlying units in the basin correlate with those in Bangemall Basin	Overlying units correlate with those in Jillawarra basin
Lower Discovery Chert up to 125 m		
Jillawarra Formation up to 1300 m		
Kiangi Creek Formation up to 1800 m	West Creek formation up to 1500 m	
Irregully Formation up to 2000 m	Gap Well formation up to 1200 m	Red zone 40 m (a) Black zone 40 m (a) Stringer zone ?900 m (a)
Tringadee Formation up to 1650 m	Arkose unit (thickness unknown)	Arkose unit (thickness unknown)
~ *Unconformity* ~		
BASEMENT		
Gneiss, schist and granite (?Lower Proterozoic)	Granitic rocks (?Lower Proterozoic)	Granitic rocks (?Lower Proterozoic)

Note: (a) denotes mineralized interval of Abra sub-basin

essentially arenaceous, while the upper divisions *GW5* and *GW6* are characterized by the occurrence of carbonates. The name Gap Well is derived from the Gap Well and Bore (24° 38'S, 118° 14'E) where low dolomite ridges are abundant (Plate 1).

Unit GW1

Distribution: This unit outcrops only in the western part of the Jillawarra area, in the central part of the Woodlands Dome. Here, the unit dips radially away from the small outcrop area of underlying basement rocks and arkose. Its thickness exceeds 100 m and it shows a variable lithology. Abundant quartz veins (up to 20 cm wide) form an irregular cross pattern.

The dominant lithologies of Unit *GW1* are laminated shale and siltstone which often have a silicified appearance, possibly due to surficial processes. In places the siltstone is very rich in irregularly distributed cubic moulds, which probably represent former pyrite.

Petrography: In thin section, the sericitic shale is intercalated with well-defined thin layers (50–700 μm) of poorly sorted and subangular siltstone. The siltstone layers consist of angular to subrounded quartz, muscovite, and a few tourmaline grains, whereas the shale bands are dominated by finely crystalline phyllosilicates with a brownish tint, some muscovite flakes (400 μm) parallel to bedding, and rare quartz grains. No feldspars have been observed. Some diffuse opaque aggregates (~200 μm in diameter) in the shale may be organic remains.

Arenite beds are more abundant in the basal portion of Unit *GW1*. They consist of poorly sorted, moderately rounded, medium- to coarse-grained quartz sandstone containing minor tourmaline and zircon. The matrix of very fine-grained phyllosilicates has a brownish tint.

Another lithology, correlated with the shale and siltstone, is massive, micritic dolomite with abundant magnetite throughout, and common quartz–carbonate–barite–magnetite veins. This rock is not exposed and has only been encountered in the lowermost 100 m of a deep (1200 m) diamond drillhole (TP-81-8) at the TP prospect, about 2.5 km east of Woodlands Dome.

Depositional environment: The lithologies in Unit *GW1* suggest a near-shore, perhaps deltaic environment, with carbonate deposition occurring in a more seaward position. This would suggest that open sea lay to the east of Woodlands Dome.

Unit GW2

Distribution: This unit forms prominent topographic highs of carbonate on both sides of the Woodlands Dome. It has been intersected in two diamond drillholes in the west of the Jillawarra area (TP-81-8, WD-81-8; Fig. 9). Farther east, in the Manganese Range Anticline, the oldest rocks exposed are also assigned to Unit *GW2*. At Manganese Range the unit consists of chloritic siltstone and coarse arenite containing cubic pseudomorphs of goethite and hematite (after pyrite). The estimated thickness of the unit is about 100 m.

At Woodlands Dome, the carbonate facies comprises silicified dolomite, often manganese capped at outcrops (Fig. 10). This dolomite is distinctly laminated and is locally stromatolitic. The stromatolites are extensively

Table 3. Stratigraphy of the Jillawarra basin

Unit	*Maximum thickness (m)*	*Lithology*
BANGEMALL GROUP		
West Creek formation		
WC4	190	Coarse-grained sandstone, quartz-pebble conglomerate intercalations: limited strike extent
WC3	75	Siltstone, in places dolomite or minor ferruginous, silicified dolomite, immature sandstone
WC2	500	Alternating sandstone and siltstone/shale beds with gradedbedding, intraclasts, slumps, scour-and-fill structures; turbidites and minor conglomerate; volcaniclastics and rhyolite near base in Coobarra Dome area
WC1	180	Coarse-grained immature arenite and polymict conglomerate (up to 40 m), dolomite, siltstone
Gap Well formation		
GW6	350	Laminated dolomitic siltstone/shale and biostromal dolomite, abundant microbial mats, syndiagenetic iron sulfides, gypsum casts; locally silicified and manganese enriched; host rocks for Red and Black zones of Abra mineralization
GW5	350	Dolomitic siltstone with coarse-grained sandstone intercalations and minor stromatolitic dolomite, host rocks for Stringer zone at Abra and low-grade Ba–Cu–Pb mineralization elsewhere in the Jillawarra basin
GWw4 (Woodlands Arenite Member)	250	Coarse-grained sandstone with barite veining and disseminated Ba–Cu mineralization at Woodlands prospect; limited strike extent
GW3	150	Siltstone with ripple marks; interbedded sandstone
GW2	100	Dolomite and dolomitic shale
GW1	100	Laminated dolomite/ siltstone and feldspathic sandstone
Arkose unit	?	Fluvial, first-cycle detritus from granitic source rocks
~~	~~~~~~~~~~	*Unconformity* ~~~~~~~~~~~~~~~~~~~~~~~~~~~~
BASEMENT		Biotite–muscovite adamellite and gneiss or schist (?Lower Proterozoic)

altered (at least partially) through surficial processes, making it impossible to determine species.

On both sides of Woodlands Dome the carbonate lithology forms ridges each with a strike length of about 1 km. The southern ridge is almost surrounded by coarse-grained arenites — possibly former limesands — while the clastites in the vicinity of the northern ridge are finer grained.

Petrology: The dolomite is micritic with some lenses and streaks of neomorphic sparite. Layering is defined by variable amounts of dispersed organic material. The proportion of clastic quartz grains is probably less than 5%; some of the quartz now visible in thin section seems to have been introduced by early silicification processes as suggested by small, wispy and discontinuous quartz veinlets bordered by sparitic carbonate. In some lenses of neomorphic sparite, newly grown euhedral carbonate crystals have incorporated organic material during growth (Fig. 11).

Crystal growth has been intermittent, as indicated by repeated layers of organic material which mark the trigonal edges of several growth stages. These sparitic carbonates commonly form the margin of the lenses while the centre is filled with quartz. On the scale of a thin section it becomes evident that the lenses are a disrupted thin layer (~1 mm) of a microbial mat.

If one assumes that the decay of the microbial mats mainly occurs diagenetically, it then follows that sparitization (into open space created by the organic decay) was also diagenetic. The central quartz filling could not have occurred much later, becauses voids in a soft sediment would have been destroyed by incremental compaction.

In the Manganese Range Anticline, Unit *GW2* is predominantly a clastic facies. Chloritic shale and siltstone, locally with strong schistosity obliterating the bedding, occur in the core of the anticline. The appearance of these schistose lithologies in Unit *GW2* and the overlying Unit *GW3*, at Manganese Range, initially led to the suggestion that the rocks were part of a basement inlier, and that they were equivalent to the Padbury Group of the western Nabberu Basin (Muhling et al., 1978; Brakel et al., 1982; Muhling and Brakel, 1985). The schistose chloritic lithologies of Unit *GW2* contain abundant cubic pseudomorphs of iron oxides/hydroxides, presumably after pyrite. Towards the west (towards the probable syn-sedimentary Manganese Range Fault) Unit *GW2* is marked by a prominent cross-bedded arenite ridge which is overlain and underlain by dolomitic siltstone and shale.

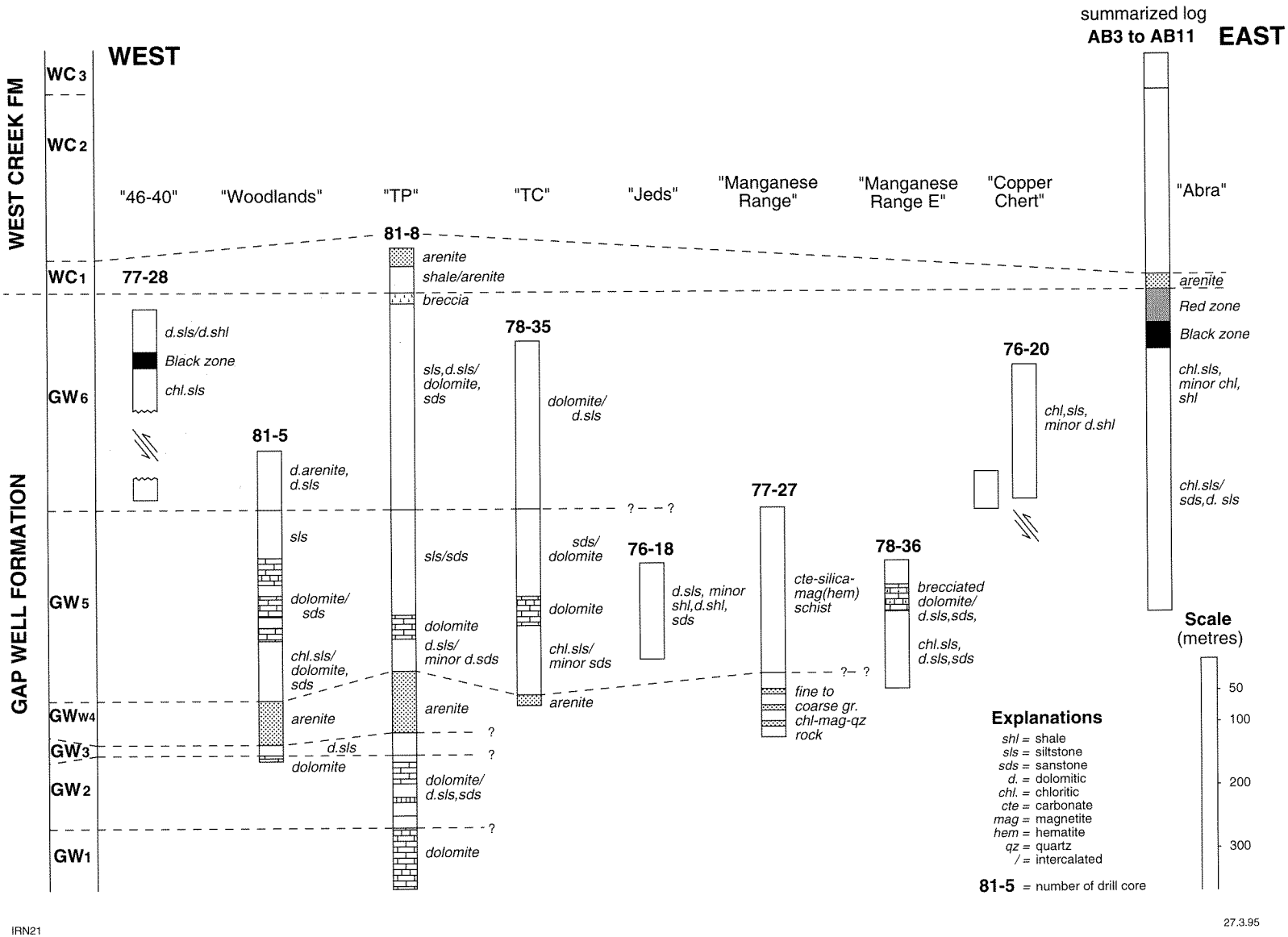

Figure 9. Diagrammatic stratigraphic correlation through the Jillawarra basin using drillholes projected onto a W–E section, over a strike distance of 51 km (not to scale). Datum is the boundary between Unit *GW6* and Unit *WC1*. Names of prospects and numbers of drillholes are shown; prospect and drillhole locations are shown on Plate 1. Core length is approximately true length. Stratigraphic subdivision is based mainly on lithology, but also with some consideration of thickness

The arenite is a quartz sandstone which is well rounded, moderately sorted, and medium to coarse grained. On fractures in the quartz grains carbonate rhombs can be found. The interstices are filled either with silica cement, or with some opaque cubes (pyrite) and some clusters of dark brown to black needle-like minerals (20 μm in length) of rutile or pseudobrookite.

Depositional environment: The presence of stromatolites in Unit *GW2* in the west indicates a shallow-water environment. The limited strike extent of the dolomite and surrounding clastics suggests that the dolomites of the Woodlands Dome represent patch reefs, which occur almost symmetrically on both sides of the dome.

The high degree of rounding of the arenite at the Manganese Range Anticline suggests a similar environment, with a barrier built of beach sand. The dolomitic siltstones and shales and the chloritic 'schists' just to the east (probably chloritized former dolomitic lutites, discussed in Chapter Eight) possibly represent a corresponding intertidal facies.

Unit GW3

Distribution: This unit is up to 150 m thick in the central part of the basin where it forms extensive outcrops in the Manganese Range Anticline. In the western part of the Jillawarra area, on the limbs of Woodlands Dome and in diamond drillholes (TP-81-8-8, WD 81-5; Fig. 9), the thickness of Unit *GW3* is more variable and is significantly less than that in the Manganese Range Anticline.

In the area of Woodlands Dome, outcrop of the unit is poor and discontinuous. The dominant lithology is a dolomitic fine-grained siltstone with some interbeds of ferruginous arenite. In drillcore, the dolomitic siltstone is interbedded with carbonate-cemented arenite, suggesting that the ferruginous arenites at the surface were originally dolomitic.

A similar lithology on the southern limb of the Manganese Range Anticline, however, lacks carbonate. Instead, the sericitic, chloritized siltstone is rich in magnetite and there are numerous interbeds of arenites, from 5 to 300 cm in thickness. These arenites commonly show ripple marks of the irregular, symmetrical type, but these are not current ripples. On the northern limb of the anticline (particularly in proximity to Quartzite Well Fault) there is a marked schistosity due to strong deformation, which obliterates the bedding. Significant amounts of iron and manganese (associated with minor base-metal mineralization) have apparently been added to the original sediment at Manganese Range, so that the field appearance of the siltstone is that of a black manganiferous magnetite–chlorite–quartz schist, which forms the prominent strike ridge of the southern part of Manganese Range.

Petrography: In thin section the siltstone is fine grained and sericitic. It contains ubiquitous dispersed opaques (magnetite), and there are some very coarse-grained detrital quartz grains scattered irregularly through the rock. Chlorite is abundant and is concentrated in certain layers. There are areas of complete quartz recrystallization where chlorite is absent. Chlorite has frequently grown in the pressure shadows of magnetite grains (Fig. 12). This can be taken as evidence that

(a) chlorite generation postdates that of magnetite; and

(b) the formation of this chlorite is related to tectonometamorphism.

Muscovite behaves similarly to chlorite: it has clearly formed later than the magnetite it encloses (Fig. 13).

Figure 10. Silicified, laminated dolomite of Unit *GW2*, with overlying manganiferous outcrops (top of picture), Woodlands area

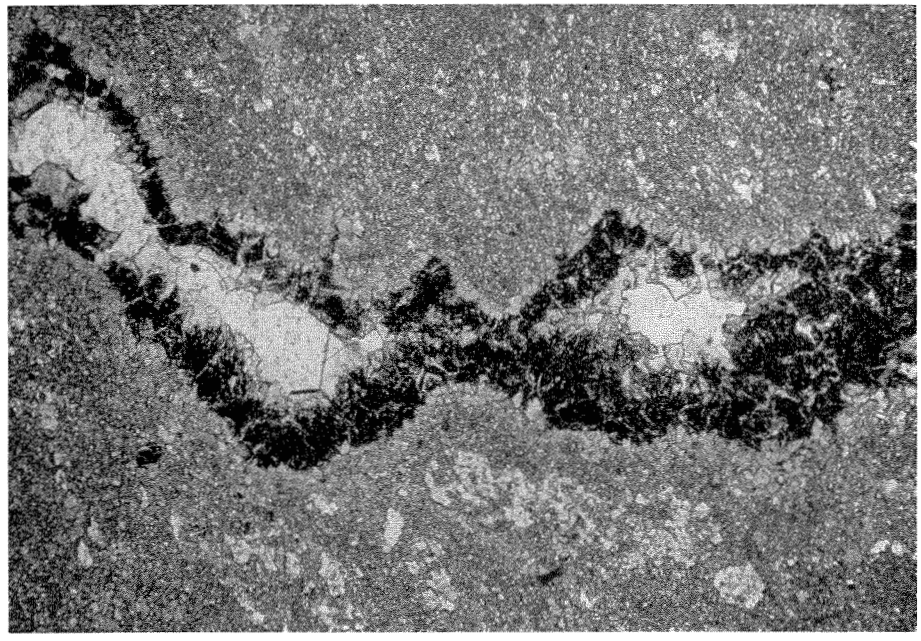

Figure 11. Part of a disrupted algal layer in micritic carbonate, Unit *GW2*. During decay of the organic material sparitic carbonate has grown into the layer. Central parts of the layer consist of quartz. Base of picture is 3.6 mm (plane-polarized light)

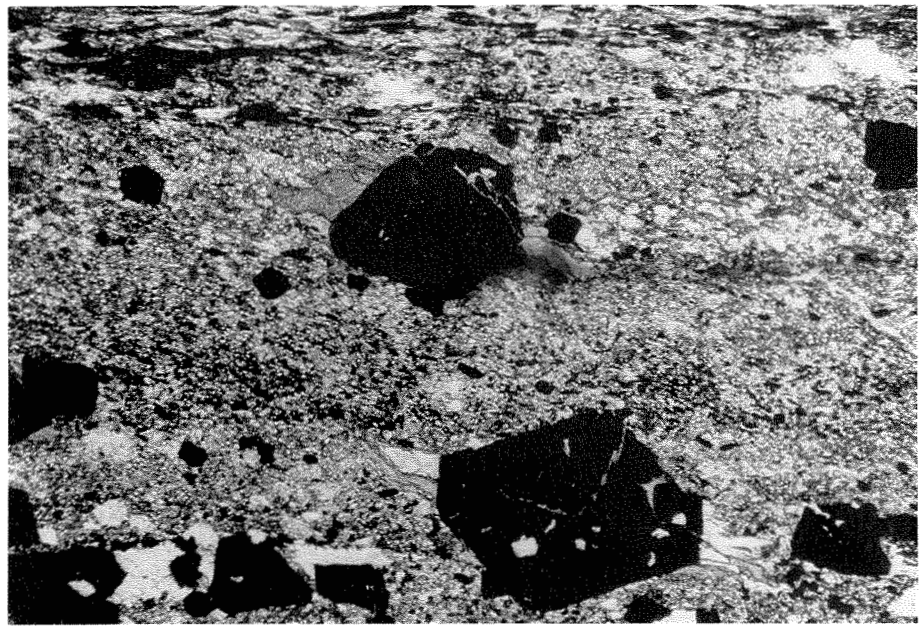

Figure 12. Growth of chlorite in the pressure shadow of magnetite grains. Siltstone in Unit *GW3* Manganese Range area. Base of picture is 3.6 mm (crossed polars)

Muscovite also forms tails to the edges of euhedral magnetite grains, indicating that it has grown in the pressure shadows of magnetite grains. Both chlorite and muscovite were probably generated by the same process at the same time. It is assumed, therefore, that compositional variations in the original sediment have had some control on the type of phyllosilicate that eventually developed.

In the Manganese Range area the arenites, often interbedded with siltstones, are poorly sorted and subangular, medium- to coarse-grained quartz sandstones with minor tourmaline. The matrix consists of fine-grained chlorite and a few scattered muscovite flakes; 10–15% magnetite is embedded in the matrix as subhedral (sometimes fractured) grains.

In both arenite and siltstone the opaque material may consist of the following:

(a) Disseminated subhedral or euhedral magnetite grains (0.1–1 mm) which have grown prior to deformation. The grain size seems to decrease with the grain size of the surrounding silicates.

(b) Thin (0.05–0.5 mm) wispy layers — up to 5 mm long — of an amorphous dark-brown material (arranged parallel to the incipient schistosity). This may be a late diagenetic product of iron oxides which were formerly more dispersed and existed prior to final compaction. These layers 'wrap' around some detrital quartz grains (Fig. 14).

(c) Fine grains (15–50 μm), which are dispersed in phyllosilicate-rich portions and recrystallized quartz layers. These grains are either anhedral or subhedral and are elongated parallel to the bedding. From their elongated crystal shape (in places resembling distorted rhombs) it is inferred that the grains are hematite.

Depositional environment: Facies analysis of Unit *GW3* is complicated by poor outcrop in the west (Woodlands Dome) and strong deformation in the central part of the basin (Manganese Range). In order to evaluate the nature of the original sediments, the lack of carbonate in Unit *GW3* at Manganese Range requires consideration. In the west, as well as at Manganese Range, the sediment is a siltstone containing several arenite interbeds. It is assumed that in both areas the sediment originally contained carbonate. At Manganese Range, however, later hydrothermal activity caused extensive silicification and the introduction of iron, manganese (and base metals), and at the same time resulted in the expulsion of carbonate. The nature and significance of these processes will be discussed later (Chapter Eight).

Thus, for the facies interpretation it is assumed that the lithologies of Unit *GW3* are fine-grained, laminated, carbonate-bearing siltstones (with symmetrical ripple marks) with irregular intercalations of medium- to coarse-grained, poorly sorted and subrounded, carbonate-cemented arenites. Such sediments are commonly encountered in an intertidal environment. Symmetrical ripple marks suggest the action of tidal currents, and the poor rounding and sorting of the interbedded arenites suggest deposition by storm action (Dimroth, 1979).

Woodlands Arenite Member (GWw4)

Distribution: The member is named after the Woodlands Dome, around the northern edge of which it forms a prominent ridge with a strike length of about 2 km . The unit has been given member status because it is a consistently mineralized unit, containing abundant barite,

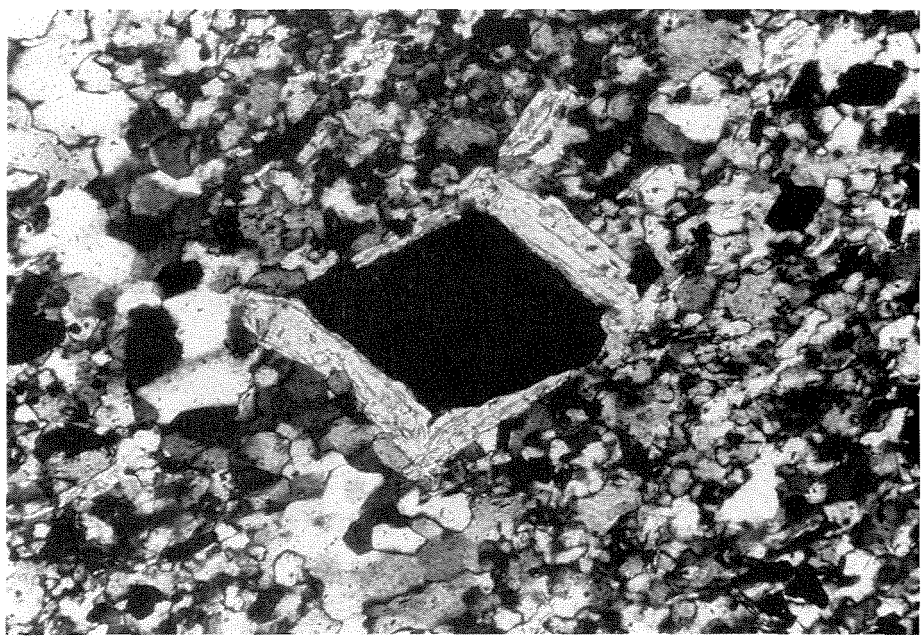

Figure 13. Muscovite surrounding euhedral magnetite. Siltstone in Unit *GW3* Manganese Range area. Base of picture is 0.9 mm (crossed polars)

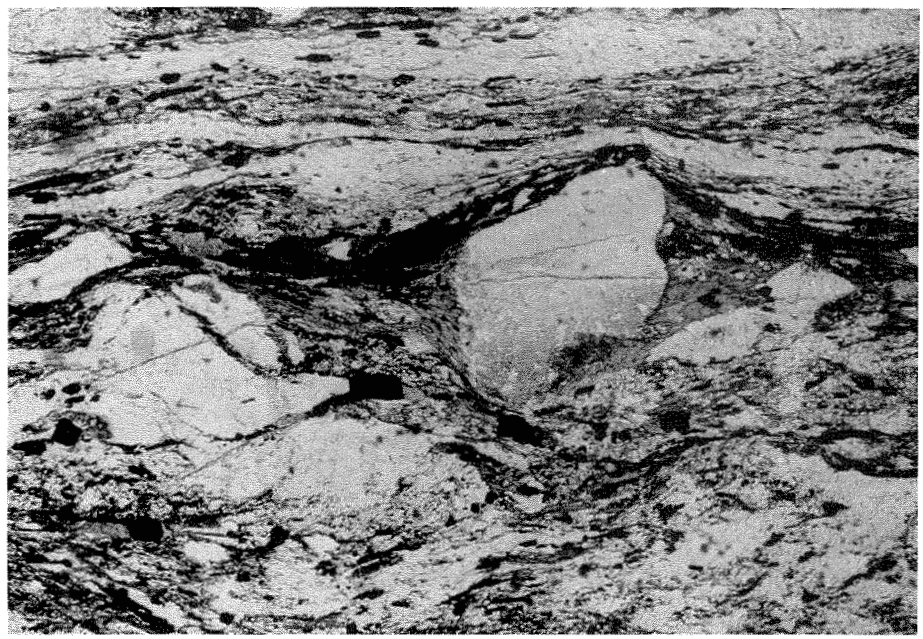

Figure 14. Amorphous iron oxide (hydroxide) layer (dark) wrapped around quartz grains. Siltstone in Unit *GW3*, Manganese Range area. Base of picture is 3.6 mm (plane-polarized light)

Figure 15. Barite vein in coarse-grained Woodlands Arenite (*GWw4*), Woodlands area

chalcopyrite, and magnetite (Fig. 15). The arenite is absent on the southern side of Woodlands Dome.

A similar arenite member (but without abundant barite and chalcopyrite) is exposed to the east in the Jeds Anticline and in the Manganese Range Anticline. In the Manganese Range Anticline, massive magnetite-rich arenite is restricted to the northern limb and the eastern closure. On the southern limb there is abundant intercalated siltstone which makes it difficult to distinguish the Unit *GWw4* from Unit *GW3*, so that it could be argued that the arenite member is absent here. In the area of Woodlands Dome the arenite is usually manganiferous and massive, with indistinct bedding. Only in the western outcrops has some medium scale (1 m) planar cross-bedding been observed. In Jeds Anticline, planar cross-bedding and ripple marks are common. In the Manganese Range Anticline the arenite is also manganiferous and massive, and planar cross-bedding (of trough type in places) is visible. Locally, in Jeds Anticline and Manganese Range Anticline, intercalated conglomerates occur, which consist mainly of well-rounded quartz pebbles (about 0.5 cm in diameter).

Petrography: The Woodlands Arenite Member is a coarse-grained, rounded, moderately sorted quartz sandstone, with the quartz grains showing wide rims of secondary quartz. The interstices are occupied by ferroan carbonate (ferroan dolomite; about 10% Fe as determined by electron microprobe). Abundant anhedral to subhedral opaques (mainly magnetite) are generally dispersed in the carbonate (Fig. 16), which intermittently contains anhedral barite grains.

All contained feldspars seem to be authigenic. The existence of chlorite along the cleavage of some plagioclase grains suggests they formed early, probably during diagenesis (Tröger, 1969). Some feldspars associated with magnetite are distinctly zoned; microprobe analysis revealed that they are barium-bearing hyalophane (Fig. 17).

All components are cemented by abundant secondary quartz, the amount of which could hardly be produced by the recrystallization of the detrital grains. It is likely that additional quartz, together with barite, carbonate and magnetite were introduced into the coarse-grained arenite, possibly during diagenesis. Some interstices are filled by material which is predominantly secondary quartz, euhedral carbonate and dispersed opaques. Figure 18 illustrates the mobility of these components.

Depositional environment: A barrier-beach complex is proposed for the depositional features observed. The arenite is well rounded and coarse grained, possibly with some penecontemporaneous carbonate as a cementing component. Planar cross-bedding is dominant over trough cross-bedding. Although strike length is restricted, the occurrence of the unit is widespread in the basin. According to the facies model of barrier-island systems (Reinson, 1979), these features would be compatible with the tidal delta/barrier island parts of such systems.

Assuming the above facies interpretation, the Woodlands Arenite Member could then be regarded as the time-equivalent of Unit *GW3*. The Woodlands Arenite would represent a barrier-island system to the *GW3* intertidal flats. This is also supported by differences in the thickness of Unit *GW3* around the Woodlands Dome. In the north where the Woodlands Arenite has a thickness of more than 100 m, the outcrop of Unit *GW3* is small. However, on the southern side the Woodlands Arenite is absent, but the

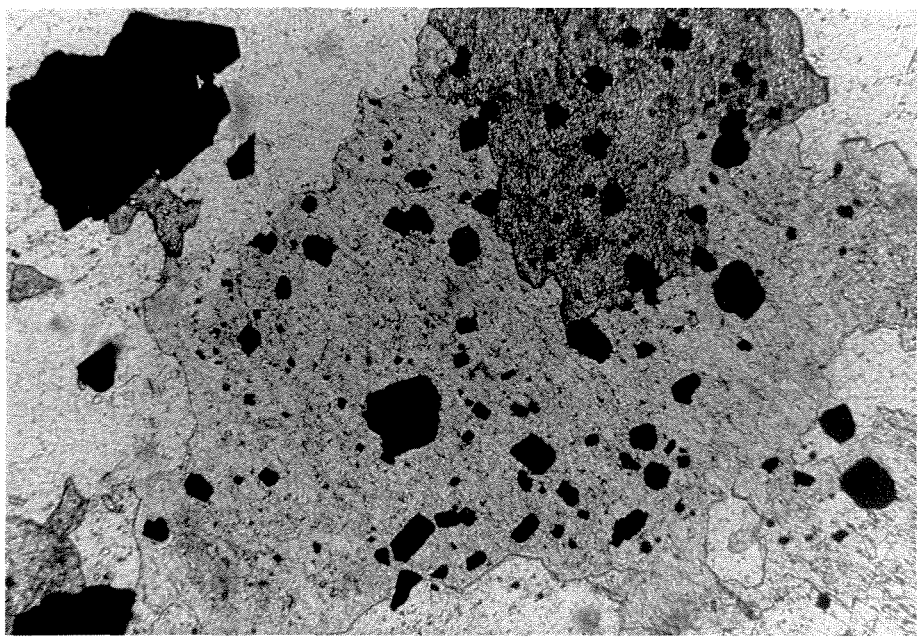

Figure 16. Magnetite grains dispersed in ferroan carbonate, Woodlands Arenite (*GWw4*). Base of picture is 0.9 mm (plane-polarized light)

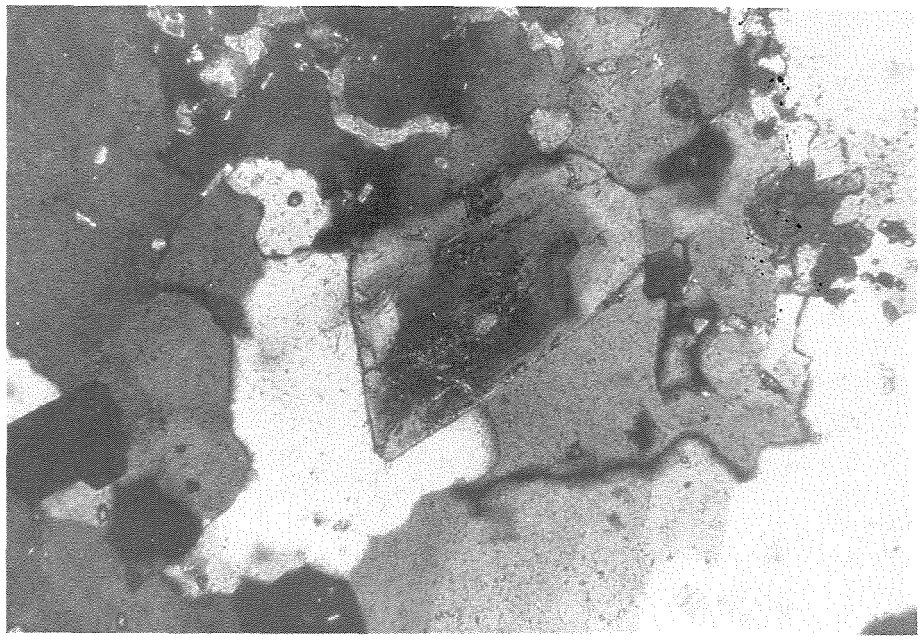

Figure 17. Zoned subhedral hyalophane in recrystallized quartz, Woodlands Arenite. Base of picture is 0.9 mm (crossed polars)

thickness of Unit *GW3* is significantly greater than in the north.

Unit GW5

Distribution: The unit varies in lithology and thickness. It was intersected in several diamond drillholes (Fig. 9) where the thickness of the unit ranges from 250 to 330 m. Defining the upper and lower limits (particularly when Unit *GWw4* is absent) can be difficult owing to the generally similar lithologies of Units *GW3*, *GW5* and *GW6*. The lower part of Unit *GW5* contains stratabound base-metal mineralization at Woodlands, TP, TC, and Manganese Range prospects (Ruddock, I., 1982, pers. comm.).

Laminated siltstone with interbedded arenite is predominant. The siltstone is frequently calcareous, and ripple marks are common. At one locality in Jeds Anticline, the method of Tanner (1971) for water-depth calculation was applied to some short, irregular, symmetrical ripple marks in fine-grained sandstone. With an assumed grain size of 120 μm the calculation yielded a water depth of tens of centimetres, a wave height of about 10 cm and a fetch (distance from shoreline) of tens of kilometres. If the value for the fetch (which is commonly less with such a water depth) is real, an unusually wide shallow-water area prevailed at that time.

Arenite intercalations with planar cross bedding are abundant. They occur either as massive bodies of less than 50 m strike length or as thin sheets (10–30 cm thick) with somewhat greater strike length. Towards the top of this unit, regular intercalations of fine-grained dolomitic siltstone and calcareous wacke are common, giving the rock a rhythmically bedded appearance (Fig. 19).

In places, the unit is represented by isolated dolomite bodies. One of these occurs north-northeast of Jillawarra exploration camp and contains some hitherto unknown stromatolites (Fig. 20). The dolomite forms the top of a well-laminated (?microbial mats) fine-grained dolomitic wacke sequence. These stromatolites have been described in detail by Grey (1985).

South of Woodlands Dome there is a prominent ridge, which consists of chloritic fine-grained arenite with intercalations of coarse-grained arenite plus thin (about 20 cm) quartz-pebble conglomerate. There is also some very coarse-grained, poorly sorted conglomerate with flat, rounded silicified shale clasts of up to 10 cm length.

Petrography: It is evident that Unit *GW5* comprises a number of different lithologies which are subject to rapid changes both vertically and along strike. The microscopic features of the various calcareous siltstones, wackes, and arenites are described below in three groups.

(a) The laminated siltstone varies from fine to coarse grained and usually has a considerable carbonate component. The epiclastic content can become minor, so that the lithology then becomes a micritic carbonate. The carbonate is frequently ferruginous and is usually micritic with patches of neomorphic sparite. Locally, bedding is defined by thin (0.4 mm) organic layers into which euhedral carbonate has grown. The siltstone is sericitic and in places contains large muscovite flakes. Where the siltstone is carbonate-rich, biotite and sub-ordinate chlorite are abundant. The biotite (composition confirmed by electron microprobe) is a brownish, weakly pleochroic variety. Authigenic albite is widespread.

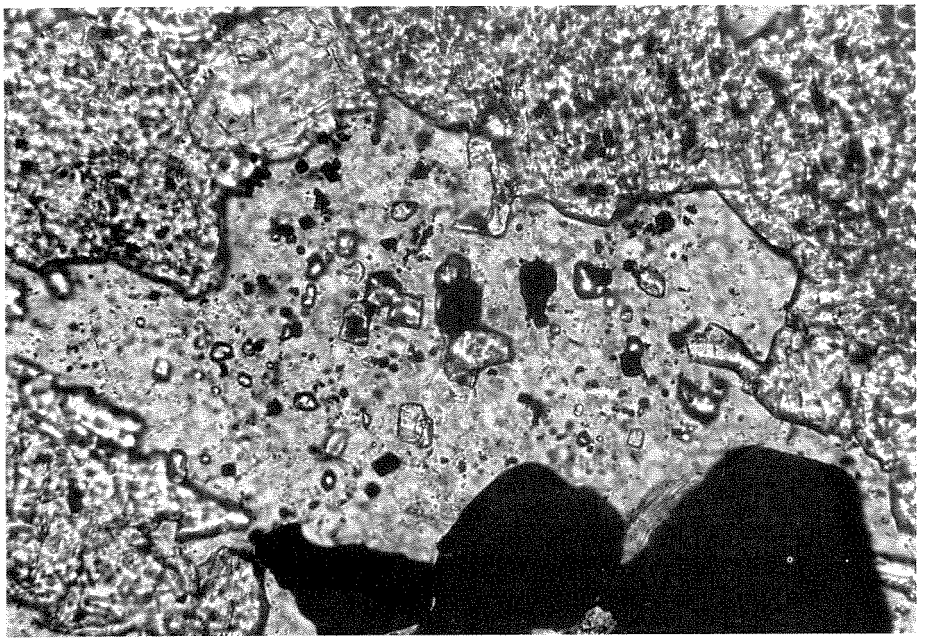

Figure 18. Quartz phase interstitial to carbonate, containing inclusions of subhedral carbonate, opaques (mainly magnetite) and barite in Woodlands Arenite (*GW*$_{W4}$). Base of picture is 0.36 mm (plane-polarized light)

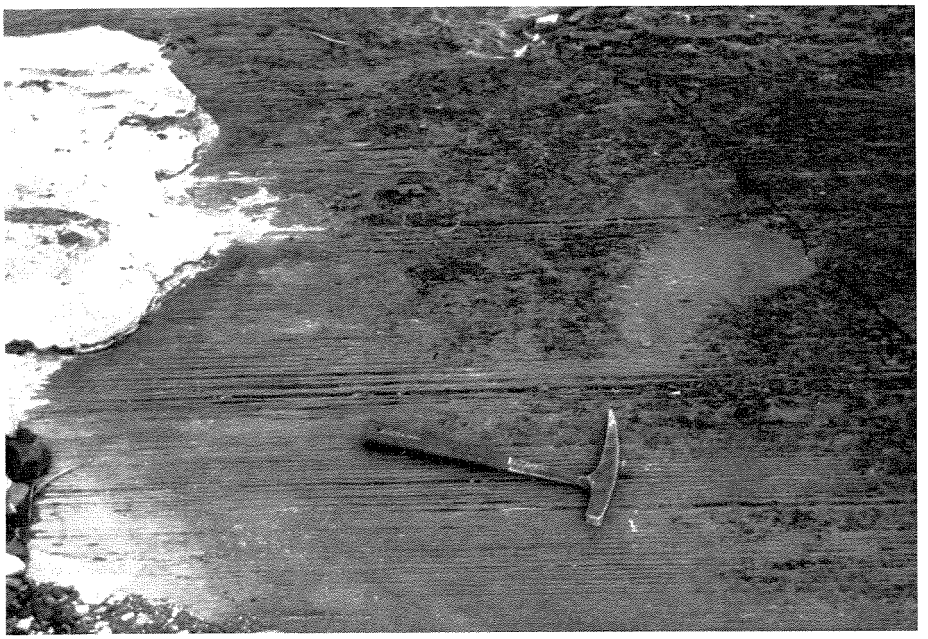

Figure 19. Rhythmically interbedded dolomitic siltstone and calcareous wacke, of Unit *GW*$_5$, in Jeds Anticline

Figure 20. Unknown stromatolites in dolomite of the upper part of Unit *GW5*, 1.5 km north-northeast of Jillawarra exploration camp

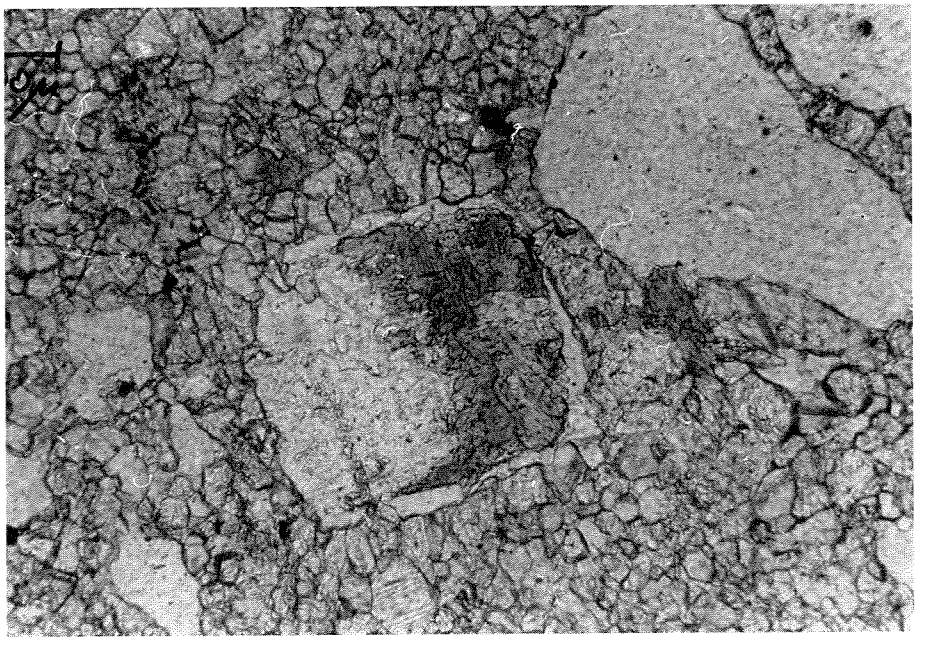

Figure 21. Biotite replacing possible authigenic albite, in siltstone of Unit *GW5*. Base of picture is 0.9 mm (plane-polarized light)

There is textural evidence to suggest that biotite is one of the latest minerals to have formed:

(i) biotite is replacing authigenic albite (Fig. 21) that has grown diagenetically;

(ii) biotite has formed at the rims of a quartz–galena vein in micritic carbonate; and

(iii) biotite formation may also be related to tectonic processes, because biotite occurs in pressure shadows around magnetite grains, oblique to bedding; it may thus be termed metamorphic biotite as it behaves similarly to chlorite.

However, the composition of the original sediment may also influence biotite formation. Some detrital clasts and pellets of micritic (minor sparitic) carbonate in a micritic carbonate matrix may contain abundant biotite, whereas the surrounding carbonate is almost devoid of it. The pellets were probably enriched originally in ferroan dolomite, which provided a source of Fe and Mg for biotite formation during alteration. Regardless of the mechanism of biotite generation, it is obvious that biotite has formed later than the opaque phases and the authigenic plagioclase.

Strong alteration can be seen in core from drillhole MRE 78-36, from the Manganese Range East Prospect. A calcareous wacke (described in (b) below) is intercalated with some shale bands of about 10–30 cm in thickness. The shale consists predominantly of pale-green phyllosilicate aggregates, which are intergrown with biotite. In coarser grained areas authigenic plagioclase is very abundant and associated with quartz. Minor relic carbonate is preserved within the shale portion, and rare titanite occurs. The alteration processes, here, have removed carbonate and, most importantly, have led to the formation of sudoite, which has been determined by X-ray diffraction. Sudoite — $K_{<1}(Al, Mg)_2(SiAl)_4O_{10}(OH)_2.nH_2O$ — belonging to the group of Al-mica clay minerals, has been described by Sudo et al. (1981) as a minor component of the alteration zone (stockwork level) of Kuroko deposits. However, occurrences of sudoite in marls and sandstones with diagenetic overprint are also known (Tröger, 1969).

(b) The calcareous wacke is another abundant lithology, which may be classified as a 'wack-stone' (Dunham, 1962). Various clasts (20–50%) have the appearance of floating in a micritic carbonate matrix, which contains biotite similar to that described for the laminated siltstone (in (a) above). Where clastics are absent the rock is commonly recrystallized to sparite.

The clasts are mainly angular (but some are well rounded) and comprise coarse-grained quartz, microcline, ferruginous carbonate pellets and minor shale. Myrmekitic quartz grains indicate that granite was exposed in the source region of the epiclastics. Authigenic albite plus secondary muscovite are common. Some of the shale clasts have been entirely altered to biotite. When the clast content increases relative to the carbonate matrix, euhedral magnetite and pyrite grains in the interstices become common; so that the opaques are more abundant in the coarser, porous parts of the rock.

While most of the plagioclase obviously is authigenic albite, much of the potash feldspar is detrital and, in coarser grains, was probably subject to significant alteration. Some elongated but rounded grains now consist of a diffuse, fine crystalline intergrowth of sericite and quartz. However, some microcline in a sandy dolomite at Manganese Range East occurs in seams (Fig. 22) which apparently have grown in situ. According to Tröger (1969), the alkalinity of a CO_2-free carbonate solution is sufficient for the low-temperature generation of authigenic potash feldspar. Hypersaline conditions favour this process. Thus it is possible that within Unit *GW5* there was a lateral variation in the salinity of diagenetic waters in the Jillawarra basin such that salinity increased towards the east.

(c) Arenaceous rocks, with a thickness of about 170 m, form a prominent ridge on the southern rim of the Woodlands Dome. They represent a local facies variant of Unit *GW5*, and have the distinctive feature of pervasive chloritization. The basal section consists of very coarse-grained, moderately sorted, rounded quartz sandstone (plus minor quartz-pebble conglomerate) which is considerably recrystallized. No feldspars have been observed. The matrix is dominated by barite, finely crystalline chlorite, minor 'cherty' quartz and white micas (Fig. 23).

Above the basal section there is a thick sequence of fine- to very fine-grained, subangular, moderately sorted lithic quartz sandstone, containing clasts of shale, chloritized shale, and a network of 'cherty' quartz with sericite. The matrix is of fine-grained, pale-green chlorite with interstitial anhedral iron-oxyhydrates.

Eastwards along strike the arenites grade into medium- to coarse-grained wackestones; these are calcareous in places and contain shale clasts. The carbonate matrix here is dominantly sparite with angular, anhedral grains; occasional euhedral rhombs in quartz indicate that recrystallization has taken place. As the carbonate content of the wackestone increases, the brown biotite (common in all calcareous rocks of Unit *GW5*) becomes the dominant phyllosilicate, while chlorite is rare and possibly in chemical disequilibrium with biotite (Fig. 24).

Depositional environment: The sedimentary environment, deduced from the facies variations, was probably a shallowing-upward carbonate sequence in the sense of James (1979). The common laminated calcareous siltstones

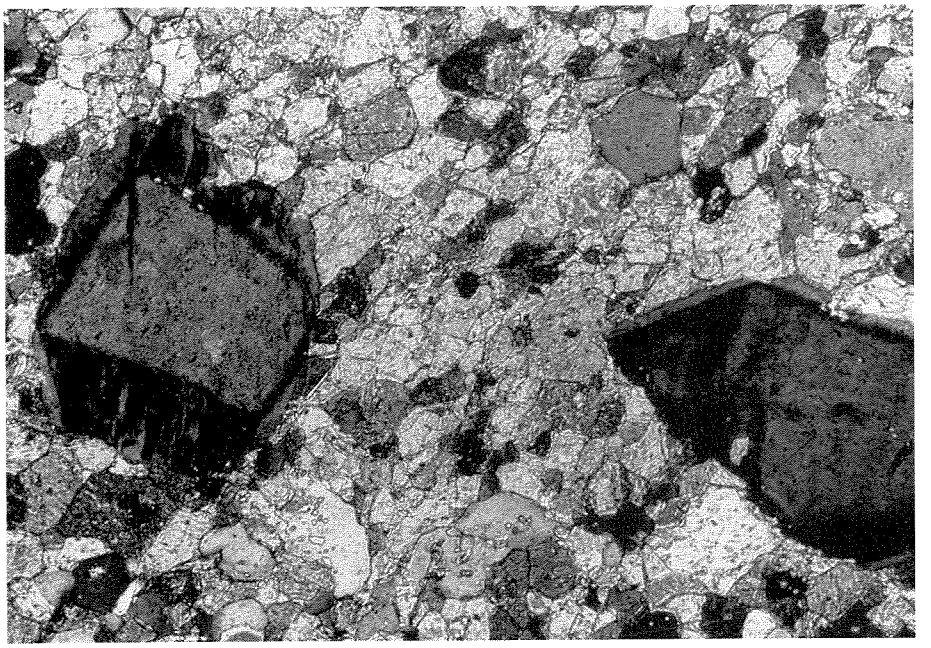

Figure 22. Authigenic seams of detrital microcline in sandy dolomite, Unit *GW5*, Manganese Range East (drillhole MRE 78-36). Base of picture is 0.9 mm (crossed polars)

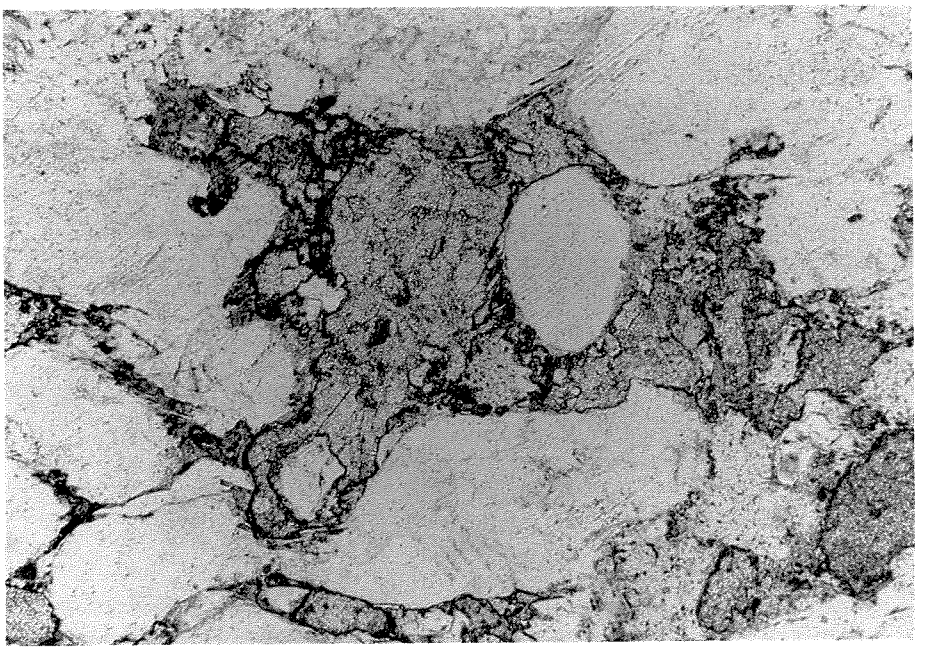

Figure 23. Barite (grey) and chlorite (dark grey) matrix in a coarse-grained quartz sandstone, Unit *GW5*, south of Woodlands prospect. Base of picture is 3.6 mm (plane-polarized light)

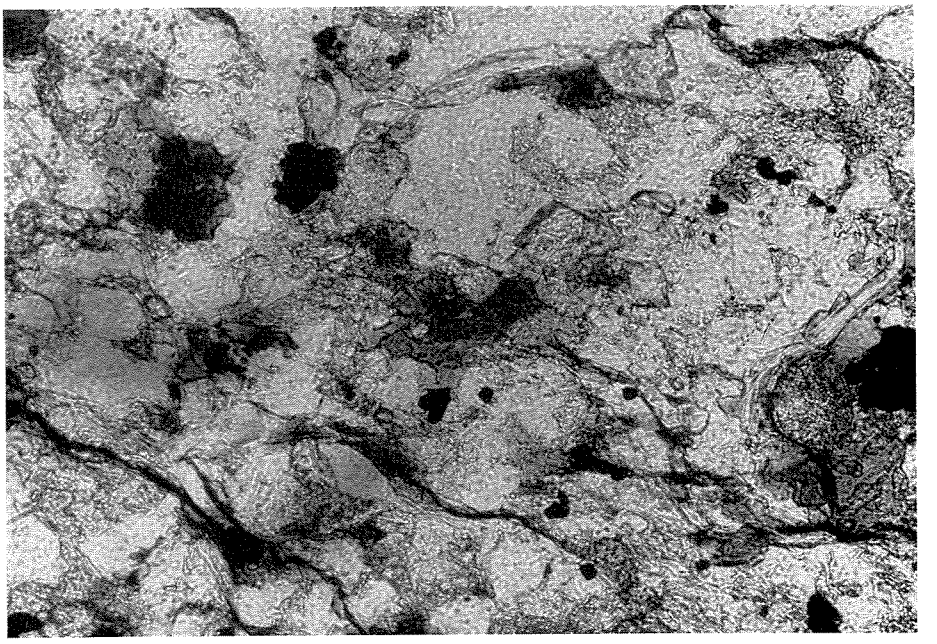

Figure 24. Biotite (dark grey) in disequilibrium with chlorite (medium grey). Both are intergrown with, or possibly have grown at the expense of, carbonate (light grey, high relief); calcareous wackestone of Unit *GW5*, south of Woodlands prospect. Base of picture is 0.9 mm (plane-polarized light)

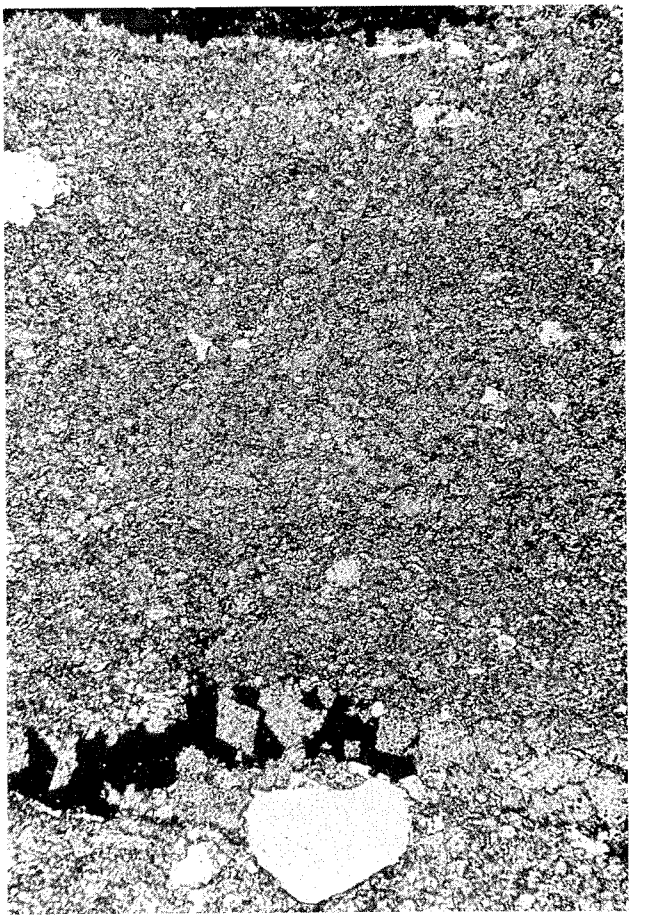

Figure 25. Disrupted microbial mats with sparitization of the micritic carbonate enhanced in these layers. Calcareous siltstone of Unit *GW5*. Base of picture is 3.6 mm (plane-polarized light)

may represent intertidal 'muddy' deposits, in which there was intermittent growth of microbial mats (Fig. 25).

Occasional quartz or feldspar grains were introduced by tidal currents, and shale clasts were derived from reworked intertidal pond deposits. The interbedded carbonate wackestones may represent storm deposits, containing quartz and feldspar clasts that have been derived from subtidal regions offshore; the roundness of most larger clastic grains indicates prolonged reworking in barrier/beach regions.

Towards the top of Unit *GW5* (Fig. 19) quiet conditions produced (upper) intertidal carbonates, while the occasional addition of more clastic material produced calcareous wackestones. A characteristic feature of such sediments are pellets, ooids and related structures (Dimroth, 1979). No ooids have been found, but Figure 26 shows some ferruginous pellets in a thin section prepared from the outcrop in the Jeds area shown in Figure 19. Outcropping possibly at the same stratigraphic level (near the top of Unit *GW5*), but farther eastwards (north-northeast of Jillawarra exploration camp), is a similar, more fine-grained laminated dolomitic siltstone, which grades upwards into stromatolitic dolomite (Fig. 20). This may indicate a shallowing-upward carbonate sequence and regressional development towards the top of Unit *GW5*.

Unit GW6

Distribution: This unit most closely resembles the 'Irregully Formation' of the Bangemall Group. It contains large dolomite biostromes that form large areas of outcrop in the west and central parts of the Jillawarra basin, but consists mainly of dolomitic siltstones and shales. Unit *GW6* was intersected in several diamond drillholes (Fig. 9), and outcrops of lithologies in Unit *GW6* extend westward beyond the Jillawarra basin for more than 30 km.

The thickness generally is around 350 m, but locally it may be greater than this. The lower boundary is gradational. It is marked by the last significant arenite and wacke interbeds of Unit *GW5*, and where laminated dolomitic siltstones and shales begin to predominate. In most cases, the top of the sequence is marked by a very coarse-grained conglomerate, which represents the basal lithology of the overlying Unit *WC1* (Fig. 39). Locally, the uppermost 20 cm of *GW6* are characterized by intense silicification and manganese enrichment (Fig. 27).

Where this conglomerate of Unit *WC1* is absent, dolomitic siltstones of Unit *GW6* grade through minor coarse clastic intercalations into ferruginous dolomitic shale of Unit *WC1*. The latter sequence itself locally shows thin conglomerate bands (5–30 cm) of the same type as the basal conglomerate. In some diamond drillholes at Abra, Unit *WC1* is entirely missing so that Unit *GW6* is overlain by Unit *WC2* with a sharp contact (Chapter Seven).

In the eastern and central parts of the basin the main lithologies of Unit *GW6* are sericitic mudstones, laminated dolomitic siltstones, and shales which often show undulatory folding. East of the Manganese Range Fault there is an increase in the overall grain size, so that the dominant rock type becomes a coarse dolomitic siltstone with thin (in the range of centimetres) calcareous sandstone intercalations.

In the area between Woodlands Fault and Manganese Range Fault (Plate 1), the unit is marked by abundant elongated dolomite biostromes. The largest bodies all appear to occur at the same stratigraphic interval and form

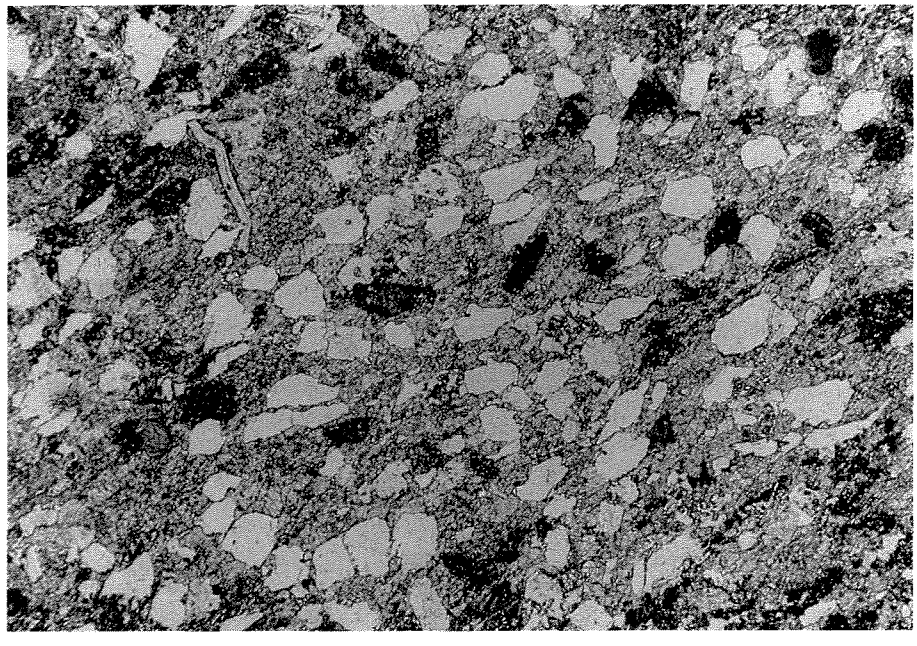

Figure 26. Ferruginous pellets (altered and stretched) in a calcareous wackestone, Unit *GW5*, at Jeds prospect. Base of picture is 3.6 mm (plane-polarized light)

an intermittent strike ridge of more than 11 km, with the individual bodies ranging in strike length between 0.3 and 2.3 km. The dolomite is either massive or laminated, commonly with grey to yellowish colours. Locally, it was subject to silicification which seems strongest in the same areas of silicification as for the dolomitic siltstones described below.

West of the Woodlands Fault, Unit *GW6* consists predominantly of dolomitic siltstone that is rich in pyrite cubes up to 3 cm on edge. The siltstone shows low or flat ripple marks with variable spacings.

Within the Jillawarra basin there are local concentrations of veins and layers of hematite and jaspilite (Fig. 28) in Unit *GW6*, possibly indicating that sabkha processes similar to those of the Red zone at Abra (Chapter Seven) were occurring elsewhere in the Jillawarra area. Some outcrops are intensely silicified and there is possibly a regional control on the degree of silicification. Intense silicification has been observed in Unit *GW6* in the area of the TP prospect, in the southern area of Jeds prospect, and in the area of the Copper Chert prospect. At the Copper Chert prospect, silicification accompanied by manganese enrichment has entirely obliterated the original features of the rocks. Another important feature of some coarse-grained, laminated dolomitic siltstones at the Copper Chert prospect and the TP prospect is the occurrence of blade-like, sometimes twinned casts (~1 cm long). These are irregularly distributed throughout the bedding and are interpreted as former, diagenetic gypsum crystals (Fig. 28).

Petrography: The petrology of the dominant rock types of Unit *GW6* in the Jillawarra basin is summarized as follows.

Some 20 km west of the Jillawarra basin, Unit *GW6* is represented by a monotonous sequence of micritic carbonates with layers of silt-sized clastic quartz. The proportion of clastics is, on average, above 20%. Abundant muscovite (average length 130 μm) and authigenic albite with carbonate inclusions occur irregularly. The carbonate shows incipient sparitization.

Within the Jillawarra basin the unit becomes more variable. A common lithology is micaceous 'mudstone', which is a fine- to medium-grained, sericitic siltstone characterized by detrital quartz grains in a matrix consisting of finely intergrown quartz and sericite; locally the matrix is calcareous (Fig. 29). In some coarser portions, authigenic potash feldspar can be seen. Finer layers of the rock are rich in organic material and iron hydroxides, and minor leucoxene has been observed. Fine-grained brown biotite is common and may contain intergrown chlorite in places.

An important feature of the micaceous siltstones is that they contain syndiagenetic pyrrhotite (and minor pyrite) occurring in single laminae 1–2 mm thick or in groups of several layers (Fig. 30). Pyrrhotite is intimately intergrown with large, pale, Fe–Mg chlorites (Fig. 31). The layers of iron sulfide have most likely formed contemporaneously with the chlorite. Because such layers of iron sulfide are usually generated during early diagenesis, provided that sulfate reducing bacteria are present (Renfro, 1974; Trudinger et al., 1972), it may be inferred that the chlorite also is diagenetic.

In a drillhole at the TP prospect (TP 78-37, Fig. 9) a fine-grained sericitic and biotite bearing siltstone is veined by pyrrhotite–quartz–carbonate (Fig. 32). The vein margins now consist of biotite prisms (Fig. 33) elongated

Figure 27. Silicification and manganese enrichment at the contact between dolomitic shales (Unit *GW6*) and coarse grained arenites (Unit *WC1*) in the area to the south of the TP prospect

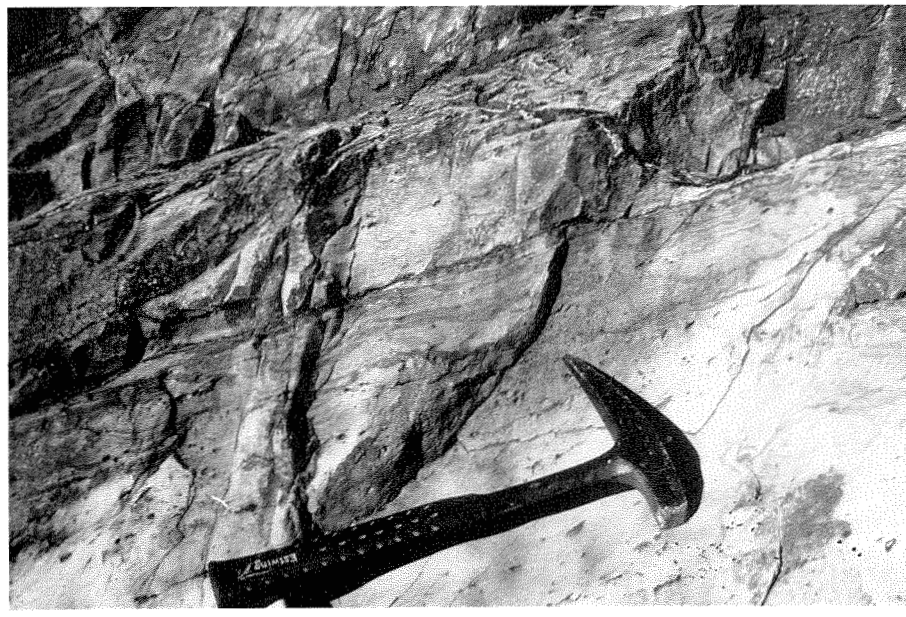

Figure 28. Red zone-type laminae of hematite (or possible liesegang structures) in dolomitic siltstone of Unit *GW6* near the TP prospect. Note elongated casts (possibly after gypsum) in the bottom half of the photograph

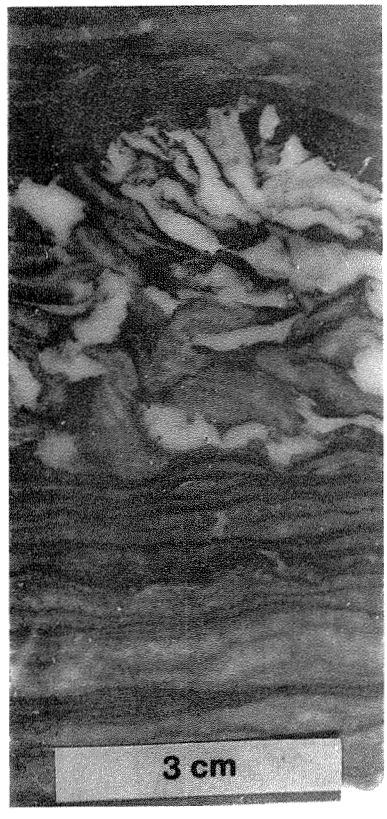

Figure 29. Soft-sediment deformation in a calcareous mudstone, Unit *GW6*

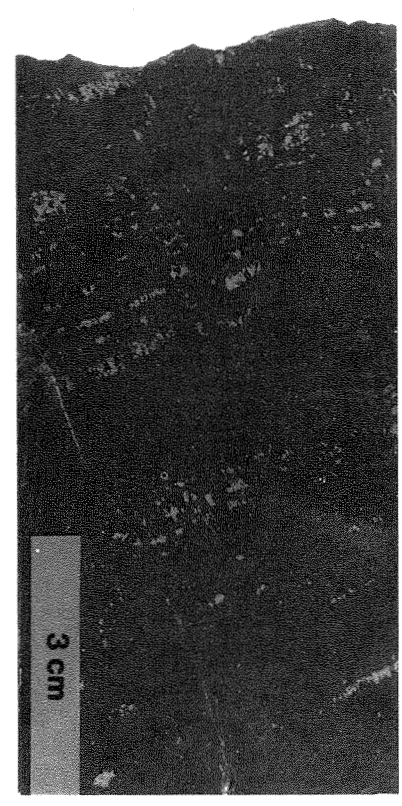

Figure 30. Syndiagenetic pyrrhotite layers in micritic dolomite, Unit *GW6*

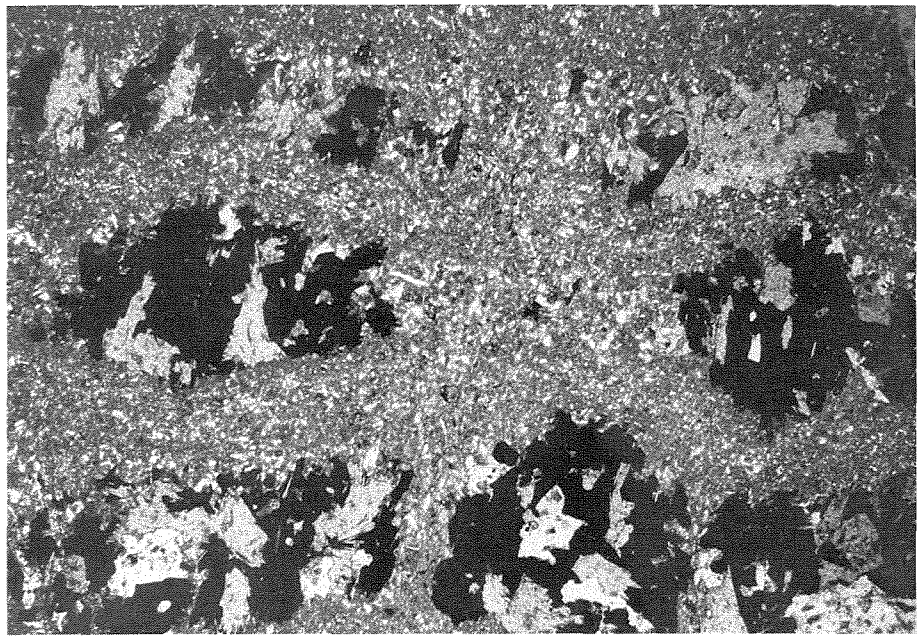

Figure 31. Pyrrhotite intergrown with chlorite in dolomite of Unit *GW6*. Base of picture is 3.6 mm (crossed polars)

at a high angle to the vein; chlorite occupies the centre of the vein where pyrrhotite and quartz are missing. The biotite apparently formed by wall-rock reaction with the fluid, whereas the chlorite composition may rather resemble the chemistry of the hydrothermal fluid.

The most abundant rock type of Unit *GW6* is laminated dolomitic siltstone (and shale), consisting of micritic dolomite which often shows neomorphic sparite; sometimes the sparite is restricted to poorly defined layers.

Figure 32. Pyrrhotite–quartz–carbonate vein in fine-grained siltstone of Unit *GW6* (drillhole TP 78-37, 309.1 m). Note marginal biotite (black)

Layering is usually defined by thin bands (0.1–0.5 mm) of organic material which is most probably the remains of microbial mats. Within the dolomite, secondary muscovite and brown biotite are common with chlorite a minor constituent. Authigenic plagioclase occurs throughout.

The carbonate is often intergrown with a diffuse 'matrix' of cryptocrystalline quartz, which was probably not derived from detrital quartz but was introduced after deposition (i.e. the rock is silicified). The extent of silicification grades from a few quartz specks to almost complete replacement of the carbonate. Abundant coloured inclusions (~10 μm) are scattered through the secondary quartz (Fig. 34). These inclusions do not contain a fluid phase and are probably composed of carbonate.

Because of this silicification, it is difficult to determine the amount of epiclastic quartz, potash, feldspar, and tourmaline. It is estimated that the content of clastic material in dolomitic siltstones in the Jillawarra basin varies between 10 and 40%. Thus, Unit *GW6* has the lowest epiclastic content of any unit within the Gap Well formation.

Another common feature of the dolomitic siltstone–shale sequence is the occurrence of abundant micritic pellets of various sizes (0.5–5 mm), in a sparite matrix (Fig. 35). The pellets mostly consist of ferruginous carbonate. However, in one occurrence of less calcareous siltstone, the pellets are significantly enriched in biotite, chlorite (Fig. 36), galena, and pyrite, with concomitant silicification. Because brown biotite is usually abundant in calcareous rocks, it can be assumed that the pellets were originally more calcareous than the matrix, and that biotite formation was enhanced in the pellets during alteration and mineralization of the whole rock.

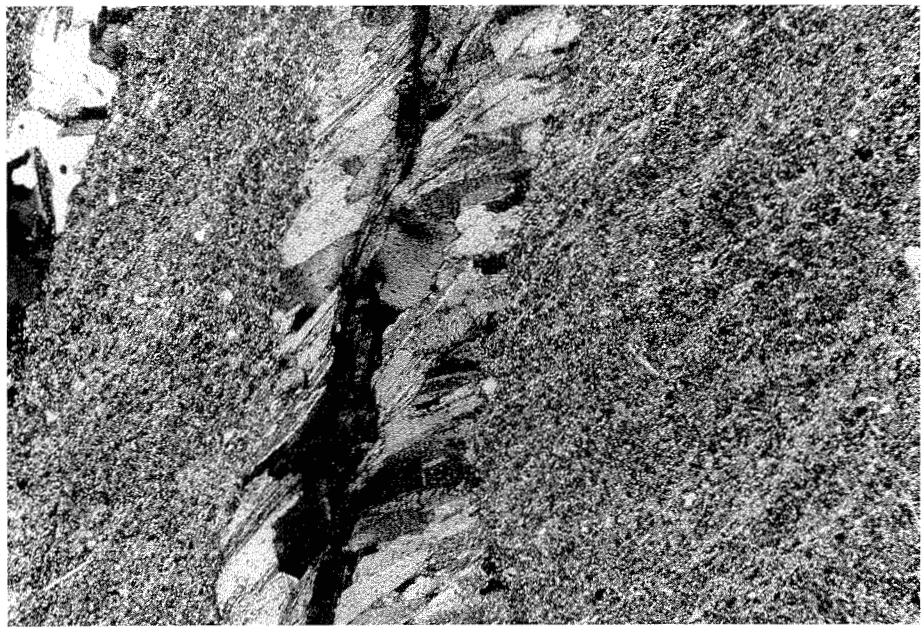

Figure 33. Vein in micaceous fine-grained siltstone of Unit *GW6* (Fig. 32) with central chlorite and marginal prismatic biotite. Base of picture is 3.6 mm (crossed polars)

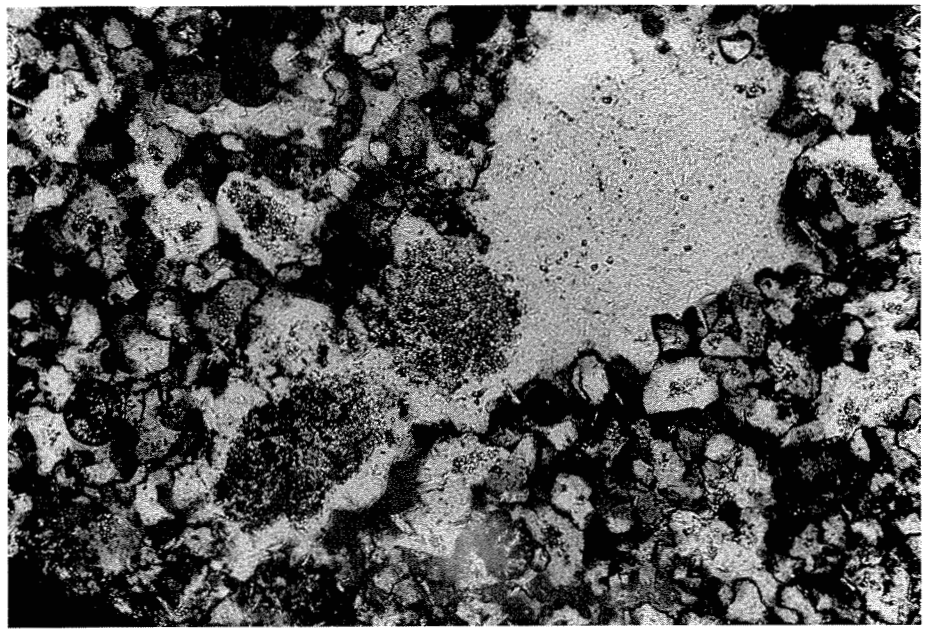

Figure 34. Quartz with abundant inclusions of carbonate in dolomitic siltstone of Unit *GW6*. Note that many quartz 'grains' have accumulations of these inclusions in their centres. Base of picture is 0.9 mm (crossed polars)

Figure 35. Ferruginous micritic carbonate pellets in a sparitic carbonate in dolomitic siltstone of Unit *GW6*. Base of picture is 3.6 mm (plane-polarized light)

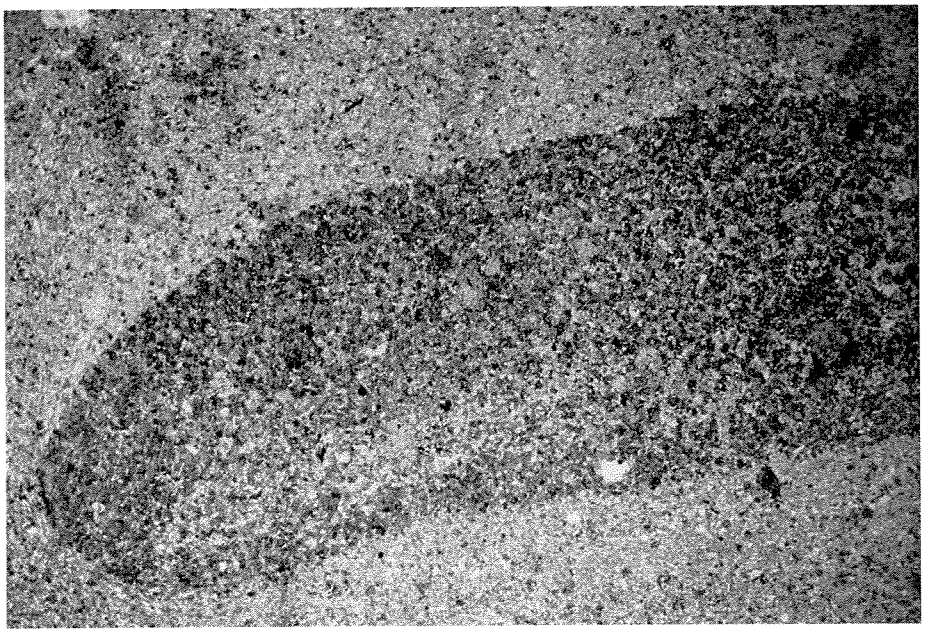

Figure 36. Large pellet (4 mm) is enriched in biotite–chlorite–pyrite–galena, in quartz–mica rock in Unit *GW6*. Base of picture is 3.6 mm (plane-polarized light)

The massive dolomite, forming the abundant low ridges in the western and central parts of the basin, consists mainly of micritic, often ferruginous carbonate. Oval patches or nodules of neomorphic sparite are common, some with secondary quartz in the centre. Rare clastic quartz grains have been observed in the micrite. Stromatolites and cryptalgal laminations are present at several localities; they also occur at Abra in the top of Unit *GW6* in drillhole AB 7. These stromatolites are of an indeterminate form, but have been described by Grey (1985).

Depositional environment: The facies of Unit *GW6* are characterized by dominant carbonate sedimentation with subordinate epiclastic input. Abundant stromatolites, cryptalgal laminations, and shallow irregular ripple marks suggest that Unit *GW6* was deposited in a shallow-water, low-energy environment. An upper intertidal zone is inferred. Reducing conditions appear to have prevailed within the sediments, resulting in the formation of occasional layers of diagenetic iron sulfide.

Some features indicate that, locally, the upper intertidal environment changed to supratidal. Figure 37 shows 'tee pee' structures in dolomitic cryptalgal laminates; such structures are characteristic of a supratidal environment (James, 1979). The occurrence of gypsum suggests hypersaline conditions similar to a sabkha environment. Further evidence of hypersaline, low-energy conditions (favourable for the growth of authigenic potash feldspar) is the abundance of authigenic plagioclase and potash feldspar in the fine-grained calcareous rocks (Fig. 38).

It is significant that Unit *GW6* has the lowest content of epiclastic material (10–40%) of the units of the Gap Well formation, indicating a period of emergence in the area of the Jillawarra basin. Emergence was more pronounced in the eastern parts, as suggested by the more common occurrence of supratidal (hypersaline) features like 'tee pee' structures, gypsum casts, and abundant cryptalgal lamination. In contrast, to the west of the Manganese Range Fault (which may have acted as a facies divide) biostromal dolomite and pelletal carbonates prevail. This suggests an intertidal environment, because the growth of biostromes requires a predominance of water cover. However, in this western area there is also some evidence at the TP prospect of hypersaline, shallow-water conditions; Figure 28 shows an interval with wispy laminae of red iron hydroxides and some casts of bladed crystals, probably after gypsum.

West Creek formation (*WC*)

This formation is subdivided into four units (named *WC1* to *WC4*). It has an average thickness of about 900 m and a maximum thickness of 1500 m. The thickness is variable because in some areas Unit *WC1* and Unit *WC4* may be absent. In most places the formation conformably overlies the Gap Well formation, but minor disconformities occur in a few areas. The name is derived from the West Creek (a tributary of Deverell Creek), north of which the formation shows its maximum development (Plate 1).

Unit WC1

Distribution: The characteristic lithology of this unit is a basal, massive coarse-grained arenite and conglomerate, with a maximum thickness of about 40 m. This is variably overlain by dolomitic shale and siltstone. At the Copper Chert prospect there is a massive dolomite occurrence. The thickness of Unit *WC1* is quite variable, and in places probably exceeds 200 m. Where the basal arenite is

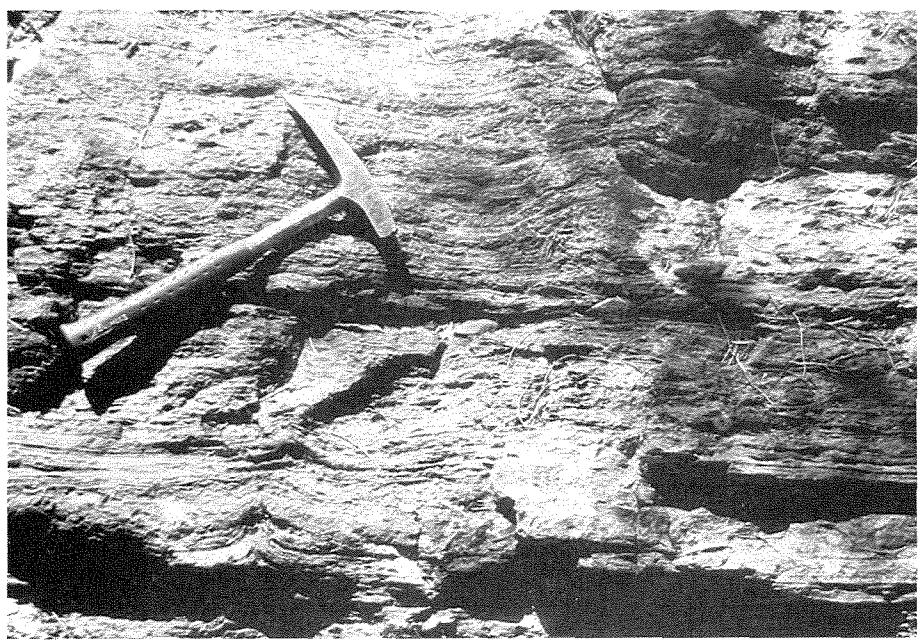

Figure 37. 'Tee-pee' structures (lower left) in dolomitic cryptalgal laminites, Unit *GW6*

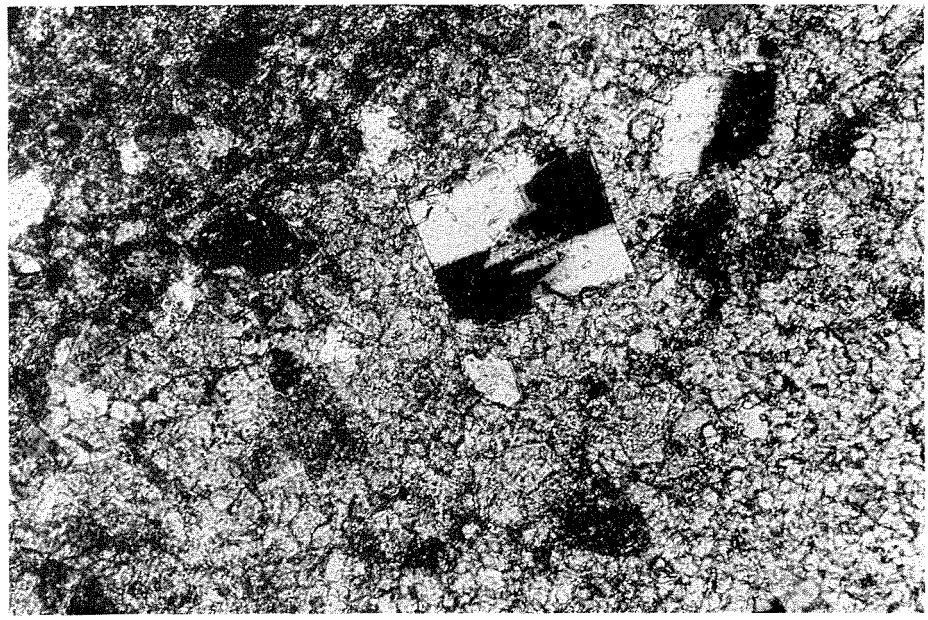

Figure 38. Authigenic potash feldspar in microsparite, in fine-grained calcareous rock of Unit *GW6*. Base of picture is 0.9 mm (crossed polars)

missing, it is difficult to distinguish the siltstones of Unit *WC1* from the laminated dolomitic siltstone and shale of the underlying Unit *GW6*. The lower contact of the unit can only be defined where the basal arenites are present.

The upper contact of Unit *WC1* is marked by the appearance of the overlying massive arenites of Unit *WC2*, which form impressive strike ridges throughout the Jillawarra area in contrast to the softer weathering dolomitic shale and siltstone of the upper part of Unit *WC1*.

In drillcores from the Abra deposit, the basal arenite of Unit *WC1* is either absent (AB 6, 7, 11) or present as a massive conglomeratic arenite (Fig. 39) up to 40 m in thickness, with no overlying dolomitic shale and siltstone. At Abra the top contact is defined by a pyrite layer (AB 9) containing complex Cu, Pb, and Sb sulfosalts (AB 4).

The coarse clastic rocks of Unit *WC1* are discontinuous along strike. Between Copper Chert prospect and Jillawarra exploration camp this facies occurs as small lenses, which are a few metres thick (Fig. 40).

In contrast, at Abra (Fig. 39), Copper Chert prospect and in the areas around TP prospect and Woodlands prospect, the coarse clastic rocks are massive and are up to 40 m in thickness (Plate 3). To the west of the Jillawarra basin, a lithology similar to Unit *WC1* forms a relatively continuous horizon (2 to 20 m thick) in the southern part of Teano Range (Ruddock, I., 1982, pers. comm.).

Petrography: The clastites are rounded to moderately rounded, moderately sorted, coarse-grained arenite with abundant large (up to 1 cm) rounded clasts of vein quartz, potash feldspar (5–10%), micaceous and ferruginous shales, siltstone, chert, and minor tourmaline. Although potash feldspar has not been identified at Abra, there is strong alteration here, and the original presence of potash feldspar cannot be ruled out.

In the Abra area the matrix of this arenite is of sparitic carbonate and minor barite (0.5 to 6.4% Ba, in whole-rock analyses). In some arenites the matrix is absent and the rock is completely cemented by quartz. Detrital titanium-bearing iron oxides, which commonly outline cross-bedding, have been altered to titanite; this alteration is possibly related to silicification (Ramdohr, 1975).

Depositional environment: For a facies interpretation the following observations are considered important:

(a) Although locally there may be considerable thicknesses of clastites in Unit *WC1*, the prevailing sedimentary environment is represented by dolomitic shale and siltstone plus minor dolomite.

(b) Due west of the Manganese Range Fault the basal conglomerate is thickest and coarsest (Fig. 40) with decreasing thickness and grain size westwards away from the fault, indicating that such syn-sedimentary faults have controlled the sites of deposition of coarse clastites. This fault has also controlled the facies of Unit *GW6*, because massive biostromal dolomite does not occur to the east of the fault.

(c) Regionally, the thick (30–40 m) clastic facies may define sub-basins where pronounced clastic deposition has occurred. These sub-basins — around TP prospect, Copper Chert prospect and Abra prospect — are the exploration target areas for base metals. These areas have remained prospective after more than 8 years of exploration (1975–1983) in the Jillawarra basin (Amoco, Geopeko, 1991).

Figure 39. Carbonate- and barite-cemented conglomerate, basal conglomerate of Unit *WC1* at Abra, drillhole AB 5

Figure 40. Basal conglomerate in Unit *WC1* (about 5 m thick) discontinuous along strike, southwest of the Manganese Range Fault

The sedimentary environment proposed for Unit *WC1* is similar to that for Unit *GW6*: an upper intertidal to supratidal zone with low clastic input and quiet carbonate deposition. However, in certain areas of the basin, synsedimentary faults have initiated sub-basins. These filled with coarse clastic rocks, while carbonate and silt deposition continued outside.

A significant portion of the coarse clasts in the basal conglomerate is derived from granitic and/or metamorphic terrane, as suggested by the presence of quartz grains with undulose extinction, potash feldspars, muscovite, and tourmaline. In contrast, jaspilite and chert clasts, plus some pellets, were derived from a nearby source, probably from the uppermost levels of Unit *GW6*. Although this suggests that sediments of Unit *GW6* had reached a lithified state, it should not be assumed that this is evidence for a significant time break between the Gap Well formation and West Creek formation. It is also possible for sediments of the supratidal zone (particularly sabkhas) to lithify rapidly due to evaporation (Kendall, 1979).

In summary, Unit *WC1* marks the onset of clastic deposition after a prolonged period of waning clastic input to the Gap Well formation. Within an intertidal zone, fault-bounded depressions developed where coarse clastic infill took place due to rapid subsidence. As discussed later in Chapter Ten, movement along the faults and concomitant subsidence of the sub-basin provided favourable sites for ascending metal-bearing hydrothermal fluids. The presence of a thick conglomerate facies at this stratigraphic level could, therefore, be used as a guide to Abra-type mineralization.

Unit WC2

Distribution: The unit is characterized by prominent strike ridges of arenite (with siltstone interbeds) and this renders the unit a useful marker horizon throughout the Jillawarra basin. A thickness of 320 m can be determined quite accurately from drillcores at the Abra prospect. In other areas, however, thickness of the unit can only be estimated from field data. There appears to be an increase in thickness to about 500 m at the longitude of the Copper Chert prospect. Thickness gradually decreases westwards from here to a minimum of about 17 m at the Manganese Range Fault. West of this fault the thickness is about 300 m.

At outcrop, the basal contact appears sharp and is marked by the appearance of the first major arenite bed which overlies the softly weathering dolomitic shale of Unit *WC1*. In Abra drillcores, the basal contact is marked either by a thin pyrite layer, within the arenites, or by a shale band. Unit *WC2* differs from Unit *GW1* merely in finer grain size and better sorting. The upper contact, on the other hand, is gradational. In Abra drillcores the contact is difficult to define. In outcrop, elsewhere in the Jillawarra basin, the upper contact is marked by a decrease in arenites and an increase in dolomitic siltstone and shale. For mapping purposes, the contact has been taken as the zone in which dolomitic siltstone and shale begin to predominate over arenites.

The arenites are fine- to medium-grained quartz sandstones or may consist of a gritty, coarse-grained and ferruginous arkose. Common cross-bedding and rare ripple marks are present. Where the arenites have a massive (silicified) appearance, moulds of weathered shale clasts are visible (Fig. 41).

The most important feature of Unit *WC2*, best seen in Abra drillcores, is the abundance of graded beds showing micro-Bouma cycles (Fig. 42), flaser bedding, scour and fill structures, and abundant rip-up clasts.

Figure 41. Moulds of weathered shale clasts in silicified arenite, Unit *WC2*

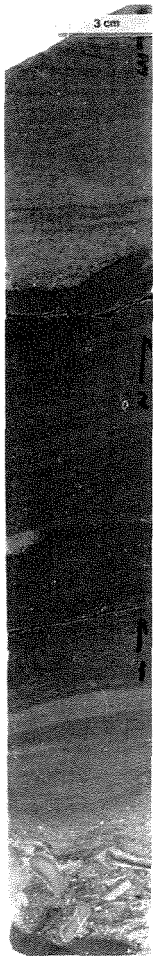

Figure 42. Complete Bouma cycle (A to E) in Unit *WC2* at Abra, drillhole AB 4

Locally, complete Bouma cycles are encountered (divisions after Walker, 1979):

E and (D)	pelitic interval of shale, in places black shale
C	cross-laminated interval, fine-grained arenite and siltstone, rarely developed
B	parallel-laminated interval, fine- to medium-grained arenite
A	graded interval, coarse arenite with shale and lithic clasts of more than 2 cm in length

Unfortunately, no drillcores from Unit *WC2* elsewhere in the Jillawarra basin are available; in outcrop, weathering and silicification render recognition of turbidite cycles difficult. Therefore, it cannot be concluded unequivocally that turbidites are present elsewhere, other than at Abra. However, the common occurrence of shale clasts (Fig. 41) and the frequent interbedding of sandstone/siltstone with minor shale may be taken to indicate that some turbidites are present.

Petrography: The examination of about 30 thin sections throws some light on the nature of Unit *WC2*. The petrology ranges from organic shale and ferruginous shale to very coarse-grained wacke with various clasts, some as much as 2 cm in length. Most rocks with grains exceeding silt-size can be termed wacke. They contain clasts of quartz, potash feldspar, siltstone, shale, ferruginous and black shale and minor ferruginous carbonate pellets. The matrix consists of fine-grained micaceous material, cherty quartz, or carbonate (predominantly sparitic).

There are two groups of clasts. One group comprises undulose quartz grains, potash feldspars and tourmaline that appear to be derived from pre-Bangemall granitic basement. A second group consists of lithic clasts of micaceous siltstone, shale (locally chloritized), ferruginous carbonate pellets (locally chloritized) and some chert. This second group is characterized by elongated rounded shapes. This feature, together with the mineralogy of the clasts (mica, quartz, tourmaline, micritic carbonate, but no metamorphic minerals), indicates that the clasts were derived from contemporaneous or slightly older sediments. Although the provenance of micaceous siltstone or shale clasts cannot unequivocally be inferred, some ferruginous shale clasts which contain euhedral iron-hydroxide cubes (after pyrite) probably were derived from tidal sediments (Fig. 43).

As mentioned, field observations suggest the dominant rock type of Unit *WC2* is an arenite, although petrological study shows it to be a wacke in places. Three classes of clastites can be distinguished, using differences in texture, composition of clasts and composition of matrix.

(a) The first comprises a medium- to coarse-grained, moderately to poorly rounded feldspathic arenite with about 15–30% potash feldspar and minor ferruginous shale clasts. Because of its feldspar content it could alternatively be termed arkose. Whereas most of the quartz grains are moderately rounded, the feldspars are subangular to angular (Fig. 44).

The amount of matrix with respect to clasts is generally small and it consists of a fine-grained, ferruginous quartz–phyllosilicate material; it is not known whether a carbonate component was present originally in the matrix. The angularity and abundance of potash feldspar clearly points to this being first-cycle detritus from a nearby source area. Deposition from turbulent water would explain the small amount of matrix as well as the relatively good sorting. The above features are encountered in alluvial-fan deposits close to source areas, where the micaceous clasts may be derived from mud banks within a braided delta.

(b) This class commonly is represented by medium- to very coarse-grained, moderately to well-rounded lithic wackestones. The population of clasts differs from group (a) in that feldspars (microcline) are subordinate (0–5%) to clasts of shale, micaceous siltstone, and possibly some formerly ferruginous carbonate pellets (now chloritized). The lithic clasts are often very large (more than 2 cm) and some consist of fine-grained wacke, indicating reworking of contemporaneous *WC2* sediments. Pyrite pseudomorphs containing shale and siltstone

fragments are abundant (Fig. 43). Some very large clasts of fine-grained wackestone (up to 1 cm across) themselves contain ferruginous pellets.

The matrix is composed of very fine-grained sericite, chlorite, and quartz, with some chlorite pellets (Fig. 45), and texturally is similar to a micritic dolomite. In addition, some clasts and pellets are of chlorite while others are not; this suggests that the original carbonate content of the matrix and the clasts (including pellets) influenced chloritization.

A relationship between carbonate–iron–chlorite becomes evident from Figure 46, which shows part of the matrix consisting of iron-bearing carbonate while the other part consists of chlorite. The processes of chloritization are discussed in more detail in Chapter Eight. However, for the following facies analysis it is assumed that the wacke type considered in this paragraph has a carbonate matrix.

Constraints on any facies interpretation are the relatively low content of potash feldspar, the abundance of lithic clasts of penecontemporaneous sediments of which at least some are derived from tidal sediments (abundant pyrite in micaceous, probably calcareous shale and clasts of pelletal rock), and a high degree of roundness of the clasts. A beach or barrier-beach environment could be inferred, where carbonate deposition is possible and frequent reworking of the clastics occurs. Here, the clastic grains from a granitic provenance are certainly a 'poly-cycle deposit', and the proportion of feldspars is considerably reduced. The lithic clasts, derived from adjacent tidal sediments, were transported and deposited by storm waters or in flood-tidal deltas.

(c) The third group of clastites is recognized, unequivocally, only in cores from Abra drillholes, but the group probably also occurs in outcrops to the east of Woodlands Fault and to the south of Jillawarra exploration camp. This group comprises fine to very coarse-grained, subrounded calcareous wacke, micaceous and calcareous siltstone and some organic shale. The wackes contain a moderate proportion of clasts (other than quartz), which are mainly of micaceous siltstone, black shale, potash feldspar, and some pellets of iron carbonate. Graded bedding and scouring of shales is common. Some rocks are fine-grained quartz arenites, containing occasional coarse quartz grains and shale clasts, and are rich in detrital tourmaline (representing comparatively mature sediments).

The most important feature of this third group is the presence of turbidites (Fig. 42), a few complete Bouma cycles, and abundant rip-up clasts. As turbidites may form in a number of environ-ments (Pettijohn, 1975; Walker, 1979) further features need to be considered in order to evaluate the probable facies. The omnipresence of carbon-ate matrix, the occurrence of large sub-angular potash feldspar grains, and the frequency of carbonate pellets clearly point to a near-shore facies. However, the preservation of fine-grained mature wackes, with one-directional low-angle cross-bedded foresets, could suggest facies developed below wave base. In a model section the above features would be attributed to the foreshore zone (just below wave base) but still within the range of carbonate deposition.

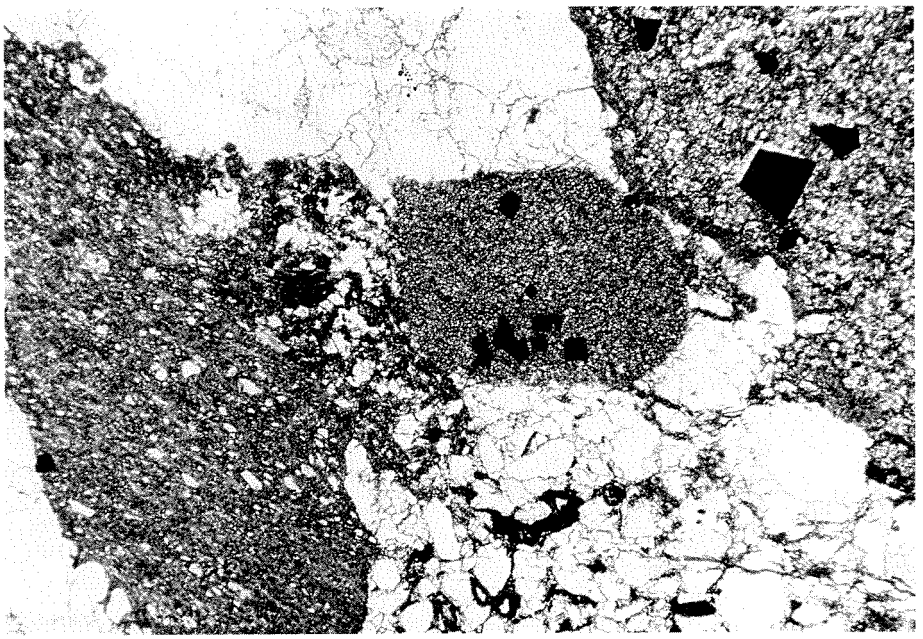

Figure 43. Ferruginous shale clasts containing pyrite cubes, Unit *WC2*. Base of picture is 3.6 mm (plane-polarized light)

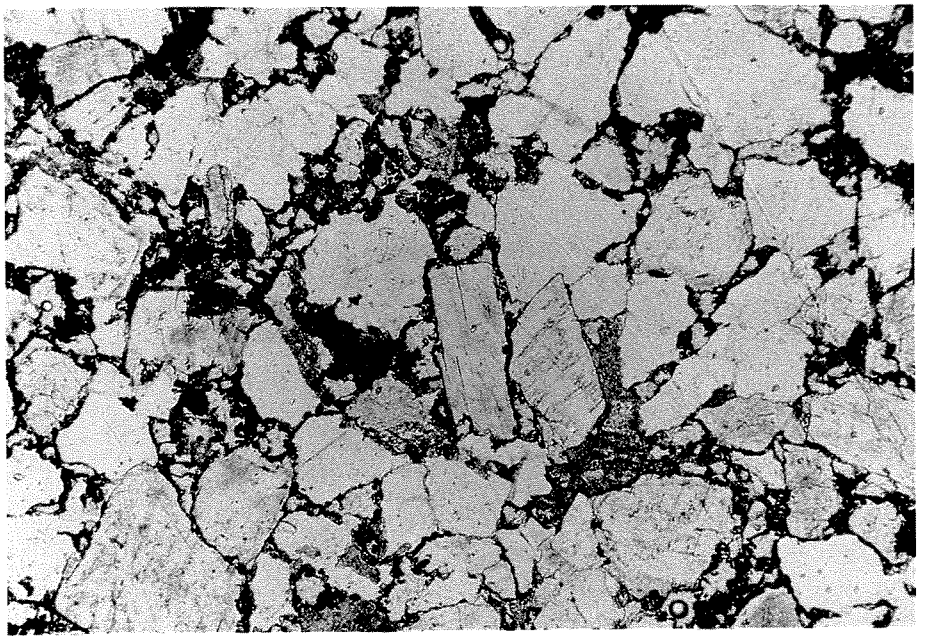

Figure 44. Arkose with angular potash feldspar, Unit *WC2*. Base of picture is 3.6 mm (plane-polarized light)

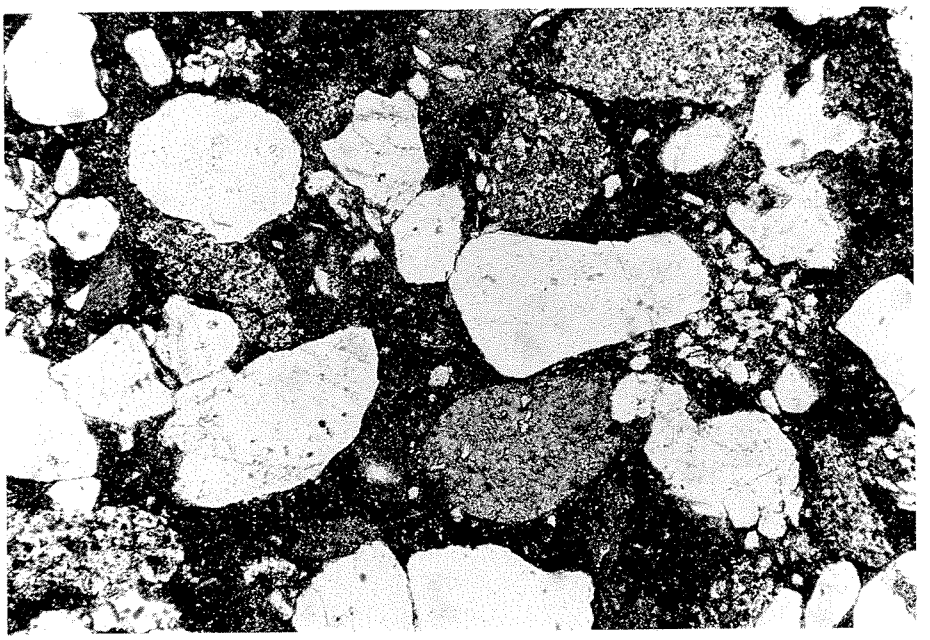

Figure 45. Chloritic matrix with chlorite pellet (lower middle) in a coarse-grained wacke, Unit *WC2*. Base of picture is 36.6 mm (plane-polarized light)

However, the occurrence of the beach-type wackes (class (b)) on three sides of the Jillawarra basin suggests that the turbidites formed in a basin into which clastics were transported from the surround-ing terestrial or beach areas. It is likely that the basin was subsiding due to syn-sedimentary fault activity and that the turbidites are 'earthquake-induced turbidites' (corresponding to fault movement) as described by Robbins (1983) for intracratonic rifted basins. In this case the depositional environment may be compared with an extensive delta where the erosional gradient is maintained through the repeated subsidence of the depository.

Depositional environment: In summary, within Unit *WC2* three facies are recognized: near-shore alluvial deposits; beach or barrier-beach deposits; and shallow-water, more-basinwards turbidites. A regional facies distribution for Unit *WC2* is presented in Figure 47, which shows the Jillawarra basin surrounded by alluvial and beach facies. Palaeocurrent analysis of cross-bedding in coarse arenites at the Abra prospect indicates that transport direction was towards the west-southwest, i.e. basinwards (Ballinger, T. A., 1982, pers. comm.), and this supports the proposed facies zones. Figure 47 also shows a change from beach to turbidite facies in the vicinity of inferred synsedimentary fault zones; one is the Woodlands Fault in the west, and the other is the fault system east of Abra.

As the occurrence of Unit *WC1* is broadly within the limits of the inferred turbidite facies in Unit *WC2*, it is likely that there was one basin (the Jillawarra basin) where submergence commenced at the onset of the deposition of Unit *WC1* and continued through the interval when Unit *WC2* was deposited.

Unit WC3

Distribution: The sequence consists predominantly of whitish, porous siltstone and shale, often manganese stained or varicoloured; subordinate arenite intercalations are also common. West of the Jeds prospect a chert horizon (0–5 m thick) occurs in the lower part of the unit, and persists westwards along strike for several kilometres, extending outside the mapped area. Siltstones prevail adjacent to (and overlying) the chert.

In the vicinity of the Abra prospect, dolomitic rocks are common. Southwest of Abra there is a massive dolomite, with a strike length of some 400 m. To the east and southeast of Abra, at a comparable stratigraphic level, dolomitic siltstone is abundant with a few lenses (less than 1 km along strike) of coarse-grained ferruginous dolomitic wackestone with abundant shale intraclasts and subangular potash feldspar. Near the top of Unit *WC3* some manganiferous gossans, containing 3000 ppm Pb, occur in the area to the southeast of Abra; one is located close to the Abra fault system.

The thickness of Unit *WC3*, estimated from field mapping, ranges from 0 to 750 m. The unit attains a maximum thickness to the south of Jillawarra Camp. The lower boundary of the unit is gradational and is marked by the disappearance of significant arenite intercalations. The upper boundary is generally sharp and marked by coarse arenites of the overlying Unit *WC4*. However, where these arenites are absent, it is difficult to distinguish the dolomitic siltstone and shale of Unit *WC3* from the overlying lower parts of the Jillawarra Formation, which in general consists of similar rock types.

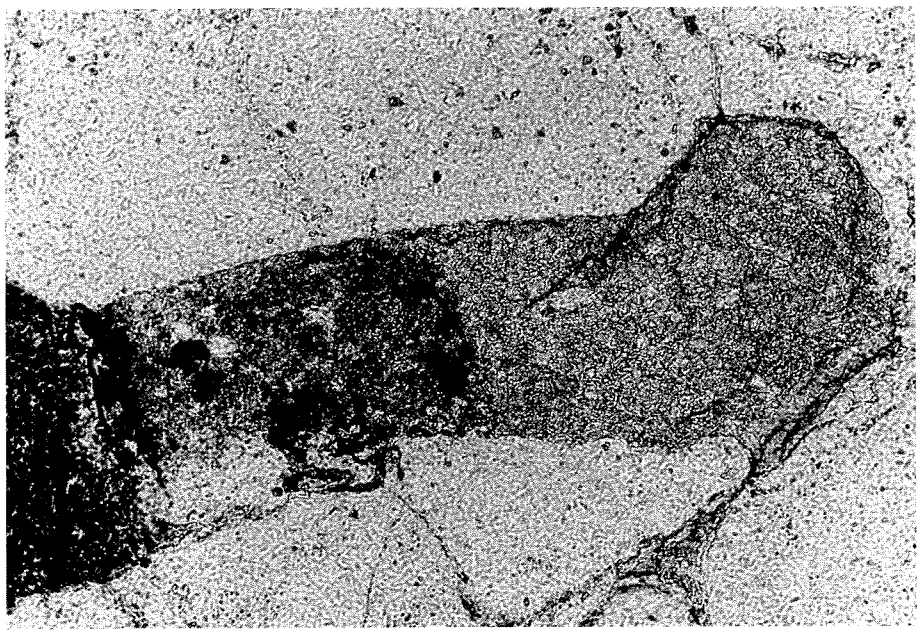

Figure 46. Ferruginous carbonate grading into chlorite (from left to right), interstitial to quartz. Base of picture is 0.9 mm (plane-polarized light)

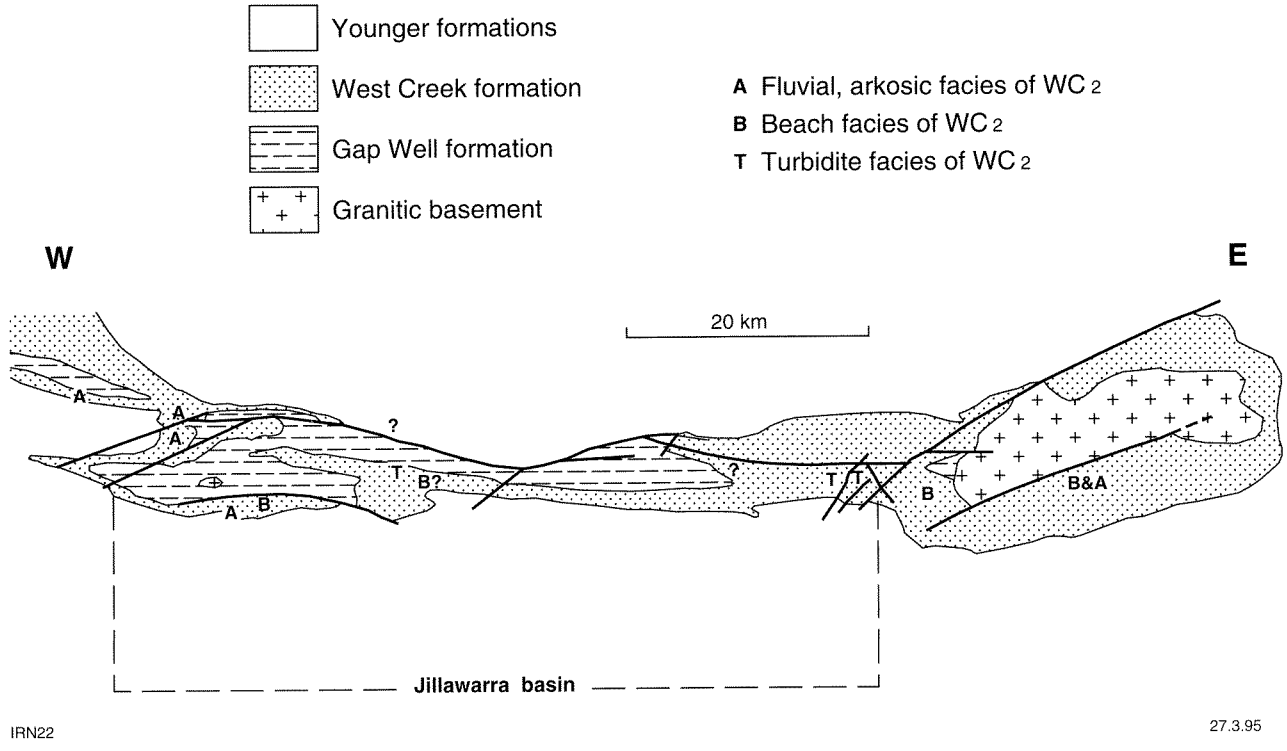

Figure 47. Facies distribution in the lower part of West Creek formation (Unit *WC2*) in the vicinity of basin-margin faults within the Jillawarra basin and adjacent areas

Petrography: In thin section, the fine-grained clastites are evenly laminated shale and micaceous siltstone, often ferruginous, with 2–10% detrital potash feldspar and a moderate amount of rounded shale clasts. As all thin sections were prepared from samples taken at outcrops, the carbonate content of some has been dissolved. Chemical analysis of a ferruginous micaceous siltstone yields 2.85% CaO plus 2.7% MgO, indicating greater than 5% dolomite. The Ba content of 304 ppm is comparable with the average content for arenite of 440 ppm Ba (Pettijohn et al, 1973).

Samples from one outcrop of Unit *WC3* consist entirely of micritic dolomite (27.30% CaO/15.97% MgO) veined by wispy quartz stringers (31.71% SiO_2). Besides 1.52% Al_2O_3 and 1.55% Fe_2O_3, no significant major- or trace-element values have been detected.

Chert horizons are common in Unit *WC3*, and they were probably a silicified dolomite. The rocks now consist of fine-grained chert and quartz material with diffuse iron hydroxide layers in places. Small carbonate inclusions indicate the former presence of carbonate, which has been silicified to form chert. In one section, the texture of ferruginous and pyritic ooids and ferruginous pellets within the cherty quartz is common (Fig. 48).

Depositional environment: For a facies interpretation, the lithologies in Unit *WC3* may be summarized as dolomitic siltstone and shale with minor interspersed dolomite lenses and oolitic, pelletal dolomite horizons. Locally, dolomite-cemented coarse-grained, subrounded wackestones are embedded in the dolomitic siltstone.

Hence, it is likely that quiet, shallow-water, tidal-flat conditions were re-established (similar to those in the Gap Well formation) after a period of high-energy clastic deposition (i.e. Units *WC1* and *WC2*). The dolomitic siltstone and shale represent intertidal sediments which received some terrigenous clastic input, as indicated by subangular potash feldspars. Possibly some mounds or swells did exist, where micritic carbonate could be deposited without clastic contribution. The occurrence of ooids suggests reworking of some material at the sediment–water interface by alternating tidal currents or wave action. Over these tidal flats some tidal channels meandered, depositing coarse-grained clastics within their banks; such deposits are now recognized as the isolated carbonate wackestone bodies. The abundance of lithic clasts and the angularity of potash feldspar in these rocks support their interpretation as channel deposits which had a nearby source of clastics. Figure 49 shows a small, coarse-grained and cross-bedded channel filling containing dolomitic siltstone.

Unit WC4

Distribution: This unit consists of coarse-grained, often cross-bedded ferruginous arenite with locally abundant quartz-pebble conglomerate interbeds some tens of centimetres in thickness. The maximum strike length of continuous outcrops is about 8 km at two localities (south of the Abra prospect and at the West Creek type locality). Elsewhere in the Jillawarra basin the unit is either absent or the arenite bodies have a limited strike extent. About 18 km west of the basin, a similar arenite unit appears (at the same horizon) over a strike length of 5 km in the southern part of Teano Range (Ruddock, I., 1982, pers. comm.).

The unit has a maximum thickness of 230 m, estimated from outcrop at the West Creek type locality. The basal contact against the softly weathering dolomitic siltstone of Unit *WC3* is well defined (although not sharp). In the

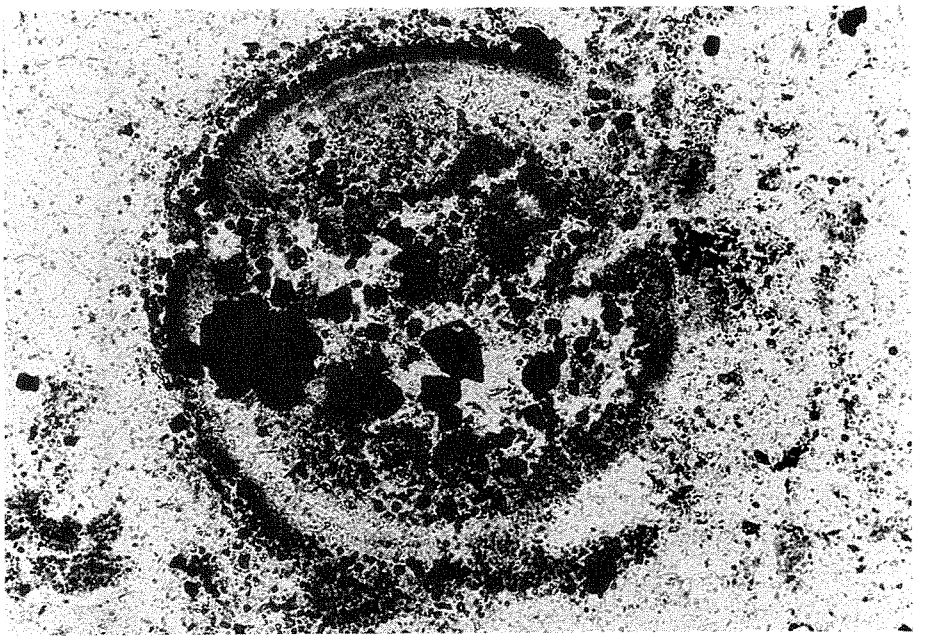

Figure 48. Ferruginous and pyritiferous possible ooid in chert horizon of Unit *WC3*. Base of picture is 0.9 mm (plane-polarized light)

uppermost portion the lithology gradually changes through micaceous and chloritic siltstone, towards the dolomitic siltstone of the lower part of the Jillawarra Formation.

In the vicinity of the Abra prospect, it is noticeable that the arenites are intensely silicified, causing a bluish colouring and the appearance of the rock as massive quartzite (Fig. 50). This is also a feature of the arenite occurrence in the southern part of Teano Range (Ruddock, I., 1982 ,pers. comm.).

Petrography: In thin section the arenites are moderately to well-rounded, well-sorted, coarse-grained quartz sandstones, which contain up to 8% subangular potash feldspar (microcline). The sandstone is completely recrystallized to massive quartzite (120° angles of 3-grain boundaries). Some interstices are filled with cherty quartz. The abundance of small carbonate inclusions suggests a former carbonate matrix.

Depositional environment: The following facts may be considered in relation to a facies interpretation:

(a) high maturity of the arenite with comparatively low content of potash feldspar;

(b) absence of lithic clasts and pellets;

(c) limited strike extent;

(d) in the Abra area Unit *WC4* seems to surround the granitic Coobarra Dome;

(e) at the West Creek type locality the strike length of the unit is somewhat limited by the Manganese Range and West Creek faults.

A beach or barrier-beach facies is inferred for Unit *WC4*, where the frequent reworking of clastics resulted in the increased maturity and sorting of the deposits. Shale clasts and calcareous pellets would have rapidly been destroyed in such an environment, resulting in 'clean' deposits of sand. A barrier beach is interpreted to have developed around the Coobarra Dome, which was probably a basement high during the deposition of Unit *WC4*. Due west of the Abra area, Unit *WC4* is absent. However, in the vicinity of the Manganese Range Fault, Unit *WC4* reappears, where it might tentatively be interpreted as a barrier beach that lay to the east of the Woodlands Dome. In this case the two faults (West Creek and Manganese Range Faults), which limit the extension of Unit *WC4*, may also define the boundaries of a basement high.

Despite the apparent control of faults on the outcrop pattern of Unit *WC4*, particularly at the West Creek type locality, it is considered unlikely that the arenite accumulated in sudsiding basins, as in the suggested depositional environment of the coarse-grained wackestone of the Unit *WC1*. The maturity of the sandstone in Unit *WC4* and the absence of lithic clasts seems to indicate beach deposits (Reinson, 1979) that developed through the growth of submarine sand and siltstone bodies, such as bars and spits.

Jillawarra Formation (*Mj*)

The Jillawarra Formation and higher stratigraphic units in the Jillawarra basin are characteristic of the overall Bangemall Basin and have been discussed earlier in the general description of the Bangemall Group (Chapter Two). In the stratigraphy established for the Bangemall Group by Daniels (1966) and Brakel and Muhling (1976), the Jillawarra Formation is regarded as one lithological unit. However, recent mapping in the Jillawarra basin has established that the formation may be subdivided into a lower calcareous unit (*Mjd*), and an upper unit consisting

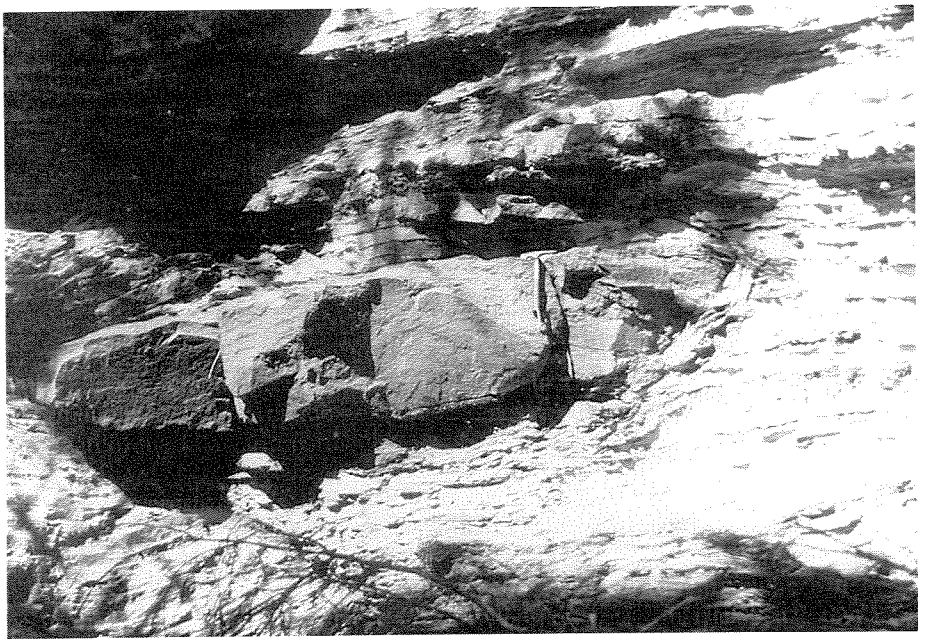

Figure 49. Coarse-grained arenaceous channel filling within dolomitic siltstone, Unit *WC3*

Figure 50. Quartzitic appearance of silicified arenite in Unit *WC4*, 3 km south of Abra

of variably coloured shale and minor chert (*Mjs*). This upper unit is comparable with the Jillawarra Formation elsewhere in the Bangemall Basin.

Unit Mjd

Distribution: The dominant lithology of this unit is dolomitic shale and subordinate massive pelletal dolomite beds. In the area north of the Quartzite Well Fault, to the east of Deverell Creek, ferruginous arenites and calcareous shale are equally abundant. South of the West Creek Fault there is a thick lens of greyish (sometimes chloritic) laminated shale that has a strike length of 5 km. Towards the margins, there is a facies change which is seen as an interlayering of whitish dolomite shale.

Because the dolomitic rocks are susceptible to weathering, the thickness of the unit can only be estimated. It is estimated that Unit *Mjd* may thin from 450 m at Jillawarra Bore (in the centre of the area) to virtually zero at Coobarra Dome in the east. The lower contact against the West Creek formation is well defined where the coarse beach deposits of Unit *WC4* are present, but the contact is somewhat arbitrary when the unit is absent.

Petrography: The ferruginous shale consists of thin layers of micaceous, fine-grained siltstone and thin layers of shale that is particularly rich in iron. Within the siltstone layers, subangular potash feldspar is present. Only insignificant amounts of lithic clasts have been observed. Within some dolomites abundant rounded to subrounded micrite pellets (0.2–0.5 cm in diameter) occur in a ferruginous micritic carbonate matrix, the latter containing subordinate fine-grained, well-rounded detrital quartz. According to Folk, (1959), if the pellet/matrix ratio exceeds three, the rock can be classified as a 'pellet dolomite'.

Depositional environment: The facies of the lower part of the Jillawarra Formation (*Mjd*) does not differ significantly from the facies of Unit *WC3*, although it is probably more variable. While the pellet dolomite probably formed in an upper intertidal environment, the arenites may represent tidal-channel fillings or beach deposits. Although a shallow-water, intertidal environment has been assumed for Unit *WC3*, the *Mjd* unit contains less-coarse clastic intercalations and there are no wackestones. This decrease in terrigenous clastics may indicate that the transgression of a shallow sea had commenced, but that there was no great increase in water depth.

Unit Mjs

Distribution: The main features of the upper Jillawarra Formation (equivalent to the facies of the Jillawarra Formation elsewhere in the Bangemall Basin) are described by Muhling and Brakel (1985).

Depositional environment: For the interpretation of facies development in the Jillawarra basin it is pertinent to note that, to the west of the Woodlands Fault, fine-grained, moderately sorted, rounded, quartz arenites are more abundant than the shale facies. In addition, there is probably a decrease in thickness west of the fault. It is likely that in this area there was some interfingering of open-marine shale facies with barrier-bar facies. A barrier bar to the west of the Woodlands Fault could have represented the western barrier to the evolving Jillawarra basin, within which shale deposition was taking place.

Chapter Four

Structure of the Jillawarra basin

The Jillawarra basin may be divided into eastern and western structural zones, which are characterized by style and intensity of deformation. East of the Abra fault system there is gentle deformation, and normal faulting in the area of the Coobarra Dome. This granitic basement dome marks the western margin of the stable Bullen Platform (Chapter Two). West of the Abra fault system the Jillawarra basin is within the Edmund Fold Belt, which is a structural zone of both open and tight folds and various types of faults. The intensity of folding decreases to the west of Woodlands Fault.

Folding

Folds observed range from gentle undulations, through tight upright folds with axial-plane cleavage, to thrusted overturned folds with cleavage parallel to bedding planes. For the convenience of terminology, folds are referred to as regional (half wavelength more than 2 km), major (0.5–2 km) or minor (10s to 100s of metres).

The overall structure of the Jillawarra basin is a regional easterly striking anticlinorium comprising the Jeds Anticline, Manganese Range Anticline, and Coolina Anticline which plunge eastwards towards the Abra fault system. Towards the west, the axis of the anticlinorium runs parallel to the Quartzite Well Fault, and extends beyond the mapped area in a west-northwesterly direction. Equally important, but restricted to the western half of the Jillawarra basin, is a regional anticline whose axial trace trends easterly and plunges both to the east and west, to form the Woodlands Dome. While these regional anticlinal structures have a tight style of folding, the major synclines (Woodlands Syncline, West Creek Syncline, the syncline south of Abra) and the major Abra Anticline are of more open style with moderate to shallow dips. The occurrence of tight anticlines and open synclines is in contrast to the general style of deformation in the Bangemall Basin, where synclines are the tighter structures. In the Bangemall Basin most tight regional folds (regardless of whether they are synclines or anticlines) occur in grabens, and this is also the case in the Jillawarra basin. Folding in the Jillawarra basin comprises four types which are described in their presumed order of development.

Slump folds

Slump folding and sliding, on low-angle slide planes, are evident in drillcores from the Gap Well and West Creek formations within the Jillawarra basin. Similar structures have been noted by Muhling and Brakel (1985) in the Kiangi Creek Formation of the Glen Ross Anticline (about 25 km north of the Jillawarra basin). These features are interpreted to be the result of deformation within plastic sediments.

Drape folds

With progressive burial of the sediments (involving dewatering and higher confining pressure) large thicknesses of strata were subjected to plastic deformation, in the form of drape folding. This ductile style of folding develops in the sedimentary strata ('cover') over the edges of vertically moving basement blocks. The geometry and strain pattern of this fold style has been demonstrated in experiments by Friedman et al. (1976) and Weinberg (1979). The resultant folds are box shaped, with relatively steep limbs and a flat central axial zone.

Many fold structures in the Jillawarra basin, particularly the anticlines, cannot be described as drape folds as they are tightly folded with steeply dipping limbs. However, they probably were drape folds initially, and it is presumed that this style of folding was once widespread in the Jillawarra basin.

Tight folds

The main tight-fold structures are the Jeds and Manganese Range Anticlines and the Woodlands Dome Anticlinorium. However, small-scale tight folds have been observed in the limbs of open folds, as in the southern limb of the major West Creek Syncline, in the regional Range Creek Syncline (3 km northwest of Quartzite Well), and in the southern limb of the Abra Anticline. Minor tight folds are abundant in the Gap Well formation, between the West Creek Syncline and the Woodlands Syncline. These subsidiary tight folds probably formed through a process of shortening, subsequent to the extensional period, and were superimposed onto major open folds.

It is evident from a consideration of structure in the Bangemall Basin (Muhling and Brakel, 1985), and from the Jillawarra basin (e.g. thrusting along the Quartzite Well Fault), that shortening occurred after the extensional period. Although shortening of basement can generate drape folds (Weinberg, 1979), further compression would lead to a tightening of these drape-fold structures. This mechanism could have produced the tight folds in the Jillawarra basin.

The style of folds is roughly similar to those described by Hobbs et al. (1976). For synclines, thinned limbs and thickened hinge zones, as measured parallel to the axial surface, are inherent in drape folding. The tight anticlinal structures were sites for the upward release of strain, which was created by differential shear in response to the development of folds at depth (Ramsay, 1962). The structures are not ideal similar folds, but because of the alternation of competent and incompetent layers, they are of class 1c (convergent isogons) and class 3 (divergent isogons) according to Ramsay (1967).

It is possible that in the western part of the Jillawarra basin, the area between the Quartzite Well Fault to the north and the West Creek Fault to the south was a regional box-shaped, drape-folded syncline (the 'Jillawarra basin') which was initially related to graben formation. When the shortening strain regime commenced, the graben was uplifted so that compressional forces were applied to the overlying sedimentary strata. The drape-folded margins of the former graben continued to shorten to form two tight anticlines; the Jeds Anticline and the Woodlands Dome Anticlinorium. The principal process of formation of two tight anticlines at the margins of a graben is depicted in Figure 51.

Folds associated with thrusting

In areas where the increase in lateral shortening could not be compensated for by the upward movement of the former graben, thrusting of the basement occurred. On Plate 1, section C–D shows the presumed style of thrusting of the basement and the concomitant folding in the cover. The thrusting took place along the Quartzite Well Fault, one of the two major thrust-fault systems in the Bangemall Basin.

The Manganese Range Anticline — in which thrusting was most intense — has its anticlinal axis truncated by the Quartzite Well Fault in the west, because of the arcuate nature of that fault. The southern limb of the anticline has steep southerly dips (60–70°) and shows no subsidiary folds; the fold style of the southern limb is therefore that of the tight folds described above. The northern limb of the anticline, however, has been thrust towards the north-northeast. In this limb there is abundant tight, subsidiary folding, together with tight minor folds which are locally overturned towards the main thrust zone in the north. In some subsidiary folds, break thrusting has resulted in the northerly dipping limbs being either suppressed or absent.

It is proposed that the tight folding is related to thrusting, and this is supported by the following evidence:

(a) The vergence — in the sense of Stille (1930), the facing of a geological structure — of all minor folds in the northern limb of the Manganese Range Anticlinorium (section C–D, Plate 1) is in a northerly direction. Thus the minor tight folds are asymmetrical in profile, showing very steeply dipping north limbs and shallow dipping south limbs.

(b) The trend of the tight, minor fold axes is parallel to the strike of the main (northernmost) thrust of the Quartzite Well Fault. This fact alone indicates a relation between thrusting and folding. Furthermore, the folds are asymmetrical in plan view as shown schematically in Figure 52A.

Sometimes there is small-scale break thrusting along the axial-plane surfaces. Remarkably, the plunge of these minor folds is often in a west-southwesterly direction, whereas the overall plunge of the Manganese Range Anticline is to the east.

The mechanism of formation for these fold structures becomes evident when the tectonic forces are regarded as the resultant of three principal vectoral forces, as illustrated in Figure 52B. While the initial tight folding can be ascribed to the northerly component and break thrusting to the upward component, the asymmetry in plan view of the fold traces is probably due to an easterly component. Thus the tight, asymmetrical minor folds in the northern limb of the Manganese Range Anticline may be drag folds formed by thrusting along the Quartzite Well Fault.

Variations in fold style

Lateral variation

The regional easterly trending anticlinorium determining the overall structure of the Jillawarra basin (Jeds Anticline–Manganese Range Anticline–and its closure east of the Copper Chert prospect) is characterized by different styles of folding along strike.

(a) East of Copper Chert prospect, where the closure of the regional anticlinorium is marked by the Y-shaped ridges of the lower part of West Creek formation (*WC2*), the dips of arenite ridges are steep, even though the fold style approaches that of open folds. Open-style folding with shallow dipping limbs occurs in the western extension of Jeds Anticline (Fig. 1), at the northwestern edge of the area mapped for this study.

(b) In the western parts of the Jillawarra basin, north of the Woodlands Syncline (section A–B on Plate 1), folding is tight and symmetrical with steep dips on both limbs.

(c) Finally, in the Manganese Range Anticline the last stage of folding is related to thrusting, and this has resulted in tight, north-vergent, asymmetrical folding.

There appears to be a relation between faulting and the style of folding. Where faults are absent the resultant fold style is open (case (a) above). These open folds are interpreted to have formed on rigid basement blocks. Tight folds (case (b)) occur in the vicinity of easterly

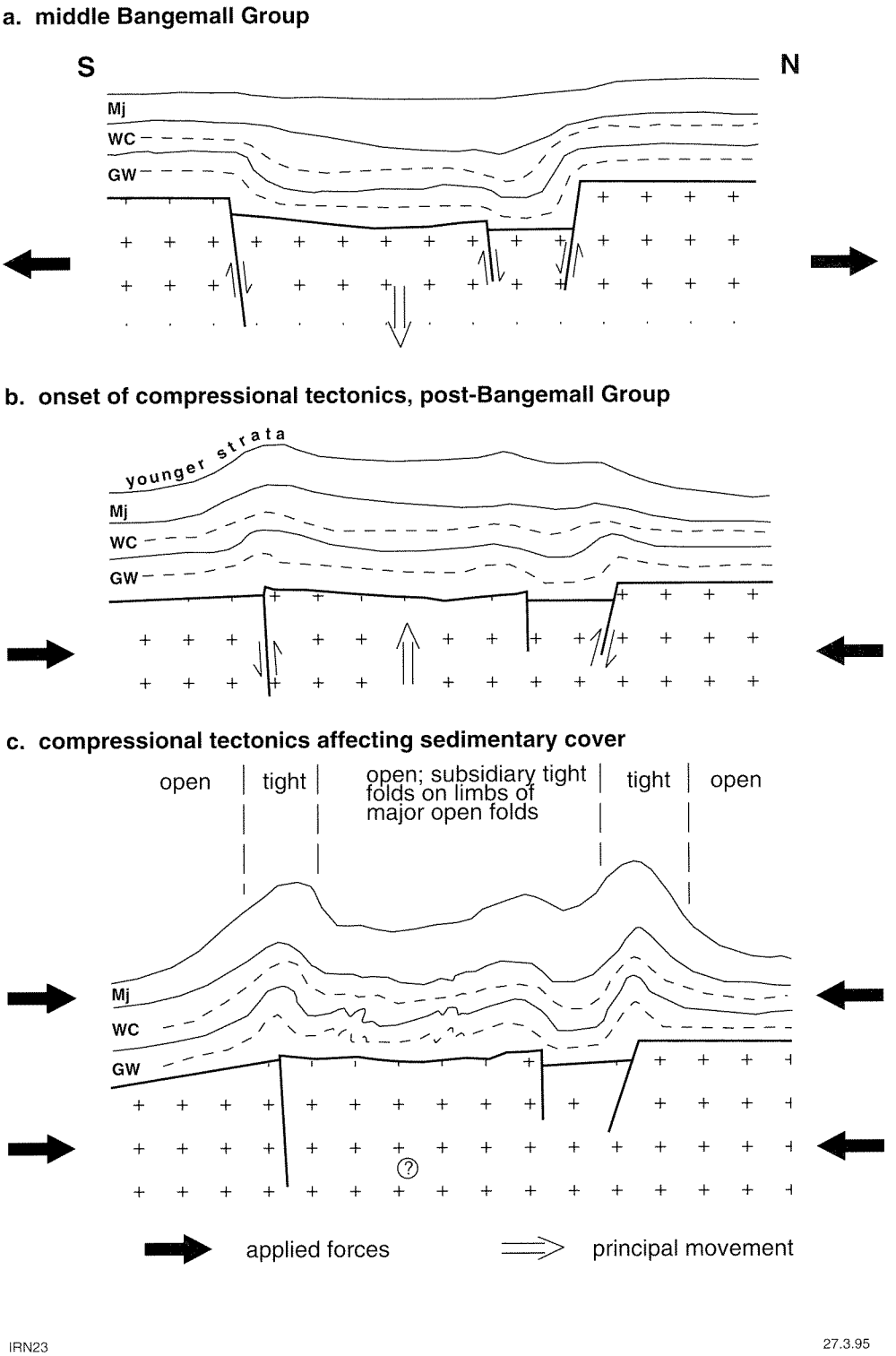

Figure 51. Schematic structural cross section through the western part of the Jillawarra basin (near section A–B, Plate 1) showing the development of tight folds at the margins of an upfaulted graben

trending faults, e.g. the Quartzite Well Fault, which probably mark the boundaries between basement blocks. Where the basement blocks are thrusted case (c) applies.

It may be concluded, therefore, that the basement has controlled deformation in the cover, in that the location and the intensity of block faulting in the basement have determined the location and the extent of deformation in the sedimentary cover.

Vertical variation

Locally there is a marked difference in degree of deformation between the Gap Well formation, plus Unit *WC1*, and Units *WC2* to *WC4* of the West Creek formation plus overlying formations. This difference is apparent in the abundant small-scale subsidiary (parasitic) folding of the lower parts and in a possible disconformity between Units *WC1* and *WC2* in the area to the southeast of the Copper Chert prospect.

These variations in deformation may be interpreted as follows:

(a) A difference in competency between the Gap Well formation (dolomitic shale which deforms plastically) and the West Creek formation (arenite) which is far more competent.

(b) However, Unit *WC1*, even with its coarse arenite portions, behaves similarly to the incompetent Gap Well formation. Unit *WC1* has been interpreted to represent the filling of localized, rapidly subsiding basins. So it is likely that, for such coarse clastic deposits, a single sediment complex would be wedge shaped and horizontally inclined. Later subsidence, on a more regional scale, could then have further inclined the surface of Unit *WC1* with respect to the sedimentary base of Unit *WC2*, which was deposited disconformably on Unit *WC1*. However, this disconformity does not necessarily indicate a significant time break.

(c) When drape folding commenced over the moving basement blocks, strain was greatest in the lowermost strata, and decreased upwards as the differential shear transferred from below was progressively compensated for by the deformation of these strata (Weinberg, 1979). Although this process may be important on a large scale with respect to the Bangemall Group as a whole, it probably had little significance for the deformational difference between the Gap Well and West Creek formations in the Jillawarra basin.

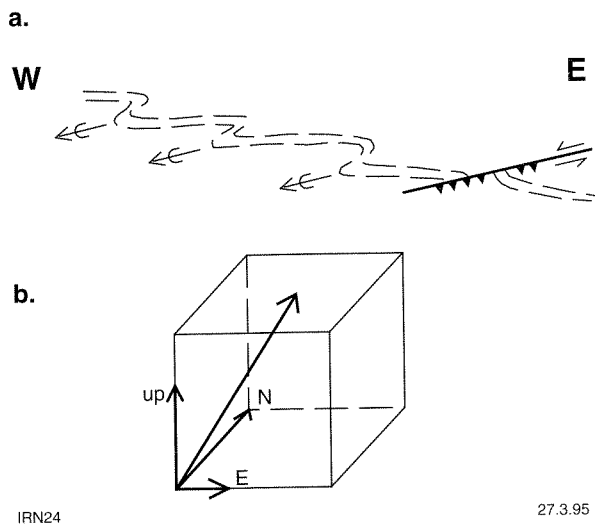

Figure 52. Schematic plan view of tight minor folds, showing: (a) symmetry of fold traces and break thrusting; and (b) vectoral forces inferred from the resultant movement to the north-northeast. Northern limb of Manganese Range Anticline

Cleavage

Within the central zone of the Jillawarra basin, where open folds predominate, cleavage is poorly developed. Newly grown muscovite usually lies parallel to bedding; a result of compaction during burial. However, axial-plane cleavage is common in the hinge zones of subsidiary tight folds, which are common in the Gap Well formation within the central zone of open folds (Fig. 51C).

Cleavage, expressed by the development of chlorite, occurs in the Manganese Range. However, as the latest folding was related to thrusting, the cleavage strikes parallel to Quartzite Well Fault in the northern limb of the Manganese Range Anticline, and deviates from the strike of the regional axial plane by about 20°. Thus the cleavage — at least in the vicinity of the Quartzite Well Fault — developed through differential shear associated with thrusting, such that movement along cleavage planes probably took place in an upward, northward and eastward direction. Shear cleavage is also in good agreement with the frequent parallelism of bedding and cleavage, particularly in the northern limb of the Manganese Range Anticline.

The dominant cleavage direction throughout the Jillawarra basin is 110° and dips are mainly vertical. The cleavage maintains its strike of 110° irrespective of the local trends of minor and major folds. The mean strike of 110° lies normal to the regional north-northeast to south-southwest compressional forces, which are inferred from thrusting along the Quartzite Well Fault. However, this cleavage is not related to the thrusting itself, because the 110° strike is still dominant where no thrust faults have been observed.

Faulting

Within the Jillawarra basin there are three main trends of faults; northeasterly, subordinate southeasterly, and easterly. The latter fault trend may have an arcuate fold trace, like the Quartzite Well Fault and the West Creek Fault. Most faults are normal except the easterly trending Quartzite Well Fault, which is thrusted.

Normal faults

Although very few fault planes are exposed, it is assumed that the normal faults have steeply dipping fault planes.

(a) Northeasterly trending faults are the most abundant. They have confined the depositional system of the Jillawarra basin in the west (Woodlands Fault) and in the east (Abra fault system).

Commonly, they affect lower stratigraphic units in the basin. While the offset is obvious in the Gap Well formation and lower units of the West Creek formation, faulting has only a minor influence on strata of the Jillawarra Formation and higher stratigraphic units. For example, in the southern area of the Woodlands Fault the arenite ridge of Unit *WC2* is displaced about 300 m by the fault, whereas in the outcrop of Jillawarra Formation (*Mjs*), to the south of this, the horizontal offset by faulting is less than 100 m (Plate 1).

Northeasterly trending faults were active during the earliest deposition of the Bangemall Group. The Manganese Range Fault probably acted as a boundary between the deposition of reef carbonate and sandy carbonate in the upper Gap Well formation (Chapter Three), whereas the Woodlands Fault marks the transition from beach deposits to shallow-water slope turbidites at the western margin of the Jillawarra basin, as seen in Unit *WC2* of the West Creek formation.

Movement along northeasterly trending faults occurred earlier than folding. This is shown by a folded fault in the eastward extension of the anticline south of Jeds Anticline (in the north-western part of Plate 1). Except for the Manganese Range Fault, the sense of the last horizontal movement of the northeasterly trending normal faults (which may have occurred after deposition of the Bangemall Group) has been dextral, i.e. to the east of the fault, the rocks have moved relatively to the southwest.

The Abra fault system is a component of the regional northeasterly trending Tangadee Lineament. About 100 km due west there is another northeasterly trending regional lineament known as the Flint Hill Lineament. Thus the area of the Jillawarra basin (plus some 15 km to the west) appears as a structural domain which is limited by two regional lineaments. The north-easterly trending normal faults within the Jillawarra basin are most probably related to these lineaments and may have been produced by the same regime of crustal strain as were the regional lineaments (Chapter Two). This regime extended from the time of deposition of upper Gap Well formation to later than deposition of the top of the Bangemall Group.

(b) Southeasterly trending faults occur in the eastern part of the Jillawarra basin, and they affect the West Creek formation (e.g. east of Abra) as well as units stratigraphically higher (e.g. displacing the Discovery Chert northwest of Copper Chert). Variations in displacement with respect to the stratigraphic level could not be quantified in the field. Although little is known about the south-easterly trending faults, their relative abundance in the eastern part of the Jillawarra basin (i.e. at the eastern margin of the Edmund Fold Belt) suggests that there is an additional structural trend in the eastern part of the Jillawarra basin.

(c) The easterly trending arcuate West Creek Fault is a normal fault, which dips at about 60° in a northerly direction. Other easterly trending normal faults occur in three areas; to the north of West Creek Well, in the closure of the regional Coolina Anticline to the south and southeast of Copper Chert prospect, and in the southern limb of the Abra Anticline. The occurrence of easterly trending faults in the hinge zone of anticlinal structures north of West Creek Well and southeast of Copper Chert prospect suggests that they formed during folding. This style of faulting is characteristic of a higher strain rate. Only minor displacement is associated with this late-stage faulting.

The West Creek Fault (or fault system) formed early in the deposition of the Bangemall Group, and it has influenced deposition of the West Creek formation (*WC2*). The fault system has also been active during the late-stage deformation of the Jillawarra basin because brecciation and silicification, within the fault zone, suggest faulting of lithified rocks. Late-stage faulting has resulted in considerable east-northeasterly movements (2 to 3 km).

The easterly trending fault in the southern limb of the Abra Anticline has formed in the lowermost West Creek formation. It lies parallel to the inferred margin of the Jillawarra basin, and it defines the northern limit of the Abra sub-basin. This fault zone probably had a major control on the mineralizing processes that produced the Abra deposit. Late-stage movement along the fault probably caused upfaulting of the former sub-basin.

Of the normal faults described above, the West Creek Fault and the easterly trending fault in the southern limb of the Abra Anticline may originally have been normal faults. The last movement, however, was developed in the opposite (reverse) sense, due to the late-stage upfaulting of the former graben.

Reverse faults and thrust faults

Faults associated with the arcuate, easterly trending Quartzite Well fault system are either reverse or thrust faults. The Quartzite Well Fault, which is probably a major basement fault, defined the northern margin of the Jillawarra basin. During crustal shortening, the graben was uplifted so that reverse faults developed, e.g. north of the Woodlands Syncline and north of the Abra prospect (as

shown in sections A–B and E–F, respectively, Plate 1). Where lateral shortening was most pronounced, thrust faults were produced.

Both types of fault developed during late-stage tectonism in the Jillawarra basin, because faulting has affected lithified rocks (evident from brecciation and silicification in fault zones). The truncation of north-easterly trending faults by the Quartzite Well fault system provides further evidence that movement along the fault system was a late-stage event.

Maximum stratigraphic displacement (upward movement) along the Quartzite Well Fault may, theoretically, reach 3 km in the vicinity of Quartzite Well. There has also been sinistral displacement where the fault system bends to the northeast. However, the above estimate of displacement could change if facies variations across the presumed basin-margin fault are considered.

Westwards from Jillawarra exploration camp, the fault trace gradually becomes northeasterly trending and the north-northeasterly direction of movement is oblique to the fault. Therefore, a number of easterly and east-northeasterly trending subsidiary faults have formed in order to compensate for the deviation from the direction normal to the compressional forces. To the east, near Copper Chert prospect, the displacement along the Quartzite Well Fault decreases rapidly and the fault splays towards the east.

In the Jillawarra basin it would appear that the amount and the rate of lateral shortening (both within the basement and in the sedimentary cover) have determined the amount of thrusting and whether or not reverse or thrust faults could develop. However, these factors alone cannot account for the contrast between considerable thrusting at Quartzite Well, and the splay fault north of the Copper Chert prospect.

There seems to be some relationship between the nature of the basement and the amount of thrusting in the basin. It is possible that the location and strike of the early margin faults (i.e. the shape) of the Jillawarra basin has influenced later deformation. But, it could also be possible that the degree of subsidence (i.e. extension of the basement) was highest in the central part of the Jillawarra basin, and that this caused the most pronounced uplift and thrusting in that area during the period of compression. Perhaps both factors, the shape of the basin and the degree of subsidence, influenced the eventual amount and degree of deformation.

Summary

The Jillawarra basin — bounded by northeasterly trending and easterly trending normal faults — formed as a result of a tensional crustal regime during the early stages of sedimentation. While infilling of the basin took place, drape folding (initiated by normal block faulting in the basement) caused stronger deformation in the lower stratigraphic units. Probably after all of the Bangemall Group had been deposited, compressional forces were applied to the basement. In areas of greatest shortening, the forces acting on the basement transmitted strain to the sedimentary cover. The compressional forces caused an uplift of the Jillawarra basin along the easterly trending margin faults. The upward movement was most intense in the area of Quartzite Well and eventually caused thrusting in a north-northeasterly direction. Shearing associated with uplifting of the basin caused the development of a regional cleavage direction striking 110°.

Throughout the deformation of the Jillawarra basin, the fold style remained open in areas where no major basement faults occurred. However, in the areas where basement faults occur, the former open-style drape folds were converted to tight folds, or to north-vergent tight folds that were related to thrusting. The general structure of the modern Jillawarra basin is marked by a northern, regional, easterly trending anticlinorium (Coolina Anticline), which is asymmetric in the area of Quartzite Well. In the western half of the Jillawarra basin there is a southern, major, easterly trending anticlinorium which plunges eastwards and disappears at about longitude 118° 23'E. Both the northern and southern anticlinoria probably mark the margins of the original Jillawarra basin.

Chapter Five

Igneous rocks of the Jillawarra basin

Most igneous rocks in the Jillawarra area are dolerite intrusions (mainly sills and some dykes), which have affected the Jillawarra Formation and higher stratigraphic levels. No igneous rocks have been found within the Jillawarra basin; i.e. in the Gap Well and West Creek formations between the Woodlands Fault and the Abra fault system.

Mafic intrusions

East of the Jillawarra basin (i.e. east of the Abra fault system) minor dolerite was encountered in two percussion drillholes south of Cadabra Hill. The dolerite intrudes the upper Gap Well formation or lower West Creek formation. The emplacement was probably controlled by the main northeasterly trending fault (Plate 2) or its splay fault, which separates the granitic, stable basement of the Coobarra Dome from the Jillawarra basin and its underlying more mobile basement.

Since this northeasterly trending fault is related to the regional Tangadee Lineament, and since the emplacement of dolerite related to the regional Flint Hill Lineament has been noted further west at Teano Range (Ruddock, I., 1982, pers. comm.), it seems likely that the dolerite intrusion (either as a dyke or a sill) at Cadabra Hill was controlled by the northeasterly trending fault.

Felsic volcanics of Coobarra Dome area

Rhyolite

At 23°37'S, 118°47'E approximately 60 m above the basal unconformity of the Bangemall Group there occurs a line of six small rhyolite bodies (Tangadee rhyolite) within the lower part of Unit *WC2* (Plate 1, Fig. 53). The rhyolite shows varicoloured banding of uncertain origin. In thin section the felsic rock consists mainly of euhedral quartz and feldspar phenocrysts, in a cryptocrystalline groundmass of quartz and minor microcline, with accessory biotite, chlorite, zircon, and opaques.

The quartz phenocrysts show hexagonal or rhomboidal outlines, preserving the bipyramidal shape of ß-quartz. Most phenocrysts are embayed, indicating resorption or corrosion by the groundmass, and many phenocrysts have become well rounded. The feldspar phenocrysts consist of a granular intergrowth of quartz and microcline, and were considered by Gee et al. (1976) to have originally been sanidine. These authors also reported rare, irregular or distinctly spherical-shaped lithophysae of pyrite, ilmenorutile, chlorite, and carbonate encased by quartz and microcline. The lithophysae are wrapped by the banding and therefore were in existence as solid objects while the volcanic material was still moving.

Chemical analyses of four samples of Tangadee rhyolite are given in Table 4. It is obvious from comparison with the average chemical composition of rhyolites (Nockolds et al., 1968) that this rock is highly altered, as emphasized by extremely high K_2O, extremely low Na_2O and a slight increase in SiO_2. The enrichment of K at the expense of Na is a common type of alteration and has been reported by Nockolds et al. (1978) and Fischer and Schmincke (1984).

Gee et al. (1976) concluded, from the excellence of textural preservation and the occurrence of fresh sulfides, that alteration of the Tangadee rhyolite considerably predates any recent weathering. However, complete chemical reconstitution of the rock does not allow the determination of timing and mechanism of the alteration. The Rb/Sr-age of 1098 ± 42 Ma is believed to date this alteration event. According to Gee et al. (1976), the rhyolite formed by local melting on a movement plane in the granitoid basement of the Coobarra Dome. However, experimental data yield no indication of the true initial $^{87}Sr/^{86}Sr$ ratio, so there is no isotopic evidence of the origin. The ryholite occurrence has been interpreted as an extrusion of felsic material along fissures with an east-northeasterly trend, parallel to the regional Tangadee Lineament.

Lapilli tuff

South of Cadabra Hill, about 10 km west of the occurrence of Tangadee rhyolite, there is a small elongated outcrop of lapilli tuff. It has a thickness of about 1 m, a strike length of 50 m at 070°, and probably is conformably overlain and underlain by rocks of the lower part of Unit *WC2*. The lapilli tuff is composed of layers of lapilli of varying grain size (1–8 mm) showing graded bedding

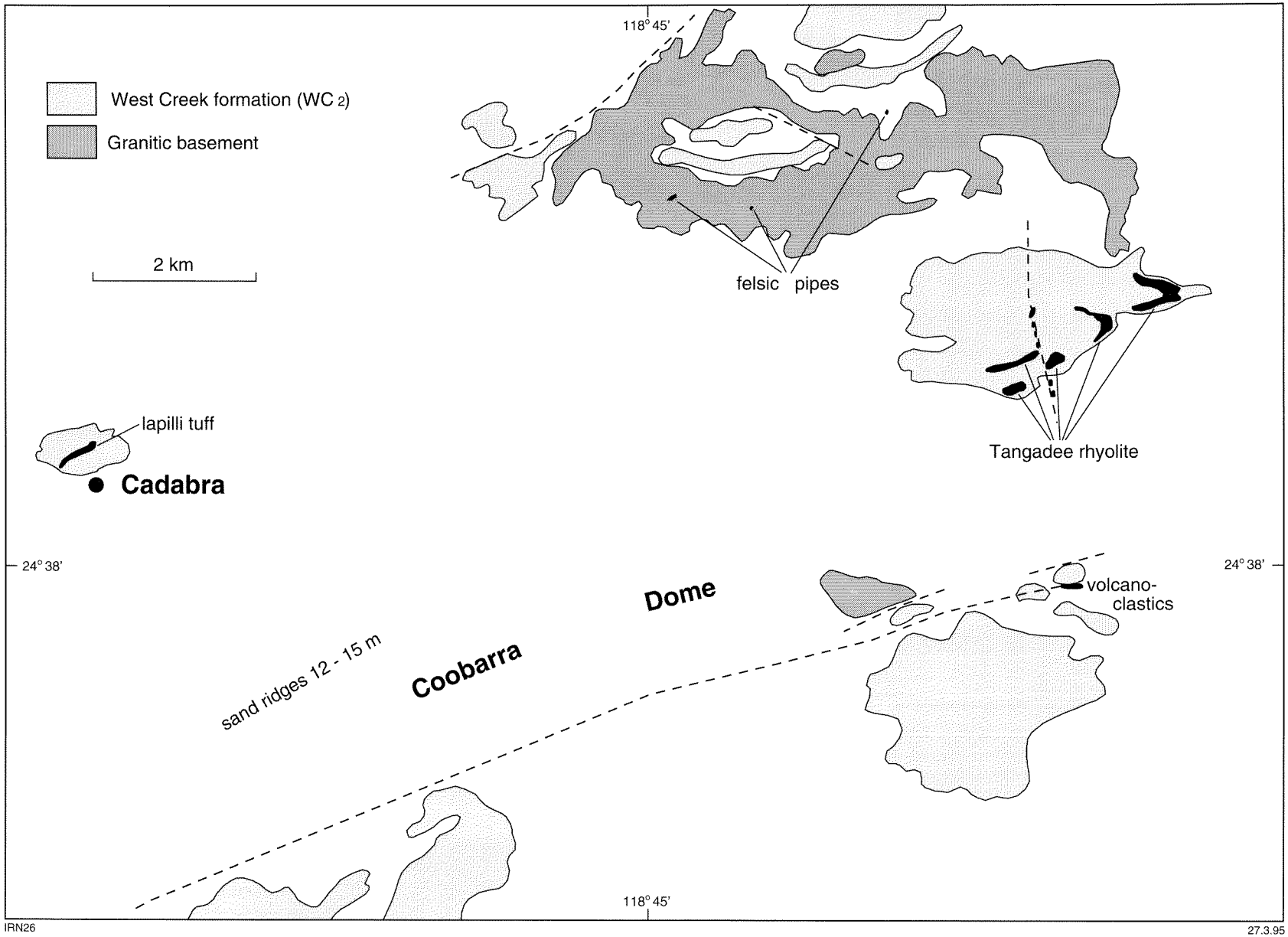

Figure 53. Locations of felsic volcanogenic rocks in the area of Coobarra Dome

within the individual layers. These layers are separated by bands (1–3 cm thick) of lapilli-free tuffaceous material.

The lapilli are ovoid with their longer axis almost perpendicular to the bedding. A similar orientation of the longer axis of quartz crystals perpendicular to the laminations of crystal tuffs has been noted by Pettijohn (1975, p. 307) who suggested that this orientation is inherited from the 'way they have fallen into it'. In thin section the lapilli resemble accretionary or armoured lapilli (Fisher and Schmincke, 1984) with coarse vesicular pumice shards in the core and fine-grained tangentially aligned platy shards forming the rim (Fig. 54). Minor angular, sometimes embayed, quartz grains occur in the coarse parts of the lapilli.

It is possible to use the type of lapilli to distinguish between pyroclastic eruptions (caused by expansion of gases initially contained within the magma) and hydroclastic eruptions (caused by vaporization of external water in contact with hot magma or lava). These are the two general categories of eruption according to Fisher and Schmincke (1984). Armoured lapilli have only been reported from hydroclastic eruptions. As the lapilli in the Cadabra Hill area are probably intermediate between the accretionary type (pumice and ash aggregates) and the armoured type (crystalline aggregates, such as the quartz grains mentioned above), it is possible that they formed during hydroclastic eruptions.

The type of magma can be inferred from the nature of the glass shards. Although there are many variables affecting the shape of glass shards, there is evidence to show that pumice shards will tend to develop from magmas with relatively high viscosity at temperatures below 850°C (Fisher and Schmincke, 1984).

Table 4. Chemical analyses of siliceous volcanogenic rocks in the area of Coobarra Dome

	1	*2*	*3*	*4(a)*	*5(a)*	*6(b)*	*7(b)*
				percentage			
SiO_2	78.0	76.1	74.9	83.4	79.7	85.23	76.45
Al_2O_3	11.1	12.3	12.3	10.24	9.97	9.02	10.62
Fe_2O_3	0.66	0.62	1.06	0.43	2.93	1.97	5.18
MgO	0.02	0.02	0.23	0.17	0.71	1.03	1.92
CaO	0.10	0.06	0.04	0.18	0.11	0.07	0.08
Na_2O	0.15	0.15	0.20	0.55	0.27	0.10	0.23
K_2O	9.06	9.21	10.45	9.66	3.59	1.99	0.04
MnO_2	<0.01	<0.01	<0.01	<0.01	0.02	0.01	0.03
TiO_2	<0.01	<0.01	<0.01	0.04	0.11	0.13	0.34
P_2O_5	<0.01	<0.01	<0.01	<0.01	0.03	0.03	0.04
H_2O^+	0.51	0.80	0.29	n.d.	n.d.	2.95	1.13
SO_3	0.04	0.03	0.03	n.d.	n.d.	0.03	0.03
				parts per million			
As	n.d.	n.d.	n.d.	<0.2	<0.2	n.d.	n.d.
Ba	n.d.	n.d.	n.d.	460	2 950	3 356	85
Be	n.d.	n.d.	n.d.	<0.5	3	n.d.	n.d.
Bi	n.d.	n.d.	n.d.	<2	<2	n.d.	n.d.
Cd	n.d.	n.d.	n.d.	<0.5	<0.5	n.d.	n.d.
Co	n.d.	n.d.	n.d.	<1	2	<1	3
Cr (c)	2 189	1 779	274	325	85	26	16
Cu	45	190	110	5	10	17	24
Mo	<10	<10	<10	2	1	n.d.	n.d.
Ni	n.d.	n.d.	n.d.	4	5	3	16
Pb	110	110	65	6	46	n.d.	n.d.
Rb	150	160	180	n.d.	n.d.	111	<1
Sr	20	20	20	18	71	57	83
W	5	<5	<5	<10	<10	n.d.	n.d.
Zn	17	16	15	7	46	<1	24
V	<56	<56	<56	<1	14	28	12
Total (%)	**99.97**	**99.57**	**99.87**	**104.78**	**97.74**	**102.53**	**96.43**

Notes: 1,2,3. Tangadee rhyolite, Coobarra Dome area (Gee et al., 1976)
4. Tangadee rhyolite
5. Lapilli tuff south of Cadabra Hill
6. Lapilli tuff south of Cadabra Hill
7. Black, felsic, pipe-like intrusion in granite, about 2.5 km north-northwest of Tangadee rhyolite. Weathered surface of sample has not been removed

(a) Analyst: Chemex Labs Ltd, Canada, using ICP and AAS
(b) Analyst: Geology and Palaeontology Institute, University of Hamburg, West Germany, using XRF
(c) Cr values in excess of 60 ppm are probably analytical artefacts

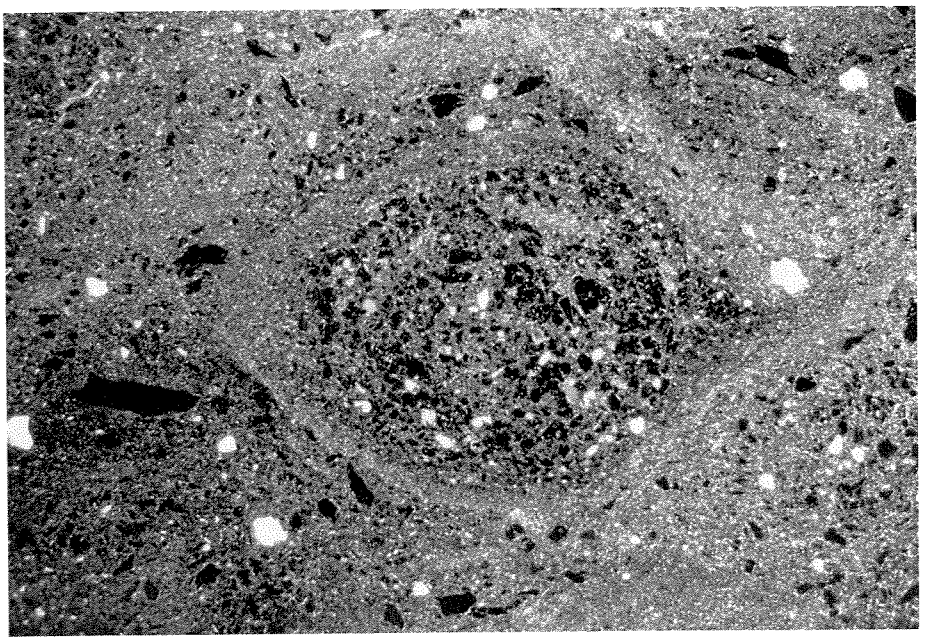

Figure 54. Lapilli with coarse pumice shards in the core and fine-grained platy shards as rims. Lapilli tuff, south of Cadabra Hill. Base of picture is 5.6 mm (crossed polars)

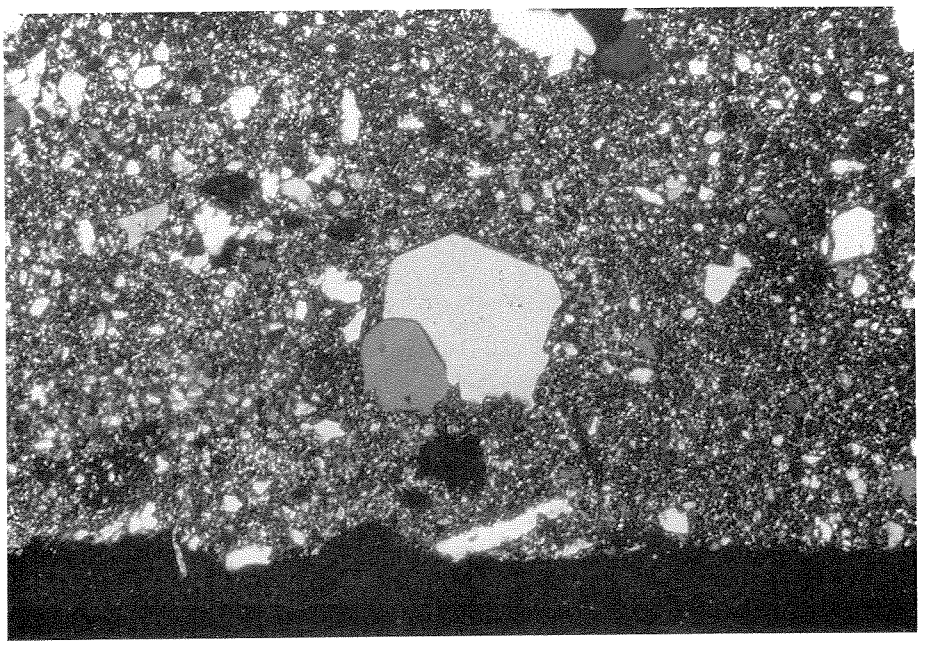

Figure 55. Euhedral quartz grain in siliceous matrix, volcaniclastic rocks, 2 km south of Tangadee rhyolite. Base of picture is 3.6 mm (crossed polars)

The whole-rock chemistry (Table 4) indicates that the K-alteration shown by the rhyolite did not affect the lapilli tuff. By comparison with chemical analyses of 7 tephras of rhyolitic fall-out and flow deposits presented by Fisher and Schmincke (1984), it is evident that the lapilli tuff is impoverished in both K and Na, but enriched in Si. This chemical trend may best be explained by the leaching of Na^+ and K^+ ions accompanied by the concomitant relative enrichment of SiO_2. However, the timing of this leaching remains unclear. Leaching could have occurred either when the lapilli (presumably subaerially deposited) were first covered by water during the period of deposition of Unit *WC2*, or during recent weathering. Recent weathering, indicated by the occurrence of liesegang rings, may also have caused an increase in Fe content (Table 4).

In comparison with the results of the above authors, barium is enriched within the lapilli tuff. As the immobility of Ba during weathering has been demonstrated (Mann, 1982; Taylor, 1983), it can be inferred that the introduction of Ba was an early event. Two possible processes for Ba introduction are envisaged:

(a) The barium-rich hydrothermal system, which probably was most active during deposition of the lapilli tuff, was linked to the sites where rhyolitic magma was generated within the basement. Water added to the magma (through faulting and fracturing of the basement during deposition of the lower part of Unit *WC2*) was enriched in Ba and, during vaporization of the water, Ba was added to the vapour phase prior to eruption.

(b) After deposition and initial burial of the lapilli tuff, the diagenetic formation waters were rich in Ba. This seems to have been the case in the hanging wall of the Abra deposit, which now has about 3000 ppm Ba in rocks that lie about 30–40 m above the top of the mineralization. The barium-enriched waters could have precipitated their solute as barite or as replacement of Na and K; in this case Ba has been added after eruption.

Other volcaniclastic rocks

About 2 km south of the Tangadee rhyolite, on the down-faulted southern side of an east-northeasterly trending fault, there are two elongated bodies of poorly preserved, silica-rich volcaniclastic rocks. To the north the outcrops are limited by the fault, but to the south the rocks seem to be overlain by Unit *WC2*. The rocks consist of large, locally rounded quartz grains (up to 1 cm) in a fine-grained siliceous matrix. It is poorly sorted and no bedding or lamination is visible.

Thin sections show rounded quartz grains with enhanced undulatory extinction, probably representing a detrital sedimentary component. The volcanogenic quartz grains comprise euhedral quartz (Fig. 55) embayed grains, angular and fractured grains, and curved laths of quartz. These grains (0.01–1.0 cm in diameter) are irregularly distributed in a fine-grained siliceous matrix which may partly have formed through devitrification of pumice or glass shards. It is tentatively concluded that the rock formed by a subaqueous pyroclastic ash flow which (on its path) incorporated rounded, sedimentary quartz grains from the probably unconsolidated coarse arenites of Unit *WC2*.

Felsic pipes

Some 3 km northwest of the Tangadee rhyolite the granitoid basement is intruded by three pipe-like bodies (20–40 m in diameter) of a black siliceous rock. Chemical analysis is shown in Table 4. The rock has low contents of Na and K, which were possibly removed during weathering. The high Fe and Mg contents may be related to abundant chlorite (causing the black colour) and minor pyrite. The rock is poorly sorted, with subangular to subrounded quartz grains of various sizes (0.01–0.5 cm), plus large (more than 1 cm) irregular shaped and vermiform quartz aggregates, in a very fine-grained chloritic matrix. Some chlorite needles are enriched at the contact between the quartz aggregates and the chloritic matrix.

There are no textural or mineralogical clues as to the origin of this rock. However, its chemical composition suggests an altered, siliceous, volcanogenic rock, so that the field occurrence could be interpreted as a volcanic vent. If this is the case, then the filling of these vents (i.e. the black felsic pipes) may be a pyroclastic breccia and/or talus from the crater rims, related to the formation of the Tangadee rhyolite.

Summary

With the exception of the felsic pipes, all felsic rocks described in the area were emplaced within the lower part of Unit *WC2*, and it can reasonably be assumed that they form one suite. The felsic pipes possibly represent the vents of an eruptive system. The presence of lapilli tuff suggests that the volcanic eruption was hydroclastic, and that a rhyolitic magma had come into contact with water which, in turn, resulted in an explosive eruption. The addition of water probably was enhanced through the onset of faulting and fracturing of the basement (subsidence) in the period when the lowermost part of Unit *WC2* was deposited. Thus, the extrusion may be related to the incipient rifting. Irrespective of how Ba came to be enriched in the lapilli tuff (i.e. prior to or after eruption), introduction of Ba is related to the hydrothermal system. If the lapilli tuff is related to the rhyolite (dated 1098 ± 42 Ma) then this would place further constraints on the age of the mineralization.

Chapter Six

Development of the Jillawarra basin

Basin limits

The limits of the Jillawarra basin (Fig. 7) are defined by the Woodlands Fault in the west, the Quartzite Well fault system in the north, the Abra fault system in the east and — at least in the western portion of the basin — by the West Creek Fault in the south (Plate 2). The Jillawarra basin is about 55 km long, in an east–west direction, and 5–6 km wide.

Earliest deposition

The oldest sedimentary unit, on granitic basement, is an arkose derived from the granite. This arkose may have been deposited either as a talus-slope breccia, or in an environment analogous to that of the Tringadee Formation (100 km to the west-southwest) in the mid-position of an alluvial fan. In the case of a talus-slope breccia, it is difficult to assess whether deposition was related to a particular tectonic event.

Transgression

The beginning of marine deposition was marked by a transgression from the southwest, along a northeasterly trending elongated graben. This may have been the result of moderate subsidence of the graben along the regional Flint Hill and Tangadee Lineaments. An increase in water depth, during the period when Unit *GW2* was deposited, is indicated by the abundance of reef dolomites together with intertidal siltstones and beach arenites. At the same time, synsedimentary faulting became evident. The Manganese Range Fault apparently acted as a facies divide between a western reef-carbonate facies and an eastern fine-grained clastic intertidal facies.

During the period when Unit *GW3* was deposited, intertidal-flat deposits were laid down in many parts of the Jillawarra basin. The dolomitic fine-grained siltstones, however, are intercalated with numerous arenite beds, indicating that there was a significant clastic contribution. Unit *GWW4* (containing up to 250 m of coarse clastite) interfingers with, and is partially time-equivalent to, the intertidal siltstone of Unit *GW3*. The former unit may represent a barrier-island system while Unit *GW3* represents intertidal flats. Up to this point the depositional history is that of the transgression of a shallow epicontinental sea, which produced near-shore facies in the Jillawarra basin. The local abundance of clastites suggests that continental debris was deposited in the Jillawarra basin, which acted as a shallow sink. The hinterland from which the clastics were derived was composed of granitic rocks.

Regression (doming)

Within the lower part of Unit *GW5* the beginning of a regression is indicated. The barrier-island arenite of Unit *GWW4* is overlain by dolomitic siltstone (Unit *GW5*) which was deposited in a water depth of tens of centimetres. Intercalated lime-sand shoals developed from the reworking of clastics in an intertidal environment. Unit *GW5* terminates with laminated dolostones and columnar stromatolites, and it resembles a shallowing-upward carbonate sequence as described by James (1979).

During the period when Unit *GW6* was deposited, the amount of clastic input decreased. An upper intertidal, low-energy environment is suggested by abundant cryptalgal laminations, stromatolites, and pellets. Intermittent supratidal, hypersaline conditions are indicated by gypsum casts, authigenic potash feldspars and thin laminae of red iron hydroxides; i.e. hematite facies of sabkhas (Kendall, 1979). Because there is evidence that synsedimentary faulting occurred during deposition of the upper Gap Well formation (there are no massive biostromal dolomites in Unit *GW6* east of the Manganese Range Fault), it may be assumed that regression was also tectonically controlled. In comparison with the Irregully Formation (partially equivalent to the Gap Well formation) elsewhere in the Bangemall Basin, the regressional development in the Jillawarra basin has been enhanced (indicated locally by supratidal, hypersaline conditions). Therefore, emergence (uplift) may also have taken place locally in the area of the Jillawarra basin.

Transgression (rifting)

After regression, marked by the upper Gap Well formation, the onset of the West Creek formation marks another transgression. On a regional scale this transgression is indicated by the re-establishment of an intertidal to subtidal environment with the low-energy carbonate deposition of Unit *WC1*. Within these intertidal flats, however, there

Table 5. Jillawarra basin and parameters related to potential mineralization (after Large, 1980)

Parameters		*Jillawarra basin*
I.	**First-order basin**	
	(a) Epicratonic and intracratonic basins (100s km dimensions)	Bangemall Basin
	(b) Fault-bounded at margins	Jeeaila–Mount Vernon–Lofty Range fault system in the north Steep faults on ROBINSON RANGE, STANLEY and NABBERU in the south
	(c) Thick sequences of clastic sediments shallow-marine carbonates, deltaic sandstones, turbidites	Clastic sediments; Tringadee Formation Shallow-marine carbonates; Tringadee Formation Deltaic sandstones, turbidites; Kiangi Creek Formation
II.	**Second-order basin**	
	(a) Becken and Schwellen (10s km dimensions)	Jillawarra basin, Becken facies
	(b) Abrupt changes in sedimentary facies and thickness at basin margins	Within Unit *WC2*, the basin margin faults acted as facies divides (Fig. 47)
III.	**Contemporaneous igneous activity**	
	(a) Tuffs, tuffites, ashfalls (<1 m thick, fine grained)	Rhyolite, lapilli tuff, etc.
	(b) Bimodal volcanic activity in first-order basin	despite minor felsics only dolerites (continental tholeiites)
	(c) Minor intrusions	none
IV.	**Regional tectonic activity and lineaments**	
	(a) Active hinge zones at margins of basins	Tight and overturned folds along the Mount Vernon Fault on the northern margin of the Bangemall Basin Tight folds at northern and southern margins of the Jillawarra basin
	(b) Regional change in sedimentary environment	Facies change across the Tangadee lineament (parameter IIb)
	(c) Intersection of lineaments and hinge zones	In the Bangemall Basin, Jeeaila–Mount Vernon–Lofty Range fault system intersects Tangadee lineament. In the Jillawarra basin, Quartzite Well fault system intersects Woodlands Fault in the west and Abra fault system in the east
V.	**Third-order basin**	
	(a) Local depressions (100 m–10 km dimensions)	The Abra sub-basin (Chapter Seven)

Note: Becken = basin; Schwellen = rise

were three rapidly subsiding, fault-controlled sub-basins. These are defined by up to 40 m of coarse clastic facies at TP prospect, Copper Chert prospect and Abra prospect. In addition to northeasterly trending faults, which had already been active during deposition of the Gap Well formation, movement along easterly trending faults also became significant. The apparent relationship between these three sub-basins and areas of significant mineral-ization suggests similarities to the Middle Proterozoic Sullivan Pb–Zn–Ag deposit, B.C., Canada. Here, the zones of high-grade mineral-ization are defined by the lateral occurrence of the underlying, thick 'Footwall Conglomerate' (Ethier et al., 1976).

The shallow-water transgression of Unit *WC1*, with three isolated areas of pronounced subsidence, was followed by a marked transgression which affected many parts of the Bangemall Basin — the onset of deposition of the Kiangi Creek Formation. Within the Jillawarra basin, Unit *WC2* comprises more than 400 m of shallow-water turbidites. The occurrence of these is apparently confined to the basin; outside the basin margins, beach or fluvial facies prevail (Fig. 47). Subsidence was greatest in the Jillawarra basin which at this stage developed into an intracratonic, fault-bounded rift valley. Robbins (1983) noted that coarse-grained turbidites are common in such a rift alley, and suggested that such turbidites were induced by earthquakes generated by rifting.

Further basin development

The filling of the Jillawarra basin is marked by the upward passage of Unit *WC2* into the predominantly intertidal dolomitic siltstone of Unit *WC3*, and the coarse beach arenites of Unit *WC4*. Further slow subsidence is indicated by the re-establishment of intertidal/barrier-bar conditions of the lower Jillawarra Formation (*Mjd*), which is overlain by shelf facies of the upper Jillawarra Formation (*Mjs*).

Summary

The regression in the upper Gap Well formation and transgression in the lower West Creek formation match the first events that occur in the 'rift valley stage' of cratonic rift basins. De Rito et al. (1983) described the first events as doming, central rifting, graben formation, and the intrusion of basic magmas into the central rift. The intrusion event would correspond to the intrusion of dolerite at higher stratigraphic levels elsewhere in the Bangemall Basin.

Because lateral crustal extension continued after the incipient rifting (*WC2*), further pulses of subsidence occurred. After a period of tectonic quiescence and infill of the basin, the shelf facies of the middle to upper Jillawarra Formation marks a further, though minor, event of subsidence. According to the classification of Large (1980), who listed parameters indicative of potential mineralization, the Jillawarra basin could be distinguished as a second-order basin occurring within a first-order basin (Table 5).

Chapter Seven

Abra sub-basin

The Abra sub-basin is situated near the eastern edge of the Jillawarra basin. The boundaries of the sub-basin are not accurately known, and there are no surface outcrops of lithologies (Units *GW5*, *GW6*, *WC1*) that occur exclusively within the sub-basin. Investigations and reconstructions of the sub-basin are based on information collected from core from eight diamond drillholes at the Abra prospect.

A surface location plan of the Abra area (Fig. 56) shows the positions of the main grid lines and the position of the eight drillholes. Except towards the south where no boundary fault to the sub-basin could be identified, the plan also shows the surface trace of the probable faults which are believed to mark the boundaries of the sub-basin. Possible extension of the Abra sub-basin is indicated by the occurrence of coarse clastic facies in Unit *WC1* (Fig. 57).

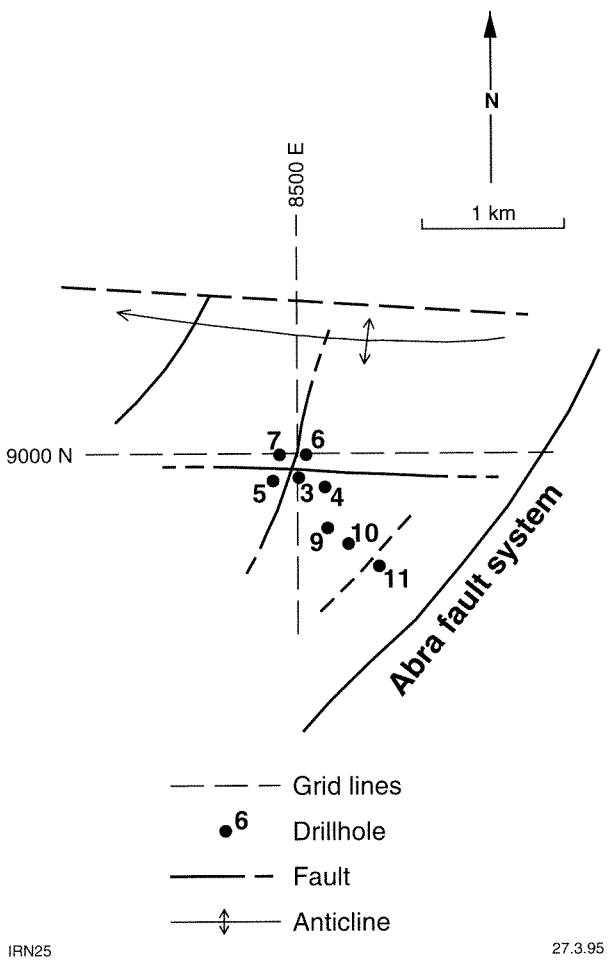

Figure 56. Plan of the Abra area showing the locations of diamond drillholes, exploration grid, and main structural features

The Abra base-metal deposit, which occurs within the sub-basin, is a shallow-water, sediment-hosted, syn-diagenetic Cu–Pb–Ba deposit (Vogt and Stumpfl, 1987). Mineralization occurs within a sequence of intertidal sediments and overlying evaporitic sediments. Within the sub-basin the deposit is overlain by 230–450 m of barren clastic sedimentary rocks. The principal ore minerals are chalcopyrite, galena, and barite, with associated pyrite, magnetite, hematite, iron carbonate, quartz, minor sphalerite, plus trace scheelite and gold. The Abra deposit is estimated to contain 130 Mt of mineralized material with an average grade of 0.25% Cu, 1.15% Pb, and 2.5% Ba. Most of the tonnage is contained in the lower part of the Abra body, known as the Stringer zone, where cross-cutting mineralized veins transgress intertidal sedimentary rocks belonging to the upper part of the Gap Well formation. Overlying this zone are the stratiform upper parts of the Abra deposit, which are known as the Red zone and Black zone. These upper zones occur within evaporitic sedimentary rocks of the upper part of the Gap Well formation.

Stratigraphy of the Abra sub-basin

The stratigraphy of the Abra area is illustrated in Figure 58, where units have been projected onto a north–south section on the 8500 m E grid line. The stratigraphic divisions encountered in the diamond drillholes appear to comprise the upper parts of the Gap Well formation (Units *GW5–GW6*) and the lower to middle parts of the West Creek formation (Units *WC1–WC3*) and may be compared with those shown in Figure 9. In this chapter, sedimentological analogies between the Abra area and those in the Jillawarra basin are discussed in order to evaluate the facies within the Abra sub-basin.

Gap Well formation

It is somewhat difficult to correlate units of the Gap Well formation in the Abra sub-basin with Units *GW5–GW6*

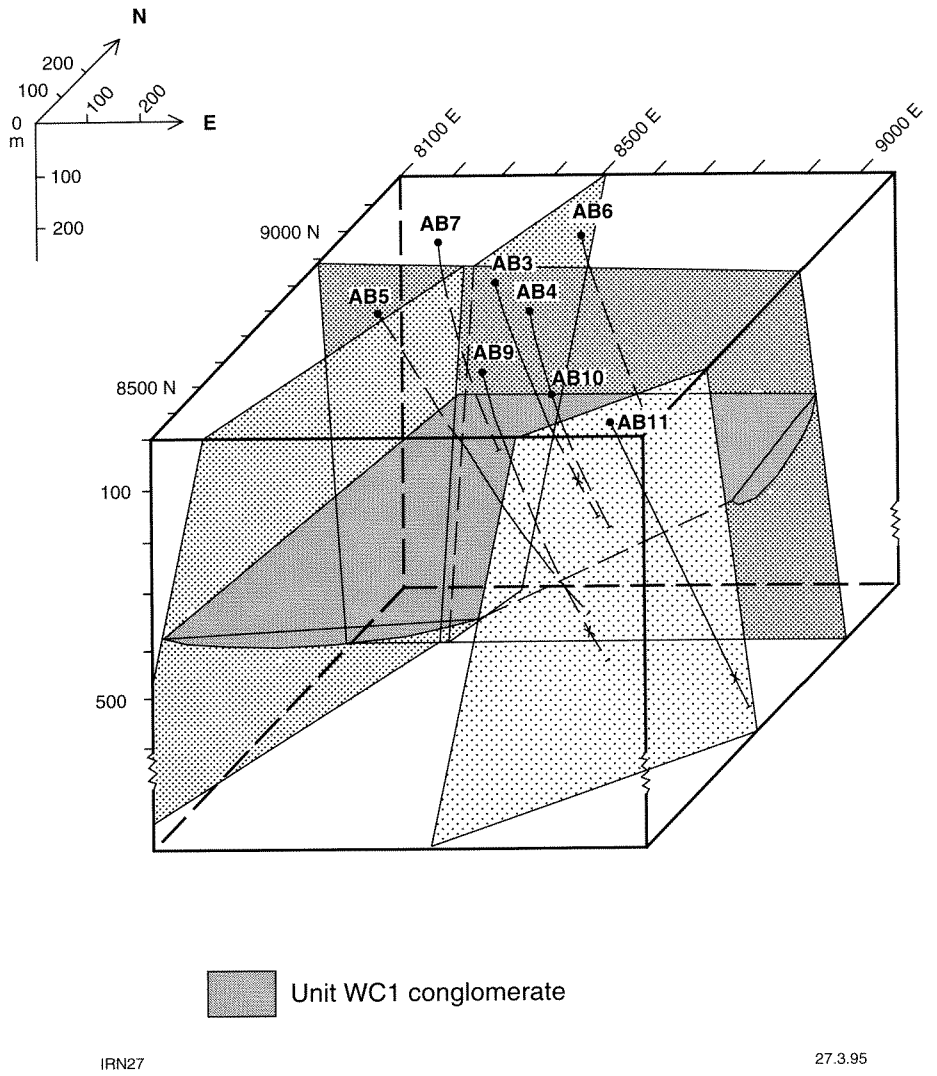

Figure 57. Block diagram of the Abra area showing the Abra sub-basin, which is defined by the occurrence of the coarse clastics of Unit *WC1* and is limited by three faults (stippled planes). Exploration grid, surface position, and downward extension of drillholes are also shown. Intersection of drillhole and fault is marked by X

in the Jillawarra basin. This is because alteration (silicification, chloritization, and brecciation) commonly obliterates the original features of the rocks in the Abra sub-basin, so that it is not appropriate to attempt subdivision into the *GW5* and *GW6* units. The Gap Well formation in the Abra sub-basin contains the ore-bearing sequence, which may be subdivided into three litho-stratigraphic units:

(a) the Stringer zone, characterized by abundant small-scale veining in fine-grained clastic sediments;

(b) the Black zone, consisting of magnetite–carbonate laminations; and

(c) the Red zone, which is dominated by jaspilite, hematite, and barite.

These zones were named by Geopeko geologists for the purposes of logging core from the Abra mineralization, which was first intersected by diamond drillhole AB 3 in September 1981.

Stringer zone

The longest drillhole intersection of the Stringer zone (416.3 m of core, corresponding to a true depth of 310 m) occurs in drillhole AB 9. Although the veining gradually decreases in the lower part, this lithostratigraphic unit probably extends below the bottom of the hole. Mineralization in the Stringer zone is limited to veins and veinlets (Fig. 59) of various composition, but it may consist of breccia zones (Fig. 60) within chloritic siltstone. The dominant rocks are chloritic siltstones and shales, with intercalations of very fine-grained arenite. These rocks are interbedded irregularly with subordinate, thin, lithic and/or feldspathic fine- to coarse-grained arenites which are often poorly sorted. Lithic arenites are more abundant in drillholes AB 4 and AB 6; in the latter the arenites comprise the upper 30 m of the Stringer zone whereas in AB 4 they are dominant throughout the hole.

Mesoscopically (scale of the drillcore), a number of sedimentary features have been observed in the Abra sub-

basin which suggest an intertidal sedimentary environment, such as that postulated for Unit *GW6* of the Jillawarra basin (Chapter 3). These features include the following:

(a) Flaser bedding; this type of ripple cross-lamination, where muddy parts occur in the troughs of the ripples, often forms in intertidal sediments (Reineck and Singh, 1973).

(b) Intraclastic brecciation; although it is not exclusively diagnostic of intertidal sediments, this feature has also been observed in Unit *GW6* near the Copper Chert prospect, and may indicate an analogous mode of origin.

(c) Subordinate thin, lithic and/or feldspathic, poorly sorted, fine- to coarse-grained arenites; these rocks are probably equivalent to the calcareous wackes of Unit *GW6* in the Jillawarra basin. The absence of significant carbonate may be the result of intense silicification which has affected all rocks in the Abra sub-basin. Abundant tiny inclusions indicate the former existence of carbonate.

(d) Scattered sand grains in muddy layers; up to about 10% scattered quartz grains in the fine-grained sedimentary rocks frequently occur in all drillcores. According to Reineck and Singh (1973, p. 359) this is a common feature of intertidal sediments, where individual sand grains are attached to algal filaments or other organic matter, and are kept in suspension prior to deposition with mud aggregates.

(e) Conformable lens-shaped pyrite layers; such layers commonly form diagenetically at the boundary between oxidizing and reducing conditions within the sedimentary column in intertidal sediments (Vogt, 1981) and are also present in the Gap Well formation of the Jillawarra basin.

The above sedimentary features support the assumption that the sediments of the Stringer zone formed in an

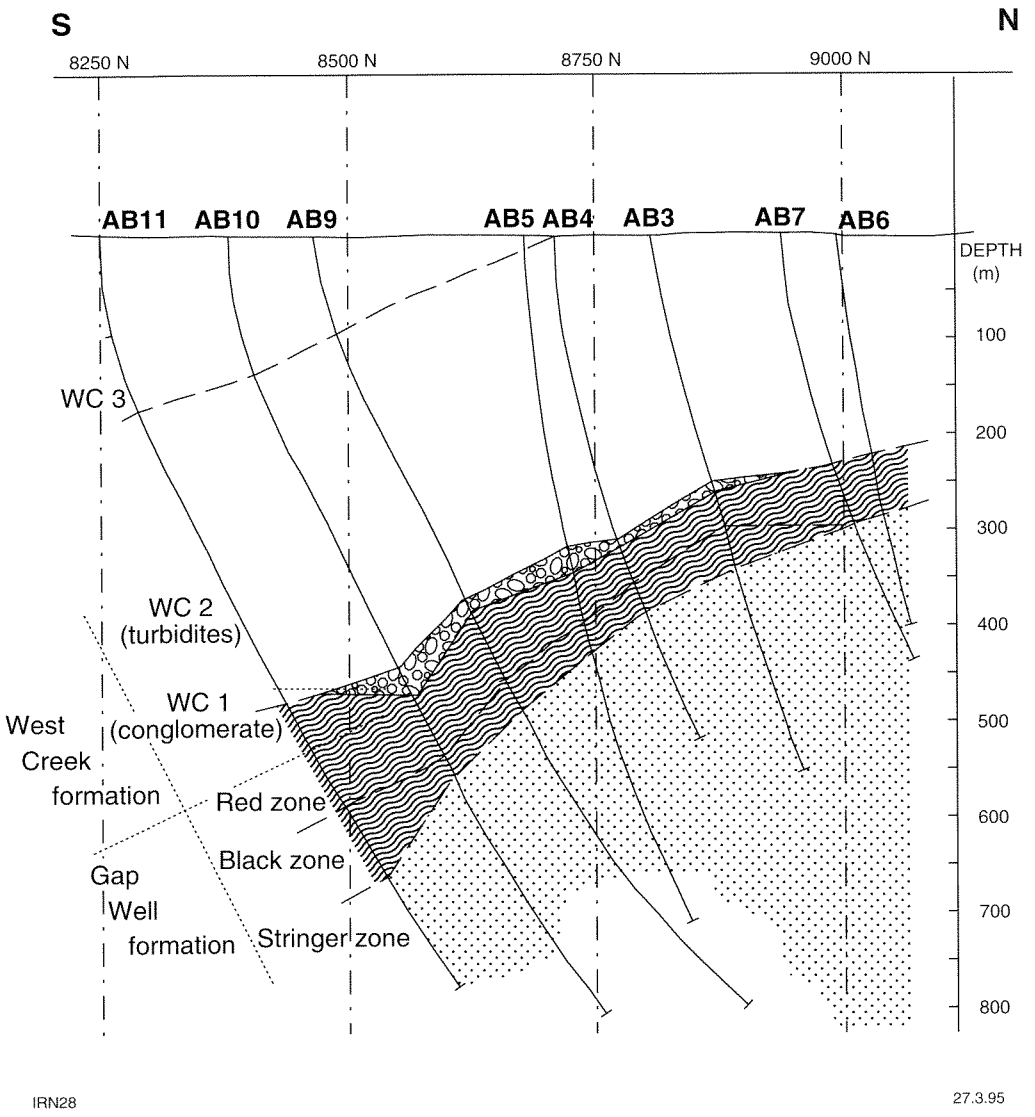

Figure 58. Cross section of the Abra area, showing lithostratigraphic units, projected onto section line 8500 E (Fig. 56). Numbers and positions of drillholes and grid lines (northings) are shown

Figure 59. Drillcore from the Stringer zone (AB 3, 499–507 m) showing veins of chalcopyrite, carbonate and quartz in chloritic siltstone

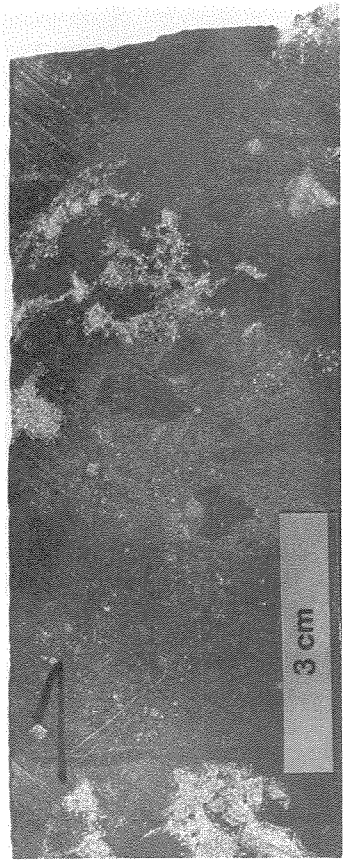

Figure 60. Brecciation of chloritic siltstone in the Stringer zone in drillhole AB 3. The fine-grained matrix also contains disseminated chalcopyrite

intertidal to subtidal environment similar to that of Unit *GW6* of the Jillawarra basin, which is exposed some 10 km to the west.

A second, dominant rock type in the Stringer zone is lithic arenite. This rock is particularly abundant in drillholes AB 4 and AB 6. The feldspar content frequently exceeds 30% of the rock, which is a medium- to coarse-grained, poorly sorted, subangular to subrounded feldspathic arenite. The cement consists of very fine-grained ('cherty') quartz; a few secondary muscovite flakes are scattered irregularly through the rock. Locally, the interstital volume ('matrix') is occupied by galena–sphalerite–barite, plus large subhedral grains of carbonate and authigenic albite. Both carbonate and albite are clearly associated with the ore minerals. Here it is not certain whether carbonate was originally present. The chloritization selectively affected muscovite and altered potash feldspar (Fig. 61). The potash feldspar shows authigenic seams which usually have been altered more intensely than the detrital grains (Fig. 62). Similar authigenic seams occur in eastern parts (Copper Chert prospect) of the Jillawarra basin and have probably formed from formation waters which had an elevated salinity, according to a process proposed by Tröger (1969).

In summary, there is evidence that there were two major rock types in the Stringer zone. The most abundant is a calcareous, micaceous siltstone which represents the common intertidal deposits comparable with Unit *GW6* of the Jillawarra basin. Intercalated with the siltstone is a medium- to coarse-grained lithic arenite which may be interpreted as tidal-channel fillings or storm deposits. Although the lithological evidence for tidal deposits is not unequivocal, the sediment structures described earlier, and

the above microscopic features provide further support for the facies interpretation that the Stringer zone lithologies represent intertidal to subtidal deposits.

Black zone

The Black zone consists of laminated, often distinctively banded, hematite/magnetite–quartz–jaspilite–carbonate–barite–galena–pyrite–chalcopyrite rocks (Fig. 63). Locally, intense veining and brecciation is well developed. The average thickness of the zone is about 35 m; however in drillholes AB 6 and AB 7 the Black zone is absent, while in drillhole AB 11 (the most southeasterly hole) the thickness increases to over 70 m.

The fine banding (often less than one 1 mm thick for an individual layer) is usually crenulated or colloform, contorted, or disrupted by blister-like structures (Fig. 64) pointing both up and down the drillhole. Sometimes the layers are condensed to form nodular aggregates now filled with quartz or carbonate. Individual layers are distinguished by their mineralogy, and there are three main types:

(a) hematite–magnetite (usually intergrown) and/or subordinate jaspilite (Fig. 65);

(b) quartz, massive, nondetrital (Fig. 65);

(c) carbonate, usually yellowish brown in colour (Fig. 65).

Locally there are layers of pyrite (Fig. 65) or, more rarely, layers of barite (Fig. 72).

No regularity or cyclicity in the sequence of layering could be found. Further details of the three types of layering are described below.

Hematite/magnetite: Layers of recrystallized hematite occur with irregularly dispersed subhedral magnetite grains. Magnetite is ubiquitous and is always intergrown with hematite. While magnetite occurs as aggregates composed of varying numbers of small (<10μm) cubes, hematite occurs as acicular crystals or clusters of crystals. Locally, layers of iron hydroxides (goethite or lepidocrocite) are associated with hematite layers (where magnetite is rare) or occur separately in quartz, imparting a jaspilitic appearance. The original lamination was probably hematite/magnetite and carbonate together with minor layers of pyrite. The banding is often colloform or completely destroyed and hematite/magnetite grains are recrystallized to form irregular masses.

Penetration of a hematite/magnetite layer by an elongated scheelite–quartz–barite aggregate suggests that the iron-rich layers formed very early (i.e. synsedimentary) whereas the barite crystallization probably occurred diagenetically (Fig. 66). In Figure 67 there is a large barite crystal (about 1.3 cm) which has grown through a hematite/magnetite–pyrite layer without significantly changing its crystallographic orientation.

Quartz: Most of the quartz either has been emplaced as an original chemical sediment, or replaces pre-existing minerals. Detrital quartz grains have not been found within the layered Black zone.

The abundance of inclusions, mainly as blebs (about 5μm in diameter) of carbonate, iron-oxides (hydroxides) or as fluid inclusions, is characteristic of all quartz types. Figure 68 shows inclusions outlining euhedral crystal shapes.

In the Black zone, silica seems to replace entire carbonate layers; this is particularly obvious in the vicinity of hematite/magnetite or pyrite layers. In Figure 69 almost

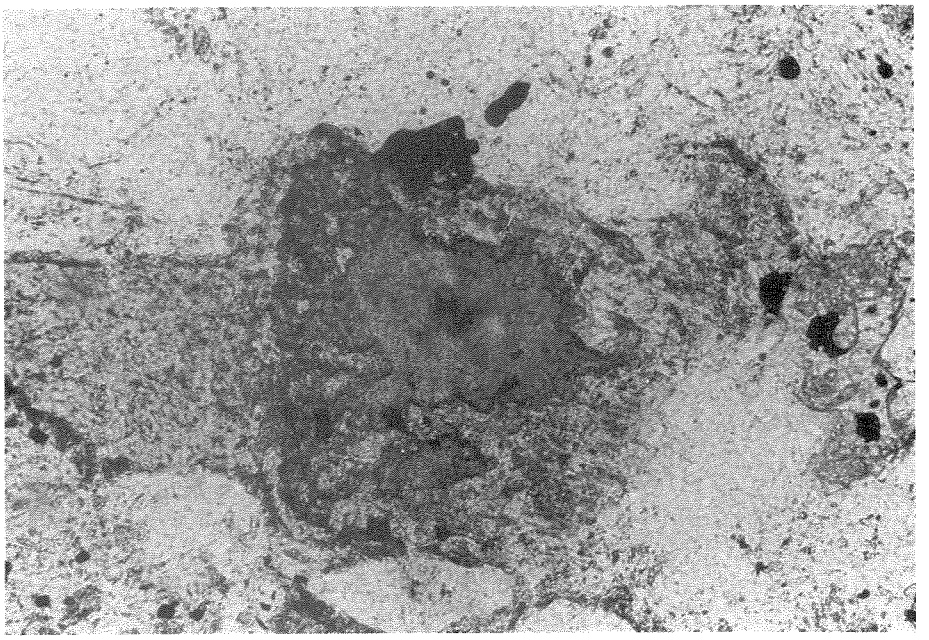

Figure 61. Partially chloritized potash feldspar, Stringer zone. Base of picture is 0.9 mm (plane-polarized light)

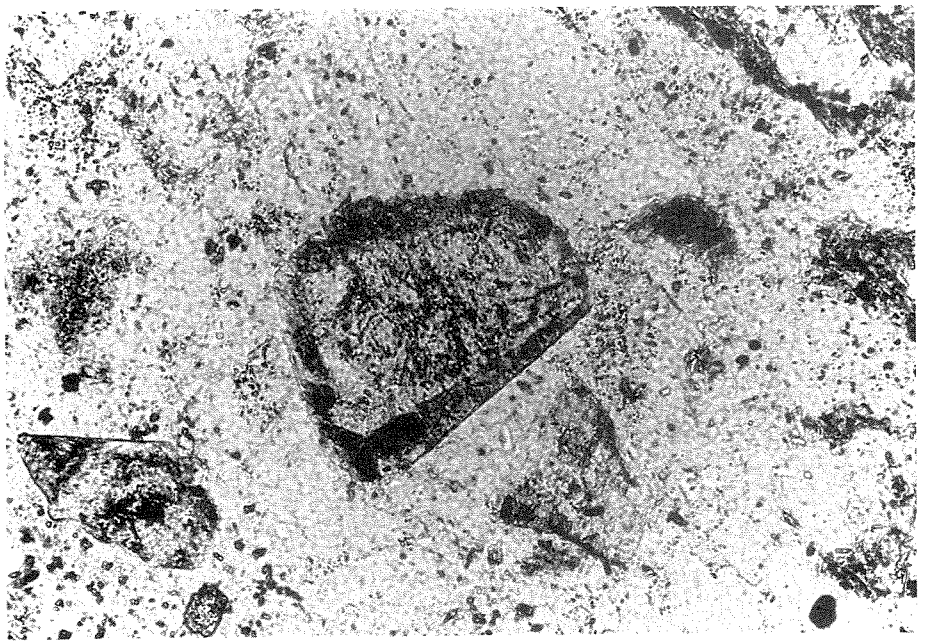

Figure 62. Authigenic seams altered to potash feldspar, Stringer zone. Base of picture is 0.9 mm (plane-polarized light)

Figure 63. Drillcore from the Black zone (AB 3, 325–333 m) showing magnetite/Fe-carbonate laminae. Note veining and brecciation in upper part of photograph

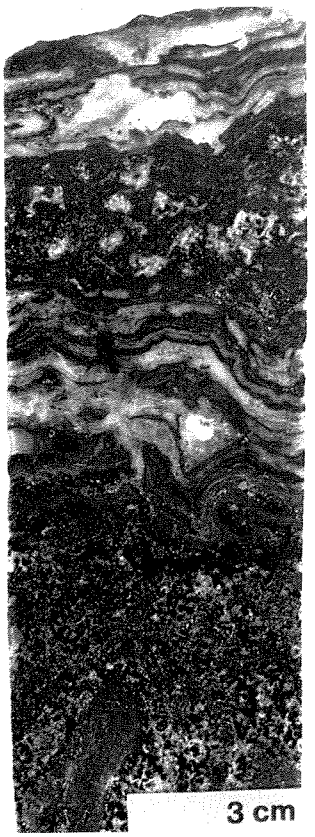

Figure 64. Core specimen from the Black zone with crenulated quartz–carbonate–magnetite layering

all 'dusting' visible in the quartz between the opaque layers consists of carbonate inclusions.

In summary there appear to be two sources of silica:

(a) chemical sedimentation in association with the hematite/magnetite as indicated by iron oxide (hydroxide) inclusions in some of the quartz;

(b) replacement solutions which preferentially affected original carbonate. This type of quartz can be free of iron hydroxide inclusions and presumably originated from the Abra hydrothermal system.

Carbonate: Although it is now subordinate to quartz in abundance, there is evidence for the widespread silicification of original carbonate, which suggests that the original sediment had a substantial carbonate component. Carbonate material now occurs as:

(a) small inclusions or relict carbonate (as described above);

(b) euhedral crystals in clear (secondary) quartz; probably formed together with the secondary quartz;

(c) dark and 'dusty' layers, or zones, of partially sparitic carbonate which contain significant amounts of Fe–Mg–Mn with a pronounced Ca deficiency.

There are indications that the carbonate has replaced sulfates (barite or gypsum). Although carbonate has usually recrystallized to subhedral or euhedral rhombs, there are local acicular or lenticular crystals of carbonate. In one sample, replacement of a nodule apparently took place: acicular carbonate crystals lie perpendicular to a micritic core (Fig. 70).

In addition to the above three types of layering there are subordinate layers of pyrite and barite.

Pyrite: Pyrite occurs as fine layers within, or clearly parallel to the hematite/magnetite layers. Despite their massive appearance the layers are composed of small individual pyrite cubes (Fig. 71) which are recrystallized. The layering and its fine-grained nature support the view that the pyrite is 'syngenetic', as in McArthur (Williams, 1978) or Mount Isa (Finlow-Bates, 1978), and thus is an integral part of the sediments of the Black zone.

It is not so certain, however, whether the pyrite indicates that euxinic conditions prevailed in the Black zone at Abra. The ubiquity of iron oxides rather suggests oxidizing conditions, and it would be more likely that pyrite formed in localized ('micro'-) environments within the sediment. The hydrogen sulfide required in such environments may have been generated by the interaction of sulfate-reducing bacteria (the sulfate ion was available in excess) and decomposition of intermittently occurring

Figure 65. Core specimen from the Black zone with magnetite carbonate layering (upper left) and quartz (white)–pyrite (light grey)–jaspilite, magnetite (black) layering. Note small, vertical quartz–chalcopyrite vein

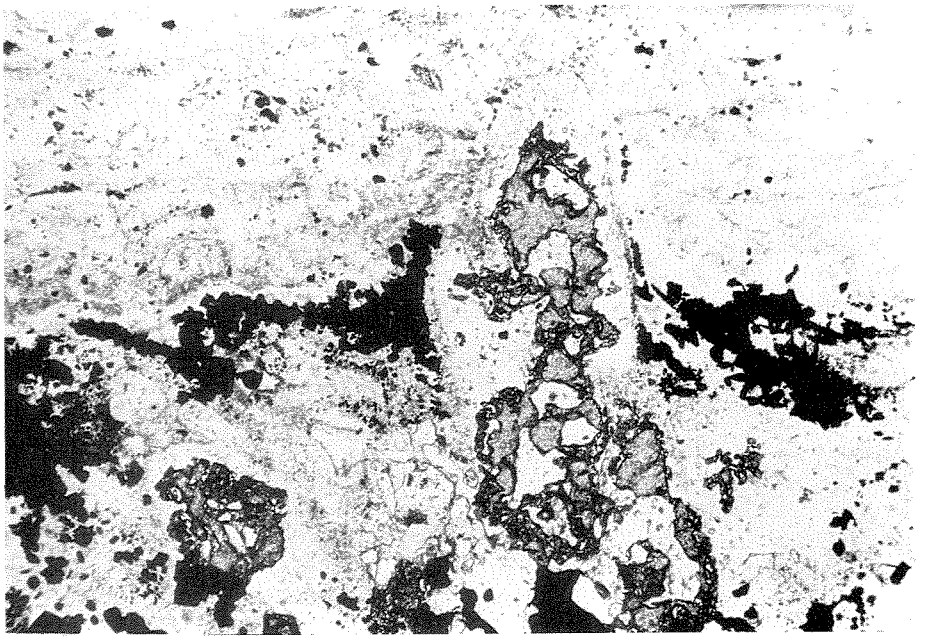

Figure 66. Protrusion of scheelite crystal into hematite/magnetite layer in the Black zone. Base of picture is 3.6 mm (plane-polarized light)

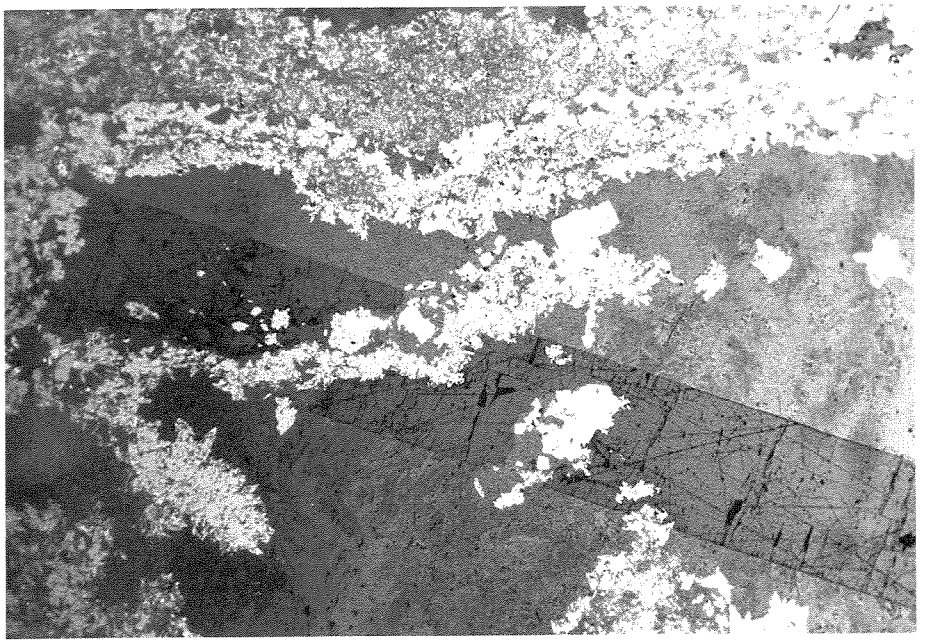

Figure 67. Diagenetic growth of barite through hematite/magnetite–pyrite layer in Black zone. Base of picture is 5.6 mm, in reflected plane-polarized light

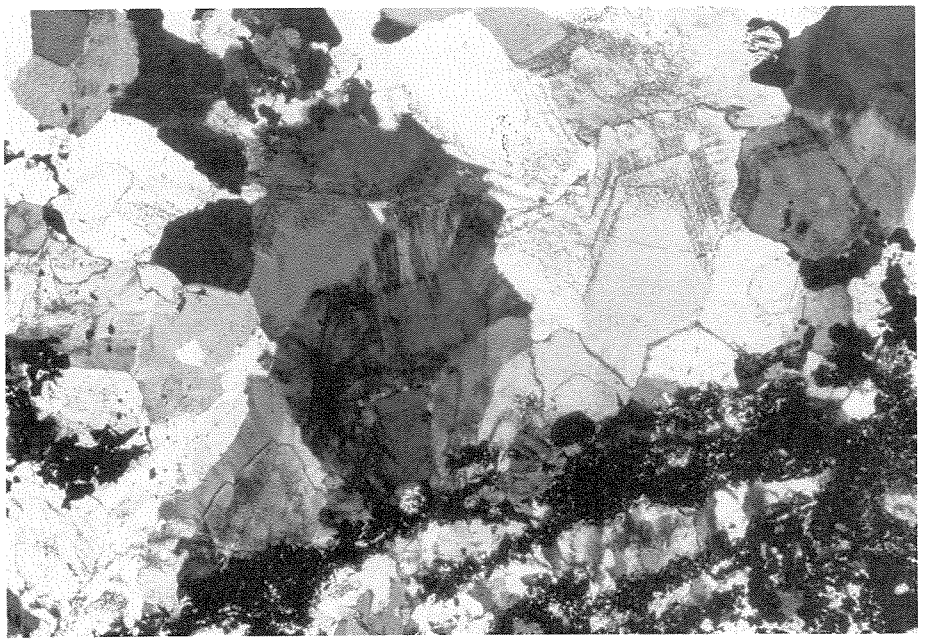

Figure 68. Flamboyant quartz along the margins of angular quartz grains in Black zone. Base of picture 3.6 mm (crossed polars)

Figure 69. Relic carbonate layers and carbonate inclusions in quartz in Black zone. Base of picture is 5.6 mm (plane-polarized light)

microbial mats (Renfro, 1974). The process of bacterial sulfate reduction is also dependent upon, and often controlled by, the supply of organic matter (Trudinger, 1981). A better term for the pyrite of the Black zone therefore is 'syndiagenetic'.

Barite: Although barite is common, it is usually associated with veining or with alteration processes. A small amount of barite occurs as massive bands or layers of acicular crystals, arranged almost perpendicular to bedding with the crystals pointing upwards from a common base (Fig. 72). Only this type of barite could be regarded as 'sedimentary' or early diagenetic and form in the sedimentary environment of the Black zone. The original sulfate appears to have been gypsum or anhydrite that has been replaced by barite (see later discussion). An example of diagenetic replacement could be interpreted for the barite in the layer of Figure 72.

Facies of the Black zone

With respect to its iron content, the Black zone could be regarded as an iron-formation developed in a basin that was hypersaline at times. The iron source could have been the continental red beds which developed on the inferred arkose underlying the Gap Well formation (discussed later).

Iron-formation can form in tidal-flat environments. This has been demonstrated by Dimroth (1979), who found stromatolitic iron-formations associated with other very shallow-water features in the Sokoman Formation, Canada. Furthermore, the occurrence of hematite layers in hypersaline environments has been reported from the Salina Basin, Michigan (Dellwig, 1955).

Although it is not clear whether barite is a primary mineral or whether it has replaced gypsum, the presence of early diagenetic sulfates indicates hypersaline or evaporitic conditions. The usual (Mg–Fe–Mn dominated) carbonate chemistry also points towards an evaporitic environment. Kendall (1979) proposed that such carbonates also should be termed evaporites because they are produced by the same processes as the more 'saline' minerals.

All of these features would suggest that the Black zone was a shallow-water, subaqueous evaporitic iron-formation that formed in an oxidizing, restricted basin with pyrite generation occurring syndiagentically within the sediments.

Red zone

The main lithology is a red-banded, veined and locally brecciated rock, which contains variable proportions of jaspilite, hematite, barite, dolomite, calcite, quartz, pyrite, galena, chalcopyrite, sphalerite, and chlorite (Figs 73 and 74).

Distinctive interbeds of lithic arenite, polymict conglomerate and silicified lutite–siltstone are also characteristic of the Red zone. Some clastic dykes are reported by Geopeko geologists in Abra drill logs.

The thickness of the zone ranges from 40 to 120 m, with increasing thickness towards the south-southeast. The Red zone occurs in all diamond drillholes at the Abra prospect. The nature of the laminations is similar to that of the Black zone. However, jaspilite–hematite–chert–pyrite–barite are dominant, resulting in an overall reddish

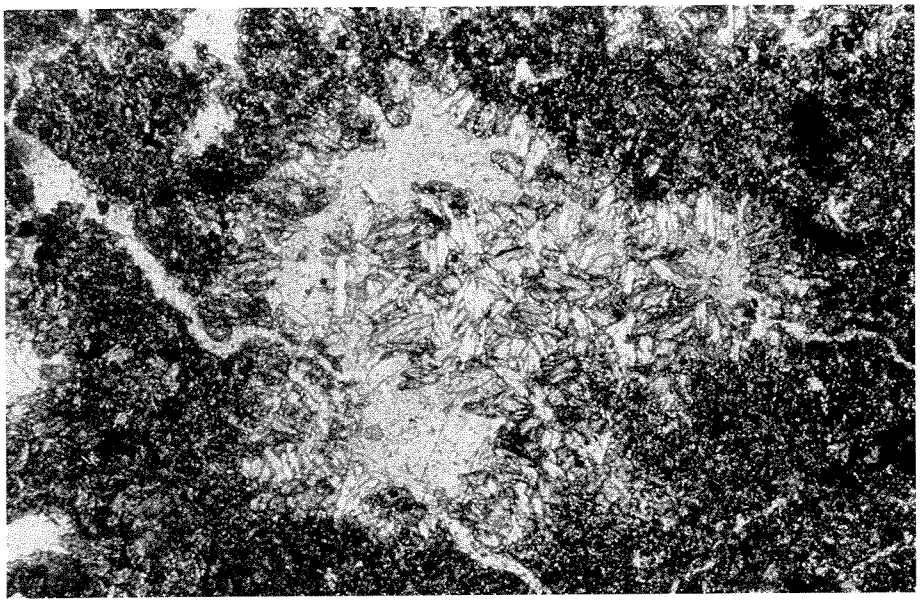

Figure 70. Acicular carbonate crystals along the margins of a micrite nodule in Black zone. Base of picture is 3.6 mm (plane-polarized light)

colouring (Fig. 75). The main components of the Red zone are described below.

Barite: Barite is a major constituent, particularly in the upper part of the Red zone (up to 49% Ba over 2 m in drillhole AB 3). Here, the barite forms massive zones and sedimentary structures are absent. Therefore, it is not certain whether the massive barite zones represent recrystallized layers or massive veins.

Carbonate: The nature of carbonate in the Red zone is similar to that in the Black zone. The dark colour and electron microprobe data suggest that they are dominantly Mg–Fe–Mn carbonates. In contrast to the Black zone there is frequent 'spherulitic extinction' in zones of apparently micritic carbonate, and a tendency to form nodules. Figure 76 shows a nodule within colloform micritic carbonate.

Nodular pseudomorphs of calcite replacing gypsum in a dolomicrite are described by Bouroullec (1980) from the Aquitaine Basin, France. The fibrous nature of the carbonate in the nodules from the Red zone suggests that carbonates may have replaced lath-shaped sulfates (barite or gypsum).

Hematite/magnetite–jaspilite–pyrite: In contrast to the Black zone, magnetite here is subordinate in abundance to hematite and jaspilite. This indicates that the Red zone represents a more oxidizing environment of sedimentation, which is compatible with a change to sabkha conditions in the Abra sub-basin.

Abundant layers of pyrite were probably generated by decomposition of abundant microbial mats within the sediments. This is a further indication of sabkha conditions where large numbers of microbial mats are common (Renfro, 1974). The co-existence of hematite and pyrite is not contradictory. It may indicate oxidizing conditions at the sediment–water interface, but with reducing conditions occurring locally within the sediment (in the vicinity of decaying microbial mats).

Clastites: A characteristic feature of the Red zone is that the banded, iron-rich rocks are often interspersed among clastites. These consist of polymict conglomerates, wackes, and minor siltstones and arenites. Coarse-grained rocks predominate. They are usually poorly sorted with subangular to subrounded grains of quartz, potash feldspar (often sericitized and/or chloritized), lithic clasts of shale, chert and jaspilitic rocks. Minor tourmaline also occurs with titano-magnetite and scheelite. The matrix, which consists of cherty quartz with some barite, is commonly jaspilitized.

The poor maturity of the clastites suggests that they were deposited as channel fillings or possibly as storm deposits within the sabkha environment. The non-correlation of the clastites between the drillholes is further evidence to support this mode of deposition. The mineralogy of most of the epiclastic grains (potash feldspar, tourmaline, scheelite) suggests a granitic source. Others, such as chert and jaspilitic clasts, were certainly derived from contemporaneous sediments without being transported over a long distance.

Further consideration: In AB 3 at 292.2 m an important texture is noted (Fig. 77). A typical banded rock is veined by barite–galena. The banded portion consists of chert–carbonate with various portions of jaspilite. The manner in which the laminae are deformed very closely resembles features of evaporitic deposits. The hummocky type of bedding just below the red jaspilite layer is identical to mammilated anhydrite structures from the Oligocene Valence Basin, Southeast France described by Guillevin (1980) as one of the common features of anhydrite (Fig. 78).

The zone immediately below, characterized by reddish contorted structures, is very similar to enterolithic structures which commonly occur in sabkha sediments. Shearman (1980) presented several examples (Fig. 79) and concluded that they are primary growth structures (i.e. not only surficial hydration of anhydrite causing contortion of former layers through up to 63% volume increase). Enterolithic structures develop where anhydrite nodules have coalesced to form layers and the continued growth of the nodules created a demand for space. The lateral pressures which result cause the layers to become contorted. Production of enterolithic structures is no doubt facilitated by the high natural moisture content of the nodules, and the platy habit of the tiny anhydrite crystals which allows easy slip between them (Shearman, 1980).

Top of the Red zone

The contact between the Red zone and the overlying West Creek formation has a variable nature, and this is demonstrated in cores from two groups of drillholes:

(a) The first group is represented by the 'southern' drillholes AB 3, AB 4, AB 5, AB 9, AB 10 and AB 11. In the uppermost Red zone, typical jaspilite–hematite-rich laminae are intercalated with layers of a conglomerate that has a jaspilitic matrix. Towards the top these conglomerate layers become more common and are eventually overlain by 'clean' clastites (matrix is no longer jaspilitic and instead consists of carbonate–quartz–barite) of the West Creek formation. Thus the upper contact of the Red zone appears conformable. Moreover, the abundance of coarse clastites in the top of the Red zone may even suggest that it is gradational.

(b) The second group is represented by the 'northern' drillholes AB 6 and AB 7, in which the upper contact of the Red zone appears different. In AB 6 the banded jaspilite–hematite–pyrite rock is overlain, with a sharp contact, by a fine- to medium-grained lithic quartz arenite. The banded jaspilite rock shows an abundance of large barite crystals, and there is oxidation of jaspilite–hematite to goethite in the uppermost few millimetres (Fig. 80). In thin section there is hardly any textural difference between the uppermost few millimetres of the Red zone (goethite-cemented clastites) and the overlying West Creek formation (carbonate-cemented clastites).

In drillhole AB 7 the uppermost Red zone is characterized by some well-developed, small (about

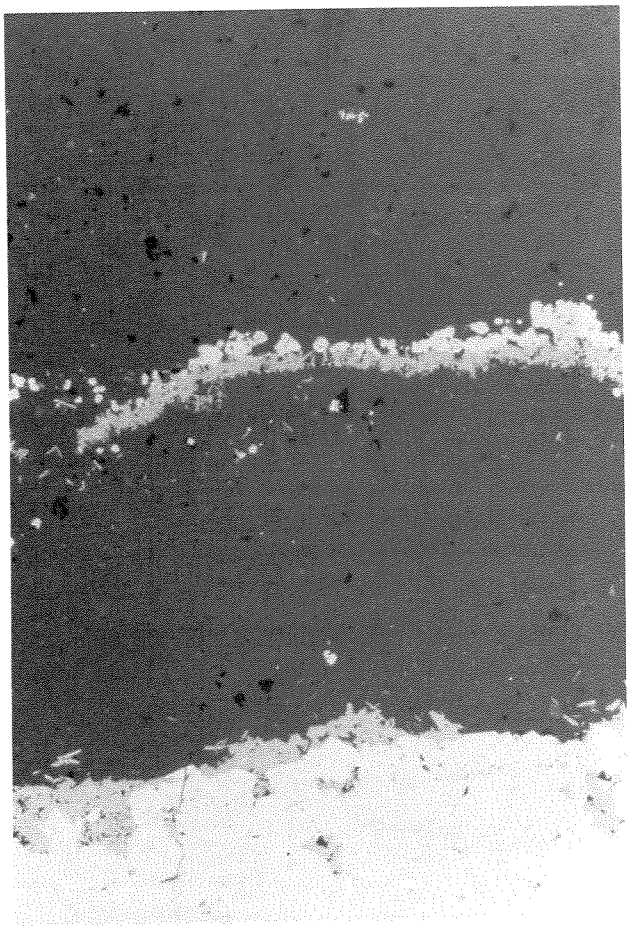

Figure 71. Pyrite layer adjacent to hematite/magnetite layer in Black zone. Base of picture is 1.15 mm, reflected light (plane-polarized light)

Figure 72. Layer of acicular crystals composed of barite and quartz in magnetite–carbonate–quartz laminae of the Black zone

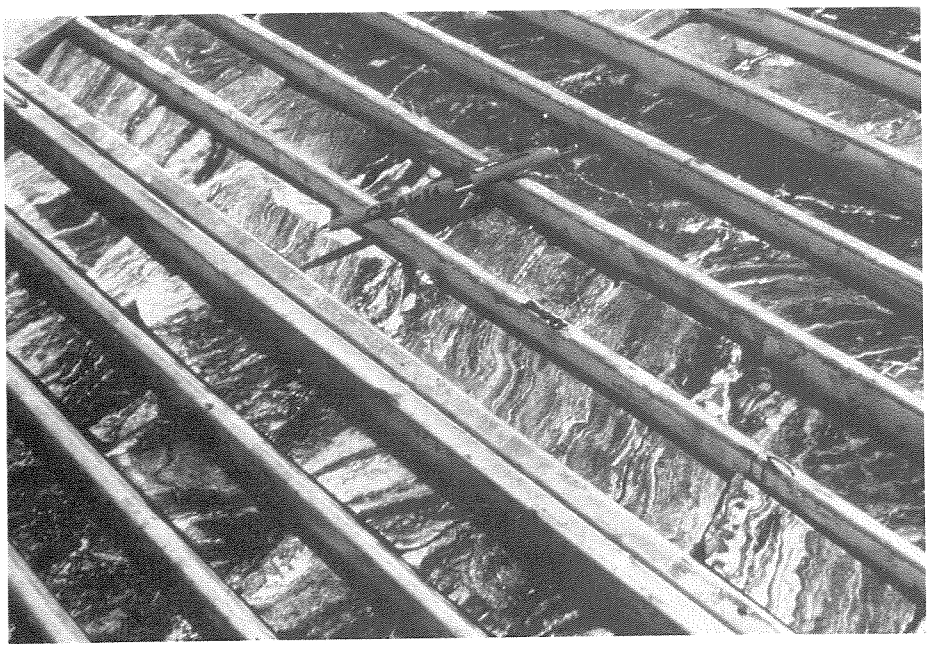

Figure 73. Drillcore from the Red zone with layers of hematite, jaspilite, quartz, carbonate and magnetite

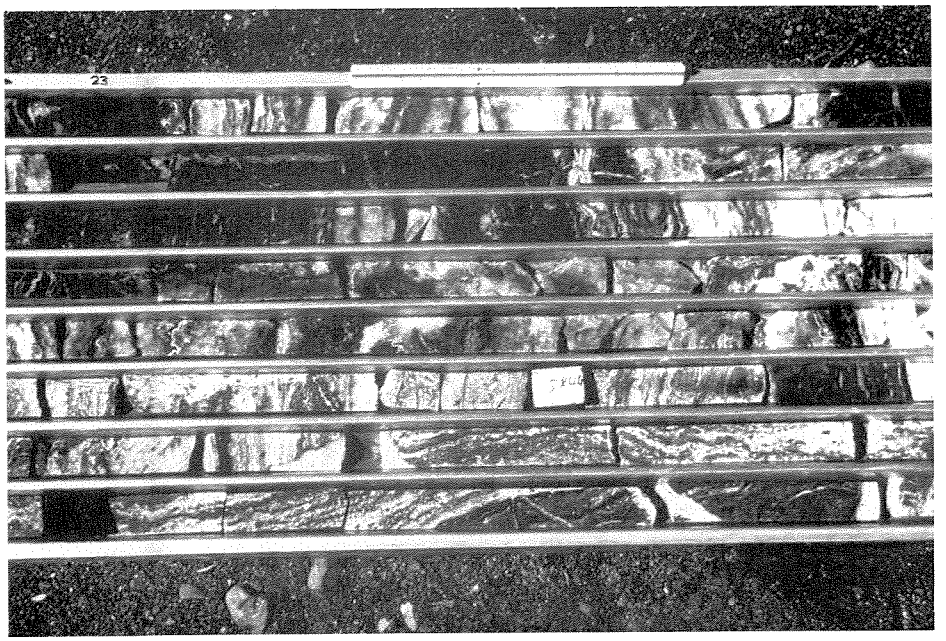

Figure 74. Drillcore from laminated Red zone, with layered hematite/magnetite–carbonate vein (bottom). Scale at top of core tray is 30 cm

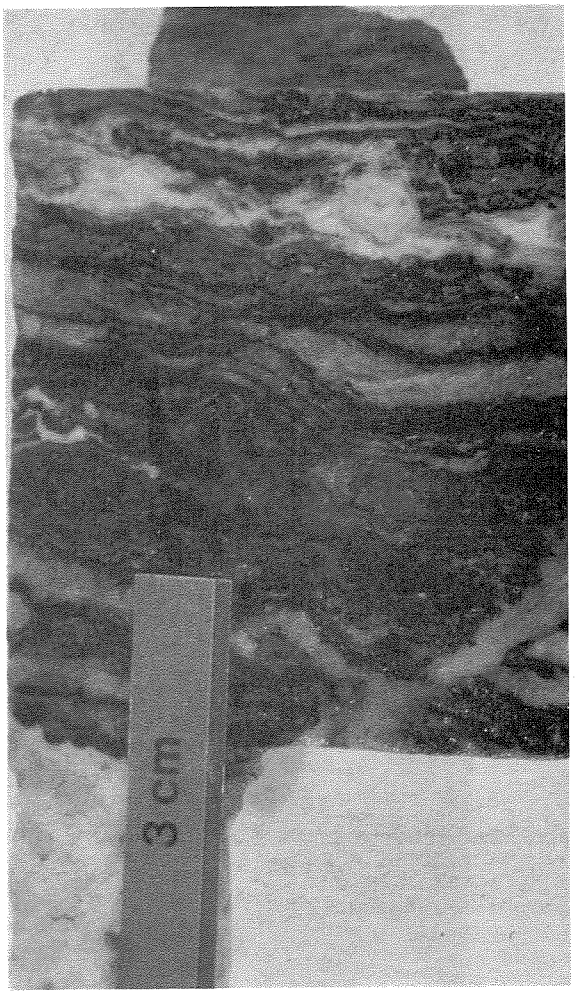

Figure 75. Core specimen from the Red zone showing layers of quartz, barite, pyrite and jaspilite

1 cm wide) digitate stromatolites above laminated jaspilite–hematite rock showing thin veins of oxidized and partially oxidized pyrite (Fig. 81).

Thus, in drillholes AB 6 and AB 7 there is evidence that chemical erosion and oxidation may have occurred in the Proterozoic. However, this does not necessarily imply that there was a significant time break between the Red zone and the overlying West Creek formation. In a sabkha environment, prolonged subaerial exposure and rapid lithification are common (Kendall, 1979). Since the Red zone probably represents coastal sabkha deposits, the pronounced oxidation and erosion seen in the northern drillholes may indicate that there was a hinterland lying due north (and east, as shown later) with respect to the Abra area.

Facies of the Red zone

From the textural features described above, there is evidence to suggest that the Red zone developed in a coastal-sabkha environment. Along the section of Abra drillholes the seaward or basinward direction would be due south. The original sediments of the coastal sabkha probably consisted mainly of layers of hematite–chert and jaspilite–carbonate, together with layers of pyrite that formed diagenetically due to the decay of microbial mats. The emplacement of barite and base-metal sulfides was not related to sedimentation, but occurred during diagenesis when a hydrothermal system was coupled with diagenetic formation waters. It is probable that the salinity of the seawater increased in the Abra area because of contemporaneous evaporation, until precipitation of sulfate occurred. Locally, within the sediments, salinity may have increased so that chloride (?NaCl) became saturated.

The absence of primary evaporite minerals is compatible with a sabkha environment. Under normal conditions these minerals are soluble in water and this would facilitate their removal and transformation even when there were only slight changes of physico-chemical parameters in the diagenetic formation waters. According to Kendall (1979) many fine-grained dolomitic red-bed sequences (e.g. the Keuper of Europe) may represent evaporite deposits, which were laid down in conditions that were not favourable for the preservation of evaporite minerals.

The sulfate problem

There is a question as to whether barite and carbonate (plus quartz) have replaced an earlier Ca sulfate mineral (gypsum or anhydrite) at Abra. Consideration of this problem has important genetic implications for the beginnings of hydrothermal activity in the area.

A number of features that suggest a replacement (non-depositional) origin for barite and carbonate have been observed.

(a) *Barite layers*: Whereas these are rare in the Black zone they are a common feature in the Red zone. Paar (1974) has described barite layers from the Breithorn Ba–Pb deposit (in eastern Greenland) which are similar to the layer shown in Figure 72 from Abra. Paar referred to the texture in the layer as 'palisade fabric', and suggested that it was produced syngenetically when Ba-rich fluids were exhaled on to the sea floor so that they penetrated earlier sediments, and barite thus replaced earlier minerals. A similar replacement process could have occurred at Abra.

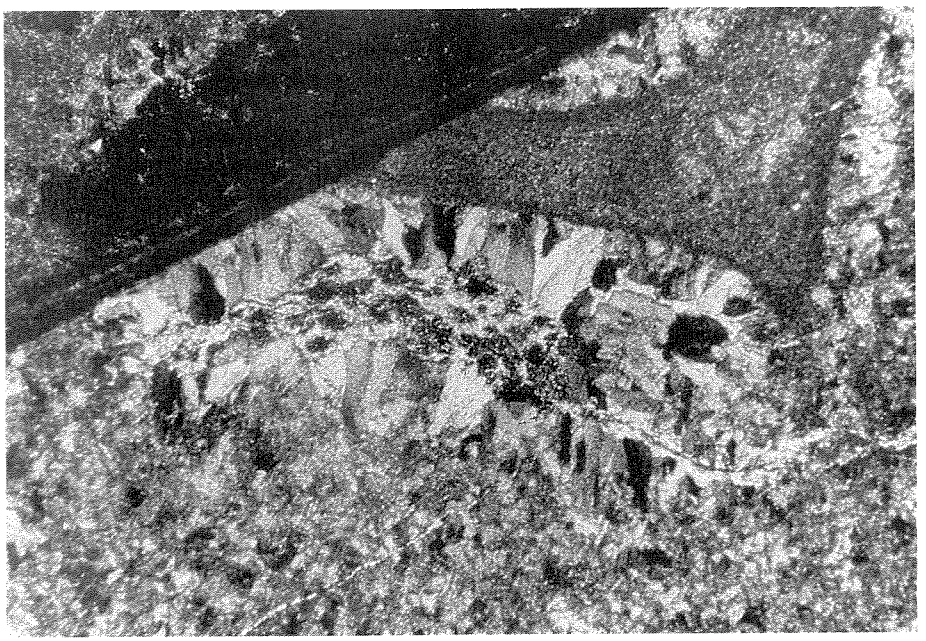

Figure 76. Nodule (in Red zone) in micrite at the margin of a thin section. Acicular carbonate crystal along the margins and diffuse, cherty quartz in the centre. Base of picture is 3.6 (crossed polars)

(b) *Strontium content of barite*: Electron-microprobe analysis of barite grains from various parts of the Abra body (Stringer, Black, and Red zones) shows a remarkably uniform Sr content varying between 0.26 and 0.86%. Similar Sr values were also obtained from barite in veins from the TP and Woodlands prospects, about 70 km west of Abra.

If any barite had been deposited in a sabkha environment (proposed for Abra), it should have a higher Sr content than vein-type barite, because sabkha sediments are enriched in Sr (Moine et al., 1981; Morrow et al., 1978). But this is not the case at Abra. It appears that barite, throughout the Jillawarra basin and at Abra, has had a common origin in that it was emplaced during hydrothermal activity after deposition of the host rocks.

(c) *Carbonate pseudomorphs (after sulfate)*: In the Red and Black zones, carbonate commonly forms acicular or lenticular grains. As this habit is unusual for carbonate minerals, it may represent the replacement of a sulfate mineral by carbonate material. An interesting occurrence of a lath-shaped calcite pseudomorph (Fig. 82) suggests that the calcite (plus some quartz) has replaced a Ca sulfate mineral, particularly as the lath-shaped grain resembles a tabular gypsum crystal. Also, whereas calcite occurs in the pseudomorph, the surrounding carbonate material is composed of Fe-rich or Mn-rich carbonate. Furthermore, as calcite is rare at Abra, it appears most likely that the original lath-shaped mineral was Ca rich; most probably Ca sulfate.

(d) *Sabkha textures*: Some mammilated and enterolithic structures have been observed at Abra (Fig. 77). As discussed earlier, these structures may initially have been composed of anhydrite.

From the above observations, it seems evident that Ca sulfates were the primary sulfates formed in the evaporitic facies of the Black and Red zones. Hydrothermal activity occurred subsequently, so that the Ca in the sulfates (gypsum or anhydrite) was replaced by Ba to form barite.

Source rocks for the Abra mineralization

Compared with other large sediment-hosted base-metal deposits around the world, the Abra deposit is unique in relation to its metal-abundance ratios of 1:5:16 for Cu:Pb:Ba and its almost negligible Zn content. This raises the question of the composition of the source rocks.

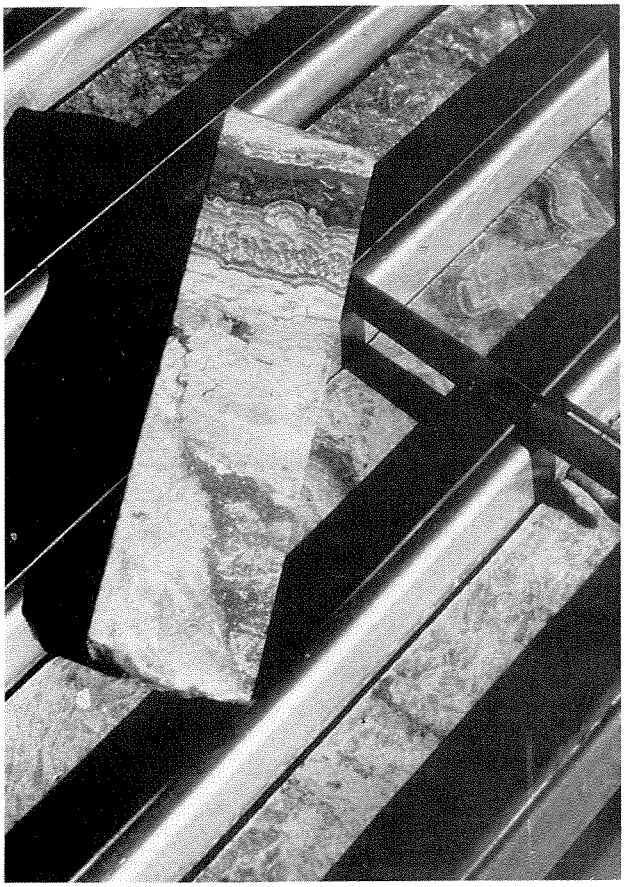

Figure 77. Sabkha textures in jaspilite–chert of the Red zone, drillhole AB 3 (292.2 m)

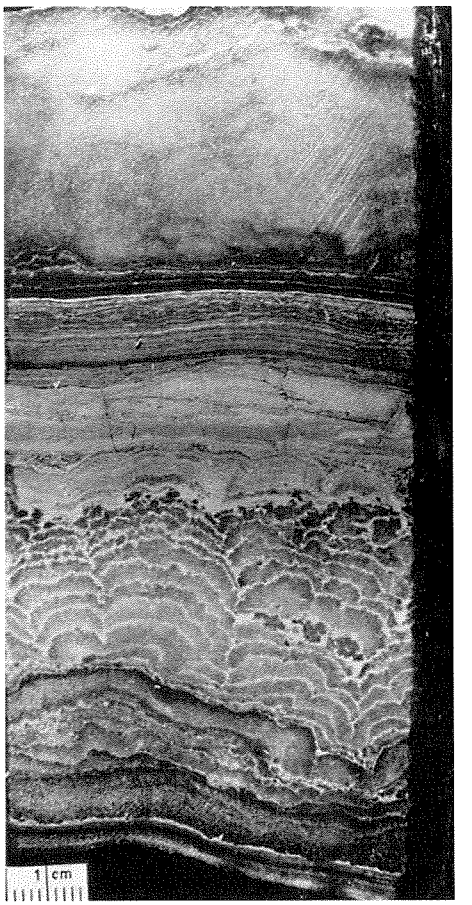

Figure 78. Mammillated anhydrite structures from the Valence Basin. Photograph from Guillevin (1980)

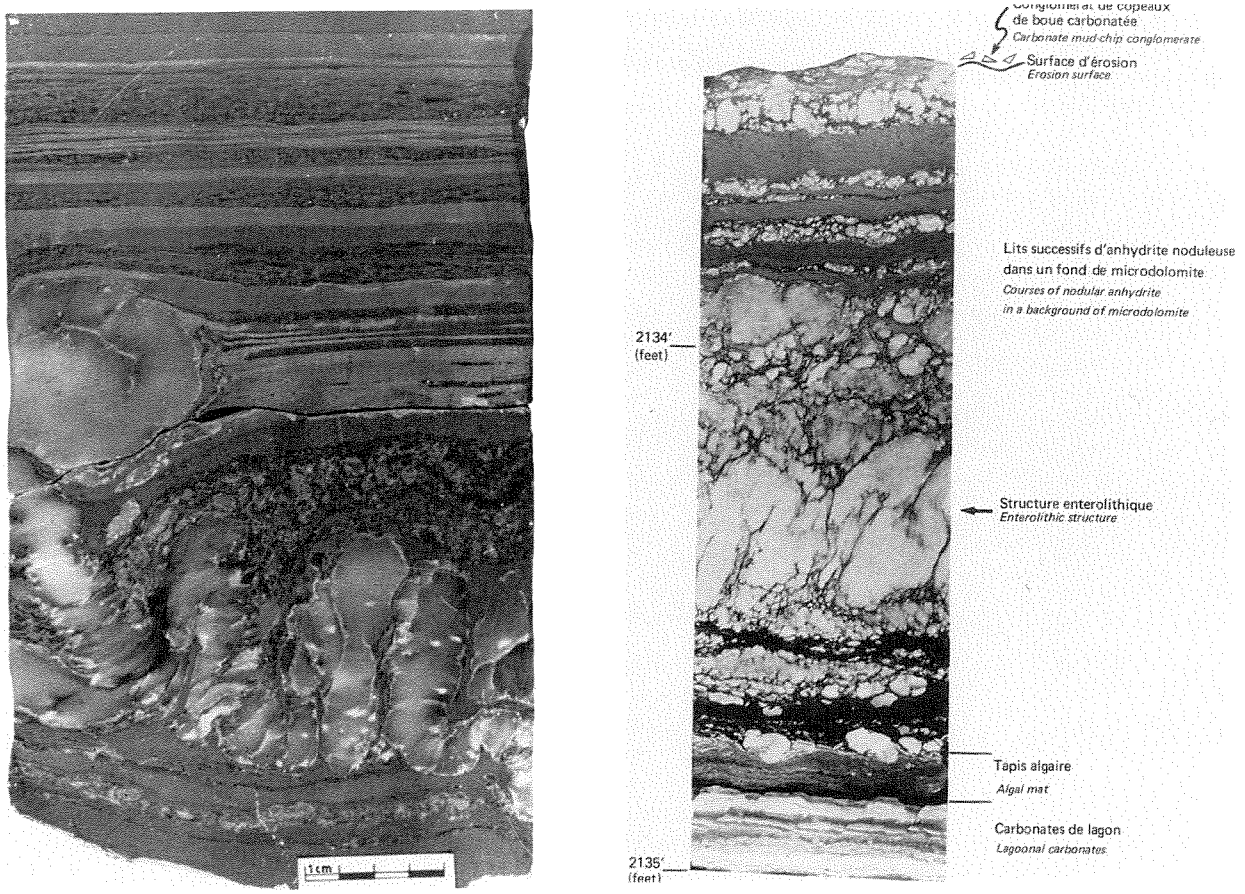

Figure 79. Enterolithic structures in sabkha deposits. Photographs from Shearman (1980)

Formation waters originating from continental rocks (basement rocks or non-pelagic sedimentary rocks) would have had the potential to be the source of the mineralization. A large amount of data has been published in support of the sedimentary genesis of various hydrothermal fluids (e.g. Dunham, 1970; Hanor, 1979; Skinner, 1979) mainly with respect to Mississippi Valley-type deposits (Carpenter et al., 1974) and shale-hosted Pb–Zn deposits (Badham, 1981). Within sedi-mentary basins and within underlying basement there are several potential source rocks. In relation to the Jillawarra basin the following five possible sources are considered:

(a) Basalts, in particular tholeiites, have high Cu and Zn values. Brines percolating through such rocks should carry Cu and Zn but not Pb, and are unlikely to account for the Abra mineralization. Furthermore, there are no basalts in the lower Bangemall Group, and the basement probably consists of granite.

(b) The granitic rocks of the basement (1600–1800 Ma) may contain reasonable quantities of Pb, Cu and Ba, but they could not provide the abundance of Mn which is present in the Abra mineralization. The average granite values are:

Pb = 15–56 ppm (Wedepohl, 1970)
Ba = 732–1605 ppm (Fischer and Puchelt, 1972)
Cu = 10–34 ppm (Zemann and Wedepohl, 1972)
Mn = 233–465 ppm (Peacor and Wedepohl, 1972)
Zn = 23–84 ppm (Brehler and Wedepohl, 1969)

Notably, the Pb/Cu ratio in Abra is 5, contrasting with about 2 in granite.

(c) Black shale is regarded rather as a sink than as a source of metalliferous brines (despite abundant metal content), because of the immobility of metals under reducing conditions (Gustafson and Williams, 1981).

(d) A potential source of sulfate brines enriched in Pb and Zn might be carbonates deposited in evaporitic basins (Thiede and Cameron, 1978). However, no evaporites are known in the basal Bangemall Group, and the basement consists of granitic rocks.

(e) In order to produce Pb-rich deposits from formation waters, the source strata should comprise large volumes of arkose derived from granites in arid environments that inhibit dispersion by chemical weathering (Gustafson and Williams, 1981).

In view of the predominance of Pb and Ba in the Abra mineralization, the source rocks should be rich in potash feldspars in which Pb and Ba substitute for K. The remaining source rock type, therefore, is either the arkose

of the basal Bangemall Group (i.e. equivalent to the Tringadee Formation), or the granitic basement. Both rock types could provide sufficient crystallographic sites for Pb and Ba. Notably, arkose has a porosity at least four times that of granite, so it would be expected to be more capable than granite of transporting large volumes of fluids in a relatively short time.

An additional mechanism is required to explain the Cu content of the Abra mineralization, which may be similar to that for red-bed copper formation. Prior to the deposition of the Bangemall Group the basement was probably subject to erosion for about 200 to 400 m.y. With the onset of the sedimentation of the Bangemall Group, some block faulting may have led to uplifting of basement blocks, which rapidly eroded and provided coarse-grained clastics (arkose) to be deposited in troughs adjacent to the blocks. This is the setting for red-bed copper formation proposed by Björlykke and Sangster (1981). Hematite-bearing sediments (i.e. red beds) principally composed of alluvial-fan deposits are also considered by Haynes (1986) as the source of the metals and the metal-transporting water for a large number of major stratiform copper deposits.

In the Jillawarra area, the presumed arkose is not exposed in the Abra area. Also, the highly weathered nature of the small outcrop of arkose at Woodlands Hills, some 50 km to the west of Abra, renders it impossible for any geological or geochemical investigation of arkose as a source rock. Some 100 km to the west-southwest there are outcrops of the Tringadee Formation (the basal formation of the Bangemall Group), which probably represents the stratigraphic equivalent of the arkose in the Jillawarra basin. The estimated maximum thickness of this formation is 1650 m (Muhling et al., 1978) and it lies unconformably on granitic and metamorphic rocks of the pre-Bangemall basement. The time gap between basement and the Bangemall Group is difficult to assess, but it may be 200 to 400 m.y.

The Tringadee Formation consists of pebbly sandstone and conglomerate, containing up to 25% feldspar in places. Most of the clasts are derived from the underlying basement. According to Muhling and Brakel (1985) the Tringadee Formation was deposited as a thick, wedge-shaped, terrestrial alluvial fan in which lithic clasts and feldspars indicate a nearby source area. For the proposed clastic basal Bangemall Group in the Abra area, an analogous depositional environment to the Tringadee Formation is inferred. The deposition of an arkose is proposed, with the granitic Coobarra Dome east of Abra as the provenance (Fig. 7).

The above geological setting is comparable with the regional depositional environment outlined by Haynes (1986) for the source rocks of some important Late Proterozoic copper deposits (e.g. Zambian Copper Belt, White Pine, Redstone copper belt). Haynes suggested that arid conditions prevailed during deposition, because sulfates and chlorides occur within the source rocks. Arid

Figure 80. Top of Red zone with abundant barite crystals overlain by quartz arenite (upper right)

Figure 81. Proterozoic chemical erosion of the top of the Red zone (in drillhole AB 7) resulting in leaching (voids) and oxidation

Figure 82. A lath-shaped pseudomorph of calcite plus quartz, after gypsum, within ferroan dolomite and quartz. Base of picture is 0.9 mm (plane-polarized light)

conditions could have occurred during deposition of the basal clastic units of the Bangemall Group, even though evaporites (as indicators of aridity) appear to be absent.

Correlation of the Black and Red zones with the Gap Well formation of the Jillawarra basin

While the Stringer zone corresponds (with respect to thickness and facies) to the upper part of Unit *GW5* plus the lower and (in places) the middle parts of Unit *GW6*, the Black and Red zones correlate with the upper part of Unit *GW6* of the Jillawarra basin (Fig. 9). However, the sedimentation rate of sabkha sediments would be slower than that of the (slightly clastic) dololutites (Kendall, 1979) of the Jillawarra basin; this prohibits correlation using the thicknesses of sequences.

Unit *GW6* of the Jillawarra basin is characterized by a regressional development with intertidal to supratidal deposits. The units in the Abra sub-basin also indicate regression: from intertidal to subtidal sediments of the Stringer zone, through shallow-water subaqueous evaporitic iron-formation of the Black zone, to coastal sabkha deposits of the Red zone. There are only minor differences between the depositional controls on lithologies in Unit *GW6* of the Jillawarra basin and equivalent lithologies at Abra (restricted basin and slightly shallower water). However, the resultant sediments are quite different, suggesting that regression in the Abra area was more pronounced than in the Jillawarra basin to the west.

Summary

In the Abra sub-basin, lithologies of the Gap Well formation are characterized by two groups of minerals: those of sedimentary association (which may have been mobilized during the course of subsequent developments); and those which have formed in connection with hydrothermal processes.

The minerals of sedimentary association are carbonates, iron oxides, Ca sulfates and pyrite which occur in the Black and the Red zones, and carbonate plus clastic minerals (quartz, feldspars, micas) which occur in the Stringer zone. The post-sedimentary, 'hydrothermal' minerals comprise all sulfides (except syndiagenetic pyrite), possibly some Fe oxides, quartz, barite, chlorite, albite, and hyalophane. The mode of emplacement of these minerals differs within the stratigraphic sequence. In the Stringer zone, sulfide veining, silicification, and chloritization prevail, whereas in the Black and Red zones additional processes are shown by the replacement of carbonate (by quartz), of sulfate (by barite, quartz, carbonate), and of pyrite (by other sulfides), plus some albitization.

There is also a variation in the mineral composition of the veins, within the sequence at Abra. In the lower parts

of the Stringer zone, the veins contain chalcopyrite, quartz, magnetite, chlorite, carbonate, and pyrite. In the upper Stringer zone and lower Black zone, the abundant minerals are galena, pyrite, magnetite/hematite, quartz, carbonate, chlorite, and barite. Veins in the Red zone consist predominantly of barite, pyrite, hematite, quartz, and carbonate. In places throughout the sequence the veining is accompanied by brecciation and, in the Stringer Zone in particular, the fine-grained breccia 'matrix' is preferentially mineralized by sulfides.

Replacement of pyrite by other sulfides in the Black and Red zones has been preceded by the syndiagenetic growth of pyrite, within the upper layers of the sediment pile ('syngenetic pyrite'), in connection with bacterial sulfate reduction. With the onset of hydrothermal activity, metal-bearing fluids percolated through the sedimentary pile and replaced pyrite. Further precipitation of sulfides was controlled by the availability of H_2S from bacterial sulfate which was trapped in the sediments. Recrystallization of fine-grained syndiagenetic pyrite continued throughout the period of base-metal mineralization. Tetrahedrite in recrystallized pyrite is rich in both Fe and As, suggesting that its formation was related to the recrystallization of pyrite.

In the Black and Red zones, the abundance of replacement textures and minerals, and the occurrence of veins, suggest that hydrothermal activity commenced after deposition of the host sediments and that synsedimentary exhalative processes were not significant in the two zones.

The onset of hydrothermal activity is linked to the generation of deep-seated faults during incipient rifting, which also led to deposition of the coarse clastic Unit *WC1* overlying the host-rock sequence at Abra. The host rocks would then still be undergoing diagenesis, so that there was an abundance of diagenetic formation waters and of pore spaces to allow the widespread replacement of Ca sulfates, carbonates, and pyrite. With respect to the host-rock sequence, the mineralization at Abra is best described as syndiagenetic.

West Creek formation

This formation is intersected in all Abra drillholes, with intersections ranging from 220 m (AB 6) to over 500 m (AB 11) in the southeast of the area. Mineralogical and sedimentological characteristics are very similar to the West Creek formation in the Jillawarra basin, so further detailed discussion is not necessary here. Short descriptions of some features of the formation, considered unique to the Abra sub-basin, are provided below.

Unit WC1

This coarse clastic unit has a maximum thickness of 40 m, but it is absent in drillholes AB 6 and AB 7 in the north, and AB 11 in the southeast (Fig. 58). Dominant rock types are: medium- to coarse-grained, moderately sorted, rounded to subangular lithic quartz arenite, and polymict granule conglomerate to pebble conglomerate (Fig. 39). The cement usually consists of carbonate and minor cherty quartz. In the lower part of this unit, barite occurs locally as cement (up to 6.4% Ba over 2 m). The barite has probably been introduced post-depositionally, and may have been either remobilized from the underlying Red zone or emplaced through hydrothermal activity.

The epiclastic grains comprise quartz, potash feldspar, chert, shale, and jaspilitic rock. Some of the shale clasts are chloritized, others consist entirely of chlorite. Locally, the bedding is defined by detrital Ti-bearing iron oxides which have been altered in situ to sphene; this phenomenon is also observed in the underlying Red zone. Although clasts of shale, chert, and jaspilite are obviously derived from the underlying Red zone, the abundance of quartz, potash feldspar and Ti-bearing iron oxides is indicative of a granitic source. The overall composition of the clastics is very similar to that in the clastic intercalations occurring in the Red zone, suggesting a common source for both clastic occurrences.

Unit *WC1* was deposited in a near-shore environment, as a coarse clastic carbonate-cemented sediment, possibly in a fluvial fan. Rapid subsidence of the depository is indicated by the presence of up to 40 m of coarse clastics. An important observation is that the drillholes which contain Unit *WC1* are separated by faults from drillholes in which this unit is absent (Fig. 57). This implies that clastites of Unit *WC1* have probably been deposited in a fault-bounded, subsiding basin; i.e. the Abra sub-basin. The limits of the Abra sub-basin are thus defined by the presence of Unit *WC1*.

Unit WC2

Whereas there is a difference between lithologies present in Unit *WC1* in the Abra sub-basin and the Jillawarra basin (the common dolomitic shale and siltstone of the latter is absent in the Abra sub-basin), Unit *WC2* of the Abra sub-basin is probably identical to that in the Jillawarra basin. At Abra the thickness of the unit is about 330 m, and it represents the shallow-water turbidite facies previously described in Chapter Three. Following the period of subsidence of local sub-basins, represented by occurrences of Unit *WC1*, the turbidites of Unit *WC2* indicate a prolonged period of subsidence which (in contrast to Unit *WC1*) affected the entire Jillawarra basin.

Unit WC3

This unit was intersected only in the southernmost drillholes (AB 9, AB 10, and AB 11). It comprises interbedded lutite–siltstone (frequently carbonaceous), fine-grained quartz arenite with subordinate coarse-grained lithic quartz arenite, and rare conglomerate. The absence of significant carbonate (massive or as dolomitic siltstone) is the main difference between Unit *WC3* here and Unit *WC3* elsewhere in the Jillawarra basin. However, a similar depositional environment, that of a tidal flat, is indicated. The change from shallow-water turbidites (Unit *WC2*) to tidal-flat sediments may signal a decrease in rate of subsidence throughout the Jillawarra basin.

Structure of the Abra sub-basin

The Abra sub-basin lies close to the eastern end of the Jillawarra basin, which is marked by the regional Tangadee lineament. The latter also marks the boundary between the structural domains of the Edmund Fold Belt and the Bullen Platform. The Abra sub-basin is located in the southern shallow limb of a broad major anticline (Section E–F, Plate 1).

Faults

The area of the Abra mineralization is limited by three faults (Fig. 56). Two northeasterly trending faults are probably related to the Abra fault system in the east, whereas the easterly trending fault parallels the regional Quartzite Well Fault to the north. By comparison with northeasterly trending faults elsewhere in the Jillawarra basin, it can be assumed that similar faults in the Abra area are normal and steeply dipping. The faults have been active from the period of deposition of Unit *GW6* onwards; i.e. they are synsedimentary faults with respect to the sequences in the Abra sub-basin.

Synsedimentary tectonic activity is evident from deposition of the Stringer zone onwards; soft-sediment deformation and slump structures are abundant. Clastic dykes, particularly abundant in the Stringer zone, are further indications of synsedimentary tectonics, because they represent the injection of sedimentary material into fractures that were created by shock waves or slumping (Reineck and Singh, 1973).

Cleavage

It has not been possible to identify any penetrative cleavage in core specimens or thin sections from Abra. Because of the open-style folding of the Abra anticline plus the siliceous, non-micaceous nature of the rocks, conditions were not favourable for the development of a pervasive cleavage.

Development of the Abra sub-basin (a third-order basin)

The Abra sub-basin is limited by an easterly trending fault to the north and by two northeasterly trending faults to the east and west respectively. The sub-basin has an east–west dimension of 600 to 1000 m, while from drilling it is known to extend at least 600 m in a north–south direction (open towards the south). The deposition in the Abra sub-basin is analogous to that in the Jillawarra basin (Chapter Three). Following a period of regression, represented by Unit *GW6* (Stringer, Black, and Red zones), there was an initial period of localized transgression (Unit *WC1*), which was followed by a period of widespread transgression turbidites (of Unit *WC2*). While trans-gression is clearly related to subsidence of the Abra sub-basin and, later, the whole of the Jillawarra basin, the events that occurred during the period of regression at Abra are more complex, and these are discussed in detail below.

Sediments of the Stringer zone formed in the same intertidal to subtidal environment as those in the lower to middle parts of Unit *GW6* in the Jillawarra basin. However, in the upper part of Unit *GW6* at Abra there is evidence that the regressional development was enhanced. Proterozoic erosion is shown not in the most easterly or most northerly drillholes but in the most westerly (AB 7). This suggests that emergence was taking place in the west (with respect to the Abra sub-basin) and that a barrier zone could have formed the western limit of the sub-basin (along a synsedimentary fault). The existence of such a zone could explain the preservation of the subaqueous evaporites of the Black zone: a barrier would be required to prevent the exchange of waters between the saline basin and the open sea. To account for the deposition of up to 40 m of subaqueous evaporites, subsidence of the (fault-bounded) sub-basin must be invoked (Kendall, 1979). There were apparently two conflicting senses of movement in the underlying basement. In one sense the enhanced regression and the formation of a barrier indicate uplift in the Abra area, but in the other sense the subaqueous evaporites suggest subsidence of the Abra sub-basin. Furthermore, it might be expected that a fault-bounded basin developed in a normal coastal environment would be a sink where tidal channels could deposit clastic material. But at Abra, there is an absence of significant clastics in the Black zone, which suggests that a different situation prevailed.

A possible explanation for the situation at Abra is that such a basin could have formed on the slope, or the summit, of an emergent basement complex (dome). The downfaulting of the basin could be the result of crustal strain through extension, which was most effective around the periphery of the dome. In such a case the area could then have been sufficiently elevated to cause any rivers and tidal channels to be diverted elsewhere. Thus, a limited amount of clastic material would be transported into the basin. A similar situation is envisaged by Jackson and Seni (1983) to explain the paucity of terrigenous sediments in evaporites and shallow-marine carbonates in a marginal-rift basin in the Gulf of Mexico. It is therefore proposed that doming took place in the Abra area (active emergence is also inferred for the Jillawarra basin; Chapter Three) accompanied by the development of a fault-bounded basin, with the faulting due to crustal extension in the domed area. The elevation of Coobarra Dome east of Abra further corrobates domal uplift in this region. Because of the limited number of drillholes and the general lack of outcrop, other than quartz arenites, the evidence for active emergence of the Abra area and the existence of the western barrier is equivocal.

A proposed six-period model for the development of the Abra sub-basin is illustrated in Figures 83 to 88. The following notes serve to highligh the characteristics of each period.

Period representing deposition of middle parts of Unit GW6 (Stringer zone)

The contemporaneous coastline lay to the north and east of Abra, and the sub-basin seems to have become deeper

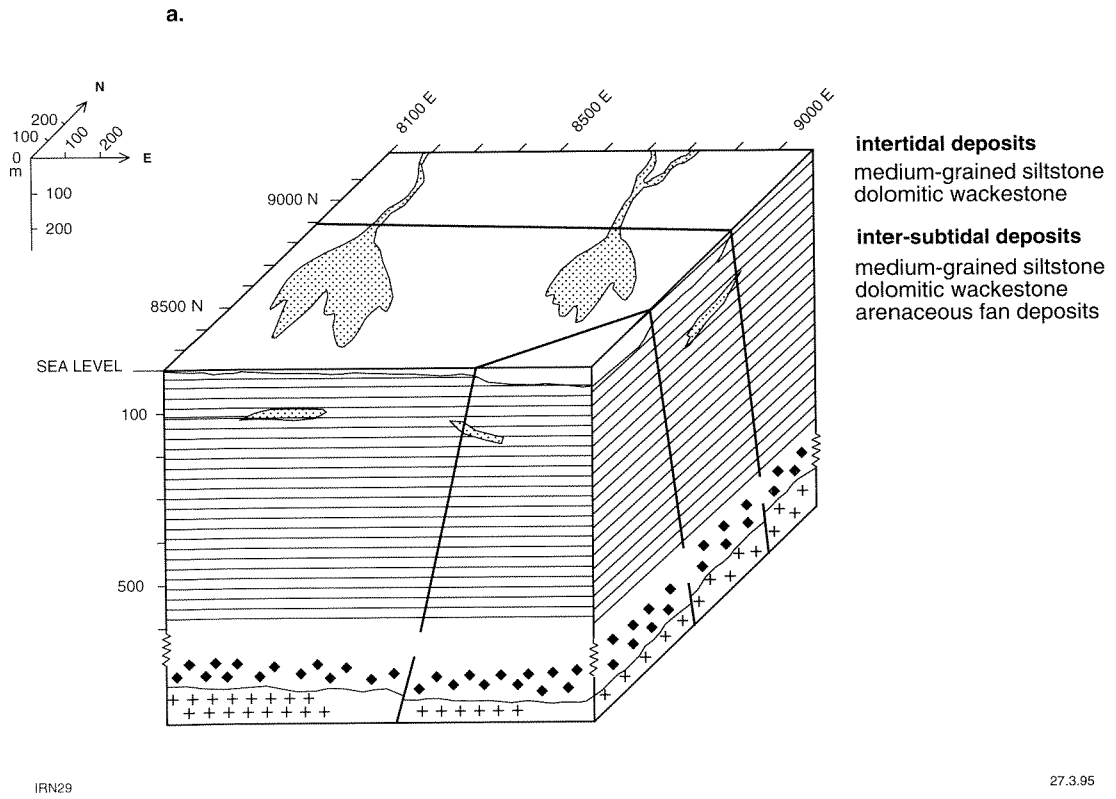

Figure 83. Abra area, deposition of middle of Unit *GW6* (Stringer zone sediments)

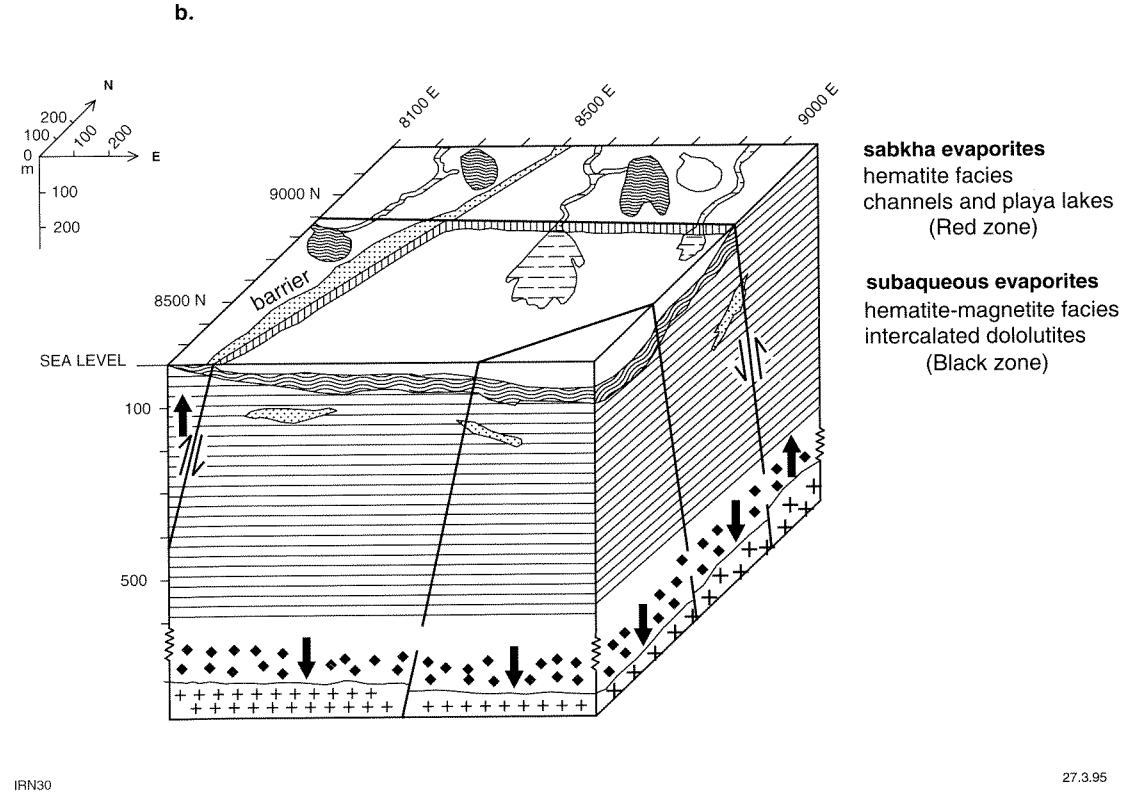

Figure 84. Abra sub-basin, deposition of upper part of Unit *GW6* (Black zone)

c.

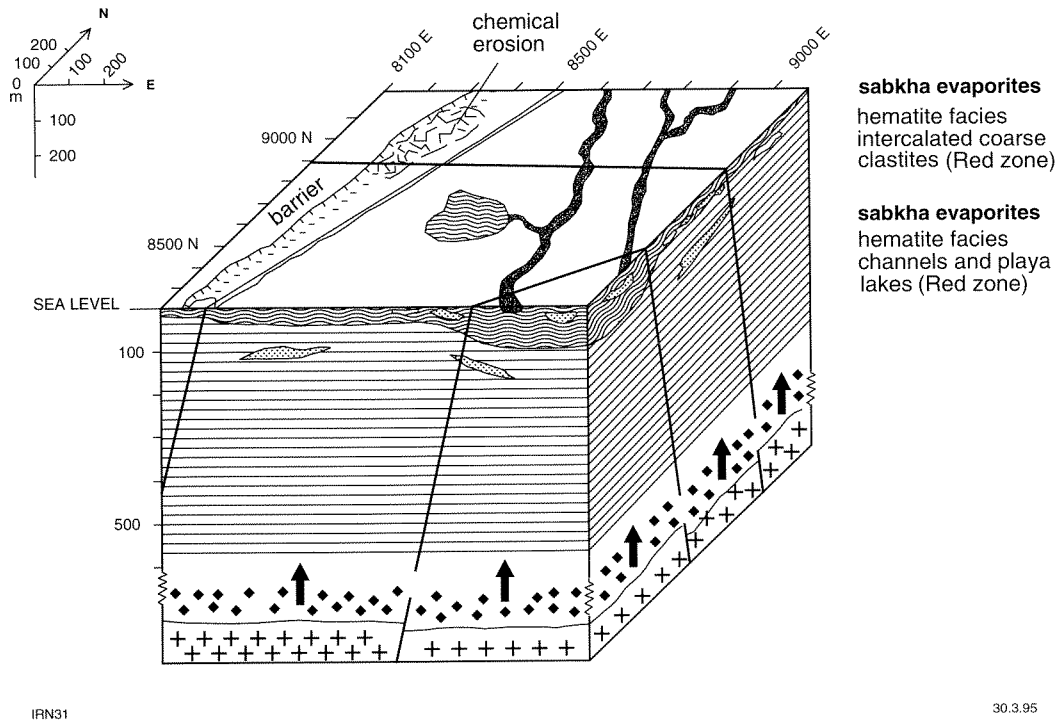

Figure 85. Abra sub-basin, deposition of uppermost part of Unit *GW6* (top of the Red zone)

d.

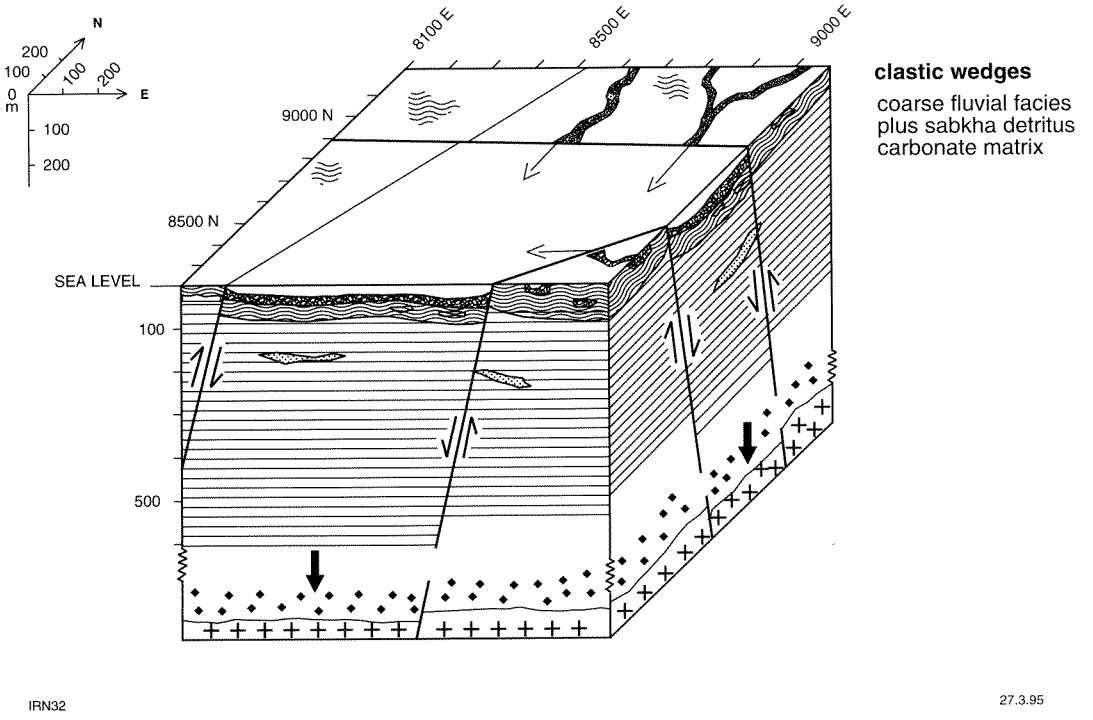

Figure 86. Abra sub-basin, deposition of Unit *WC1* (coarse clastites)

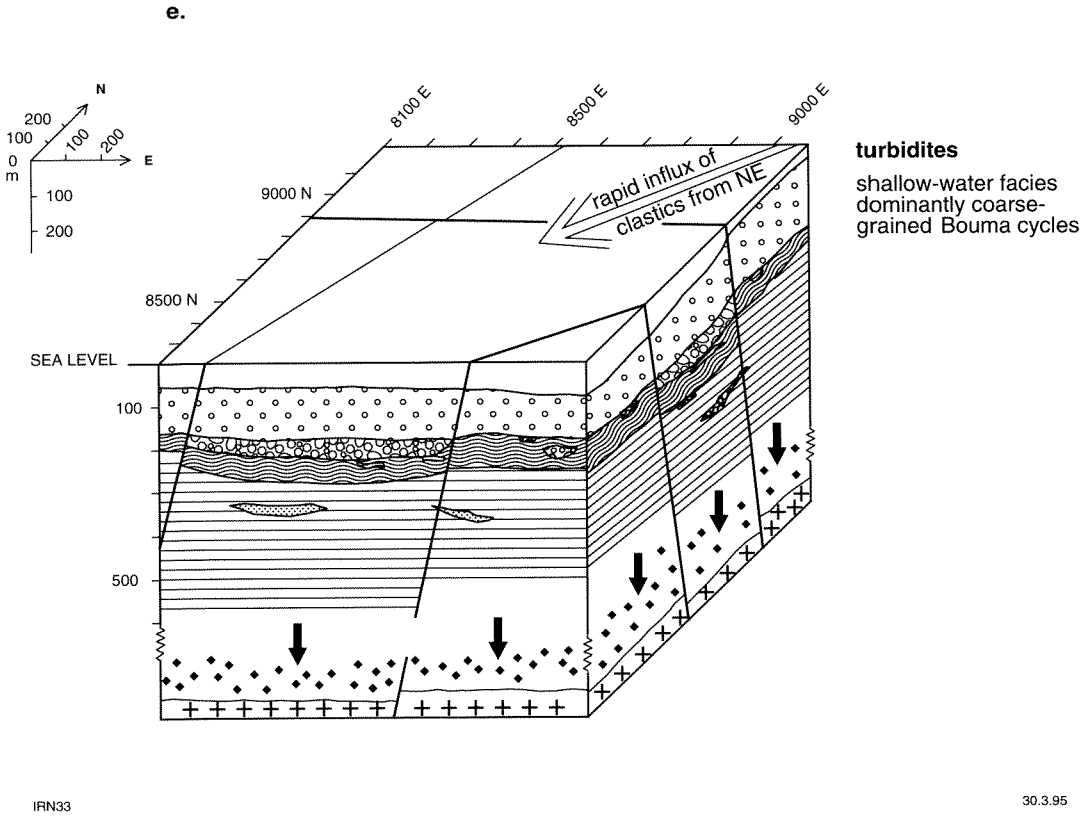

Figure 87. Abra sub-basin, deposition of Unit *WC2* (turbidites)

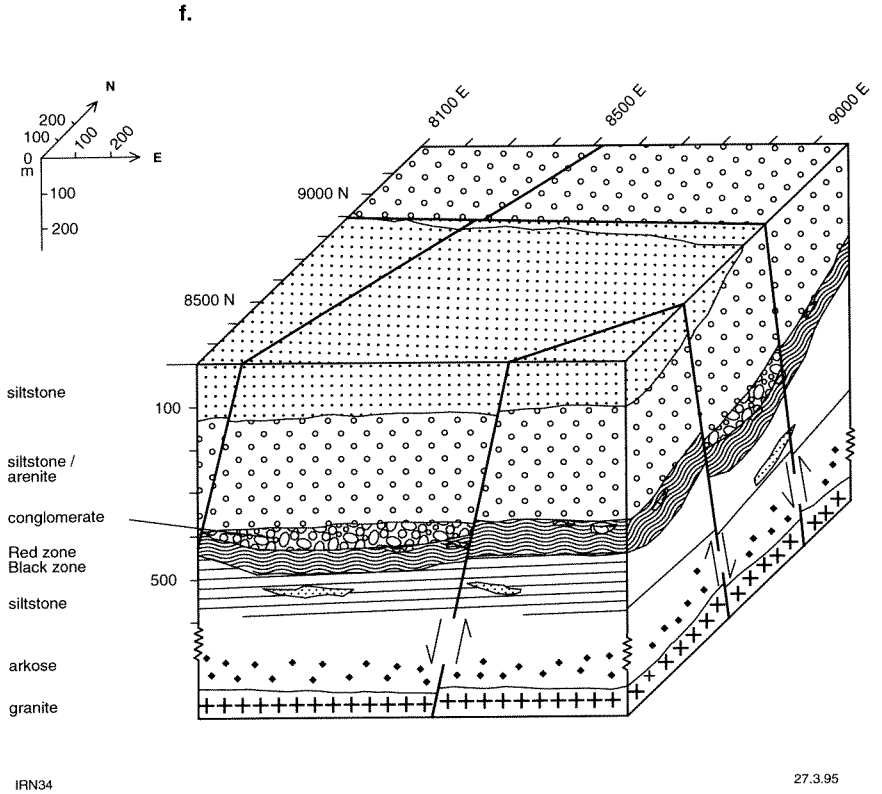

Figure 88. Abra area, present day

towards the southeast. Sediments were predominantly intertidal to subtidal calcareous silts, with some arenaceous fan deposits (Fig. 83). Towards the centre of the sub-basin, these sediments were intercalated with minor turbidites. There was no significant fault activity during this period, and the Abra sub-basin had not yet begun to develop. The whole area was probably undergoing slight emergence.

Period representing deposition of upper part of the Unit GW_6 (Black zone)

While surrounding areas were progressively uplifted, the Abra sub-basin began to develop through local down-faulting. It is uncertain whether movement occurred along the southeastern fault. Because of the continuing uplift of the surrounding areas a barrier began to form and this separated the Abra sub-basin from the sea (Fig. 84). Subsidence of the sub-basin resulted in the deposition of subaqueous evaporitic iron-formations (Black zone), while in the adjacent areas, tidal flats became supratidal and a coastal sabkha was developed (lower Red zone in drillholes AB 6 and AB 7).

Period representing deposition of uppermost part of Unit GW6 (top of the Red zone)

There was no further subsidence of the Abra sub-basin, and the whole area was affected by general uplift. The subaqueous evaporites graded into coastal sabkhas with minor clastic sedimentation (Fig. 85). The former coastal sabkhas in the north were characterized by abundant clastic intercalations and resembled continental sabkhas. Locally, in the zone of the former barrier, there was prolonged subaerial exposure which led to Proterozoic chemical erosion of the sabkha sediments.

Period representing deposition of Unit WC1 (coarse clastites)

Rapid subsidence of the Abra sub-basin occurred along the three faults (Fig. 86). The subsiding basin was filled by up to 40 m of coarse, carbonate-cemented shallow-water clastites in a fluvial environment. The clastics were derived mainly from a granitic source, probably from the northeast. Some of the areas adjacent to the Abra sub-basin remained as sabkhas. The sabkha deposits were rapidly lithified and contributed a minor portion of jaspilitic rocks to the clastites.

Period representing deposition of Unit WC2 (turbidites)

Regional subsidence resulted in the deposition of several hundreds of metres of coarse-grained shallow-water turbidites, with complete Bouma cycles in places. The clastics were derived from a landmass in the northeast (Fig. 87).

Period of folding (present disposition of Abra sub-basin)

During regional folding of the Bangemall Group, a major, broad, asymmetrical anticline formed (Coolina Anticline). The Abra sub-basin is located on the southern limb of the anticline, which has a shallow plunge towards the west. This has produced an average dip of 20–30° to the south-southwest, in the Abra area (Fig. 88). The arrows on Figure 88 indicate the latest sense of relative movement along faults which is related to the late-stage folding of the Bangemall Group.

Chapter Eight

Hydrothermal alteration in the Jillawarra basin

Hydrothermal processes leading to the formation of the Abra mineralization were accompanied by certain alteration assemblages associated with silicification, albitization, and chloritization. Preliminary fluid inclusion data suggest that this alteration took place at 190–260°C.

Silicification

This is the most significant and widespread type of alteration and can be recognized in all rocks of the Jillawarra basin. It is strongest in the Abra area, and also to the west at the TP and Copper Chert prospects, where it shows decreasing intensity away from the areas of mineralization. Silicification, therefore, may be regarded as a large-scale indicator of the proximity of a mineralized area. When silicification affects calcareous sediments it replaces carbonate to various extents, leaving remnants of the original lithology such as small relics of carbonate inclusions in quartz. Silicification of arenites leads to exclusively quartz-cemented quartz arenites, resulting in massive rocks with a quartzite appearance, in particular in Units *WC1* and *WC4* (Chapter Three). Silicification may also be involved in the chloritization of carbonate rocks.

Albitization

Albitization, though less common than silicification, is also recognized throughout the Jillawarra basin. Authigenic albite (<2% An) is mainly associated with galena at Abra, occurring at the contact of wall rock and veins, or within the wall rock. Although authigenic albite in calcareous pelites in Units *GW5* and *GW6* of the Jillawarra basin does not contain any galena inclusions, it could also have formed from hydrothermal solutions, which were more distal and, therefore, devoid of metals.

In the Sullivan deposit, British Columbia, albite–chlorite alteration occurs as a pervasively altered zone in the hanging wall up to 100 m above the sulfide horizon (Ethier et al., 1976). This zone is spatially restricted to the immediate vicinity of the massive-sulfide mineralization.

In the Abra area albitization is more widespread, occurring in distal and proximal positions to the mineralization. As it is related to the ubiquitous hydrothermal silicification, it is likely that SiO_2 (and possibly Al) reacted with Na in formation waters to produce albite.

Chloritization

This is most common in the vicinity of Abra, and is related to hydrothermal processes. Chloritization affected carbonates, micas, clay minerals, and potash feldspars.

Chloritization of potash feldspar took place indirectly through chloritization of sericite which had formed earlier as a product of decomposition of potash feldspar.

Chloritization of principally the same type, but less intense, is prevalent throughout the Jillawarra basin. However, there is an exception to this in the development of chlorite in the Manganese Range Anticline, which defines foliation in a quartz–chlorite–magnetite schist of Unit *GW2*. Chlorite development is interpreted to be due to tectono-metamorphic processes (thrusting of the rocks towards the north-northeast after the termination of hydrothermal activity) rather than to hydrothermal processes associated with mineralization. In addition to chlorite, biotite is widespread in the Jillawarra basin. Notably, biotite is absent in the Abra area.

In general, the occurrence of chlorite and biotite seems to characterize two extreme environments during the alteration phase (or late diagenesis?) of the Jillawarra basin, including Abra. Chlorite clearly represents the proximal ore environment while biotite occurs in the distal, non-ore environment. In an intermediate position (with respect to proximal/distal) there is a low-K phyllosilicate in the low-grade mineralization at the 46–40 prospect, in the west of the Jillawarra basin. This is a high-Si, Mn (Fe), low-K phyllosilicate that occurs in veins, suggesting that it was a product of hydrothermal fluids. However, in this case the phyllosilicate is rich in SiO_2 and Mn but depleted in Mg when compared with proximal vein chlorite.

In summary, there appears to be a genetic relationship between the type of phyllosilicate formed during alteration, and the proximity to hydrothermal systems (provided that the phyllosilicates formed contemporaneously). The various phyllosilicates possibly represent differences in the chemistry of hydrothermal fluids, but they may also have formed in response to different temperatures as follows:

(a) proximal: chlorite; indicating high-grade or high-temperature hydrothermal activity;

(b) intermediate: low-K phyllosilicate; indicating low-grade or low-temperature hydrothermal activity;

(c) distal: biotite; indicating low-temperature alteration.

The composition of chlorites as proximity indicators to mineralization has been demonstrated by Reimann and Stumpfl (1985), and Kalogeropoulos (1983). To date, a relationship between the mineralogy of phyllosilicates and the proximity of ore environments has not been observed and it may be useful to investigate the mineralogy and chemistry of phyllosilicates in order to examine their use as an instrument in exploration.

Chapter Nine

Mineralization in the Jillawarra basin (outside the Abra sub-basin)

Muhling and Brakel (1985) discussed various mineral occurrences in the Bangemall Basin, and divided these into a number of groups:

(a) stratabound zinc with minor copper;

(b) fault-zone deposits of lead and zinc;

(c) copper and lead in carbonates of the Irregully Formation;

(d) fault or fissure deposits of copper at the contact between shale and dolerite (at Ilgarari and Kumarina);

(e) gold (at the Bangemall Mining Centre);

(f) surface enrichment of manganese;

(g) stratabound phosphate.

Within the Jillawarra basin three of these groups may be recognized; groups (a) and (b) at the Quartzite Well prospect (Davy, 1980), and group (f) at the Manganese Range and Woodlands Hill (de la Hunty, 1963). The remaining groups appear to be unrelated to the mineralizing processes that have operated in the Jillawarra basin.

The stratabound lead–copper–barite mineralization in the Gap Well formation, in the Jillawarra basin, is one of the main subjects of this study. It was not considered by Muhling and Brakel (1985) because they had compiled their data for Bulletin 128 during 1978, before the exploration drilling results in the Jillawarra area were available.

Mineralization in the Jillawarra basin

Since exploration for base metals in the Jillawarra area commenced in 1974, several target areas have been defined by magnetic surveys and soil and rock-chip geochemical surveys. Although geochemical and geophysical anomalies have been delineated, no significant gossans have been observed to date, except for the gossan at Quartzite Well and the barite–copper mineralization that occurs at the surface at the Woodlands prospect. The various geochemical and geophysical anomalies have been tested by some 30 diamond drillholes at nine prospects (the locations of which are shown on Plate 2). All prospects are situated within the limits of the Gap Well formation, within the limits of the Jillawarra basin.

Using data from diamond drillholes, the stratigraphic interval of significant mineralization in the Jillawarra basin may be correlated with the stratigraphic interval of Abra mineralization in drillhole AB 3 (Fig. 89). Table 6 lists the grades and characteristics of mineralization in the Jillawarra basin. Prospects with negligible grades of mineralization (e.g. Jeds prospect, Manganese Range East prospect) are excluded from Table 6 and are not discussed further.

Two types of mineralization similar to those at Abra can be distinguished at a number of prospects elsewhere in the Jillawarra basin:

(a) Black zone type; and

(b) Stringer zone type.

Black zone type mineralization

This type of mineralization was observed in drillcores from the 46–40 prospect in the west of the basin. The host rock is a laminated magnetite–quartz–carbonate rock (Fig. 89) which is commonly brecciated and veined. In DDH 77-28 a 'Black zone' thickness of 37 m was intersected (Fig. 89). The sequence is at a stratigraphic level similar to that of the Black zone at Abra, and is similar in thickness. However, the zone is not overlain by sabkha lithologies, as is the case with the Red zone at Abra. This may suggest that there was a less pronounced regressional development in the 46–40 area.

During the deposition of this Black zone at 46–40, the environment was probably less oxidizing and less saline than that at Abra. Hematite is almost entirely absent. There are very few pyrite layers, which suggests that microbial mats were not very abundant. This points to a permanent cover of only moderately oxidizing water. The commonly distinct layering of magnetite–quartz–carbonate

Table 6. Features of low-grade mineralization

Features of mineralization	*Name of prospect* '46–40' representative drillhole: 77–28	'Woodlands' representative drillhole: 81–5	'TP' representative drillhole: 81–8
Significant intersections (over core m)			
Pb	3.10% (110–114 m), 1.30% (131–134 m)	—	3.60% (594–598 m), 4,70% (623–625 m)
Cu	0.30% (113–115 m), 0.25% (135–147 m)	0.29% (372–410 m), ~0.40% (442–460 m)	—
Ba	15.00% (132–138 m), no continuous assays	5.90% (372–410 m), ~4.00% (422–460 m)	10.90% (593–598 m), 990% (623–625 m)
Zn	—	—	0.25% (890–891 m)
'Background' range (enriched in:)			
Pb	50–1 500 ppm (Black zone, footwall)	0–325 ppm	50–10 000 ppm (400–960 m)
Cu	10–500 ppm (lower Black zone)	10–75 ppm	25–375 ppm (594–598 m)
Ba	not determined	300–1 800 ppm	4 000–60 000 ppm (570–1 200 m)
Zn	35–100 ppm (upper Black zone)	10–450 ppm (above mineralized zone)	40–350 ppm
Mode of occurrence	chalcopyrite in veins (with quartz–magnetite)	Barite, chalcopyrite in veins, chalcopyrite disseminated within chloritic fine-grained sedimentary rock;	Within calcareous vein breccia
	galena in veins and disseminated; barite in irregular patches	Barite disseminated; cement and chalcopyrite disseminated in Woodlands Arenite	
Associated minerals	pyrite in veins and conformable layers <1% between 151 and 255 m	abundant magnetite;	magnetite, pyrite
		subordinate pyrite and pyrrhotite in hangingwall	
	Fe–Mn carbonate, magnetite	Fe–Mn carbonate	
	chlorite, jaspilite	chlorite, biotite, hyalophane	biotite, chlorite
Host rock	Brecciated magnetite–quartz–chlorite–barite–carbonate rock, laminated (Black zone-type)	370–410 m: silicified chloritic siltstone/ sandstone	593–598 m: brecciated dolomicrite
		422–460 m: silicified coarse grained arenite (Woodlands Arenite)	678–788 m: Woodlands Arenite shows high magnetite content and high Mn values, but no sulfides present
Stratigraphic position of best intersection	Upper *GW6*	Lower *GW5*	Lower middle *GW5*
		Upper *GWw4*	
Zoning	Not clear; Mn enriched in upper part of Black zone and above Black zone	More Ba in upper mineralized zone; absence of Pb in Cu-rich zones	Extreme 'telescoping': highest assays of Pb, Cu, Ba, Ag in 4 m interval (594–598m)
Correlation	Ag (Zn) with Pb	Possibly Mn with Ba	Ba with Pb Ba with Mn, however, Mn is more widespread Ag with Pb
Alteration	Silicification, chloritization, brecciation	Silicification, chloritization	Silicification, chloritization, brecciation
Remarks	Highest Mn values in lower part of hole, associated with magnetite veins; several thin jaspilite interbeds in Black zone	Ag, Au ≤1 ppm: within mineralized zones Pb, Zn do not exceed 90 ppm; highest Mn values in lower part of hole; no significant mineralization above 360 m	Highest Mn values associated with magnetite enrichment, 678–788 m, in Woodlands Arenite and 970–1200 m in dolomite/ siltstone; mineralization clearly related to veining and brecciation; Au <0.01 ppm

in the Jillawarra basin (excluding Abra)

'TC' representative drillhole: 78–35	*'Manganese Range' representative drillhole: 77–27*	*'Copper Chert' representative drillhole: 76–20*
—	0.23% (118–130m)	—
0.31% (519–565m)	0.91% (332–345m)	1 vein with 2–5% (216.8–217.0 m)
not determined	not determined	—
—	—	—
0–70 ppm	0–50 ppm (≤ 670 ppm above 86 m)	No assays
5–670 ppm	35–8 500 ppm (313–370 m)	No assays
not determined	not determined	No assays
15–225 ppm	25–115 ppm (≤410 ppm above 74 m)	No assays
Disseminated, magnetite–chalcopyrite vein; barite–quartz–carbonate veins	Chalcopyrite–magnetite–quartz veins; patches of chalcopyrite	Chalcopyrite–sphalerite–pyrite veins
Pyrite, minor pyrrhotite magnetite, in layers and disseminated carbonate, barite chlorite, biotite	Magnetite, layers and disseminated minor pyrite barite chlorite	Pyrite, pyrrhotite layers and disseminated
Silicified, chloritic, siltstone/sandstone, magnetite-rich (in layers and disseminated)	Chlorite–magnetite–quartz schist, partly brecciated	Laminated chloritic and dolomitic siltstone
Lower *GW5*	Lower *GW5* (or upper *GWw4*)	Lower *GW6*
Not clear because only Cu mineralization present; Mn enriched above Cu zone (455–500 m) Au with Cu (no continuous assay)	Mn enriched above 250 m	
Silicification, chloritization; minor brecciation	Silicification, chloritization	Silicification, chloritization
Intense barite–quartz veining below about 450 m (no assays); chalcopyrite and pyrite generally associated with magnetite-rich beds; Au <0.1 ppm (no continuous assay)	Barite veining and magnetite very abundant throughout the hole	No significant mineralization; probably no barite or magnetite

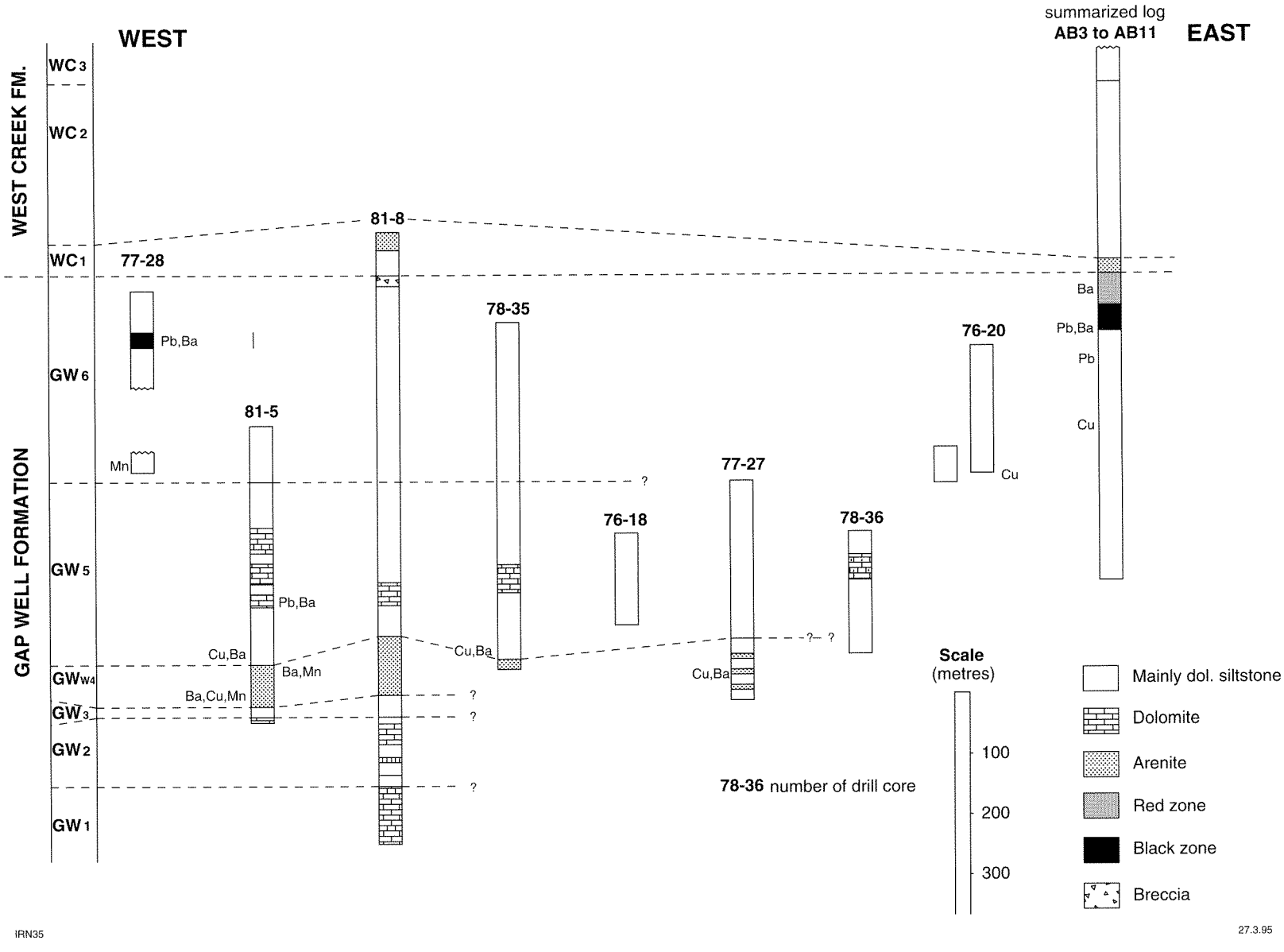

Figure 89. Stratigraphic position of significant mineralization in the Jillawarra basin, projected onto a W–E section of 51 km (no horizontal scale). See Figure 9 for names of prospects and Plate 2 for locations

(i.e. chemical sediments) suggests very quiet conditions of sedimentation, probably in a restricted basin. However, the absence of conformable sulfate layers (all barite seems vein-related) implies that salinity levels were below sulfate saturation within the sediments and basin waters.

The mineralization at 46–40 prospect is dominated by galena and barite with subordinate amounts of chalcopyrite. It is discordant (veins and disseminated) and is accompanied by silicification (replacing carbonate), chloritization and brecciation.

In summary, the Black zone of the 46–40 prospect differs from the Black zone of Abra with respect to the following features:

(a) Red zone is absent;

(b) depositional environment is less oxidizing and less saline;

(c) mineralization is of lower grade; and

(d) there is less syndiagenetic pyrite, therefore probably lower fS_2 during times of mineralization.

Despite these differences the Black zone sediments of the 46–40 prospect belong to the same genetic class (subaqueous evaporite iron-formation) as the Black zone at Abra. The mineralization is almost identical in style (discordant) and in mineralogy to the Abra mineralization (Pb, Ba, Cu, very minor Zn).

Stringer zone type mineralization

This type of mineralization is encountered in all drillholes listed in Table 6, including the footwall of the Black zone at 46–40. The host rock is usually a chloritic, magnetite-bearing siltstone and fine-grained sandstone of the *GW5* and lower *GW6* units (Fig. 90).

A feature common to all rock types in the Stringer zones is the abundance of magnetite, either as layers in fine-grained siltstone (up to 60% magnetite in rocks from the Manganese Range prospect) or disseminated in arenites (e.g. Woodlands Arenite) and dolomites (Fig. 91). Hematite and jaspilite are occasionally associated with magnetite but they are not abundant.

In drillhole TP-81-8, the host rock to mineralization is a brecciated dolomicrite containing chlorite/biotite stringers and secondary (whitish, sparitic) carbonate (Fig. 92).

The mineralization is predominantly Cu–Pb–Ba (lacking Zn) with chalcopyrite, galena and barite being the only ore minerals. Galena usually occurs with pyrite, either within pyrite or as seams to pyrite, which may indicate a post-pyrite emplacement of galena (i.e. pyrite

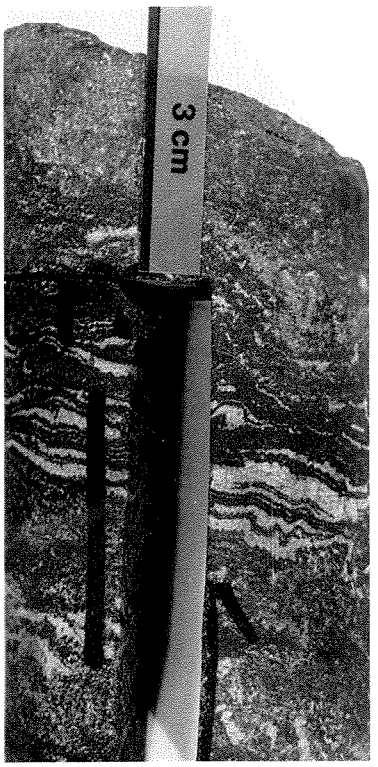

Figure 90. Black zone-type magnetite–carbonate laminae in core specimen from the 46–40 prospect

Figure 91. Laminated chloritic siltstone with layers of magnetite, and disseminated blebs of magnetite (subhedral) and pyrite (subhedral)

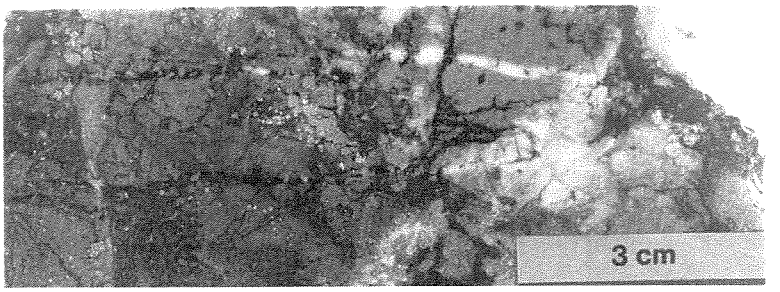

Figure 92. Brecciated dolomicrite with chlorite/biotite stringers and secondary carbonate

has formed diagenetically and was later replaced by galena during diagenesis). Abundant inclusions of magnetite/hematite in pyrite suggest that pyrite formed diagenetically within the sediments and incorporated pre-existing iron oxides. Although some chalcopyrite occurs on fractures in pyrite most of the chalcopyrite is associated with magnetite, usually as inclusions.

The style of mineralization comprises three types:

(a) vein;

(b) vein breccia;

(c) disseminated, patchy.

All are discordant to bedding and are associated with silicification and chloritization, and with the emplacement of barite, Fe–Mn carbonates, magnetite, and minor pyrite. Vein mineralization is by far the dominant type. Figure 93 shows a chalcopyrite–siderite vein in chloritic siltstone that is almost identical to veins seen in the Stringer zone at Abra.

The stratigraphic position of the mineralized intervals is below that reached by Abra drillholes (Fig. 89). However, the host rocks are comparable with those of the lower Stringer zone at Abra, consisting chiefly of chloritic siltstone and fine-grained sandstone (with the exception of a brecciated dolomicrite in drillhole TP-81-8).

Significant Ba and local Cu mineralization occurs in the Woodlands Arenite Member (*GWw4*) which underlies the chloritic siltstone/sandstone interval of Unit *GW5*. Higher grades of mineralization always occur in the hanging wall of the member.

Metal zonation

It is difficult to recognize vertical metal zonation within a single drillhole. This is mainly because only one metal is dominant in one drillhole, while concentrations of other metals are at 'background' levels and are distributed irregularly throughout the hole. However, comparison of the stratigraphic position of mineralization between various drillholes reveals a faint vertical zonation pattern. Whereas all Cu mineralization occurs within the *GWw4* and/or lower *GW5* unit (except drillhole 76-20 where the mineralization seems fault-related) Pb-rich mineralization occupies higher stratigraphic levels (drillholes 81-8; 77-28).

Copper-rich mineralization, at lower stratigraphic levels overlain by an interval enriched in Pb is comparable with metal zonation at Abra. However, a comparable Ba-rich interval stratigraphically above the Pb-rich interval (i.e. the Red zone at Abra) cannot be distinguished. Instead, Ba is closely associated with Pb and Cu mineralization. Another important difference from Abra is that the mineralization is generally 100–200 m stratigraphically below the mineralized lithologies at Abra.

The occurrence of Ba with Pb and Cu and the lower stratigraphic level of mineralization suggest that, compared with Abra, the hydrothermal fluids elsewhere in the Jillawarra basin were at lower temperatures and of smaller volumes. Lower temperatures prevented the ascent of the fluids to the stratigraphic levels at Abra. Also, smaller volumes of hydrothermal fluids resulted in a higher wall-rock/hydrothermal-fluid ratio, which in turn made the hydrothermal solutions susceptible to wall-rock reactions and caused close spatial precipitation of most metals (including barite).

The 46–40 prospect is the only exception to the trend described above. The host rock of Black zone type and the mineralization reaches the same stratigraphic levels as at Abra, which suggests that a similar temperature regime

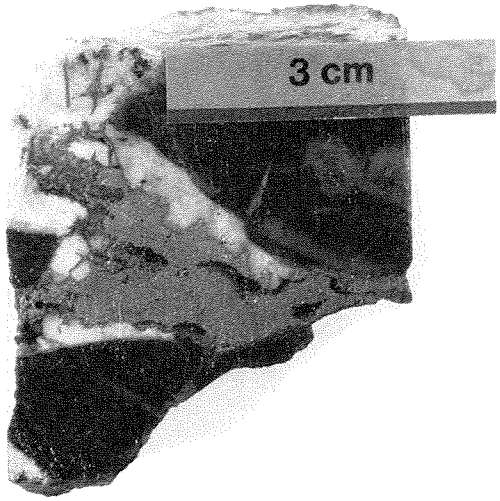

Figure 93. Chalcopyrite–siderite vein in chloritic siltstone (46–40 prospect)

occurred at 46–40. A localized high geothermal gradient was probably present in this area, because the 46–40 mineralization occurs in the vicinity of the Woodlands Fault, which forms the western margin of the Jillawarra basin. By comparison, the Abra mineralization is located near the faults which mark the eastern margin of the Jillawarra basin).

Quartzite Well Fault mineralization

A detailed study of the mineralization has been made by Davy (1980). Further points are discussed here to highlight features that may be pertinent to the proposed ore-forming processes at Abra. The mineralized zone is located in siltstone and calcareous siltstone of the Jillawarra Formation, which has been overthrusted on the northern side of the Quartzite Well Fault in the central Jillawarra basin (Plate 1).

The main sulfide mineral is pyrite (up to 60% of whole rock) in several morphological types ranging from fine-grained disseminated pyrite, through massive pyrite to authigenic pyrite euhedra. Locally, pyrite forms pseudomorphs probably after gypsum (Fig. 94) indicating hypersaline conditions of sedimentation. This is similar to the conditions proposed for the Abra sub-basin. A similar environment has also been interpreted for the Jillawarra Formation at the Glen Ross Spring prospect of Inco Australia, located about 30 km west-northwest of Quartzite Well, where hypersaline or sabkha conditions were proposed (Harrison, P., 1983, pers. comm.).

Pyrite also forms atoll structures (Fig. 95), which are described by Love and Zimmermann (1961) from the Mount Isa Shale. However, no replacement of the core or the rim by other sulfides has been observed.

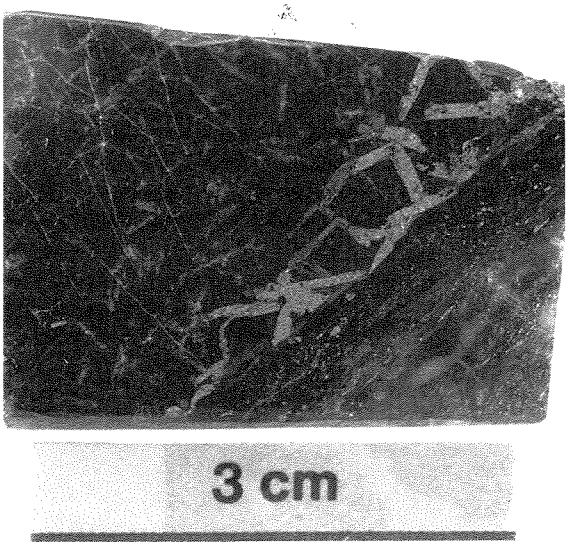

Figure 94. Lath-shaped pyrite, possibly after gypsum, in black siliceous shale, Jillawarra Formation, Quartzite Well prospect

Table 7. Electron microprobe analyses of sphalerite, Quartzite Well drillhole 76–12, 195.2 m, 'Ore Chert'

Element	*Percentage*			
Fe	0.687	2.378	2.246	1.280
Cu	4.004	1.170	0.294	1.407
S	30.819	32.647	33.795	33.167
Zn	64.581	66.376	62.045	61.664
Cd	0.123	0.180	0.258	0.278
Mn	0.003	0.000	0.000	0.000
In	0.000	0.000	0.000	0.000
Total	**100.217**	**102.751**	**98.737**	**97.933**

The main difference between mineralization at Quartzite Well and mineralization at Abra is that sphalerite is the main ore mineral. It occurs in veins, as disseminated grains, or as irregular masses within aggregates of pyrite. Microprobe analyses (Table 7) are in accordance with the Fe content reported by Davy (1980) for sphalerite from other occurrences of stratabound zinc with minor copper in the Bangemall Basin.

Davy (1980) suggested that the source of metals could be either connate water or palaeoriver (spring) water for Zn, and the mechanical erosion of older strata for (?detrital) copper. However, it may also be argued that connate or other groundwaters should transmit the geochemical characteristics of underlying strata. In that case the dominant minerals should be Cu and Pb, and there should be little or no Zn. In terms of a possible detrital origin for chalcopyrite from an adjacent 'basement high' (i.e. rocks of the Manganese Range Anticline, Plate 2), this seems unlikely. This area was covered by younger sediments at the time of mineralization. The area was upfaulted and eroded after deposition of the Bangemall Group (Chapter Three).

This study concludes that the metals were derived from hydrothermal solutions which ascended along the Quartzite Well Fault. The proximity of stratabound Zn with minor Cu to major fault zones or lineaments throughout the Bangemall Basin was recognized by Muhling and Brakel (1985), and it is tentatively suggested here that all the metals have the same mode of origin.

The Ba content of the Quartzite Well mineralization, about one order of magnitude higher than that of other copper–zinc mineralization in the Bangemall Basin, may indicate a link to the Abra-type hydrothermal system.

Summary

The other mineralized areas of the Jillawarra basin are similar to Abra in regard to the following features:

(a) metals; predominantly Cu–Pb–Ba, paucity of Zn;

(b) association of ore minerals; while galena prefer-

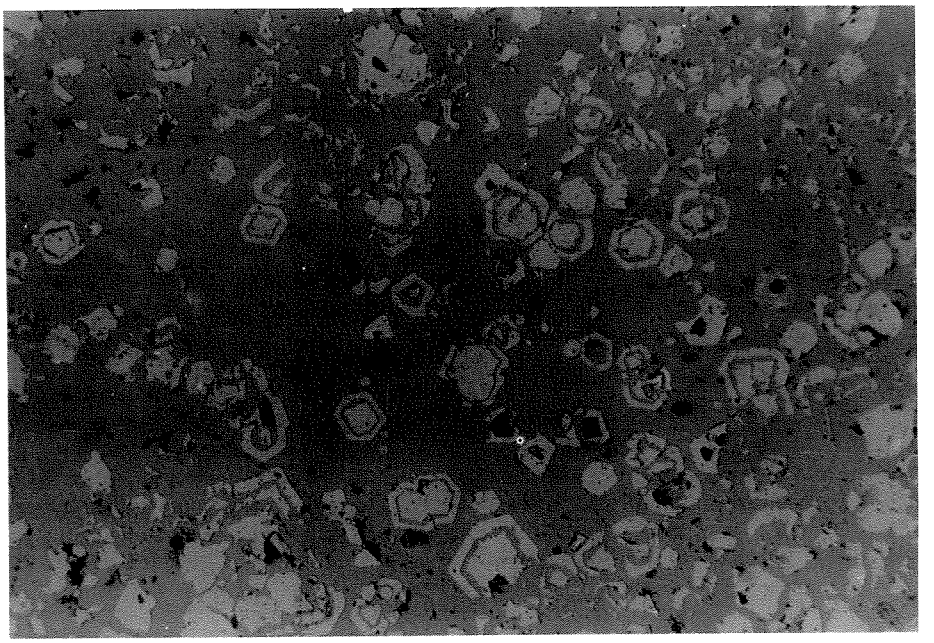

Figure 95. Atoll pyrite in black siliceous shale, Jillawarra Formation, Quartzite Well prospect. White is pyrite, grey is shale, black is hole in section. Base of picture is 0.58 mm. Reflected plane-polarized light

entially is concurrent with pyrite, chalcopyrite shows an affinity with magnetite;

(c) association of 'gangue' minerals; mineralization is usually accompanied by Fe–Mn carbonates, magnetite, pyrite, chlorite, quartz and minor jaspilite;

(d) alteration; mainly silicification, chloritization, and minor albitization;

(e) host rock; both Stringer zone-type chloritic siltstone/sandtone and Black zone-type laminated magnetite–quartz–carbonate rock;

(f) mode of emplacement; chiefly veins and disseminations, locally with concomitant brecciation;

(g) zoning; poorly developed;

(h) fO_2; abundant magnetite, slightly less hematite may be due to lower stratigraphic level;

(i) fS_2; magnetite dominant over iron sulfide and common syndiagenetic pyrrhotite indicates lower fS_2 within the sediments.

Most mineralization in the Jillawarra basin may be classified as low-grade Abra type, comprising Black zone type (46–40 prospect) and lower Stringer zone type (all prospects including the lower part of the 46–40 prospect). The hydrothermal system(s) was probably related to the Abra hydrothermal system, with respect to timing and metal source. The main difference between the Abra deposit and the low-grade mineralization elsewhere may be resolved by proposing that, outside the Abra sub-basin, a lower geothermal gradient existed throughout most of the Jillawarra basin during the period when mineralization took place.

The mineralization in the Jillawarra basin has features in common with the Zambian Copperbelt (Fleischer et al., 1976) and McArthur River (Lambert, 1976), carbonate hosted lead–zinc deposits (Sangster, 1976), and sediment-hosted massive sulfide deposits (Sangster and Scott, 1976). However, the metal abundances within these groups of mineralization are unique, and comparison with the above deposits may be impracticable.

Chapter Ten

Genesis of the Abra mineralization

A comprehensive model is now presented for the genesis and chronology of Abra-type ore formation in relation to the geotectonic development of the Jillawarra basin.

Geotectonic setting

The intracratonic sedimentary Bangemall Basin is one of the larger intrusive continental tholeiite provinces of the world. The intrusion of dolerite commenced at about the time of deposition of the middle Bangemall Group, and the intrusions were obviously related to a tensional crustal regime in the sialic basement (Muhling and Brakel, 1985).

Two sets of folds (northeasterly trending and easterly trending) are dominant, and were active both during and after deposition of the Bangemall Group. These folds, which are present mainly in the Edmund Fold Belt (one of three structural provinces distinguished), developed over mobile basement. Open-style drape folds were produced initially, but in the final stage of deformation these folds were tightened by compressional forces directed from the north-northeast and south-southwest.

The history of deposition in the Bangemall Basin indicates very shallow-water conditions during deposition of the lower Bangemall Group. Following this there was a regressional interval and two major transgressions, which were followed in turn by another regressional interval that marked the infill of the basin.

Structural and depositional evolution of the Bangemall Basin are interpreted as being in accordance with the development of an intracratonic rift that failed to develop further into an intercratonic rift. During the periods of crustal extension, transgressional sequences were deposited in the basin; the termination of extension is marked by a regression. Sawkins (1976) presented a list of worldwide examples of continental rifting between 1200 and 1000 Ma that have many features in common with the Bangemall Basin.

The irregular quantitative distribution of dolerite (Fig. 96) in relation to major basin faults and lineaments suggests the former presence of a triple junction (Chapter Two) in the area of the granitic Coobarra Dome, east of which the intracratonic rift bifurcates.

A recent study by Eriksson and Chuck (1985) concluded that the Bangemall Basin represented an aulacogen. This interpretation was related to a three-armed rift junction which developed close to the Paterson Province to the east. The study also concluded that the sediments of the rifting stage were largely confined to the southwestern basin margin, and equivalents of the Gap Well and West Creek formations were probably deposited during the thermal subsidence stage.

However, geological data from the Jillawarra area show that the West Creek formation was deposited in response to considerable faulting and rapid subsidence (more than 300 m of shallow-water turbidites), a situation incompatible with the thermal subsidence stage (McKenzie, 1978). Therefore, it is proposed that at least in the central Bangemall Basin (Jillawarra area), the West Creek formation (the equivalent of the Kiangi Creek Formation elsewhere) represents the rifting stage. Furthermore, if rifting occurred in an aulacogen from a three-armed rift junction in the east, the rift-stage deposits should not be concentrated in the southwest but rather in the central, early rift zone.

The Jillawarra basin principally reflects the depositional and tectonic history of the Bangemall Basin. However, subsidence within the Jillawarra basin (Fig. 47) occurred earlier than elsewhere in the Bangemall Basin. This early subsidence is characterized by Unit *WC1*. Subsidence during deposition of Unit *WC2* was more pronounced (shallow-water turbidites) within the Jillawarra basin than in surrounding parts of the Bangemall Basin. This indicates that rifting in the Bangemall Basin commenced within the Jillawarra basin, which was the initial, easterly trending, axial rift valley.

The development of the Abra sub-basin in relation to the Jillawarra basin indicates that crustal doming and the formation of a triple junction occurred in the vicinity of the Abra area. This is characterized by an interval of pronounced regression from subtidal siltstones, through subaqueous evaporitic iron-formation, to coastal sabkha. This sequence was deposited in a fault-bounded restricted basin (the Abra sub-basin) which, owing to greater strain in the periphery, formed in the apical zone of the crustal dome.

Doming in the Abra area implies that the adjacent granitic Coobarra Dome also was subject to doming in the period when the upper Gap Well formation was deposited. It is inferred that a thermal plume (hot spot) in the underlying mantle was responsible for doming in the Abra–Coobarra Dome area, analogous to the development

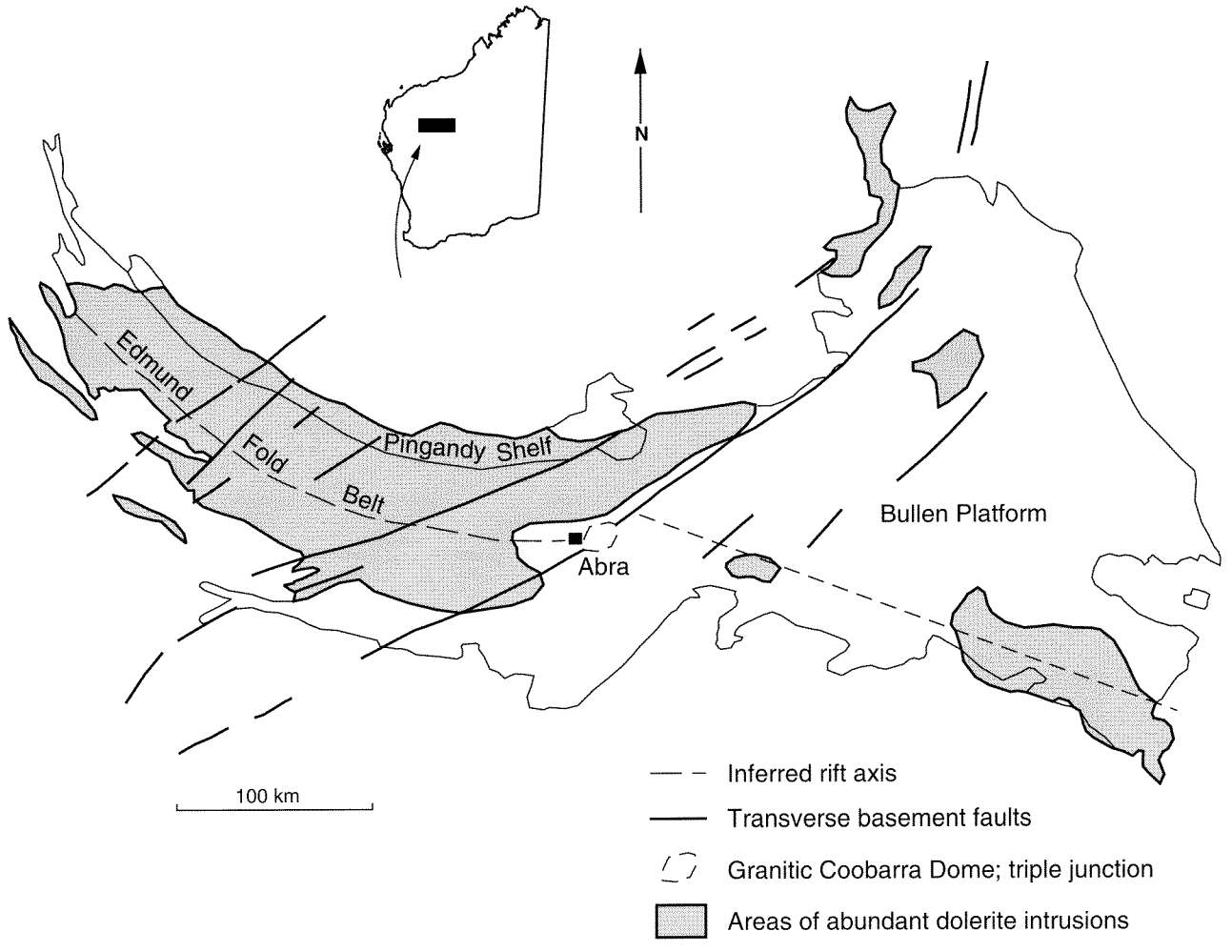

Figure 96. Distribution of dolerite in relation to lineaments and structural provinces in the Bangemall Basin. Abra is located in the inferred rift adjacent to a basement dome which formed in the area of the triple junction. The offset of the rift axis in this area is due to movement along the northeasterly trending lineament after deposition of the Bangemall Group

of 'high spots' over mantle plumes in Africa (Thiessen et al., 1979). From the hot spot, sufficient heat was transferred to high crustal levels, which in turn produced a steep geothermal gradient and resulted in the mobilization and ascent of large amounts of metal-bearing fluids. The following model is based on this concept.

Source rocks

It has been concluded that the source rock of the Abra metals was arkose with features of red-bed copper mineralization (Chapter Seven). The tectonic setting of the depository of the arkose adjacent to a rising granitic dome permits accumulation of great thicknesses (possibly in excess of the 1650 m maximum thickness of the Tringadee Formation), and is in accordance with the typical tectonic setting of continental red-beds. Because of the unusually high heat flow, rapid breakdown of potash feldspars occurs releasing Pb and Ba which substitute for K. For an assumed thickness of 1650 m, and 30 ppm average Pb content, an area of 4 x 4 km would provide sufficient volume to account for some 1.5 Mt of Pb at Abra. Red-bed arkose in the source region also explains the abundance of magnetite/hematite in the Stringer zone; hematite, abundant in red-beds, would be reduced to magnetite when the arkose was heated.

Red-bed formation on the basement in the areas surrounding the Jillawarra basin also provided a huge source of Fe, which was transported into the Abra sub-basin (and the Jillawarra basin) by weathering solutions, where it was deposited as iron formation of the Black and Red zones.

Accumulation of metal-bearing fluids

Progressive burial and increasing heat flow induced the continuous production of water and metal ions by metamorphic mineral reactions. The high porosity of the arkose allowed rapid lateral and vertical migration of the metal-bearing fluids.

The dome structure of sedimentary rocks, lying over the Coobarra Dome, led to trapping of the fluids near the top of the permeable strata, analogous to structural traps in petroleum geology. The Tringadee Formation is characterized by an increasing number of siltstone interbeds towards the top (Muhling et al., 1978). Assuming some impermeable horizons in the upper arkose, large volumes of hot metal-bearing fluids could have migrated up-dip and accumulated in a structural trap. There was no further ascent of the fluids to higher stratigraphic levels because at this stage there were no deep-seated faults which could serve as conduits.

Ascent of hydrothermal fluids

Tensional forces in the crust led to incipient rifting which is expressed by the generation of deep-seated normal faults. One of these faults forms the northern margin of the Abra sub-basin, controlling the distribution of the coarse clastic facies of Unit *WC1*. It is proposed that this fault extended into the basement, and cut through the arkose. The hot, metal-bearing solutions in the structural trap, within the upper arkose, could then be channelled into the conduit provided by the fault zone. Because of the comparatively low permeability of lithologies in the Black and Red zones, a convective system developed. Widespread brecciation seen in the Stringer zone indicates that hydraulic fracturing took place, which facilitated the percolation of hydrothermal fluids. No significant exhalation onto the contemporaneous sea floor occurred. These processes are shown schematically in Figure 97. Of the three margin faults of the Abra sub-basin, it was mainly the easterly trending, northern fault that served as a conduit for metalliferous solutions; possibly because not all faults penetrated the arkose, or because they have also been boundary faults of the arkose depository and therefore did not have access to large amounts of fluids.

The driving force of the hydrothermal system was the heat source at depth, whereby significant vertical temperature gradients controlled the ascent of hydrothermal fluids. Contemporaneous faulting along the feeder channel suggests that the ascent of hydrothermal fluids was supported by seismic pumping as described by Sibson et al. (1975).

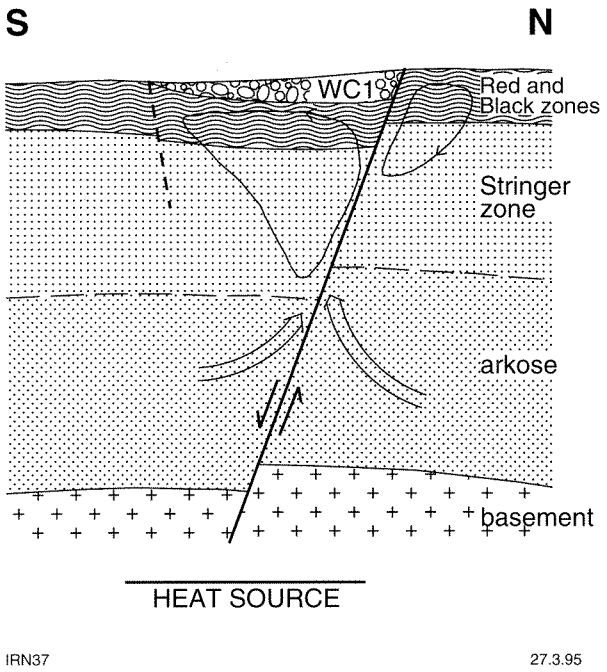

Figure 97. North–south schematic section (not to scale) showing ascent of hydrothermal fluids derived from red-bed arkose. The shape of the convective cells at the mineralization level is after Henley and Thornley (1979) and Large (1981). The size of the convective system penetrating the arkose is unknown

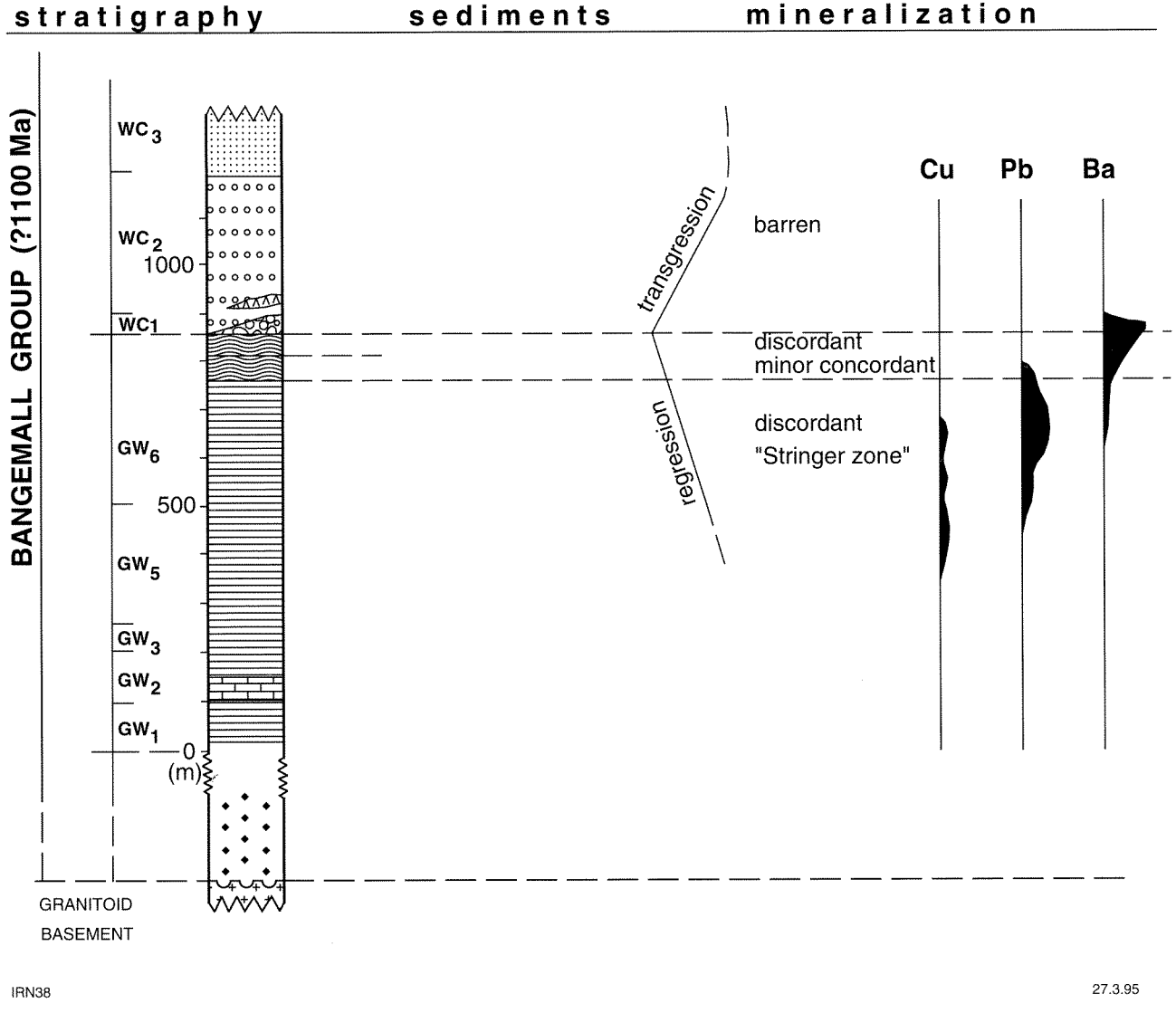

Figure 98. Summary of the host rock sequence and the main features of the Abra mineralization

A side-effect of the anomalously high heat flow was felsic volcanism on the Coobarra Dome, characterized by hydroclastic eruptions induced by faulting in the basement. Despite their spatial separation, hydro-thermal processes and felsic volcanism are related in that both were contemporaneous, and both were generated by the same principal mechanism.

Emplacement of the Abra mineralization

The metals were transported in hot (up to 260°C) solutions in small veinlets radiating from the main feeder channel, and which penetrated the sediments of the Stringer, Black, and Red zones. These strata were in the process of diagenesis, so that they still contained abundant, partly hypersaline formation waters. The hydrothermal system was coupled to this system of diagenetic formation water, which facilitated percolation of the fluids and distribution of metals to distal locations.

Sulfides were emplaced mainly in small veins, in the Stringer and Black zones, but also in the Red zone. Emanating from the main feeder channel and transgressing lithological boundaries, galena and chalcopyrite precipitated in two elongated, concentric zones according to their solubility, which was largely a function of temperature. In addition to occurrences in veins, galena (and minor chalcopyrite) also formed as replacement minerals for pre-existing, syndiagenetic pyrite layers within hematite/magnetite bands. This replacement is expressed by the formula:

$$3\ Fe\ S_2 + 5\ Pb\ Cl_2 + 3\ Fe_2O_3 + 5H_2O$$
$$= 5\ PbS + 3\ Fe_3O_4 + 10\ HCl + SO_2$$

This reaction is thermodynamically favoured at 200°C, and pH6 in the presence of Pb ions (Tluih, A., 1984, pers. comm.). Further galena precipitation occurred where the fluids carrying Pb encountered free H_2S, which was generated by bacterial sulfate reduction and then trapped in the sediment.

Some barite precipitated in veins concurrently with the sulfides, but the bulk of barite occurs as stratiform layers within the Red zone. Here, barite formation is due to quantitative replacement of Ca sulfates in the sabkha lithologies of the Red zone. This reaction is favoured because of the very low solubility of barite. The quantitative nature of this replacement was due to high water content, sufficient porosity (intercalated clastites) and the non-consolidation, at that stage, of sediments in the Red zone.

Summary

A continental hot spot below the area of the Coobarra Dome initiated intracratonic rifting of the Bangemall Basin in a triple-junction pattern. Prior to rifting, doming occurred which resulted in deposition of a thick sequence of red-bed arkose adjacent to the dome. High heat flow linked to the hot spot brought about the breakdown of minerals through metamorphism and the mobilization of metal-bearing fluids.

With the onset of rifting, faults penetrated into the basement and through the arkose, and channelled the fluids principally into one fault zone. The hydrothermal fluids ascended along this fault zone and percolated through the sediments of the upper part of the Gap Well formation. Sulfides formed mainly in veins and as replacement of pre-existing pyrite. Barium-bearing solutions, however, penetrated the sediments until they encountered abundant sulfate in the Red zone. This sulfate was present in the form of gypsum, or anhydrite, and was quantitatively replaced by barite. Figure 98 summarizes the main features of the metal distribution and the host sediment sequence of the Abra mineralization.

References

AMOCO MINERALS AUSTRALIA CO., GEOPEKO, 1991, Jillawarra base metals exploration: Western Australia Geological Survey, M-Series Open File Item 4641.

ANHAEUSSER, C. R., and BUTTON, A., 1976, A review of southern African stratiform ore deposits — their position in time and space, *in* Handbook of stratabound and stratiform ore deposits, Volume 5 *edited by* K. H. WOLF, New York, Elsevier, p. 257–319.

ANNELS, A. E., 1984, The geotectonic environment of Zambian copper–cobalt mineralisation: Journal of the Geological Society of London, v. 141, p. 279–289.

BADHAM, J. P. N., 1981, Shale-hosted Pb–Zn deposits: products of exhalation of formation waters?: Institute of Mining and Metallurgy, Transactions (Section B), v. 90, B70–B76.

BJÖRLYKKE, A., and SANGSTER, D. F., 1981, An overview of sandstone lead deposits and their relation to red-bed copper and carbonate-hosted lead–zinc deposits: Economic Geology, 75th Anniversary Volume, p. 179–213.

BODDINGTON, T. D. M., 1987, Abra, a Middle Proterozoic mineralized body, Western Australia: Australasian Institute of Mining and Metallurgy, Proceedings, v. 292, p. 59–69.

BOUROULLE, C. J., 1980, Sequential studies of the top of the evaporitic series of the Lower Lias in a well in the Aquitaine basine (Auch 1), south-western France, *in* Evaporite deposits *edited by* G. BUSSON:Paris, Editions Technip, p. 29–31 and p. 146–159.

BRAKEL, A. T., ELIAS, M., and BARNETT, J. C., 1982, Collier, Western Australia: Western Australia Geological Survey, 1:250 000 Geological Series Explanatory Notes.

BRAKEL, A. T., and MUHLING, P. C., 1976, Stratigraphy, sedimentation, and structure in the western and central part of the Bangemall Basin, Western Australia: Western Australia Geological Survey, Annual Report 1975, p. 70–79.

BREHLER, B., and WEDEPOHL, K. H., 1969, Zinc, *in* Handbook of Geochemistry *edited by* K. H. WEDEPOHL, Vol. II/3, 30-E-15–30-E-17: Berlin, Springer-Verlag.

CARMICHAEL, I. S. E., TURNER, F. J., and VERHOOGEN, J., 1974, Igneous Petrology: New York, McGraw-Hill, 739p.

CARPENTER, A B., TROUT, M. L., and PICKETT, E. E., 1974, Preliminary report on the origin and chemical evolution of lead- and zinc-rich oil fields brines in Central Mississippi: Economic Geology, v. 69, p. 1191–1206.

COMPSTON, W., and ARRIENS, P. A., 1968, The Precambrian geochronology of Australia: Canadian Journal of Earth Science, v. 5, p. 561–583.

DANIELS, J. L., 1966, Revised stratigraphy, palaeocurrent system and palaeogeography of the Proterozoic Bangemall Group: Western Australia Geological Survey, Annual Report 1965, p. 48–56.

DAVY, R., 1980, A chemical and mineralogical study of low-grade zinc mineralization at three localities in the Proterozoic Bangemall Basin of Western Australia: Western Australia Geological Survey, Report 10, p. 1–70.

de la HUNTY, L. E., 1963, The geology of the manganese deposits of Western Australia: Western Australia Geological Survey, Bulletin 116.

De RITO, R. F., COZZARELLI, F. A., and HODGE, S. D., 1983, Mechanism of subsidence of ancient cratonic rift basins, *in* Processes of continental rifting *edited by* P. MORGAN and B. H. BAKER: Tectonophysics, v. 94, p. 141–168.

DIMROTH, E., 1979, Models of physical sedimentation of iron formations, *in* Facies Models *edited by* R. G. WALKER: Geoscience Canada, Reprint Series 1, p. 175–182.

DUNHAM, K. C., 1970, Mineralization by deep formation waters: a review: Institute of Mining and Metallurgy, Transactions (Section B), v. 79, B127–B136.

DUNHAM, R. J., 1962, Classification of carbonate rocks according to depositional texture, *in* Classification of carbonate rocks *edited by* W. E. HAM, American Association of Petroleum Geologists, Memoir 1, p. 108–121.

ERIKSSON, K. A., and CHUCK, R. G., 1985, Aulacogens: sedimentological and tectonic evolution and association mineralization, *in* Handbook of strata-bound and stratiform ore deposits, volume 12 *edited by* K. H. WOLF: New York, Elsevier, p. 461–529.

ETHIER, V. G., CAMPBELL, F. A., BOTH, R. A., and KROUSE, H. R., 1976, Geological setting of the Sullivan orebody and estimates of temperatures and pressure of metamorphism: Economic Geology, v. 71, p. 1570–1588.

FINLOW-BATES, T., 1978, Control on the genesis of submarine exhalative ore deposits — with particular reference to Mt Isa Mines, Queensland, Australia: Dissertation, Montan-Universität Leoben, Austria, (unpublished), p. 244.

FISCHER, K., and PUCHELT, H., 1972, Barium, *in* Handbook of Geochemistry *edited by* K. H. WEDEPOHL, v. II/4, 56-E-6: Berlin, Springer-Verlag.

FISHER, R. V., and SCHMINCKE, H. V., 1984, Pyroclastic Rocks: Berlin, Springer-Verlag, 472p.

FLEISCHER, V. D., GARLICK, W. G., and HALDANE, R., 1976, Geology of the Zambian Copperbelt, *in* Handbook of strata-bound and stratiform ore deposits, volume 6 *edited by* K. H. WOLF: New York, Elsevier, p. 223–352.

FOLK, R. L., 1959, Practical petrographic classification of limestones: Bulletin of American Association of Petroleum Geologists, v. 63, p. 1–38.

FRIEDMAN, M., HANDIN, J., LOGAN, J. M., MIN, K. D., and STEARNS, D. W., 1976, Experimental folding of rocks under confining pressure: Part III. Faulted drape folds in multilithologic layered specimens: Geological Society of America, Bulletin, v. 87, p. 1049–1066.

GEE, R. D., 1979, Structure and tectonic style of the Western Australian Shield: Tectonophysics, v. 58, p. 327–369.

GEE, R. D., de LAETER, J. R., and DRAKE, J. R., 1976, Geology and geochronology of altered rhyolite from the lower part of the Bangemall Group near Tangadee, Western Australia: Western Australia Geological Survey, Annual Report 1975, p. 112–117.

GREY, K., 1985, Stromatolites and other organic remains in the Bangemall Basin, *in* Geology of the Bangemall Group *edited by* P. C. MUHLING and A. T. BRAKEL: Geological Survey of Western Australia, Bulletin 128, p. 221–231.

GUILLEVIN, Y., 1980, Petrographical data of Oligocene evaporites in the Bresse and Valence basins (Eastern France), *in* Evaporite deposits *edited by* G. BUSSON: Paris, Editions Technip, p. 41–48 and p. 174–213.

GUSTAFSON, L. B., and WILLIAMS, N., 1981, Sediment-hosted stratiform deposits of copper, lead, and zinc: Economic Geology, 75th Anniversary Volume, p. 139–178.

HANOR, J. S., 1979, The sedimentary genesis of hydrothermal fluids, *in* Geochemistry of hydrothermal ore deposits *edited by* H. L. BARNES: Wiley and Sons, New York, p. 137–172.

HAYNES, D. W., 1986, Stratiform copper deposits hosted by low-energy sediments: II. Nature of source rocks and composition of metal transporting water: Economic Geology, v. 81, p. 266–280.

HENLEY, R. W., and THORNLEY, P., 1979, Some geothermal aspects of polymetallic massive sulfide formation: Economic Geology, v. 74, p. 1600–1612.

HOBBS, B. E., MEANS, W. D., and WILLIAMS, P. E., 1976, An outline of structural geology: New York, John Wiley and Sons, 571p.

JACKSON, M. P. A., and SENI, S. J., 1983, Geometry and evolution of salt structures in a marginal rift basin of the Gulf of Mexico, East Texas: Geology, v. 11, p. 131–135.

JAMES, N. P., 1979, Shallowing-upward sequences in carbonates, *in* Facies Models *edited by* R. G. WALKER: Geoscience Canada, Reprint Series I, p. 109–119.

KALOGEROPOULOS, S. I., 1983, Composition and oxidation state dependence of chlorites from tuffaceous exhalites associated with volcanogenic massive sulfide ore deposits: Neues Jahrbuch für Mineralogie, Monatshefte 4, p. 187–192.

KENDALL, A. C., 1979, Continental and supratidal (sabkha) evaporites and subaqueous evaporites, *in* Facies models *edited by* R. G. WALKER: Geoscience Canada, Reprint Series I, p. 145–174.

LAMBERT, I. B., 1976, The McArthur zinc–lead–silver deposit: features, metallogenesis and comparison with some other stratiform ores, *in* Handbook of strata-bound and stratiform ore deposits, volume 6 *edited by* K. H. WOLF: New York, Elsevier, p. 535–484.

LARGE, D. E., 1980, Geological parameters associated with sediment-hosted, submarine exhalative Pb–Zn deposits: an empirical model for mineral exploration: Geologisches Jahrbuch, D40, p. 59–129.

LARGE, D. E., 1981, Sediment-hosted submarine exhalative lead–zinc deposits — a review of their geological characteristics and genesis, *in* Handbook of strata-bound and stratiform ore deposits, volume 9 *edited by* K. H. WOLF: New York, Elsevier, p. 469–507.

LOVE, L. G., and ZIMMERMANN, D. O., 1961, Bedded pyrite and micro-organisms from the Mt Isa Shale: Economic Geology, v. 56, p. 873–896.

MARSTON, R. J., 1980, Copper mineralization in Western Australia: Western Australia Geological Survey, Mineral Resources Bulletin 13, p. 101–107.

McKENZIE, D., 1978, Some remarks on the development of sedimentary basins: Earth and Planetary Science Letters, v. 40, p. 25–32.

MOINE, B., SAUVAN, P., and JAROUSSE, J., 1981, Geochemistry of evaporite-bearing series: A tentative guide for the identification of metaevaporites: Contributions to Mineralogy and Petrology, v. 76, p. 401–412.

MORROW, D. W., KROUSE, H. R., GHENT, E. D., TAYLOR, G. C., and DAWSON, K. R., 1978, A hypothesis concerning the origin of barite in Devonian carbonate rocks of northeastern British Columbia: Canadian Journal of Earth Sciences, v. 15, p. 1391–1406.

MUHLING, P. C., and BRAKEL, A. T., 1985, Geology of the Bangemall Group — the evolution of an intracratonic Proterozoic Basin: Western Australia Geological Survey, Bulletin 128, 219p.

MUHLING, P. C., BRAKEL, A. T., and DAVIDSON, W. A., 1978, Mount Egerton, Western Australia: Western Australia Geological Survey, 1:250 000 Geological Series Explanatory Notes.

MUTTON, A. J., and McINERNEY, P. M., 1987, The geophysical discovery of the Abra base metal deposit, Bangemall Basin, Western Australia: Exploration Geophysics, v. 18, p. 148–151.

NOCKOLDS, S. R., KNOX, R. W. O'B., and CHINNER, G. A., 1978, Petrology for students: Cambridge, Cambridge University Press, 435p.

PAAR, W., 1974, Die Gefüge der synsedimentär-syndiagenetischen Schwerspat-Bleiglanz-Lagerstäte 'Breithorn', Ostgrönland: Archiva Lagerstätten Farschung, Ostalpen, Sonderband, v. 2, p. 215–237.

PEARCE, J. A., and CANN, J. R., 1973, Tectonic setting of basic volcanic rocks determined using trace element analyses: Earth and Planetary Science Letters, v. 19, p. 290–300.

PEACOR, D. R., and WEDEPOHL, K. H., 1972, Manganese, *in* Handbook of geochemistry *edited by* K. H. WEDEPOHL, v. II/3, 25-E-1: Berlin, Springer-Verlag.

PETTIJOHN, F. J., 1975, Sedimentary rocks: New York, Harper and Row, 628p.

PETTIJOHN, F. J., POTTER, P. E., and SIEVER, R., 1973, Sand and sandstone: New York, Springer-Verlag, 618p.

RAMDOHR, P., 1975, Die Erzmineralien und ihre Verwachsungen: Berlin, Akademie-Verlag, 1277p.

RAMSAY, J. G., 1962, The geometry and mechanics of formation of 'similar' type folds: Journal of Geology, v. 70, p. 309–327.

RAMSAY, J. G., 1967, Folding and fracturing of rocks:New York, McGraw-Hill, 568p.

REIMANN, C., and STUMPFL, E. F., 1985, Palaeozoic amphibolites, Kreuzeck Mountains, Austria: Geochemical variations in the vicinity of mineralization: Mineralium Deposita, v. 20, p. 69–75.

REINECK, H. E., and SINGH, I. B., 1973, Depositional sedimentary environments: Berlin, Springer-Verlag, 439p.

REINSON, G. E., 1979, Barrier Island systems, *in* Facies Models *edited by* R. G. WALKER: Geoscience Canada, Reprint Series I, p. 57–74.

RENFRO, A. R., 1974, Genesis of evaporite-associated stratiform metalliferous deposits — a sabkha process: Economic Geology, v. 69, p. 33–45.

RICHARDS, J. R., 1983, Lead isotopes as indicators of old stable craton in Western Australia: Geochemical Journal, v. 17, p. 241–246.

ROBBINS, E. I., 1983, Accumulation of fossil fuels and metallic minerals in active and ancient rift lakes, *in* Processes of continental rifting *edited by* P. MORGAN and B. H. BAKER: Tectonophysics, v. 94, p. 633–658.

SANGSTER, D. F., 1976, Carbonate-hosted lead–zinc deposits, *in* Handbook of strata-bound and stratiform ore deposits, volume 6 *edited by* K. H. WOLF: New York, Elsevier, p. 447–456.

SANGSTER, D. F., and SCOTT, S. D., 1976, Precambrian, strata-bound, massive Cu–Zn–Pb sulfide ores of North America *in* Handbook of strata-bound and stratiform ore deposits, volume 6 *edited by* K. H. WOLF: New York, Elsevier, p. 129–222.

SAWKINS, F. J., 1976, Widespread continental rifting: Some considerations of timing and mechanism: Geology, v. 4, p. 427–430.

SHEARMAN, D. J., 1980, Sabkha facies evaporites, *in* Evaporite deposits *edited by* G. BUSSON: Paris, Editions Technip, p. 19 and p. 96–109.

SIBSON, R. H., MOORE, J. McM., and RAKIN, A. H., 1975, Seismic pumping — a hydrothermal fluid transport mechanism: Journal of the Geological Society of London, v. 131, p. 653–659.

SKINNER, B. J., 1979, The many origins of hydrothermal mineral deposits, *in* Geochemistry of hydrothermal ore deposits *edited by* H. L. BARNES: New York, Wiley and Sons, p. 1–21.

STILLE, H., 1930, Ober Einseitigkeiten in der germanotypen Tektonik Nordspaniens und Deutschlands: Göttingen, Gesellschaft der Wissenschaften, Mathematisch-Physikalische Klasse, Nachrichten, v. 3, p. 179–219.

TANNER, W. F., 1971, Numerical estimates of ancient waves, water depth and fetch: Sedimentology, v. 16, p. 71–88.

THIEDE, D. S., and CAMERON, E. N., 1978, Concentrations of heavy metals in the Elk Point evaporite sequence, Saskatchewan: Economic Geology, v. 73, p. 405–415.

THIESSEN, R., BURKE, K., and KIDD, W. S. F., 1979, African hotspots and their relation to the underlying mantle: Geology, v. 7, p. 263–266.

TRÖGER, W. E., 1969, Optische Bestimmung der gesteinsbildenden Minerale, Teil 2/Textband: Stuttgart, Schweizerbart'sche Verlagsbuchhandlung.

TRUDINGER, P. A., 1981, Origin of sulphide in sediments: Australia BMR, Geology and Geophysics Journal, v. 6, p. 279–285.

TRUDINGER, P. A., LAMBERT, I. B., and SKYRING, G. W., 1972, Biogenic sulfide ores: a feasibility study: Economic Geology, v. 67, p. 1114–1127.

VOGT, J. H., 1984, Geological evolution and stratabound Cu–Pb–Ba mineralization of the Jillawarra Belt in the Proterozoic Bangemall Basin, Western Australia: Montan-Universität, Leoben, Austria, Ph.D. thesis (unpublished).

VOGT, J. H., and KOLLENBERG, W., 1987, Genetic implications of geochemical factor analysis in a sediment-hosted Cu–Pb–Ba mineralization: Mineralium Deposita, v. 22, p. 151–161.

VOGT, J. H., and STUMPFL, E. F., 1987, Abra — a stratabound Pb–Cu–Ba mineralization in the Bangemall Basin, Western Australia: Economic Geology, v. 82, p. 805–825.

WALKER, R. G., 1979, Turbidites and associated coarse clastic deposits *in* Facies models *edited by* R. G. WALKER: Geoscience Canada, Reprint Series I, p. 91–103.

WALTER, M. R., 1972, Stromatolites and the biostratigraphy of the Australian Precambrian and Cambrian: Palaeontological Association, Special Papers in Palaeontology, No. 11.

WEDEPOHL, K. H., 1970, Lead, *in* Handbook of Geochemistry *edited by* K. H. WEDEPOHL, v. II/5, 82-E-11/12: Berlin, Springer-Verlag.

WEINBERG, D. W., 1979, Experimental folding of rocks under confining pressure: Part VII. Partially scaled models of drape folds: Tectonophysics, v. 54, p. 1–24.

WILLIAMS, N., 1978, Studies of the base-metal sulfide deposits at McArthur River, Northern Territory, Australia: II. The sulfide–S and organic–C relationships of the concordant deposits and their significance: Economic Geology, v. 73, p. 1036–1056.

ZEMANN, J., and WEDEPOHL, K. H., 1972, Copper, *in* Handbook of geochemistry *edited by* K. H. WEDEPOHL, v. II/3: 29-E-12: Berlin, Springer-Verlag.

GEOLOGICAL MAP OF THE JILLAWARRA AREA

SHEET 1

SHEET 2

REFERENCE

CAINOZOIC — TERTIARY / QUATERNARY

- Qc, Qa, Qc — Qc Sand, wind blown; Qa Alluvium; Qc Colluvium
- Ti — Laterite, iron crust

? MIDDLE PROTEROZOIC — Basement Group

- Dy — Dolerite, dykes and sills
- Mv — **DEVIL CREEK FORMATION:** dolomitic siltstone, dolomitic shale; minor silicified shale and chert
- MC — **DISCOVERY CHERT:** massive to laminated fissile chert
- MJ, MJa, MJb — **JILLAWARRA FORMATION:** Yertsilovited silicia-rich and iron-rich shale, finely laminated; minor laminated chert. West of 118° 02' E : silicified siltstone and fine-grained sandstone near the top. Dolomitic: dolomitic shale, shale, sandstone
- WC, WCa, WCb, WCc — **WEST CREEK FORMATION:** Coarse-grained sandstone; quartz-pebble conglomerate intercalations in upper part; silicification east of 118° 20' E; high angle cross-bedding common. Siltstone, iron-rich siltstone; dolomitic siltstone; minor dolomitic sandstone; silicified dolomite with chert appearance; minor immature sandstone. Alternating sandstone and siltstone beds, intricately of various sizes, graded bedding, scour-and-fill structures, slump structures; basal sandstone crossbedded and manganese-rich; in upper parts intercalated polymict conglomerate associated with manganese- and tuffaceous-rich horizons; sequence grades laterward into coarse-grained feldspathic sandstone and conglomerate. Rhyolite and minor related spilit tuff; erupted in basal portion of WC2. Interbedded siltstone,coarse-grained immature quartz sandstone, polymict conglomerate, minor dolomite
- BW, BW4, BW3, BW2c, BW2, BW1, BW0 — **BAP WELL FORMATION:** Local silica and manganese enrichment at top. Laminated siltstone, ripple marks; dolomite shale; patchy discordant oxidized sulphides and accompanied silicification and manganese enrichment; minor concordant oxidized sulphides. Biostromal dolomite. Dolomite. Siltstone with numerous, commonly lenticular,coarse-grained sandstone intercalations; minor conglomerate near the top; minor dolomitic siltstone; barite veining in sandstone; wave ripples in siltstone. **Woodlands Arenite Member:** coarse-grained sandstone with barite veining; interbedded sandstone and siltstone. Siltstone with ripple marks; interbedded sandstone. Dolomite; dolomitic shale; minor coarse-grained sandstone. Laminated siltstone, rich in cubic moulds; sandstone; minor dolomitic siltstone; immature coarse muscovite sandstone at base
- ? — Granitic basement—biotite-muscovite adamellite (Coobarra Dome); gneiss/schist (Woodlands Dome)

SYMBOLS

- Geological boundary
- Fault: accurate; concealed; inferred; accurate
- Shear zone
- Quartz vein
- Anticline: accurate, with direction of plunge; concealed; overturned
- Minor anticline
- Syncline: accurate, with direction of plunge; concealed; overturned
- Minor syncline
- Zone of minor folds, showing plunge and vergence
- Strike and dip of bedding, dip not measured
- Top of stratum
- Cleavage: vertical; inclined
- Mineral elongation lineation, measured on bedding surface
- Stromatolite locality
- Diamond drill hole — @ 33W-79-36
- Mineral exploration prospect — Jeds
- Mineral occurrence: Barium (barite) — Ba; Copper (malachite, brochantite, cuprite) — Cu; Lead (galena) — Pb; Manganese — Mn; Zinc — Zn
- Formed road
- Track
- Fence
- Intermittent watercourse
- Well or bore, with windpump

DIAGRAMMATIC SECTIONS

NATURAL SCALE

SECTION A—B

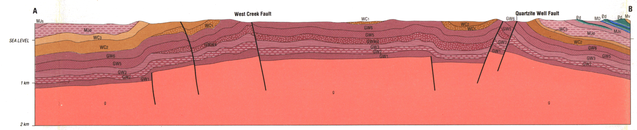

SECTION C—D

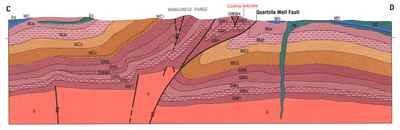

SECTION E—F

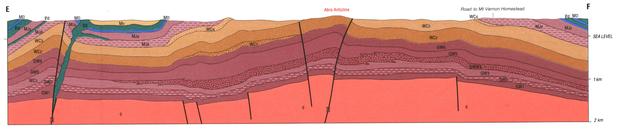

TECTONIC UNITS WITHIN THE BANGEMALL BASIN

SCALE 1:7 500 000

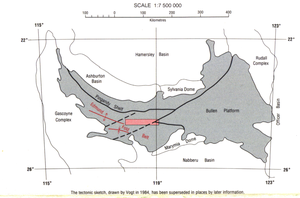

The tectonic sketch, drawn by Vogt in 1984, has been superseded in places by later information.

INDEX TO 1:250 000 SHEETS

Area of investigation

MT EGERTON SG 50-3 — WHIM 1 — WHIM 2

COLLIER SG 50-4

LOCATION MAP

Approximate outline of Bangemall Basin

Area of investigation

Cartography by the Cartographic Services Branch, Surveys and Mapping Division, Department of Minerals and Energy, Western Australia

Published by and available from the Geological Survey of Western Australia, Department of Minerals and Energy, 100 Plain Street, East Perth, WA, 6004

Printed by the State Print, Department of State Services, Western Australia

Mapped and compiled by J. Vogt, G.S.W.A., 1982-1983, incorporating data from AMOCO Minerals Pty. Ltd. and Geoplanic Pty. Ltd.

Base map courtesy of Geoplanic Pty. Ltd.

DEPARTMENT OF MINERALS AND ENERGY
HON. GEORGE CASH, J.P., M.L.C.
MINISTER FOR MINES
L. C. HANFORD, ACTING DIRECTOR GENERAL

PETER BLU
DIRECTOR, GEOLOGICAL SURVEY OF WESTERN AUSTRALIA

SCALE 1 : 50 000

1000 Metres 0 1 2 3 4 5 Kilometres

JILLAWARRA AREA

© Western Australia 1983

GEOLOGICAL SURVEY & GENERAL LIBRARY
- 9 APR 1998
DEPARTMENT OF MINES
WESTERN AUSTRALIA

SOLID GEOLOGY OF THE JILLAWARRA AREA

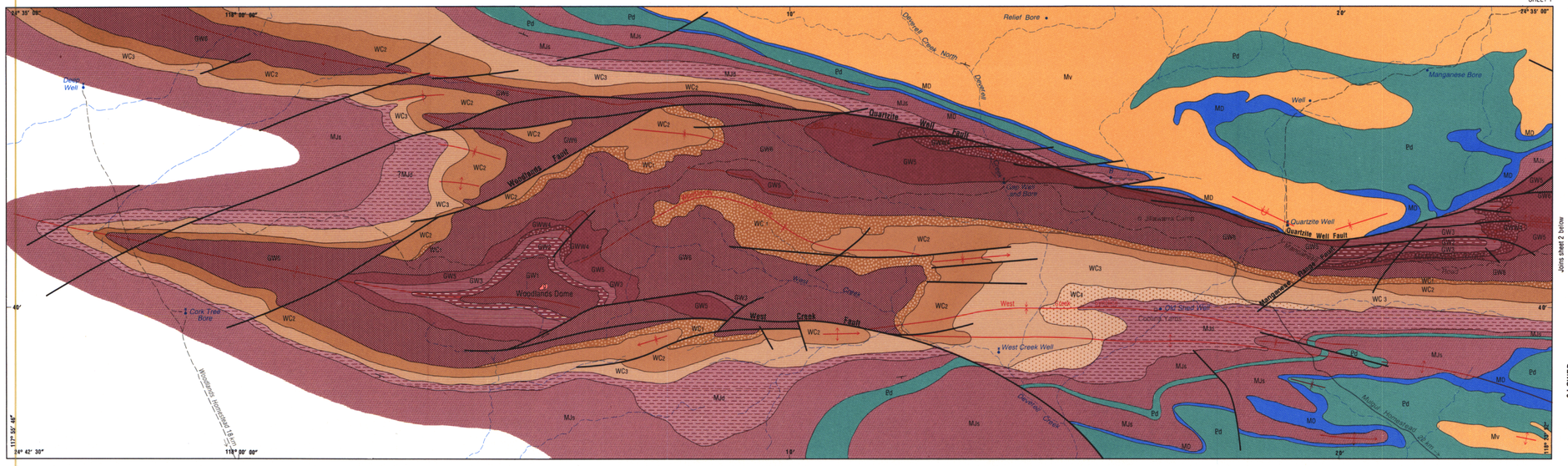

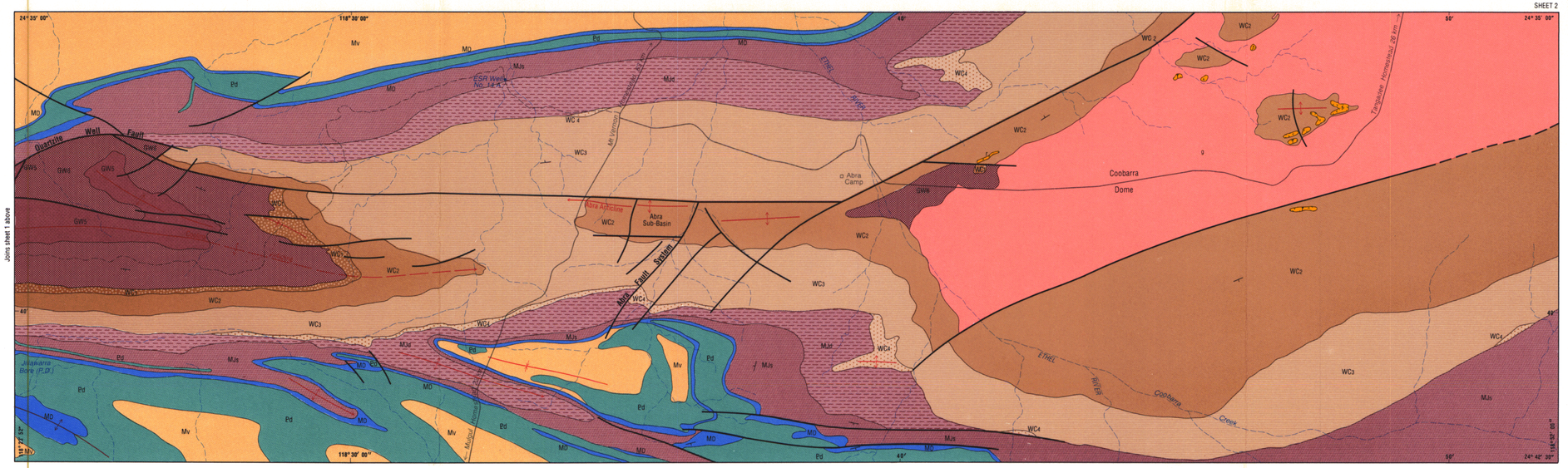

REFERENCE

- Pd — Dolerite, dykes and sills; marked when structurally significant
- Mv — **DEVIL CREEK FORMATION:** dolomitic siltstone and shale; locally large volumes of dolerite sills
- MD — **DISCOVERY CHERT:** massive to laminated chert; locally large volumes of dolerite sills
- MJs — **JILLAWARRA FORMATION:** Varicoloured silica-rich and iron-rich laminated shale
- MJd — Dolomite; dolomitic shale; shale; sandstone

Bangemall Group

- WC3 — **WEST CREEK FORMATION:** Coarse-grained sandstone; quartz-pebble conglomerate intercalations
- WC3 — Siltstone; dolomitic siltstone; minor immature sandstone
- WC2 — Turbiditic sandstone, siltstone and shale; grades eastward into feldspathic sandstone and conglomerate
- WC2 — Rhyolite and minor related lapilli tuff
- WC1 — Interbedded siltstone; coarse-grained immature sandstone and polymict conglomerate
- GW6 — **GAP WELL FORMATION:** Laminated siltstone; dolomitic shale; stromatolitic dolomite
- GW5 — Siltstone with coarse-grained sandstone intercalations; minor stromatolitic dolomite
- GW4 — **Woodlands Arenite Member:** coarse-grained sandstone
- GW3 — Ripple-marked siltstone and interbedded sandstone
- GW2 — Dolomite; dolomitic shale; minor coarse-grained sandstone
- GW1 — Laminated siltstone; sandstone; minor dolomitic siltstone

PROTEROZOIC

? LOWER PROTEROZOIC

- g — Granitic basement; biotite-muscovite adamellite (Coobarra Dome); gneiss/schist (Woodlands Dome)

SYMBOLS

- Geological boundary
- Fault, accurate
- Anticline: accurate; concealed
- Syncline: accurate; overturned
- Strike and dip of bedding
- Formed road
- Track
- Watercourse
- Well or bore, with windpump

TECTONIC SKETCH

SCALE 1 : 15 000 000

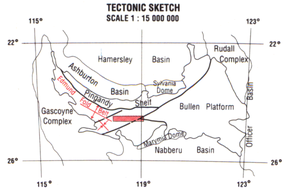

The tectonic sketch, drawn by Vogt in 1984, has been superseded in places by later information.

DEPARTMENT OF MINERALS AND ENERGY
HON. GEORGE CASH, J.P., M.L.C.
MINISTER FOR MINES
L.C. RANFORD, ACTING DIRECTOR GENERAL

PIETRO GUI
DIRECTOR, GEOLOGICAL SURVEY OF WESTERN AUSTRALIA

SCALE 1: 100 000

1000 0 1 2 3 4 5 6
Metres Kilometres

JILLAWARRA AREA

© Western Australia 1993

GEOLOGICAL SURVEY & GENERAL LIBRARY
- 9 APR 1998
DEPARTMENT OF MINES WESTERN AUSTRALIA